US Army Corps
of Engineers®

Hydrologic Engineering Center

River Analysis System
HEC-RAS

Release Notes

Version 4.0.0 Beta

November 2006

Approved for Public Release – Distribution Unlimited

Introduction

Version 4.0 of the River Analysis System (HEC-RAS) is now available. This version supersedes version 3.1.3, which was released in May of 2005 to the general public. Several new simulation features have been added to the program since that time. Version 4.0 of HEC-RAS includes the following new features:

1. Sediment Transport/Movable Bed Modeling
2. Sediment Impact Analysis Methods (SIAM)
3. Water Quality Capabilities (Temperature Modeling)
4. User Defined Rules for Controlling Gate Operations
5. Modeling Pressurized Pipe Flow
6. Pump Station Override Rules
7. New Channel Design/Modification Tools
8. Geo-Referencing Tools
9. New Gate Types
10. New Functionality for Lateral Weirs
11. Additional Graphical Outputs
12. Shortcut Keys for Graphics
13. User's Manual and Help System

Other minor enhancements were also added. The development team has also continued careful and systematic testing of the program since the last release. The results of that testing in combination with reports from users has allowed the identification and repair of various problems. Some problems that did not affect results but caused problems in the program interface have been repaired without being specifically documented.

The *Hydraulic Reference Manual* for Version 3.1 continues to accurately describe the data requirements and mathematical models included in the program. New simulation capabilities have been added to the program and are not included in the manual. The manual is currently undergoing a major revision to expand documentation of existing mathematical models and fully describe the newly added models.

The *Applications Guide* also continues to accurately describe how to apply the program to various engineering problems. However, the guide is undergoing revision to add guidance on how to use new features of the program to more efficiently solve problems.

Installation

The installation program and all documentation are available on the HEC website at http://www.hec.usace.army.mil . This new release is installed independently of any previous versions of the program. Users may have the new version and previous versions of HEC-RAS software installed simultaneously for parallel use or testing. This new version is fully compatible with projects developed in any previous version of the program. However, once a project has been opened in Version 4.0 and saved, it may not be possible to open it with an older version of the software and reproduce the old results (i.e. the software is not fully forward compatible).

The new installation package is designed to be easy to use. It will take you through the steps of selecting a directory for the program files and making other settings. Use the following steps to install the program on the Microsoft Windows® operating system:

1. Download the installation package from the HEC website to a temporary folder on the computer. If the software was provided to you on a CD-ROM or other media, insert it in the appropriate drive.
2. Run the installation program. In Windows Explorer, double-click the icon for the installation program. You must have administrator privileges to run the installer.
3. Follow the on-screen prompts to install the program.

New Capabilities

Sediment Transport/Movable Bed Analyses

This component of the modeling system is intended for the simulation of one-dimensional sediment transport/movable boundary calculations resulting from scour and deposition over moderate time periods (typically years, although applications to single flood events are possible).

The sediment transport potential is computed by grain size fraction, thereby allowing the simulation of hydraulic sorting and armoring. The model is designed to simulate long-term trends of scour and deposition in a stream channel that might result from modifying the frequency and duration of the water discharge and stage, or modifying the channel geometry. This system can be used to evaluate deposition in reservoirs, design channel contractions required to maintain navigation depths, predict the influence of dredging on the rate of deposition, estimate maximum possible scour during large flood events, and evaluate sedimentation in fixed channels.

For details on how to use the sediment transport capabilities in HEC-RAS, please review Chapter 17 of the User's Manual.

Sediment Impact Analysis Methods (SIAM)

SIAM is a sediment budget tool that compares annualized sediment reach transport capacities to supplies and indicates reaches of overall sediment surplus or deficit. SIAM is a screening level tool to compute rough, relative responses to a range of alternatives, in order to identify the most promising alternatives (which should then be modeled in more detail). The algorithms in SIAM evaluate sediment impact caused by local changes on the system from a sediment continuity perspective. The results map potential imbalances and instabilities in a channel network and provide the first step in designing or refining remediation.

Users can begin with existing geometry and flow data and develop a set of sediment reaches with unique sediment and hydraulic characteristics. The SIAM program will then perform sediment transport capacity computations to determine potential imbalances and instabilities in a channel network. SIAM does not predict intermediate or final morphological patterns and does not update cross sections, but rather indicates trends of locations in the system for potential sediment surpluses or deficits. The results can be used to design or refine remediation efforts in the system.

For details on how to perform a SIAM analysis in HEC-RAS, please review Chapter 18 of the User's Manual.

Water Quality Analysis

This component of the modeling system is intended to allow the user to perform riverine water quality analyses. An advection-dispersion module is included with this version of HEC-RAS, adding the capability to model water temperature. This new module uses the QUICKEST-ULTIMATE explicit numerical scheme to solve the one-dimensional advection-dispersion equation using a control volume approach with a fully implemented heat energy budget. Future versions of the software will include the ability to perform the transport of several water quality constituents.

For details on how to use the water quality capabilities in HEC-RAS, please review Chapter 19 of the User's Manual.

User Defined Rules for Controlling Gate Operations

The operating procedures for determining and controlling the releases from reservoirs and other types of hydraulic structures can be quite complex. HEC-RAS allows flexibility in modeling and controlling the operations of gates at hydraulic structures through the use of rules. Examples of variables that could be used to control releases from a hydraulic structure are: current flows and water surfaces at the structure, current flows and stages at a downstream or upstream cross section location, time considerations (winter,

morning, etc), and/or previously computed values (accumulated outflows, running averages, etc). Rule operations in HEC-RAS are available for inline hydraulic structures, lateral hydraulic structures, and storage area connections that contain gates.

For details on how to use the User Defined Rules Capabilities for controlling gate operations in HEC-RAS, please review Chapter 16 of the User's Manual.

Modeling Pressurized Pipe Flow

HEC-RAS can be used to model pressurized pipe flow during unsteady flow calculations. This is accomplished by using the Priessmann slot theory applied to the open channel flow equations. To model pressure flow with HEC-RAS, the user must use cross sections with a Lid option. The cross section is entered as the bottom half of the pipe and the Lid is entered as the top half of the pipe. Any shape pipe can be modeled, however, the details of the pipe shape will depend on how many points the user puts in for the bottom (cross section) and the top (Lid).

In general, lids can be added to any cross section in the HEC-RAS model. Several cross sections in succession with lids can be used to represent a pipe. Multiple interconnected pipes can be modeled. Lidded cross sections can be used around stream junctions to represent pressurized junctions. However, HEC-RAS does not compute minor losses at junctions, bends, or where pipes change size. This is currently a limitation in modeling pressurized pipe flow with HEC-RAS. Lateral flows can be modeled by either using lateral structures with culverts, or by directly inputting hydrographs as lateral flow boundary conditions. The lateral structure option can be used to mimic drop inlets connecting the surface flow to the pipe.

For details on how to use the Pressurized Pipes capabilities in HEC-RAS, please review Chapter 16 of the User's Manual.

Pump Station Override Rules

Advanced control rules have been added to the Pump Station capabilities of HEC-RAS in order to override normal pump operations. Override rules make it easy to turn pumps on and off based on time of day, as well as target flows and stages from any location in the model. Rules can also be set to override the total pump station maximum or minimum flow capacity.

For details on how to use the Pump Station Override Rules Capabilities in HEC-RAS, please review the section on Pump Stations in Chapter 6 of the User's Manual.

New Channel Design/Modification Tools

The channel design/modification tools in HEC-RAS allow the user to perform a series of trapezoidal cuts into the existing channel geometry or to create new channel geometry. The current version of HEC-RAS has two tools for performing channel modifications. These tools are available from the Tools menu of the Geometric Data editor and are labeled Channel Design/Modification and Channel Modification (original). The tool labeled Channel Design/Modification is a new tool for HEC-RAS version 4.0. The tool labeled Channel Modification (original) is the original channel modification tool developed for HEC-RAS.

For details on how to use the Channel Design/Modifications Capabilities in HEC-RAS, please review Chapter 13 of the User's Manual.

Geo-Referencing Tools

GIS tools in HEC-RAS are provided on the Geometric Data editor on the GIS Tools menu. The GIS Tools provide capabilities for editing and modifying x and y coordinates associated with the river network, cross sections, bridges/culvert, hydraulic structures, and other features in HEC-RAS. These GIS coordinate data can be edited directly through the different table options or computed based on the data available. The GIS Tools also provide visual displays of the data that can be exported to the GIS for processing.

For details on how to use the Geo-Referencing Tools in HEC-RAS, please review the section on Geo-Referencing an HEC-RAS Model in Chapter 6 of the User's Manual.

New Gate Types

Two new gate types have been added into HEC-RAS for use with Inline Hydraulic Structures, Lateral Structures, and Storage Area Connections. These gate types are: overflow gates with a closed top; overflow gates with an open top. Additionally the ability for the user to enter a set of User defined curves to represent a gate(s), has also been added as an option.

For details on the new gate types and user defined gate curves in HEC-RAS, please review the section on Inline Hydraulic Structures in Chapter 6 of the User's Manual.

New Functionality for Lateral Structures

In previous versions of HEC-RAS a lateral weir could be set up to span several cross sections of the channel it was attached to (head water side). However, for the channel receiving flow (tailwater side), the program was limited to sending the flow to only a single cross section location. The user can now set the tailwater location to a range of cross sections. The program distributes the flow across this range of cross sections, and it also uses the full range for

evaluating tailwater submergence on the lateral weir. We have also added the ability to override/set the spacing between cross sections on the lateral structure. This allows the user to have lateral structure lengths that are longer or shorter than the cross section reach lengths.

For details on the new Lateral Structures features, please review Chapter 6 of the User's manual.

Additional Graphical Outputs

New graphical outputs have been developed for Sediment Transport Computations, SIAM analyses, and Water Quality Computations. Additionally, when performing an unsteady flow analysis the user can optionally turn on the ability to view output at the computation interval level. This is accomplished by checking the box labeled Computation Level Output on the Unsteady Flow Analysis window (In the Computations Settings area on the window).

For details on the new graphical outputs for unsteady flow computations in HEC-RAS, please review the section on Viewing Computational Level Output for Unsteady Flow in Chapter 9 of the User's Manual. For more information on graphical outputs for Sediment Transport Analysis, SIAM, and Water Quality Analysis, please review their perspective chapters in the User's manual.

Shortcut Keys for Graphics

A couple of shortcut key features have been made available for all of the graphic windows. They are:

Shift Key: When the shift key is held down and the mouse pointer is over the graphic window, the mouse pointer will change to a "hand" which puts it in a panning mode.

Control Key: When holding down the control key and the mouse pointer is over the graphic window, the pointer changes to a measuring tool. The user can create a line or polygon by clicking the mouse pointer with as many points as they want. When the Control Key is released, the program will display a dialog containing: the line length, area of a polygon when the first and last point are closed; the x distance traveled; the y distance traveled; the slope of the bounding box containing the data. The X and y coordinates of the data points are also sent to the windows clipboard, which is very handy for getting GIS coordinates for cross sections.

User's Manual and Help System

The HEC-RAS User's Manual has been completely updated for the 4.0 software release. All of the chapters have received updated text and graphics. New information has been added to chapters 13 and 16 of the

manual, and completely new chapters have also been added (Chapters 17, 18, and 19). Additionally, the help system has been completely revamped. The new help system directly uses the user's manual PDF file. The software still has context sensitive help, in that, while on any editor if you select the help menu option or press the F1 key, a help window will appear with the correct section of the manual displayed.

Problems Repaired

The following is a list of bugs that were found in version 3.1.3 and fixed for version 4.0:

1. **Velocity Output at Bridges.** During unsteady flow calculations, if reverse flows occurred through a bridge, the software would report values of zero for velocities at the cross section just upstream of the bridge. This was only an output mistake, and did not effect the computation of the water surface and flow.

2. **Family of Rating Curves for Unsteady Flow.** For bridges, culverts, storage area connections, and lateral structures, in which a family of curves are generated from the Unsteady flow pre-processor, several changes have been made to the code that generates these curves. The previous version of HEC-RAS was on occasion getting some bad points in the curves, which would cause all of the curves in that zone to have a problem. We have fixed several known problems, as well as improved the way we interpolate between the curves.

3. **Submerged Culvert Flow.** When the outlet of a culvert is submerged, the culvert can act as a siphon if the inlet is also submerged. In some cases, RAS was treating the culvert as a siphon even though the water surface at the inlet was slightly below the top of the culvert (that is, the inlet was not fully submerged).

4. **Storage Area Connections.** Having more than 10 storage area connections in the model could, in rare cases, cause a "GUI didn't allocate arrays large enough," error.

5. **Perched Bridges.** A perched bridge (the low chord on the bridge is higher than minimum elevation in the overbanks) that was being modeled as a cross section with a lid, was not always computing flow in the overbanks properly.

6. **Dam Break Piping Failure.** During a dam break, the transition from a piping failure to an open breach was not always being computed correctly.

7. **Bridge Momentum Computations.** For a bridge that was being solved with the momentum method, version 3.1.3 would allow a slight drop in the energy grade line as the calculations proceeded

from the downstream internal bridge section to the upstream internal bridge section. Version 4.0 will disregard the momentum solution if this happens (and usually defaults to the energy solution).

8. **Bridge Pressure and Weir Flow Computations.** For bridges with pressure and weir flow, the reported flow distribution (the amount of flow in the channel versus the left and right overbanks) was not always correct. This was only an output reporting problem, not a problem with the calculations of the water surfaces.

9. **Pump Station Inflow to a Storage Area.** For a storage area that was receiving flow from a pump station, the inflow to the storage area was being incorrectly reported in some cases. This was not a problem with the computations (i.e. the correct flow was being used for the computations), just in reporting the flows in the output file and interface.

10. **GIS Data Import of Levees.** The data importer would not import levees unless the cross section bank stations were also imported.

11. **Importing HEC-HMS Version 3.0 and Greater Flow Data from HEC-DSS.** With the release of HEC-HMS version 3.0, there was a change to they way flow data was sent to HEC-DSS files. Before all data was sent as single precision numbers. Now HEC-HMS sends all its results as double precision numbers. Previous versions of HEC-RAS (Version 3.1.3 and earlier) were only set up to read the data as single precision numbers. So, versions 3.1.3 and earlier of HEC-RAS would not correctly read flow data from HEC-DSS if it was created by HEC-HMS version 3.0 and later.

    If you are still using HEC-RAS 3.1.3 or earlier, users can download HEC-DSSVue and a special plug-in that will allow you to convert a double precision HEC-DSS file to a single precision HEC-DSS file. HEC-DSSVue and the plug-in are available from our web page.

12. **Cross Section Interpolation.** A few data sets were sent to us where the cross section interpolation routines were not correctly interpolating geometry and/or other cross section properties. Many of these data sets had cross sections with "Lids", while some were problems with interpolating Manning's n values.

13. **Lateral Structure Stationing.** If a lateral structure did not start at a stationing of zero, it was not always located exactly correct along the cross sections.

14. **Metric Units Output for Hydraulic Radius.** The program was incorrectly reporting the Hydraulic radius to the 2/3 power in the output. This was a conversion from English to metric units error.

15. **Abutment Scour Problem.** On occasion the program would compute a projected abutment/road embankment length that was incorrect. This only came up under rare circumstances, and depended on how the stationing of the cross section just upstream of the bridge, and the approach cross section, were entered.

16. **K2 Factor for Abutment Scour.** This factor was being interpolated from a graph that was presented in an earlier version of the HEC-18 manual. For abutment attack angles that were very mild, the interpolated values were not very good. The latest HEC-18 manual now has an equation. We have changed the code to use this equation.

17. **Pipe Arch Culverts.** For very small pipe arch culverts, the user would enter a Rise and the program was incorrectly calculating the span. This was only for Pipe Arch Culverts with smaller than 18 inch corner radius.

18. **Corrugated Metal Box Culverts.** Many corrugated metal box culverts actually have sloping inward side walls and rounded corners at the top. The slope of these walls and the curvature of the corner radius can vary with manufacturers. HEC-RAS does not account for the sloping wall or the rounded corner radius. User's must come up with an equivalent span and rise in order to match the area correctly. It is suggested to use the correct rise, and adjust the span to get the correct area of the culvert. That way the program will get the transition from low flow to pressure flow at the correct elevation.

19. **Storage Area of a Cross Section for Unsteady Flow.** HEC-RAS was incorrectly calculating the available storage area above a permanent ineffective flow area, when the permanent ineffective area intersects the ground between the first two or last two points of the cross section.

20. **Limit of 500 Hydrograph Output Locations for Unsteady Flow.** The previous version of HEC-RAS had a limit of 500 locations for output hydrographs when performing unsteady flow calculations. The problem was also enhanced by the fact that HEC-RAS automatically computed output hydrographs at specific locations by default. This limit has been done away with. The number of hydrograph locations is now allocatable, and only limited by the memory in your computer.

21. **Restart File for Unsteady Flow Calculations.** There were some problems in reading a Re-Start file for use as initial conditions of an unsteady flow run. These problems have been corrected.

Support Policy

Technical support for program users within the Corps of Engineers is provided through an annual subscription service. Subscribing offices can expect full support from HEC staff in the routine application of the program. Users are strongly urged to consult with HEC staff on the technical feasibility of using the program before beginning a project with unique requirements. Extended

support for large or complex projects can be arranged under a separate reimbursable project agreement.

Support can not be provided to users outside the Corps of Engineers. Domestic and foreign vendors are available that provide fee-for-service support similar to the support provided to subscribing Corps offices. Such service agreements are between the user and the vendor and do not include HEC staff. Vendors do contact HEC on behalf of their users when unusual problems or errors are encountered. A list of vendors can be found at http://www.hec.usace.army.mil .

Reporting of suspected program errors is unrestricted and we will reply to all correspondence concerning such errors. We are continuously working to improve the program and possible bugs should always be reported. Reports should include a written description of the steps that lead to the problem and the effects that result from it. If we cannot reproduce the reported problem, we may ask you to send a copy of your project.

Report program errors through the following channels:

- Go to our web site at www.hec.usace.army.mil then go to the HEC-RAS support page.
- Send email to hec.ras@usace.army.mil on the internet.
- Write to:

  U.S. Army Corps of Engineers

  Hydrologic Engineering Center

  609 Second Street

  Davis, CA 95616 USA.

CHAPTER 1

Introduction

Welcome to the Hydrologic Engineering Center's River Analysis System (HEC-RAS). This software allows you to perform one-dimensional steady and unsteady flow hydraulics. Future versions will support sediment transport calculations.

The current version of HEC-RAS supports one-dimensional, steady and unsteady flow, water surface profile calculations. This manual documents the hydraulic capabilities of the Steady and unsteady flow portion of HEC-RAS. Documentation for sediment transport calculations will be made available as these features are added to the HEC-RAS.

This chapter discusses the general philosophy of HEC-RAS and gives you a brief overview of the hydraulic capabilities of the modeling system. Documentation for HEC-RAS is discussed, as well as an overview of this manual.

Contents

- General Philosophy of the Modeling System
- Overview of Hydraulic Capabilities
- HEC-RAS Documentation
- Overview of This Manual

General Philosophy of the Modeling System

HEC-RAS is an integrated system of software, designed for interactive use in a multi-tasking, multi-user network environment. The system is comprised of a graphical user interface (GUI), separate hydraulic analysis components, data storage and management capabilities, graphics and reporting facilities.

The system will ultimately contain three one-dimensional hydraulic analysis components for: (1) steady flow water surface profile computations; (2) unsteady flow simulation; and (3) movable boundary sediment transport computations. A key element is that all three components will use a common geometric data representation and common geometric and hydraulic computation routines. In addition to the three hydraulic analysis components, the system contains several hydraulic design features that can be invoked once the basic water surface profiles are computed.

The current version of HEC-RAS supports Steady and Unsteady Flow Water Surface Profile calculations. New features and additional capabilities will be added in future releases.

Overview of Hydraulic Capabilities

HEC-RAS is designed to perform one-dimensional hydraulic calculations for a full network of natural and constructed channels. The following is a description of the major hydraulic capabilities of HEC-RAS.

Steady Flow Water Surface Profiles. This component of the modeling system is intended for calculating water surface profiles for steady gradually varied flow. The system can handle a single river reach, a dendritic system, or a full network of channels. The steady flow component is capable of modeling subcritical, supercritical, and mixed flow regime water surface profiles.

The basic computational procedure is based on the solution of the one-dimensional energy equation. Energy losses are evaluated by friction (Manning's equation) and contraction/expansion (coefficient multiplied by the change in velocity head). The momentum equation is utilized in situations where the water surface profile is rapidly varied. These situations include mixed flow regime calculations (i.e., hydraulic jumps), hydraulics of bridges, and evaluating profiles at river confluences (stream junctions).

The effects of various obstructions such as bridges, culverts, weirs, spillways and other structures in the flood plain may be considered in the computations. The steady flow system is designed for application in flood plain management and flood insurance studies to evaluate floodway encroachments. Also, capabilities are available for assessing the change in water surface profiles due to channel improvements, and levees.

Special features of the steady flow component include: multiple plan analyses; multiple profile computations; multiple bridge and/or culvert opening analysis, and split flow optimization at stream junctions and lateral weirs and spillways.

Unsteady Flow Simulation. This component of the HEC-RAS modeling system is capable of simulating one-dimensional unsteady flow through a full network of open channels. The unsteady flow equation solver was adapted from Dr. Robert L. Barkau's UNET model (Barkau, 1992 and HEC, 1997). This unsteady flow component was developed primarily for subcritical flow regime calculations.

The hydraulic calculations for cross-sections, bridges, culverts, and other hydraulic structures that were developed for the steady flow component were incorporated into the unsteady flow module. Additionally, the unsteady flow component has the ability to model storage areas and hydraulic connections between storage areas, as well as between stream reaches.

Sediment Transport/Movable Boundary Computations. This component of the modeling system is intended for the simulation of one-dimensional sediment transport/movable boundary calculations resulting from scour and deposition over moderate time periods (typically years, although applications to single flood events will be possible).

The sediment transport potential is computed by grain size fraction, thereby allowing the simulation of hydraulic sorting and armoring. Major features include the ability to model a full network of streams, channel dredging, various levee and encroachment alternatives, and the use of several different equations for the computation of sediment transport.

The model will be designed to simulate long-term trends of scour and deposition in a stream channel that might result from modifying the frequency and duration of the water discharge and stage, or modifying the channel geometry. This system can be used to evaluate deposition in reservoirs, design channel contractions required to maintain navigation depths, predict the influence of dredging on the rate of deposition, estimate maximum possible scour during large flood events, and evaluate sedimentation in fixed channels.

HEC-RAS Documentation

The HEC-RAS package includes several documents, each are designed to help the modeler learn to use a particular aspect of the modeling system. The documentation has been divided into the following three categories:

Documentation	Description
User's Manual	This manual is a guide to using the HEC-RAS. The manual provides an introduction and overview of the modeling system, installation instructions, how to get started, simple examples, detailed descriptions of each of the major modeling components, and how to view graphical and tabular output.
Hydraulic Reference Manual	This manual describes the theory and data requirements for the hydraulic calculations performed by HEC-RAS. Equations are presented along with the assumptions used in their derivation. Discussions are provided on how to estimate model parameters, as well as guidelines on various modeling approaches.
Applications Guide	This document contains a series of examples that demonstrate various aspects of the HEC-RAS. Each example consists of a problem statement, data requirements, general outline of solution steps, displays of key input and output screens, and discussions of important modeling aspects.

Overview of This Manual

This manual presents the theory and data requirements for hydraulic calculations in the HEC-RAS system. The manual is organized as follows:

- Chapter 2 provides an overview of the hydraulic calculations in HEC-RAS.
- Chapter 3 describes the basic data requirements to perform the various hydraulic analyses available.
- Chapter 4 is an overview of some of the optional hydraulic capabilities of the HEC-RAS software.

- Chapters 5, 6, 7, and 8 provide detailed discussions on modeling bridges; culverts; multiple openings; and inline weirs and gated spillways.
- Chapter 9 describes how to perform floodway encroachment calculations.
- Chapter 10 describes how to use HEC-RAS to compute scour at bridges.
- Chapter 11 describes how to model ice-covered rivers.
- Chapter 12 describes the equations and methodologies for stable channel design within HEC-RAS.
- Appendix A provides a list of all the references for the manual.
- Appendix B is a summary of the research work on "Flow Transitions in Bridge Backwater Analysis."
- Appendix C is a write up on the computational differences between HEC-RAS and HEC-2.
- Appendix D is a write up on the "Computation of the WSPRO Discharge Coefficient and Effective Flow Length."

CHAPTER 2

Theoretical Basis for One-Dimensional Flow Calculations

This chapter describes the methodologies used in performing the one-dimensional flow calculations within HEC-RAS. The basic equations are presented along with discussions of the various terms. Solution schemes for the various equations are described. Discussions are provided as to how the equations should be applied, as well as applicable limitations.

Contents

General

This chapter describes the theoretical basis for one-dimensional water surface profile calculations. Discussions contained in this chapter are limited to steady flow water surface profile calculations and unsteady flow routing. When sediment transport calculations are added to the HEC-RAS system, discussions concerning this topic will be included in this manual.

Steady Flow Water Surface Profiles

HEC-RAS is currently capable of performing one-dimensional water surface profile calculations for steady gradually varied flow in natural or constructed channels. Subcritical, supercritical, and mixed flow regime water surface profiles can be calculated. Topics discussed in this section include: equations for basic profile calculations; cross section subdivision for conveyance calculations; composite Manning's n for the main channel; velocity weighting coefficient alpha; friction loss evaluation; contraction and expansion losses; computational procedure; critical depth determination; applications of the momentum equation; and limitations of the steady flow model.

Equations for Basic Profile Calculations

Water surface profiles are computed from one cross section to the next by solving the Energy equation with an iterative procedure called the standard step method. The Energy equation is written as follows:

$$Y_2 + Z_2 + \frac{\alpha_2 V_2^2}{2g} = Y_1 + Z_1 + \frac{\alpha_1 V_1^2}{2g} + h_e \qquad (2\text{-}1)$$

Where: Y_1, Y_2 = depth of water at cross sections

Z_1, Z_2 = elevation of the main channel inverts

V_1, V_2 = average velocities (total discharge/ total flow area)

α_1, α_2 = velocity weighting coefficients

g = gravitational acceleration

h_e = energy head loss

A diagram showing the terms of the energy equation is shown in Figure 2-1.

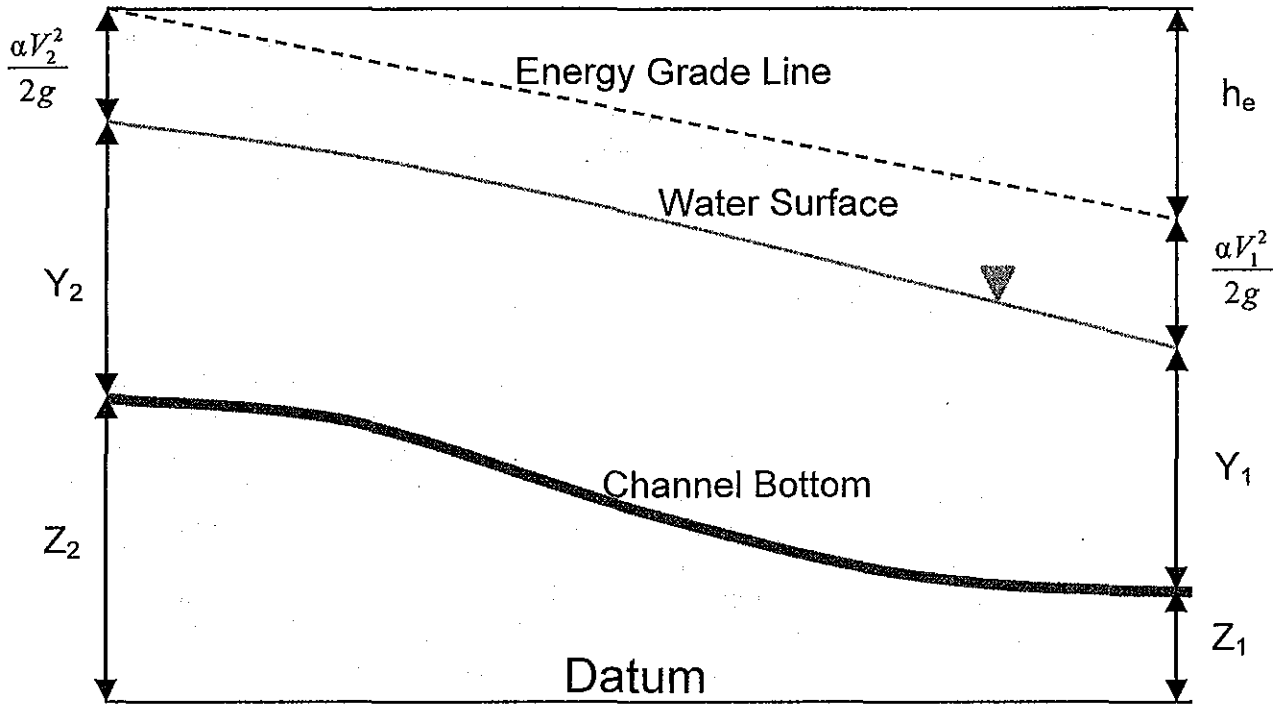

Figure 2.1 Representation of Terms in the Energy Equation

The energy head loss (h_e) between two cross sections is comprised of friction losses and contraction or expansion losses. The equation for the energy head loss is as follows:

$$h_e = L\bar{S}_f + C\left|\frac{\alpha_2 V_2^2}{2g} - \frac{\alpha_1 V_1^2}{2g}\right| \tag{2-2}$$

Where: L = discharge weighted reach length

$\bar{S}_f$ = representative friction slope between two sections

C = expansion or contraction loss coefficient

The distance weighted reach length, L, is calculated as:

$$L = \frac{L_{lob}\,\overline{Q}_{lob} + L_{ch}\,\overline{Q}_{ch} + L_{rob}\,\overline{Q}_{rob}}{\overline{Q}_{lob} + \overline{Q}_{ch} + \overline{Q}_{rob}} \tag{2-3}$$

where: L_{lob}, L_{ch}, L_{rob} = cross section reach lengths specified for flow in the left overbank, main channel, and right overbank, respectively

$\overline{Q}_{lob}, \overline{Q}_{ch}, \overline{Q}_{rob}$ = arithmetic average of the flows between sections for the left overbank, main channel, and right overbank, respectively

Cross Section Subdivision for Conveyance Calculations

The determination of total conveyance and the velocity coefficient for a cross section requires that flow be subdivided into units for which the velocity is uniformly distributed. The approach used in HEC-RAS is to subdivide flow in the **overbank** areas using the input cross section n-value break points (locations where n-values change) as the basis for subdivision (Figure 2-2). Conveyance is calculated within each subdivision from the following form of Manning's equation (based on English units):

$$Q = K S_f^{1/2} \tag{2-4}$$

$$K = \frac{1.486}{n} A R^{2/3} \tag{2-5}$$

where: K = conveyance for subdivision

n = Manning's roughness coefficient for subdivision

A = flow area for subdivision

R = hydraulic radius for subdivision (area / wetted perimeter)

The program sums up all the incremental conveyances in the overbanks to obtain a conveyance for the left overbank and the right overbank. The main channel conveyance is normally computed as a single conveyance element. The total conveyance for the cross section is obtained by summing the three subdivision conveyances (left, channel, and right).

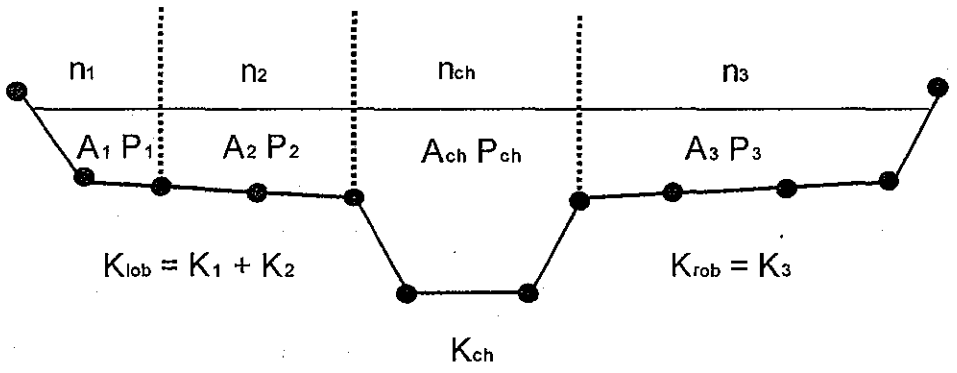

Figure 2.2 HEC-RAS Default Conveyance Subdivision Method

An alternative method available in HEC-RAS is to calculate conveyance between every coordinate point in the overbanks (Figure 2.3). The conveyance is then summed to get the total left overbank and right overbank values. This method is used in the Corps HEC-2 program. The method has been retained as an option within HEC-RAS in order to reproduce studies that were originally developed with HEC-2.

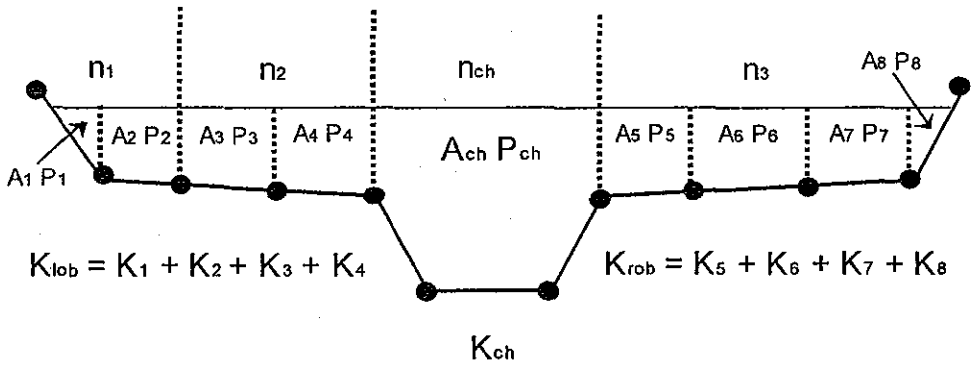

Figure 2.3 Alternative Conveyance Subdivision Method (HEC-2 style)

The two methods for computing conveyance will produce different answers whenever portions on the overbank have ground sections with significant vertical slopes. In general, the HEC-RAS default approach will provide a lower total conveyance for the same water surface elevation.

In order to test the significance of the two ways of computing conveyance, comparisons were performed using 97 data sets from the HEC profile accuracy study (HEC, 1986). Water surface profiles were computed for the 1% chance event using the two methods for computing conveyance in HEC-RAS. The results of the study showed that the HEC-RAS default approach will generally produce a higher computed water surface elevation. Out of the 2048 cross section locations, 47.5% had computed water surface elevations within 0.10 ft. (30.48 mm), 71% within 0.20 ft. (60.96 mm), 94.4% within 0.4 ft. (121.92 mm), 99.4% within 1.0 ft. (304.8 mm), and one cross section had a difference of 2.75 ft. (0.84 m). Because the differences tend to be in the same direction, some effects can be attributed to propagation of downstream differences.

The results from the conveyance comparisons do not show which method is more accurate, they only show differences. In general, it is felt that the HEC-RAS default method is more commensurate with the Manning equation and the concept of separate flow elements. Further research, with observed water surface profiles, will be needed to make any conclusions about the accuracy of the two methods.

Composite Manning's n for the Main Channel

Flow in the **main channel** is not subdivided, except when the roughness coefficient is changed within the channel area. HEC-RAS tests the applicability of subdivision of roughness within the main channel portion of a cross section, and if it is not applicable, the program will compute a single composite n value for the entire main channel. The program determines if the main channel portion of the cross section can be subdivided or if a composite main channel n value will be utilized based on the following criterion: if a main channel side slope is steeper than 5H:1V and the main channel has more than one n-value, a composite roughness n_c will be computed [Equation 6-17, Chow, 1959]. The channel side slope used by HEC-RAS is defined as the horizontal distance between adjacent n-value stations within the main channel over the difference in elevation of these two stations (see S_L and S_R of Figure 2.4).

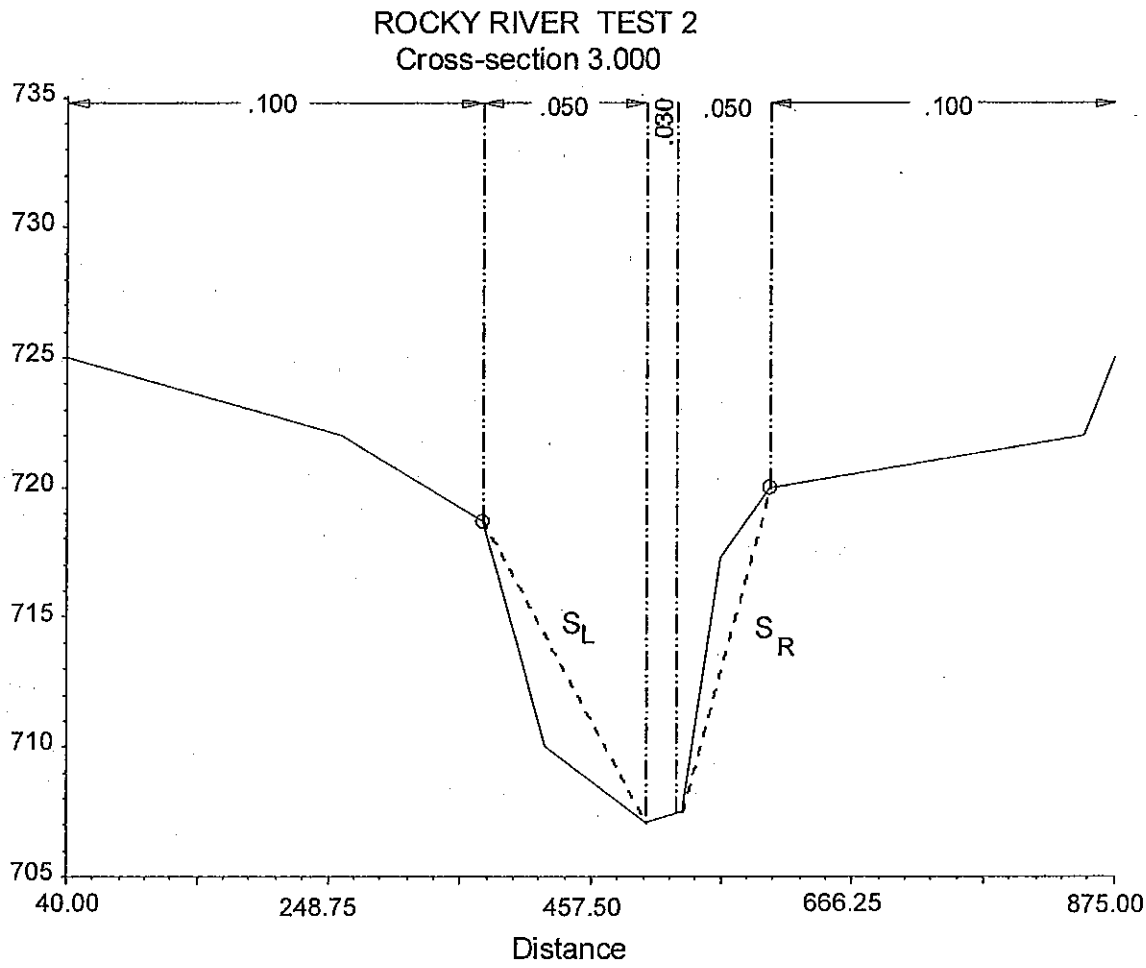

Figure 2.4 Definition of Bank Slope for Composite n_c Calculation

For the determination of n_c, the main channel is divided into N parts, each with a known wetted perimeter P_i and roughness coefficient n_i.

$$n_c = \left[\frac{\sum_{i=1}^{N} \left(P_i \, n_i^{1.5} \right)}{P} \right]^{2/3} \tag{2-6}$$

where: n_c = composite or equivalent coefficient of roughness

P = wetted perimeter of entire main channel

P_i = wetted perimeter of subdivision I

n_i = coefficient of roughness for subdivision I

The computed composite n_c should be checked for reasonableness. The computed value is the composite main channel n value in the output and summary tables.

Evaluation of the Mean Kinetic Energy Head

Because the HEC-RAS software is a one-dimensional water surface profiles program, only a single water surface and therefore a single mean energy are computed at each cross section. For a given water surface elevation, the mean energy is obtained by computing a flow weighted energy from the three subsections of a cross section (left overbank, main channel, and right overbank). Figure 2.5 below shows how the mean energy would be obtained for a cross section with a main channel and a right overbank (no left overbank area).

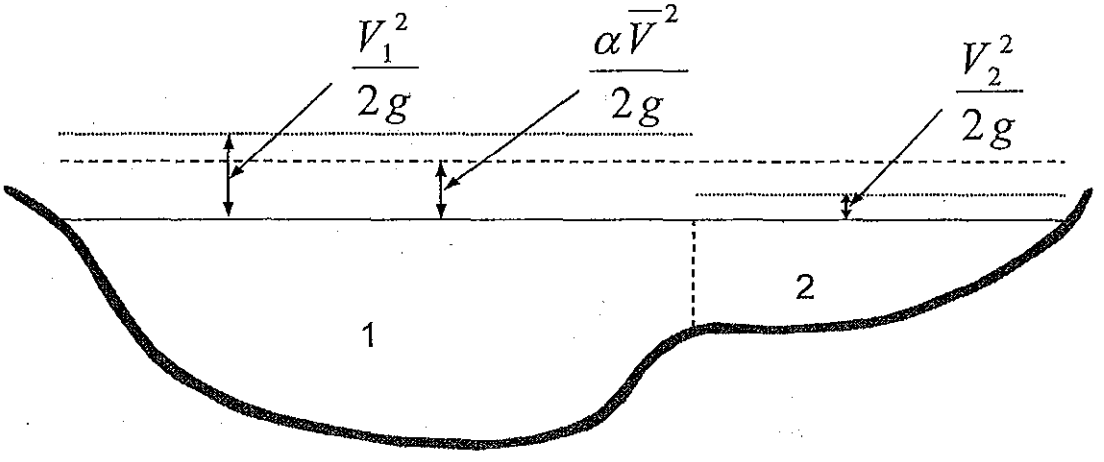

V_1 = mean velocity for subarea 1

V_2 = mean velocity for subarea 2

Figure 2.5 Example of How Mean Energy is Obtained

To compute the mean kinetic energy it is necessary to obtain the velocity head weighting coefficient alpha. Alpha is calculated as follows:

Mean Kinetic Energy Head = Discharge-Weighted Velocity Head

$$\alpha \frac{\overline{V}^2}{2g} = \frac{Q_1 \frac{V_1^2}{2g} + Q_2 \frac{V_2^2}{2g}}{Q_1 + Q_2} \qquad (2\text{-}7)$$

$$\alpha = \frac{2g\left[Q_1\frac{V_1^2}{2g} + Q_2\frac{V_2^2}{2g}\right]}{(Q_1+Q_2)\overline{V}^2} \tag{2-8}$$

$$\alpha = \frac{Q_1V_1^2 + Q_2V_2^2}{(Q_1+Q_2)\overline{V}^2} \tag{2-9}$$

In General:

$$\alpha = \frac{\left[Q_1V_1^2 + Q_2V_2^2 + \ldots + Q_NV_N^2\right]}{Q\overline{V}^2} \tag{2-10}$$

The velocity coefficient, α, is computed based on the conveyance in the three flow elements: left overbank, right overbank, and channel. It can also be written in terms of conveyance and area as in the following equation:

$$\alpha = \frac{(A_t)^2\left[\frac{K_{lob}^3}{A_{lob}^2} + \frac{K_{ch}^3}{A_{ch}^2} + \frac{K_{rob}^3}{A_{rob}^2}\right]}{K_t^3} \tag{2-11}$$

Where: A_t = total flow area of cross section

A_{lob}, A_{ch}, A_{rob} = flow areas of left overbank, main channel and right overbank, respectively

K_t = total conveyance of cross section

K_{lob}, K_{ch}, K_{rob} = conveyances of left overbank, main channel and right overbank, respectively

Friction Loss Evaluation

Friction loss is evaluated in HEC-RAS as the product of $\overline{S}_f$ and L (Equation 2-2), where $\overline{S}_f$ is the representative friction slope for a reach and L is defined by Equation 2-3. The friction slope (slope of the energy gradeline) at each cross section is computed from Manning's equation as follows:

$$S_f = \left(\frac{Q}{K}\right)^2 \tag{2-12}$$

Alternative expressions for the representative reach friction slope (S_f) in HEC-RAS are as follows:

Average Conveyance Equation

$$\overline{S}_f = \left(\frac{Q_1 + Q_2}{K_1 + K_2}\right)^2 \tag{2-13}$$

Average Friction Slope Equation

$$\overline{S}_f = \frac{S_{f1} + S_{f2}}{2} \tag{2-14}$$

Geometric Mean Friction Slope Equation

$$\overline{S}_f = \sqrt{S_{f1} \times S_{f2}} \tag{2-15}$$

Harmonic Mean Friction Slope Equation

$$\overline{S}_f = \frac{2\left(S_{f1} \times S_{f2}\right)}{S_{f1} + S_{f2}} \tag{2-16}$$

Equation 2-13 is the "default" equation used by the program; that is, it is used automatically unless a different equation is requested by input. The program also contains an option to select equations, depending on flow regime and profile type (e.g., S1, M1, etc.). Further discussion of the alternative methods for evaluating friction loss is contained in Chapter 4, "Overview of Optional Capabilities."

Contraction and Expansion Loss Evaluation

Contraction and expansion losses in HEC-RAS are evaluated by the following equation:

$$h_{ce} = C\left|\frac{\alpha_1 V_1^2}{2g} - \frac{\alpha_2 V_2^2}{2g}\right| \qquad (2\text{-}17)$$

Where: C = the contraction or expansion coefficient

The program assumes that a contraction is occurring whenever the velocity head downstream is greater than the velocity head upstream. Likewise, when the velocity head upstream is greater than the velocity head downstream, the program assumes that a flow expansion is occurring. Typical "C" values can be found in Chapter 3, "Basic Data Requirements."

Computation Procedure

The unknown water surface elevation at a cross section is determined by an iterative solution of Equations 2-1 and 2-2. The computational procedure is as follows:

1. Assume a water surface elevation at the upstream cross section (or downstream cross section if a supercritical profile is being calculated).

2. Based on the assumed water surface elevation, determine the corresponding total conveyance and velocity head.

3. With values from step 2, compute $\overline{S}_f$ and solve Equation 2-2 for h_e.

4. With values from steps 2 and 3, solve Equation 2-1 for WS_2.

5. Compare the computed value of WS_2 with the value assumed in step 1; repeat steps 1 through 5 until the values agree to within .01 feet (.003 m), or the user-defined tolerance.

The criterion used to assume water surface elevations in the iterative procedure varies from trial to trial. The first trial water surface is based on projecting the previous cross section's water depth onto the current cross section. The second trial water surface elevation is set to the assumed water surface elevation plus 70% of the error from the first trial (computed W.S. - assumed W.S.). In other words, W.S. new = W.S. assumed + 0.70 * (W.S. computed - W.S. assumed). The third and subsequent trials are generally based on a "Secant" method of projecting the rate of change of the difference between computed and assumed elevations for the previous two trials. The equation for the secant method is as follows:

$$WS_I = WS_{I-2} - Err_{I-2} * Err\_Assum / Err\_Diff \qquad (2\text{-}18)$$

Where: WS_I = the new assumed water surface

WS_{I-1} = the previous iteration's assumed water surface

WS_{I-2} = the assumed water surface from two trials previous

Err_{I-2} = the error from two trials previous (computed water surface minus assumed from the I-2 iteration)

Err_Assum = the difference in assumed water surfaces from the previous two trials. Err_Assum = WS_{I-2} - WS_{I-1}

Err_Diff = the assumed water surface minus the calculated water surface from the previous iteration (I-1), plus the error from two trials previous (Err_{I-2}). Err_Diff = WS_{I-1} - WS_Calc_{I-1} + Err_{I-2}

The change from one trial to the next is constrained to a maximum of 50 percent of the assumed depth from the previous trial. On occasion the secant method can fail if the value of Err_Diff becomes too small. If the Err_Diff is less than 1.0E-2, then the secant method is not used. When this occurs, the program computes a new guess by taking the average of the assumed and computed water surfaces from the previous iteration.

The program is constrained by a *maximum number of iterations* (the default is 20) for balancing the water surface. While the program is iterating, it keeps track of the water surface that produces the minimum amount of error between the assumed and computed values. This water surface is called the *minimum error water surface*. If the maximum number of iterations is reached before a balanced water surface is achieved, the program will then calculate critical depth (if this has not already been done). The program then checks to see if the error associated with the *minimum error water surface* is within a predefined tolerance (the default is 0.3 ft or 0.1 m). If the minimum error water surface has an associated error less than the predefined tolerance, and this water surface is on the correct side of critical depth, then the program will use this water surface as the final answer and set a warning message that it has done so. If the minimum error water surface has an associated error that is greater than the predefined tolerance, or it is on the wrong side of critical depth, the program will use critical depth as the final answer for the cross section and set a warning message that it has done so. The rationale for using the minimum error water surface is that it is probably a better answer than critical depth, as long as the above criteria are met. Both the minimum error water surface and critical depth are only used in this situation to allow the program to continue the solution of the water surface profile. Neither of these two answers are considered to be valid solutions, and therefore warning messages are issued when either is used. In general, when the program cannot balance the energy equation at a cross section, it is usually caused by an inadequate number of cross sections (cross sections spaced too far apart) or bad cross section data. Occasionally, this can occur because the program is

attempting to calculate a subcritical water surface when the flow regime is actually supercritical.

When a "balanced" water surface elevation has been obtained for a cross section, checks are made to ascertain that the elevation is on the "right" side of the critical water surface elevation (e.g., above the critical elevation if a subcritical profile has been requested by the user). If the balanced elevation is on the "wrong" side of the critical water surface elevation, critical depth is assumed for the cross section and a "warning" message to that effect is displayed by the program. The program user should be aware of critical depth assumptions and determine the reasons for their occurrence, because in many cases they result from reach lengths being too long or from misrepresentation of the effective flow areas of cross sections.

For a subcritical profile, a preliminary check for proper flow regime involves checking the Froude number. The program calculates the Froude number of the "balanced" water surface for both the main channel only and the entire cross section. If either of these two Froude numbers are greater than 0.94, then the program will check the flow regime by calculating a more accurate estimate of critical depth using the minimum specific energy method (this method is described in the next section). A Froude number of 0.94 is used instead of 1.0, because the calculation of Froude number in irregular channels is not accurate. Therefore, using a value of 0.94 is conservative, in that the program will calculate critical depth more often than it may need to.

For a supercritical profile, critical depth is automatically calculated for every cross section, which enables a direct comparison between balanced and critical elevations.

Critical Depth Determination

Critical depth for a cross section will be determined if any of the following conditions are satisfied:

(1) The supercritical flow regime has been specified.

(2) The calculation of critical depth has been requested by the user.

(3) This is an external boundary cross section and critical depth must be determined to ensure the user entered boundary condition is in the correct flow regime.

(4) The Froude number check for a subcritical profile indicates that critical depth needs to be determined to verify the flow regime associated with the balanced elevation.

(5) The program could not balance the energy equation within the

specified tolerance before reaching the maximum number of iterations.

The total energy head for a cross section is defined by:

$$H = WS + \frac{\alpha V^2}{2g} \tag{2-19}$$

where: H = total energy head

WS = water surface elevation

$\frac{\alpha V^2}{2g}$ = velocity head

The critical water surface elevation is the elevation for which the total energy head is a minimum (i.e., minimum specific energy for that cross section for the given flow). The critical elevation is determined with an iterative procedure whereby values of WS are assumed and corresponding values of H are determined with Equation 2-19 until a minimum value for H is reached.

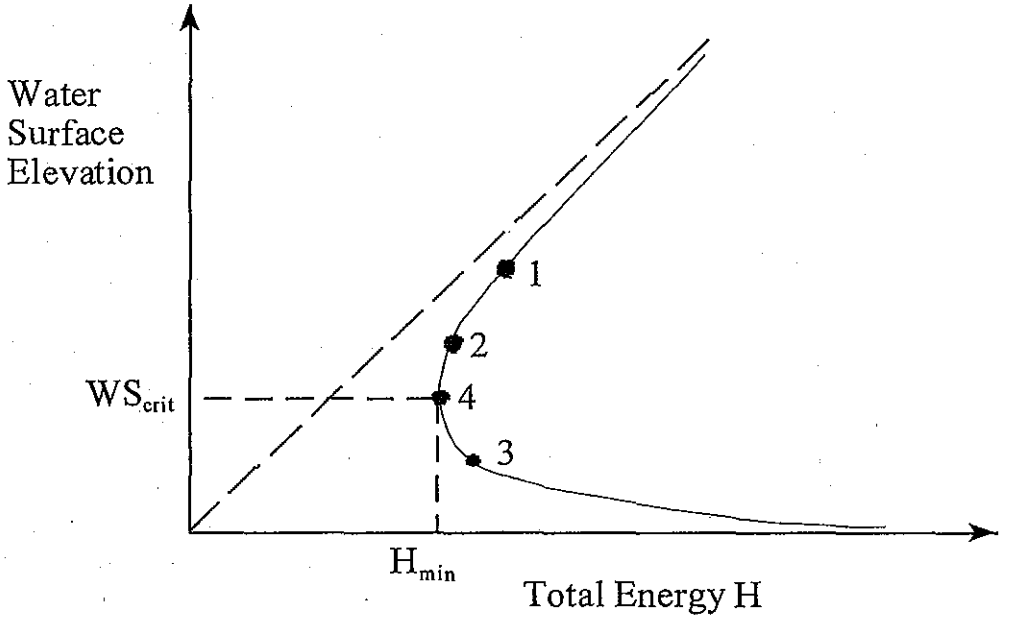

Figure 2.6 Energy vs. Water Surface Elevation Diagram

The HEC-RAS program has two methods for calculating critical depth: a "parabolic" method and a "secant" method. The parabolic method is computationally faster, but it is only able to locate a single minimum energy. For most cross sections there will only be one minimum on the total energy curve, therefore the parabolic method has been set as the default method (the default method can be changed from the user interface). If the parabolic

method is tried and it does not converge, then the program will automatically try the secant method.

In certain situations it is possible to have more than one minimum on the total energy curve. Multiple minimums are often associated with cross sections that have breaks in the total energy curve. These breaks can occur due to very wide and flat overbanks, as well as cross sections with levees and ineffective flow areas. When the parabolic method is used on a cross section that has multiple minimums on the total energy curve, the method will converge on the first minimum that it locates. This approach can lead to incorrect estimates of critical depth. If the user thinks that the program has incorrectly located critical depth, then the secant method should be selected and the model should be re-simulated.

The "parabolic" method involves determining values of H for three values of WS that are spaced at equal ΔWS intervals. The WS corresponding to the minimum value for H, defined by a parabola passing through the three points on the H versus WS plane, is used as the basis for the next assumption of a value for WS. It is presumed that critical depth has been obtained when there is less than a 0.01 ft. (0.003 m) change in water depth from one iteration to the next and provided the energy head has not either decreased or increased by more than .01 feet (0.003 m).

The "secant" method first creates a table of water surface versus energy by slicing the cross section into 30 intervals. If the maximum height of the cross section (highest point to lowest point) is less than 1.5 times the maximum height of the main channel (from the highest main channel bank station to the invert), then the program slices the entire cross section into 30 equal intervals. If this is not the case, the program uses 25 equal intervals from the invert to the highest main channel bank station, and then 5 equal intervals from the main channel to the top of the cross section. The program then searches this table for the location of local minimums. When a point in the table is encountered such that the energy for the water surface immediately above and immediately below are greater than the energy for the given water surface, then the general location of a local minimum has been found. The program will then search for the local minimum by using the secant slope projection method. The program will iterate for the local minimum either thirty times or until the critical depth has been bounded by the critical error tolerance. After the local minimum has been determined more precisely, the program will continue searching the table to see if there are any other local minimums. The program can locate up to three local minimums in the energy curve. If more than one local minimum is found, the program sets critical depth equal to the one with the minimum energy. If this local minimum is due to a break in the energy curve caused by overtopping a levee or an ineffective flow area, then the program will select the next lowest minimum on the energy curve. If all of the local minimums are occurring at breaks in the energy curve (caused by levees and ineffective flow areas), then the program will set critical depth to the one with the lowest energy. If no local minimums are found, then the program will use the water surface elevation with the least energy. If the

critical depth that is found is at the top of the cross section, then this is probably not a real critical depth. Therefore, the program will double the height of the cross section and try again. Doubling the height of the cross section is accomplished by extending vertical walls at the first and last points of the section. The height of the cross section can be doubled five times before the program will quit searching.

Applications of the Momentum Equation

Whenever the water surface passes through critical depth, the energy equation is not considered to be applicable. The energy equation is only applicable to gradually varied flow situations, and the transition from subcritical to supercritical or supercritical to subcritical is a rapidly varying flow situation. There are several instances when the transition from subcritical to supercritical and supercritical to subcritical flow can occur. These include significant changes in channel slope, bridge constrictions, drop structures and weirs, and stream junctions. In some of these instances empirical equations can be used (such as at drop structures and weirs), while at others it is necessary to apply the momentum equation in order to obtain an answer.

Within HEC-RAS, the momentum equation can be applied for the following specific problems: the occurrence of a hydraulic jump; low flow hydraulics at bridges; and stream junctions. In order to understand how the momentum equation is being used to solve each of the three problems, a derivation of the momentum equation is shown here. The application of the momentum equation to hydraulic jumps and stream junctions is discussed in detail in Chapter 4. Detailed discussions on applying the momentum equation to bridges is discussed in Chapter 5.

The momentum equation is derived from Newton's second law of motion:

Force = Mass x Acceleration (change in momentum)

$$\sum F_x = m a \tag{2-20}$$

Applying Newton's second law of motion to a body of water enclosed by two cross sections at locations 1 and 2 (Figure 2.7), the following expression for the change in momentum over a unit time can be written:

$$P_2 - P_1 + W_x - F_f = Q \rho \Delta V_x \tag{2-21}$$

Where: P = Hydrostatic pressure force at locations 1 and 2.
W_x = Force due to the weight of water in the X direction.
F_f = Force due to external friction losses from 2 to 1.
Q = Discharge.
ρ = Density of water
ΔV_x = Change in velocity from 2 to 1, in the X direction.

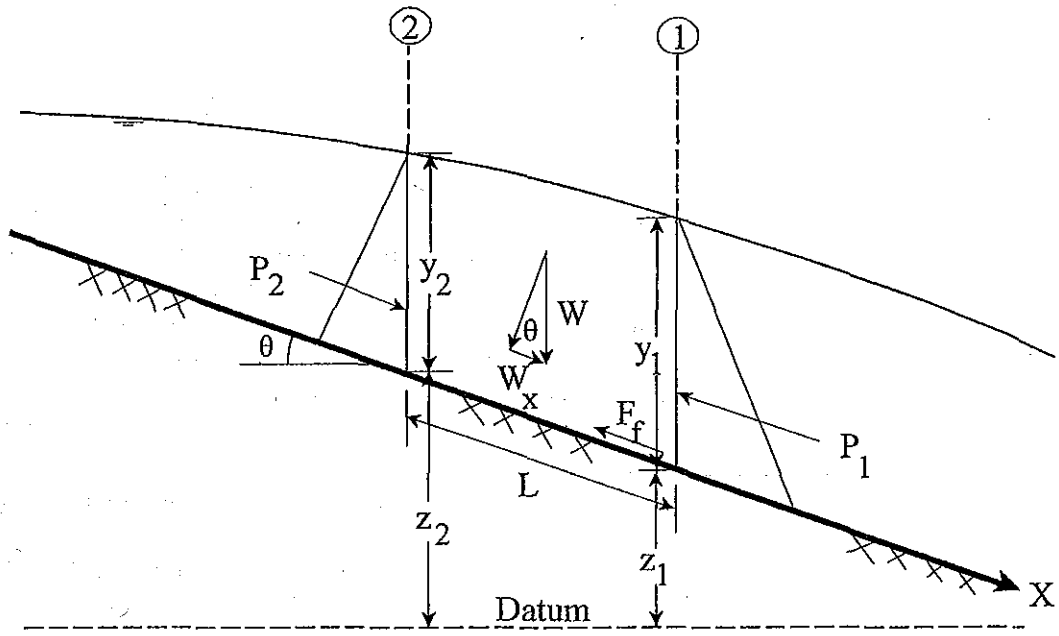

Figure 2.7 Application of the Momentum Principle

Hydrostatic Pressure Forces:

The force in the X direction due to hydrostatic pressure is:

$$P = \gamma A \overline{Y} \cos\theta \tag{2-22}$$

The assumption of a hydrostatic pressure distribution is only valid for slopes less than 1:10. The cos θ for a slope of 1:10 (approximately 6 degrees) is equal to 0.995. Because the slope of ordinary channels is far less than 1:10, the cos θ correction for depth can be set equal to 1.0 (Chow, 1959). Therefore, the equations for the hydrostatic pressure force at sections 1 and 2 are as follows:

$$P_1 = \gamma A_1 \overline{Y}_1 \tag{2-23}$$

$$P_2 = \gamma A_2 \overline{Y}_2 \tag{2-24}$$

Where: γ = Unit weight of water
A_i = Wetted area of the cross section at locations 1 and 2
$\overline{Y}_i$ = Depth measured from the water surface to the centroid of the cross sectional area at locations 1 and 2

Weight of Water Force:

Weight of water = (unit weight of water) x (volume of water)

$$W = \gamma\left(\frac{A_1 + A_2}{2}\right)L \tag{2-25}$$

$$W_x = W \times \sin\theta \tag{2-26}$$

$$\sin\theta = \frac{z_2 - z_1}{L} = S_0 \tag{2-27}$$

$$W_x = \gamma\left(\frac{A_1 + A_2}{2}\right)L S_0 \tag{2-28}$$

Where: L = Distance between sections 1 and 2 along the X axis
S_o = Slope of the channel, based on mean bed elevations
z_i = Mean bed elevation at locations 1 and 2

Force of External Friction:

$$F_f = \tau \overline{P} L \tag{2-29}$$

Where: τ = Shear stress
$\overline{P}$ = Average wetted perimeter between sections 1 and 2

$$\tau = \gamma \overline{R} \overline{S}_f \tag{2-30}$$

Where: $\overline{R}$ = Average hydraulic radius (R = A/P)
$\overline{S}_f$ = Slope of the energy grade line (friction slope)

$$F_f = \gamma \frac{\overline{A}}{\overline{P}} \overline{S}_f \overline{P} L \tag{2-31}$$

$$F_f = \gamma \left(\frac{A_1 + A_2}{2} \right) \overline{S}_f L \tag{2-32}$$

Mass times Acceleration:

$$ma = Q \rho \Delta V_x \tag{2-33}$$

$$\rho = \frac{\gamma}{g} \quad and \quad \Delta V_x = (\beta_1 V_1 - \beta_2 V_2)$$

$$ma = \frac{Q\gamma}{g} (\beta_1 V_1 - \beta_2 V_2) \tag{2-34}$$

Where: β = momentum coefficient that accounts for a varying velocity distribution in irregular channels

Substituting Back into Equation 2-21, and assuming Q can vary from 2 to 1:

$$\gamma A_2 \overline{Y}_2 - \gamma A_1 \overline{Y}_1 + \gamma\left(\frac{A_1 + A_2}{2}\right) L S_0 - \gamma\left(\frac{A_1 + A_2}{2}\right) L \overline{S}_f = \frac{Q_1 \gamma}{g} \beta_1 V_1 - \frac{Q_2 \gamma}{g} \beta_2 V_2 \qquad (2\text{-}35)$$

$$\frac{Q_2 \beta_2 V_2}{g} + A_2 \overline{Y}_2 + \left(\frac{A_1 + A_2}{2}\right) L S_0 - \left(\frac{A_1 + A_2}{2}\right) L \overline{S}_f = \frac{Q_1 \beta_1 V_1}{g} + A_1 \overline{Y}_1 \qquad (2\text{-}36)$$

$$\frac{Q_2 \beta_2}{g A_2} + A_2 \overline{Y}_2 + \left(\frac{A_1 + A_2}{2}\right) L S_0 - \left(\frac{A_1 + A_2}{2}\right) L \overline{S}_f = \frac{Q_1 \beta_1}{g A_1} + A_1 \overline{Y}_1 \qquad (2\text{-}37)$$

Equation 2-37 is the functional form of the momentum equation that is used in HEC-RAS. All applications of the momentum equation within HEC-RAS are derived from equation 2-37.

Air Entrainment in High Velocity Streams

For channels that have high flow velocity, the water surface may be slightly higher than otherwise expected due to the entrainment of air. While air entrainment is not important for most rivers, it can be significant for highly supercritical flows (Froude numbers greater than 1.6). HEC-RAS now takes this into account with the following two equations (EM 1110-2-1601, plate B-50):

For Froude numbers less than or equal to 8.2,

$$D_a = 0.906\, D(e)^{0.061F} \qquad (2\text{-}38)$$

For Froude numbers greater than 8.2,

$$D_a = 0.620\, D(e)^{0.1051F} \qquad (2\text{-}39)$$

Where: Da = water depth with air entrainment
D = water depth without air entrainment
e = numerical constant, equal to 2.718282
F = Froude number

A water surface with air entrainment is computed and displayed separately in the HEC-RAS tabular output. In order to display the water surface with air entrainment, the user must create their own profile table and include the variable "WS Air Entr." within that table. This variable is not automatically displayed in any of the standard HEC-RAS tables.

Steady Flow Program Limitations

The following assumptions are implicit in the analytical expressions used in the current version of the program:

(1) Flow is steady.

(2) Flow is gradually varied. (Except at hydraulic structures such as: bridges; culverts; and weirs. At these locations, where the flow can be rapidly varied, the momentum equation or other empirical equations are used.)

(3) Flow is one dimensional (i.e., velocity components in directions other than the direction of flow are not accounted for).

(4) River channels have "small" slopes, say less than 1:10.

Flow is assumed to be steady because time-dependent terms are not included in the energy equation (Equation 2-1). Flow is assumed to be gradually varied because Equation 2-1 is based on the premise that a hydrostatic pressure distribution exists at each cross section. At locations where the flow is rapidly varied, the program switches to the momentum equation or other empirical equations. Flow is assumed to be one-dimensional because Equation 2-19 is based on the premise that the total energy head is the same for all points in a cross section. Small channel slopes are assumed because the pressure head, which is a component of Y in Equation 2-1, is represented by the water depth measured vertically.

The program does not currently have the capability to deal with movable boundaries (i.e., sediment transport) and requires that energy losses be definable with the terms contained in Equation 2-2.

Unsteady Flow Routing

The physical laws which govern the flow of water in a stream are: (1) the principle of conservation of mass (continuity), and (2) the principle of conservation of momentum. These laws are expressed mathematically in the form of partial differential equations, which will hereafter be referred to as the continuity and momentum equations. The derivations of these equations are presented in this chapter based on a paper by James A. Liggett from the book "Unsteady Flow in Open Channels" (Mahmmod and Yevjevich, 1975).

Continuity Equation

Consider the elementary control volume shown in Figure 2.8. In this figure, distance x is measured along the channel, as shown. At the midpoint of the control volume the flow and total flow area are denoted $Q(x,t)$ and A_T, respectively. The total flow area is the sum of active area A and off-channel storage area S.

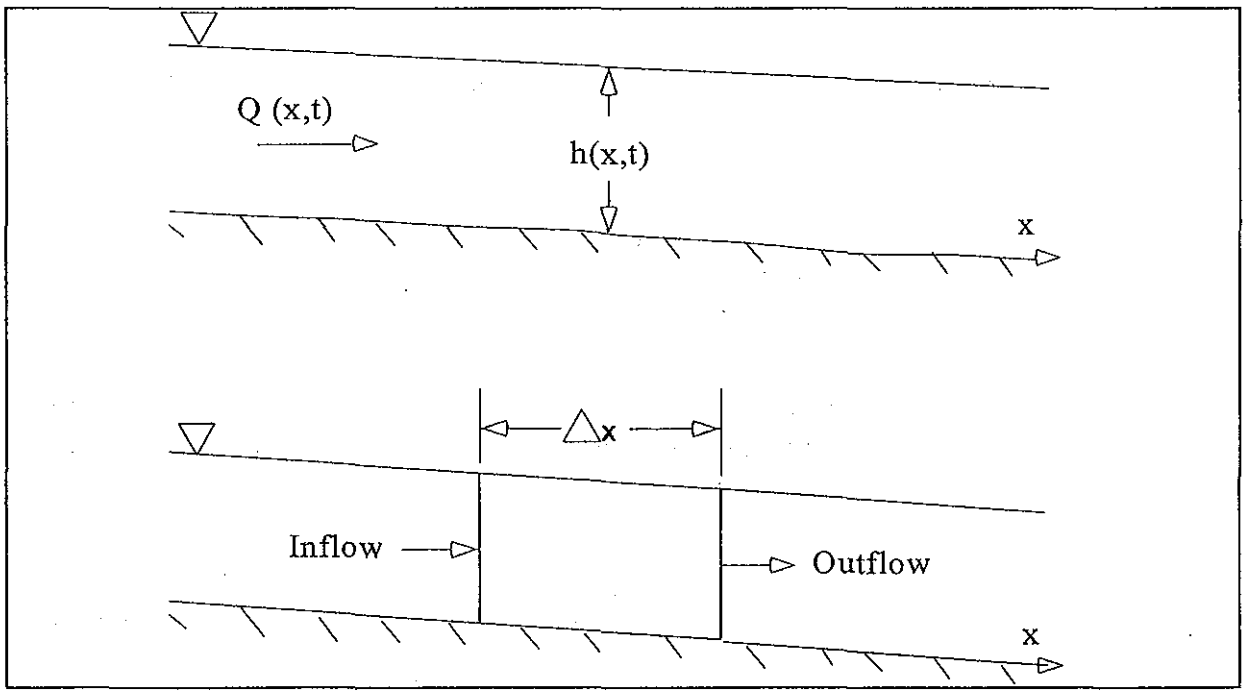

Figure 2.8 Elementary Control Volume for Derivation of Continuity and Momentum Equations.

Conservation of mass for a control volume states that *the net rate of flow into the volume be equal to the rate of change of storage inside the volume*. The rate of inflow to the control volume may be written as:

$$Q - \frac{\partial Q}{\partial x}\frac{\Delta x}{2} \tag{2-40}$$

the rate of outflow as:

$$Q + \frac{\partial Q}{\partial x}\frac{\Delta x}{2} \tag{2-41}$$

and the rate of change in storage as:

$$\frac{\partial A_T}{\partial t}\Delta x \tag{2-42}$$

Assuming that Δx is small, the change in mass in the control volume is equal to:

$$\rho\frac{\partial A_T}{\partial t}\Delta x = \rho\left[\left(Q - \frac{\partial Q}{\partial x}\frac{\Delta x}{2}\right) - \left(Q + \frac{\partial Q}{\partial x}\frac{\Delta x}{2}\right) + Q_l\right] \tag{2-43}$$

where Q_l is the lateral flow entering the control volume and ρ is the fluid density. Simplifying and dividing through by $\rho\Delta x$ yields the final form of the continuity equation:

$$\frac{\partial A_T}{\partial t} + \frac{\partial Q}{\partial x} - q_l = 0 \tag{2-44}$$

in which q_l is the lateral inflow per unit length.

Momentum Equation

Conservation of momentum is expressed by Newton's second law as:

$$\sum F_x = \frac{d\bar{M}}{dt} \tag{2-45}$$

Conservation of momentum for a control volume states that *the net rate of momentum entering the volume* (momentum flux) *plus the sum of all external forces acting on the volume be equal to the rate of accumulation of momentum.* This is a vector equation applied in the x-direction. The momentum flux (MV) is the fluid mass times the velocity vector in the direction of flow. Three forces will be considered: (1) pressure, (2) gravity and (3) boundary drag, or friction force.

Pressure forces: Figure 2.9 illustrates the general case of an irregular cross section. The pressure distribution is assumed to be hydrostatic (pressure varies linearly with depth) and the total pressure force is the integral of the pressure-area product over the cross section. After Shames (1962), the pressure force at any point may be written as:

$$F_P = \int_0^h \rho g (h - y) T(y) \, dy \tag{2-46}$$

where h is the depth, y the distance above the channel invert, and $T(y)$ a width function which relates the cross section width to the distance above the channel invert.

If F_P is the pressure force in the x-direction at the midpoint of the control volume, the force at the upstream end of the control volume may be written as:

$$F_P - \frac{\partial F_P}{\partial x} \frac{\Delta x}{2} \tag{2-47}$$

and at the downstream end as:

$$F_P + \frac{\partial F_P}{\partial x} \frac{\Delta x}{2} \tag{2-48}$$

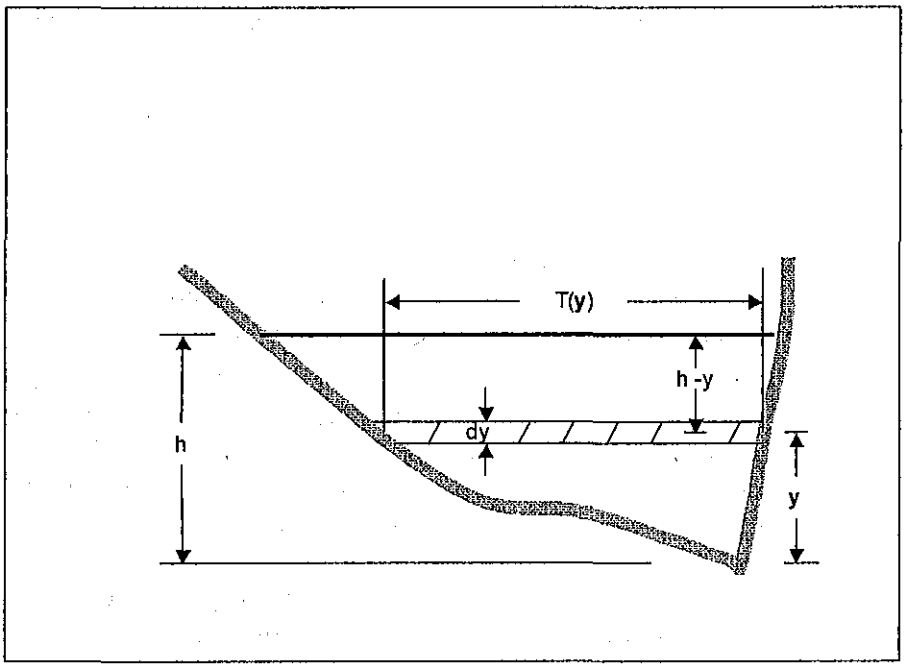

Figure 2.9 Illustration of Terms Associated with Definition of Pressure Force.

The sum of the pressure forces for the control volume may therefore be written as:

$$F_{Pn} = \left| F_P - \frac{\partial F_P}{\partial x}\frac{\Delta x}{2} \right| - \left| F_P + \frac{\partial F_P}{\partial x}\frac{\Delta x}{2} \right| + F_B \qquad (2\text{-}49)$$

where F_{Pn} is the net pressure force for the control volume, and F_B is the force exerted by the banks in the x-direction on the fluid. This may be simplified to:

$$F_{Pn} = -\frac{\partial F_P}{\partial x}\Delta x + F_B \qquad (2\text{-}50)$$

Differentiating equation 2-46 using Leibnitz's Rule and then substituting in equation 2-50 results in:

$$F_{Pn} = -\rho g \Delta x \left[\frac{\partial h}{\partial x} \int_0^h T(y)dy + \int_0^h (h-y) \frac{\partial T(y)}{\partial x} dy \right] + F_B \qquad (2\text{-}51)$$

The first integral in equation 2-51 is the cross-sectional area, A. The second integral (multiplied by $-\rho g \Delta x$) is the pressure force exerted by the fluid on the banks, which is exactly equal in magnitude, but opposite in direction to F_B. Hence the net pressure force may be written as:

$$F_{Pn} = -\rho g A \frac{\partial h}{\partial x} \Delta x \qquad (2\text{-}52)$$

Gravitational force: The force due to gravity on the fluid in the control volume in the x-direction is:

$$F_g = \rho g A \sin\theta \, \Delta x \qquad (2\text{-}53)$$

here θ is the angle that the channel invert makes with the horizontal. For natural rivers θ is small and $\sin\theta \approx \tan\theta = -\partial Z_0 / \partial X$, where z_0 is the invert elevation. Therefore the gravitational force may be written as:

$$F_g = -\rho g A \frac{\partial z_0}{\partial x} \Delta x \qquad (2\text{-}54)$$

This force will be positive for negative bed slopes.

Boundary drag (friction force): Frictional forces between the channel and the fluid may be written as:

$$F_f = -\tau_0 P \Delta x \qquad (2\text{-}55)$$

where τ_o is the average boundary shear stress (force/unit area) acting on the fluid boundaries, and P is the wetted perimeter. The negative sign indicates that, with flow in the positive x-direction, the force acts in the negative x-direction. From dimensional analysis, τ_o may be expressed in terms of a drag coefficient, C_D, as follows:

$$\tau_0 = \rho C_D V^2 \qquad (2\text{-}56)$$

The drag coefficient may be related to the Chezy coefficient, C, by the following:

$$C_D = \frac{g}{C^2} \tag{2-57}$$

Further, the Chezy equation may be written as:

$$V = C\sqrt{RS_f} \tag{2-58}$$

Substituting equations 2-56, 2-57, and 2-58 into 2-55, and simplifying, yields the following expression for the boundary drag force:

$$F_f = -\rho g A S_f \Delta x \tag{2-59}$$

where S_f is the friction slope, which is positive for flow in the positive x-direction. The friction slope must be related to flow and stage. Traditionally, the Manning and Chezy friction equations have been used. Since the Manning equation is predominantly used in the United States, it is also used in HEC-RAS. The Manning equation is written as:

$$S_f = \frac{Q|Q|n^2}{2.208R^{4/3}A^2} \tag{2-60}$$

where R is the hydraulic radius and n is the Manning friction coefficient.

Momentum flux: With the three force terms defined, only the momentum flux remains. The flux entering the control volume may be written as:

$$\rho\left[QV - \frac{\partial QV}{\partial x}\frac{\Delta x}{2}\right] \tag{2-61}$$

and the flux leaving the volume may be written as:

$$\rho\left[QV + \frac{\partial QV}{\partial x}\frac{\Delta x}{2}\right] \tag{2-62}$$

Therefore the net rate of momentum (momentum flux) entering the control volume is:

$$-\rho\frac{\partial QV}{\partial x}\Delta x \tag{2-63}$$

Since the momentum of the fluid in the control volume is $\rho Q\Delta x$, the rate of accumulation of momentum may be written as:

$$\frac{\partial}{\partial t}(\rho Q\Delta x) = \rho\Delta x\frac{\partial Q}{\partial t} \tag{2-64}$$

Restating the principle of conservation of momentum:

The net rate of momentum (momentum flux) *entering the volume* (2-63) *plus the sum of all external forces acting on the volume* [(2-52) + (2-54) + (2-59)] *is equal to the rate of accumulation of momentum* (2-64). Hence:

$$\rho\Delta x\frac{\partial Q}{\partial t} = -\rho\frac{\partial QV}{\partial x}\Delta x - \rho gA\frac{\partial h}{\partial x}\Delta x - \rho gA\frac{\partial z_0}{\partial x}\Delta x - \rho gAS_f\Delta x \tag{2-65}$$

The elevation of the water surface, z, is equal to $z_0 + h$. Therefore:

$$\frac{\partial z}{\partial x} = \frac{\partial h}{\partial x} + \frac{\partial z_0}{\partial x} \tag{2-66}$$

where $\partial z / \partial x$ is the water surface slope. Substituting (2-66) into (2-65), dividing through by $\rho\Delta x$ and moving all terms to the left yields the final form of the momentum equation:

$$\frac{\partial Q}{\partial t} + \frac{\partial QV}{\partial x} + gA\left(\frac{\partial z}{\partial x} + S_f\right) = 0 \tag{2-67}$$

Application of the Unsteady Flow Equations Within HEC-RAS

Figure 2-10 illustrates the two-dimensional characteristics of the interaction between the channel and floodplain flows. When the river is rising water moves laterally away from the channel, inundating the floodplain and filling available storage areas. As the depth increases, the floodplain begins to convey water downstream generally along a shorter path than that of the main channel. When the river stage is falling, water moves toward the channel from the overbank supplementing the flow in the main channel.

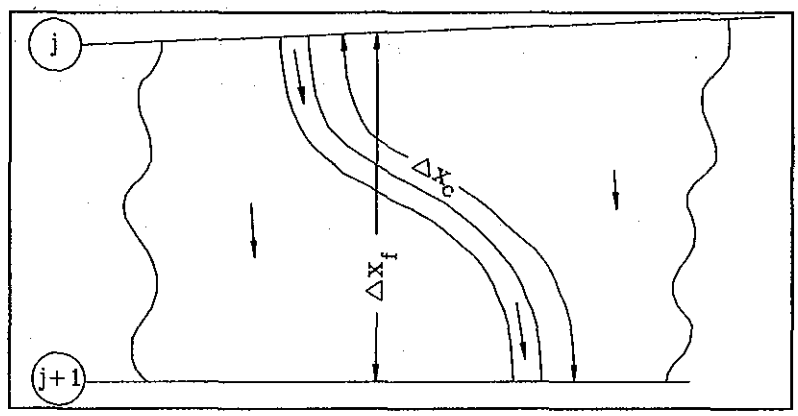

Figure 2.10 Channel and floodplain flows

Because the primary direction of flow is oriented along the channel, this two-dimensional flow field can often be accurately approximated by a one-dimensional representation. Off-channel ponding areas can be modeled with storage areas that exchange water with the channel. Flow in the overbank can be approximated as flow through a separate channel.

This channel/floodplain problem has been addressed in many different ways. A common approach is to ignore overbank conveyance entirely, assuming that the overbank is used only for storage. This assumption may be suitable for large streams such as the Mississippi River where the channel is confined by levees and the remaining floodplain is either heavily vegetated or an off-channel storage area. Fread (1976) and Smith (1978) approached this problem by dividing the system into two separate channels and writing continuity and momentum equations for each channel. To simplify the problem they assumed a horizontal water surface at each cross section normal to the direction of flow; such that the exchange of momentum between the channel and the floodplain was negligible and that the discharge was distributed according to conveyance, i.e.:

$$Q_c = \phi\ Q \tag{2-68}$$

Where: Q_c = flow in channel,
Q = total flow,
ϕ = $K_c / (K_c + K_f)$,
K_c = conveyance in the channel, and,
K_f = conveyance in the floodplain.

With these assumptions, the one-dimensional equations of motion can be combined into a single set:

$$\frac{\partial A}{\partial t} + \frac{\partial(\Phi Q)}{\partial x_c} + \frac{\partial[(1-\Phi)Q]}{\partial x_f} = 0 \tag{2-69}$$

$$\frac{\partial Q}{\partial t} + \frac{\partial(\Phi^2 Q^2 / A_c)}{\partial x_c} + \frac{\partial((1-\Phi)^2 Q^2 / A_f)}{\partial x_f} + gA_c\left[\frac{\partial Z}{\partial x_c} + S_{fc}\right] + gA_f\left[\frac{\partial z}{\partial x_f} + S_{ff}\right] = 0 \tag{2-70}$$

in which the subscripts *c* and *f* refer to the channel and floodplain, respectively. These equations were approximated using implicit finite differences, and solved numerically using the Newton-Raphson iteration technique. The model was successful and produced the desired effects in test problems. Numerical oscillations, however, can occur when the flow at one node, bounding a finite difference cell, is within banks and the flow at the other node is not.

Expanding on the earlier work of Fread and Smith, Barkau (1982) manipulated the finite difference equations for the channel and floodplain and defined a new set of equations that were computationally more convenient. Using a velocity distribution factor, he combined the convective terms. Further, by defining an equivalent flow path, Barkau replaced the friction slope terms with an equivalent force.

The equations derived by Barkau are the basis for the unsteady flow solution within the HEC-RAS software. These equations were derived above. The numerical solution of these equations is described in the next sections.

Implicit Finite Difference Scheme

The most successful and accepted procedure for solving the one-dimensional unsteady flow equations is the four-point implicit scheme, also known as the box scheme (Figure 2.11). Under this scheme, space derivatives and function values are evaluated at an interior point, $(n+\theta)\,\Delta t$. Thus values at $(n+1)\,\Delta t$ enter into all terms in the equations. For a reach of river, a system of simultaneous equations results. The simultaneous solution is an important aspect of this scheme because it allows information from the entire reach to influence the solution at any one point. Consequently, the time step can be significantly larger than with explicit numerical schemes. Von Neumann stability analyses performed by Fread (1974), and Liggett and Cunge (1975), show the implicit scheme to be unconditionally stable (theoretically) for $0.5 < \theta \leq 1.0$, conditionally stable for $\theta = 0.5$, and unstable for $\theta < 0.5$. In a convergence analysis performed by the same authors, it was shown that numerical damping increased as the ratio $\lambda/\Delta x$ decreased, where λ is the length of a wave in the hydraulic system. For streamflow routing problems where the wavelengths are long with respect to spatial distances, convergence is not a serious problem.

In practice, other factors may also contribute to the non-stability of the solution scheme. These factors include dramatic changes in channel cross-sectional properties, abrupt changes in channel slope, characteristics of the flood wave itself, and complex hydraulic structures such as levees, bridges, culverts, weirs, and spillways. In fact, these other factors often overwhelm any stability considerations associated with θ. **Because of these factors, any model application should be accompanied by a sensitivity study, where the accuracy and the stability of the solution are tested with various time and distance intervals.**

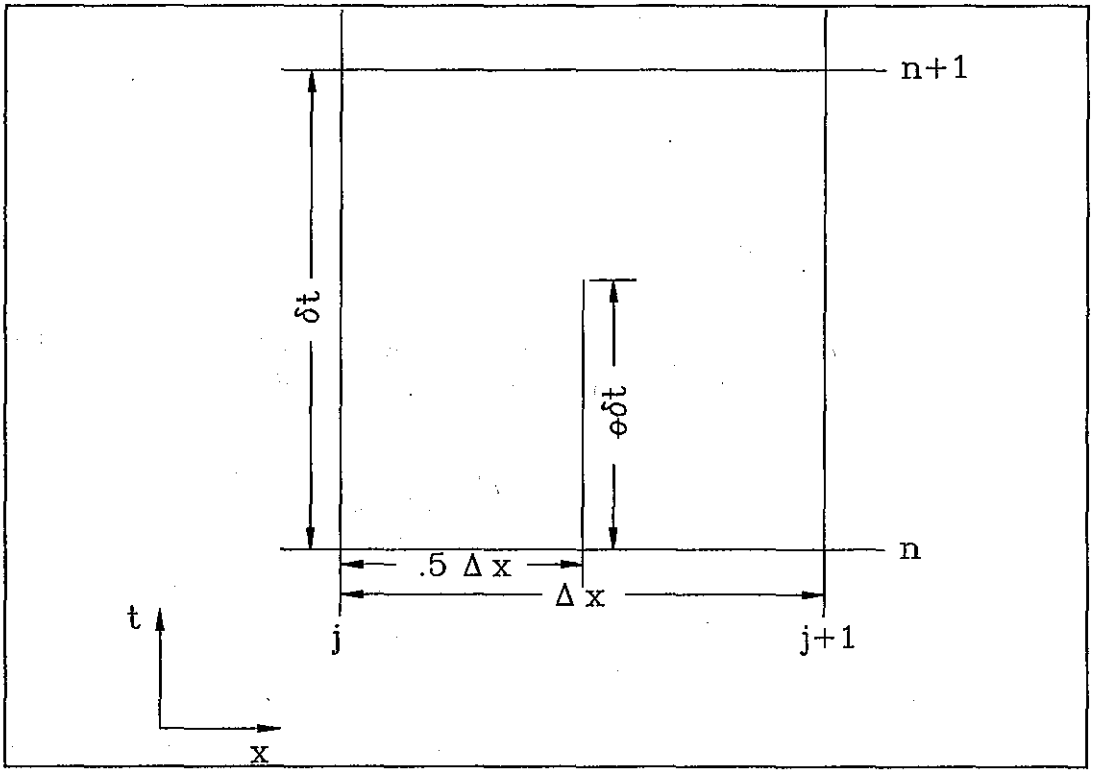

Figure 2.11 Typical finite difference cell.

The following notation is defined:

$$f_j = f_j^n \tag{2-71}$$

and:

$$\Delta f_j = f_j^{n+1} - f_j^n \tag{2-72}$$

then:

$$f_j^{n+1} = f_j + \Delta f_j \tag{2-73}$$

The general implicit finite difference forms are:

1. Time derivative

$$\frac{\partial f}{\partial t} \approx \frac{\Delta f}{\Delta t} = \frac{0.5(\Delta f_{j+1} + \Delta f_j)}{\Delta t} \tag{2-74}$$

2. Space derivative

$$\frac{\partial f}{\partial x} \approx \frac{\Delta f}{\Delta x} = \frac{(f_{j+1} - f_j) + \theta(\Delta f_{j+1} - \Delta f_j)}{\Delta x} \tag{2-75}$$

3. Function value

$$f \approx \overline{f} = 0.5(f_j + f_{j+1}) + 0.5\theta(\Delta f_j + \Delta f_{j+1}) \quad (2\text{-}76)$$

Continuity Equation

The continuity equation describes conservation of mass for the one-dimensional system. From previous text, with the addition of a storage term, S, the continuity equation can be written as:

$$\frac{\partial A}{\partial t} + \frac{\partial S}{\partial t} + \frac{\partial Q}{\partial x} - q_l = 0 \quad (2\text{-}77)$$

where:

x	=	distance along the channel,
t	=	time,
Q	=	flow,
A	=	cross-sectional area,
S	=	storage from non conveying portions of cross section,
q_l	=	lateral inflow per unit distance.

The above equation can be written for the channel and the floodplain:

$$\frac{\partial Q_c}{\partial x_c} + \frac{\partial A_c}{\partial t} = q_f \quad (2\text{-}78)$$

and:

$$\frac{\partial Q_f}{\partial x_f} + \frac{\partial A_f}{\partial t} + \frac{\partial S}{\partial t} = q_c + q_l \quad (2\text{-}79)$$

where the subscripts c and f refer to the channel and floodplain, respectively, q_l is the lateral inflow per unit length of floodplain, and q_c and q_f are the exchanges of water between the channel and the floodplain.

Equations 2-78 and 2-79 are now approximated using implicit finite differences by applying Equations 2-74 through 2-76:

$$\frac{\Delta Q_c}{\Delta x_c} + \frac{\Delta A_c}{\Delta t} = \bar{q}_f \tag{2-80}$$

$$\frac{\Delta Q_f}{\Delta x_c} + \frac{\Delta A_c}{\Delta t} + \frac{\Delta S}{\Delta t} = \bar{q}_c + \bar{q}_l \tag{2-81}$$

The exchange of mass is equal but not opposite in sign such that $\Delta x_c q_c = -q_f \Delta x_f$. Adding the above equations together and rearranging yields:

$$\Delta Q + \frac{\Delta A_c}{\Delta t}\Delta x_c + \frac{\Delta A_f}{\Delta t}\Delta x_f + \frac{\Delta S}{\Delta t}\Delta x_f - \bar{Q}_l = 0 \tag{2-82}$$

where $\bar{Q}_l$ is the average lateral inflow.

Momentum Equation

The momentum equation states that the rate of change in momentum is equal to the external forces acting on the system. From Appendix A, for a single channel:

$$\frac{\partial Q}{\partial t} + \frac{\partial (VQ)}{\partial x} + gA\left(\frac{\partial z}{\partial x} + S_f\right) = 0 \tag{2-83}$$

where: g = acceleration of gravity,
S_f = friction slope,
V = velocity.

The above equation can be written for the channel and for the floodplain:

$$\frac{\partial Q_c}{\partial t} + \frac{\partial (V_c Q_c)}{\partial x_c} + gA_c\left(\frac{\partial z}{\partial x_c} + S_{fc}\right) = M_f \tag{2-84}$$

$$\frac{\partial Q_f}{\partial t} + \frac{\partial (V_f Q_f)}{\partial x_f} + gA_f\left(\frac{\partial z}{\partial x_f} + S_{ff}\right) = M_c \tag{2-85}$$

where M_c and M_f are the momentum fluxes per unit distance exchanged between the channel and floodplain, respectively. Note that in Equations 2-84 and 2-85 the water surface elevation is not subscripted. An assumption in these equations is that the water surface is horizontal at any cross section perpendicular to the flow. Therefore, the water surface elevation is the same for the channel and the floodplain at a given cross section.

Using Equations 2-74 through 2-76, the above equations are approximated using finite differences:

$$\frac{\Delta Q_c}{\Delta t}+\frac{\Delta(V_c Q_c)}{\Delta x_c}+g\overline{A}_c\left(\frac{\Delta z}{\Delta x_c}+\overline{S}_{fc}\right)=M_f \tag{2-86}$$

$$\frac{\Delta Q_f}{\Delta t}+\frac{\Delta(V_f Q_f)}{\Delta x_f}+g\overline{A}_f\left(\frac{\Delta z}{\Delta x_f}+\overline{S}_{ff}\right)=M_c \tag{2-87}$$

Note that $\Delta x_c M_c = -\Delta x_f M_f$.

Adding and rearranging the above equations yields:

$$\frac{\Delta(Q_c\Delta x_c+Q_f\Delta x_f)}{\Delta t}+\Delta(V_c Q_c)+\Delta(V_f Q_f)+g(A_c+A_f)\Delta z+g\overline{A}_c\overline{S}_{fc}\Delta x_c+g\overline{A}_f\overline{S}_{ff}\Delta x_f=0 \tag{2-88}$$

The final two terms define the friction force from the banks acting on the fluid. An equivalent force can be defined as:

$$g\overline{A}\,\overline{S}_f\Delta x_e=g\overline{A}_c\overline{S}_{fc}\Delta x_c+g\overline{A}_f\overline{S}_{ff}\Delta x_f \tag{2-89}$$

where: Δx_e = equivalent flow path,
S_f = friction slope for the entire cross section,
A = $\overline{A}_c+\overline{A}_f$.

Now, the convective terms can be rewritten by defining a velocity distribution factor:

$$\beta=\frac{(V_c^2A_c+V_f^2A_f)}{V^2A}=\frac{(V_cQ_c+V_fQ_f)}{QV} \tag{2-90}$$

then:

$$\Delta(\beta VQ) = \Delta(V_c Q_c) + \Delta(V_f Q_f) \tag{2-91}$$

The final form of the momentum equation is:

$$\frac{\Delta(Q_c \Delta x_c + Q_f \Delta x_f)}{\Delta t} + \Delta(\beta VQ) + g\bar{A}\Delta z + g\bar{A}\bar{S}_f \Delta x_e = 0 \tag{2-92}$$

A more familiar form is obtained by dividing through by Δx_e:

$$\frac{\Delta(Q_c \Delta x_c + Q_f \Delta x_f)}{\Delta t \Delta x_e} + \frac{\Delta(\beta VQ)}{\Delta x_e} + g\bar{A}\left(\frac{\Delta z}{\Delta x_e} + \bar{S}_f\right) = 0 \tag{2-93}$$

Added Force Term

The friction and pressure forces from the banks do not always describe all the forces that act on the water. Structures such as bridge piers, navigation dams, and cofferdams constrict the flow and exert additional forces, which oppose the flow. In localized areas these forces can predominate and produce a significant increase in water surface elevation (called a "swell head") upstream of the structure.

For a differential distance, *dx*, the additional forces in the contraction produce a swell head of dh_l. This swell head is only related to the additional forces. The rate of energy loss can be expressed as a local slope:

$$S_h = \frac{dh_l}{dx} \tag{2-94}$$

The friction slope in Equation 2-93 can be augmented by this term:

$$\frac{\partial Q}{\partial t} + \frac{\partial(VQ)}{\partial x} + gA\left(\frac{\partial z}{\partial x} + S_f + S_h\right) = 0 \tag{2-95}$$

For steady flow, there are a number of relationships for computation of the swell head upstream of a contraction. For navigation dams, the formulas of Kindsvater and Carter, d'Aubuisson (Chow, 1959), and Nagler were reviewed by Denzel (1961). For bridges, the formulas of Yarnell (WES, 1973) and the Federal Highway Administration (FHWA, 1978) can be used. These formulas were all determined by experimentation and can be expressed in the more general form:

$$h_l = C\frac{V^2}{2g} \tag{2-96}$$

where h_l is the head loss and C is a coefficient. The coefficient C is a function of velocity, depth, and the geometric properties of the opening, but for simplicity, it is assumed to be a constant. The location where the velocity head is evaluated varies from method to method. Generally, the velocity head is evaluated at the tailwater for tranquil flow and at the headwater for supercritical flow in the contraction.

If h_l occurs over a distance Δx_e, then $h_l = \overline{S}_h \Delta x_e$ and $\overline{S}_h = h_l / \Delta x_e$ where $\overline{S}_h$ is the average slope over the interval Δx_e. Within HEC-RAS, the steady flow bridge and culvert routines are used to compute a family of rating curves for the structure. During the simulation, for a given flow and tailwater, a resulting headwater elevation is interpolated from the curves. The difference between the headwater and tailwater is set to h_l and then $\overline{S}_h$ is computed. The result is inserted in the finite difference form of the momentum equation (Equation 2-93), yielding:

$$\frac{\Delta(Q_c \Delta x_c + Q_f \Delta x_f)}{\Delta t \Delta x_e} + \frac{\Delta(\beta V Q)}{\Delta x_e} + g\overline{A}\left(\frac{\Delta z}{\Delta x_e} + \overline{S}_f + \overline{S}_h\right) = 0 \qquad (2\text{-}97)$$

Lateral Influx of Momentum

At stream junctions, the momentum as well as the mass of the flow from a tributary enters the receiving stream. If this added momentum is not included in the momentum equation, the entering flow has no momentum and must be accelerated by the flow in the river. The lack of entering momentum causes the convective acceleration term, $\partial (VQ) / \partial x$, to become large. To balance the spatial change in momentum, the water surface slope must be large enough to provide the force to accelerate the fluid. Thus, the water surface has a drop across the reach where the flow enters creating backwater upstream of the junction on the main stem. When the tributary flow is large in relation to that of the receiving stream, the momentum exchange may be significant. The confluence of the Mississippi and Missouri Rivers is such a juncture. During a large flood, the computed decrease in water surface elevation over the Mississippi reach is over 0.5 feet if the influx of momentum is not properly considered.

The entering momentum is given by:

$$M_l = \xi \frac{Q_l V_l}{\Delta x} \qquad (2\text{-}98)$$

where: Q_l = lateral inflow,
V_l = average velocity of lateral inflow,
ξ = fraction of the momentum entering the receiving stream.

The entering momentum is added to the right side of Equation 2-97, hence:

$$\frac{\Delta(Q_c \Delta x_c + Q_f \Delta x_f)}{\Delta t \Delta x_e} + \frac{\Delta(\beta V Q)}{\Delta x_e} + g\overline{A}\left(\frac{\Delta z}{\Delta x_e} + \overline{S}_f + \overline{S}_h\right) = \xi \frac{Q_l V_l}{\Delta x_e} \qquad (2\text{-}99)$$

Equation 2-99 is only used at stream junctions in a dendritic model.

Finite Difference Form of the Unsteady Flow Equations

Equations 2-77 and 2-83 are nonlinear. If the implicit finite difference scheme is directly applied, a system of nonlinear algebraic equations results. Amain and Fang (1970), Fread (1974, 1976) and others have solved the nonlinear equations using the Newton-Raphson iteration technique. Apart from being relatively slow, that iterative scheme can experience troublesome convergence problems at discontinuities in the river geometry. To avoid the nonlinear solution, Preissmann (as reported by Liggett and Cunge, 1975) and Chen (1973) developed a technique for linearizing the equations. The following section describes how the finite difference equations are linearized in HEC-RAS.

Linearized, Implicit, Finite Difference Equations

The following assumptions are applied:

1. If $f \bullet f >> \Delta f \bullet \Delta f$, then $\Delta f \bullet \Delta f = 0$ (Preissmann as reported by Liggett and Cunge, 1975).

2. If g = g(Q,z), then Δg can be approximated by the first term of the Taylor Series, i.e.:

$$\Delta g_j = \left(\frac{\partial g}{\partial Q}\right)_j \Delta Q_j + \left(\frac{\partial g}{\partial z}\right)_j \Delta z_j \qquad (2\text{-}100)$$

3. If the time step, Δt, is small, then certain variables can be treated explicitly; hence $h_j^{n+1} \approx h_j^n$ and $\Delta h_j \approx 0$.

Assumption 2 is applied to the friction slope, S_f and the area, A. Assumption 3 is applied to the velocity, V, in the convective term; the velocity distribution factor, β; the equivalent flow path, x; and the flow distribution factor, ϕ.

The finite difference approximations are listed term by term for the continuity equation in Table 2-1 and for the momentum equation in Table 2-2. If the unknown values are grouped on the left-hand side, the following linear equations result:

$$CQ1_j \Delta Q_j + CZ1_j \Delta z_j + CQ2_j \Delta Q_{j+1} + CZ2_j \Delta z_{j+1} = CB_j \tag{2-101}$$

$$MQ1_j \Delta Q_j + MZ1_j \Delta z_j + MQ2_j \Delta Q_{j+1} + MZ2_j \Delta z_{j+1} = MB_j \tag{1-102}$$

Table 2-1
Finite Difference Approximation of the Terms in the Continuity Equation

Term	Finite Difference Approximation
ΔQ	$(Q_{j+1} - Q_j) + \theta(\Delta Q_{j+1} - \Delta Q_j)$
$\frac{\partial A_c}{\partial t}\Delta x_c$	$0.5\Delta x_{cj}\frac{\left(\frac{dA_c}{dz}\right)_j \Delta z_j + \left(\frac{dA_c}{dz}\right)_{j+1} \Delta z_{j+1}}{\Delta t}$
$\frac{\partial A_f}{\partial t}\Delta x_f$	$0.5\Delta x_{fj}\frac{\left(\frac{dA_f}{dz}\right)_j \Delta z_j + \left(\frac{dA_f}{dz}\right)_{j+1} \Delta z_{j+1}}{\Delta t}$
$\frac{\partial S}{\partial t}\Delta x_f$	$0.5\Delta x_{fj}\frac{\left(\frac{dS}{dz}\right)_j \Delta z_j + \left(\frac{dS}{dz}\right)_{j+1} \Delta z_{j+1}}{\Delta t}$

Table 2-2
Finite Difference Approximation of the Terms in the Momentum Equation

Term	***Finite Difference Approximation***
$\frac{\partial(Q_c \Delta x_c + Q_f \Delta x_f)}{\partial t \Delta x_e}$	$\frac{0.5}{\Delta x_e \partial t}(\partial Q_{cj} \Delta x_{cj} + \partial Q_{fj} \Delta x_{fj} + \partial Q_{cj+1} \Delta x_{cj} + \partial Q_{fj+1} \Delta x_{fj})$
$\frac{\Delta \beta VQ}{\Delta x_{ej}}$	$\frac{1}{\Delta x_{ej}}\left[(\beta VQ)_{j+1} - (\beta VQ)_j\right] + \frac{\theta}{\Delta x_{ej}}\left[(\beta VQ)_{j+1} - (\beta VQ)_j\right]$
$g\overline{A}\frac{\Delta z}{\Delta x_e}$	$g\overline{A}\left[\frac{z_{j+1} - z_j}{\Delta x_{ej}} + \frac{\theta}{\Delta x_{ej}}(\Delta z_{j+1} - \Delta z_j)\right] + \theta g \Delta \overline{A}\frac{(z_{j+1} - z_j)}{\Delta x_{ej}}$
$g\overline{A}(\overline{S}_f + \overline{S}_h)$	$g\overline{A}(\overline{S}_f + \overline{S}_h) + 0.5\theta g\overline{A}\left[(\Delta S_{fj+1} + \Delta S_{fj}) + (\Delta S_{hj+1} + \Delta S_{hj})\right] + 0.5\theta g(\overline{S}_f + \overline{S}_h)(\Delta A_j + \Delta A_{j+1})$
$\overline{A}$	$0.5(A_{j+1} + A_j)$
$\overline{S}_f$	$0.5(S_{fj+1} + S_{fj})$
∂A_j	$\left(\frac{dA}{dZ}\right)_j \Delta z_j$
∂S_{fj}	$\left(\frac{-2S_f}{K}\frac{dK}{dz}\right)_j \Delta z_j + \left(\frac{2S_f}{Q}\right)_j \Delta Q_j$
$\partial \overline{A}$	$0.5(\Delta A_j + \Delta A_{j+1})$

The values of the coefficients are defined in Tables 2-3 and 2-4.

Table 2-3
Coefficients for the Continuity Equation

Coefficient	Value
$CQ1_j$	$\frac{-\theta}{\Delta x_{ej}}$
$CZ1_j$	$\frac{0.5}{\Delta t \Delta x_{ej}}\left[\left(\frac{dA_c}{dz}\right)_j \Delta x_{cj} + \left(\frac{dA_f}{dz} + \frac{dS}{dz}\right)_j \Delta x_{fj}\right]$
$CQ2_j$	$\frac{\theta}{\Delta x_{ej}}$
$CZ2_j$	$\frac{0.5}{\Delta t \Delta x_{ej}}\left[\left(\frac{dA_c}{dz}\right)_{j+1} \Delta x_{cj} + \left(\frac{dA_f}{dz} + \frac{dS}{dz}\right)_{j+1} \Delta x_{fj}\right]$
CB_j	$-\frac{Q_{j+1} - Q_j}{\Delta x_{ej}} + \frac{Q_l}{\Delta x_{ej}}$

Table 2-4

Coefficients of the Momentum Equation

Term	Value
$MQ1_j$	$0.5\frac{\Delta x_{cj}\phi_j + \Delta x_{fj}(1-\phi_j)}{\Delta x_{ej}\Delta t} - \frac{\beta_j V_j \theta}{\Delta x_{ej}} + \theta g \bar{A}\frac{(S_{fj} + S_{hj})}{Q_j}$
$MZ1_j$	$\frac{-gA\theta}{\Delta x_{ej}} + 0.5g(z_{j+1} - z_j)\left(\frac{dA}{dz}\right)_j\left(\frac{\theta}{\Delta x_{ej}}\right) - g\theta\bar{A}\left[\left(\frac{dK}{dz}\right)_j\left(\frac{S_{fj}}{K_j}\right) + \left(\frac{dA}{dz}\right)_j\left(\frac{S_{hj}}{A_j}\right)\right] + 0.5\theta g\left(\frac{dA}{dz}\right)_j(\bar{S}_f + \bar{S}_h)$
$MQ2_j$	$0.5\left[\Delta x_{cj}\phi_{j+1} + \Delta x_{fj}(1-\phi_{j+1})\right]\left(\frac{1}{\Delta x_{ej}\Delta t}\right) + \beta_{j+1}V_{j+1}\left(\frac{\theta}{\Delta x_{ej}}\right) + \frac{\theta g A}{Q_{j+1}}(S_{fj+1} + S_{hj+1})$
$MZ2_j$	$\frac{g\bar{A}\theta}{\Delta x_{ej}} + 0.5g(z_{j+1}-z_j)\left(\frac{dA}{dz}\right)_{j+1}\left(\frac{\theta}{\Delta x_{ej}}\right) - \theta g\bar{A}\left[\left(\frac{dK}{dz}\right)_{j+1}\left(\frac{S_{fj+1}}{K_{j+1}}\right) + \left(\frac{dA}{dz}\right)_{j+1} + \left(\frac{S_{hj+1}}{A_{j+1}}\right)\right] + 0.5\theta g\left(\frac{dA}{dz}\right)_{j+1}(\bar{S}_f + \bar{S}_h)$
MB_j	$-\left[(\beta_{j+1}V_{j+1}Q_{j+1} - \beta_j V_j Q_j)\left(\frac{1}{\Delta x_{ej}}\right) + \left(\frac{g\bar{A}}{\Delta x_{ej}}\right)(z_{j+1} - z_j) + g\bar{A}(\bar{S}_f + \bar{S}_h)\right]$

Flow Distribution Factor

The distribution of flow between the channel and floodplain must be determined. The portion of the flow in the channel is given by:

$$\phi_j = \frac{Q_{cj}}{Q_{cj} + Q_{fj}} \tag{2-103}$$

Fread (1976) assumed that the friction slope is the same for the channel and floodplain, thus the distribution is given by the ratio of conveyance:

$$\phi_j = \frac{K_{cj}}{K_{cj} + K_{fj}} \tag{2-104}$$

Equation 2-104 is used in the HEC-RAS model.

Equivalent Flow Path

The equivalent flow path is given by:

$$\Delta x_e = \frac{\overline{A}_c \overline{S}_{fc} \Delta x_c + \overline{A}_f \overline{S}_{ff} \Delta x_f}{\overline{A} \overline{S}_f} \tag{2-105}$$

If we assume:

$$\overline{\phi} = \frac{\overline{K}_c}{\overline{K}_c + \overline{K}_f} \tag{2-106}$$

where $\overline{\phi}$ is the average flow distribution for the reach, then:

$$\Delta x_e = \frac{\overline{A}_c \Delta x_c + \overline{A}_f \Delta x_f}{\overline{A}} \tag{2-107}$$

Since Δx_e is defined explicitly:

$$\Delta x_{ej} = \frac{(A_{cj} + A_{cj+1}) \Delta x_{cj} + (A_{fj} + A_{fj+1}) \Delta x_{fj}}{A_j + A_{j+1}} \tag{2-108}$$

Boundary Conditions

For a reach of river there are N computational nodes which bound N-1 finite difference cells. From these cells 2N-2 finite difference equations can be developed. Because there are 2N unknowns (ΔQ and Δz for each node), two additional equations are needed. These equations are provided by the boundary conditions for each reach, which for subcritical flow, are required at the upstream and downstream ends. For supercritical flow, boundary conditions are only required at the upstream end.

Interior Boundary Conditions (for Reach Connections)

A network is composed of a set of M individual reaches. Interior boundary equations are required to specify connections between reaches. Depending on the type of reach junction, one of two equations is used:

Continuity of flow:

$$\sum_{i=1}^{l} S_{gi} Q_i = 0 \qquad (2\text{-}109)$$

where: l = the number of reaches connected at a junction,
S_{gi} = -1 if i is a connection to an upstream reach, +1 if i is a connection to a downstream reach,
Q_i = discharge in reach i.

The finite difference form of Equation 2-109 is:

$$\sum_{i=1}^{l-1} MU_{mi} \Delta Q_i + MUQ_m \Delta Q_K = MUB_m \qquad (2\text{-}110)$$

where: $MU_{mi} = \theta S_{gi}$,
$MUQ_m = \theta S_{gK}$,
$MUB_m = - \sum_{i=1}^{l} S_{gi} Q_i$

Continuity of stage:

$$z_k = z_c \tag{2-111}$$

where z_k, the stage at the boundary of reach k, is set equal to z_c, a stage common to all stage boundary conditions at the junction of interest. The finite difference form of Equation 2-111 is:

$$MUZ_m \Delta z_K - MU_m \Delta z_c = MUB_m \tag{2-112}$$

where: $MUZ_m = 0$,
$MU_m = 0$,
$MUB_m = z_c - z_K$.

With reference to Figure 2.12, HEC-RAS uses the following strategy to apply the reach connection boundary condition equations:

- Apply flow continuity to reaches upstream of flow splits and downstream of flow combinations (reach 1 in Figure 2.12). Only one flow boundary equation is used per junction.
- Apply stage continuity for all other reaches (reaches 2 and 3 in Figure 2.12). Z_c is computed as the stage corresponding to the flow in reach 1. Therefore, stage in reaches 2 and 3 will be set equal to Z_c.

Upstream Boundary Conditions

Upstream boundary conditions are required at the upstream end of all reaches that are not connected to other reaches or storage areas. An upstream boundary condition is applied as a flow hydrograph of discharge versus time. The equation of a flow hydrograph for reach m is:

$$\Delta Q_k^{n+1} = Q_k^n - Q_k \tag{2-113}$$

where k is the upstream node of reach m. The finite difference form of Equation 2-113 is:

$$MUQ_m \Delta dQ_K = MUB_m \tag{2-114}$$

where: $MUQ_m = 1$,
$MUB_m = Q_l^{n+1} - Q_l^n$.

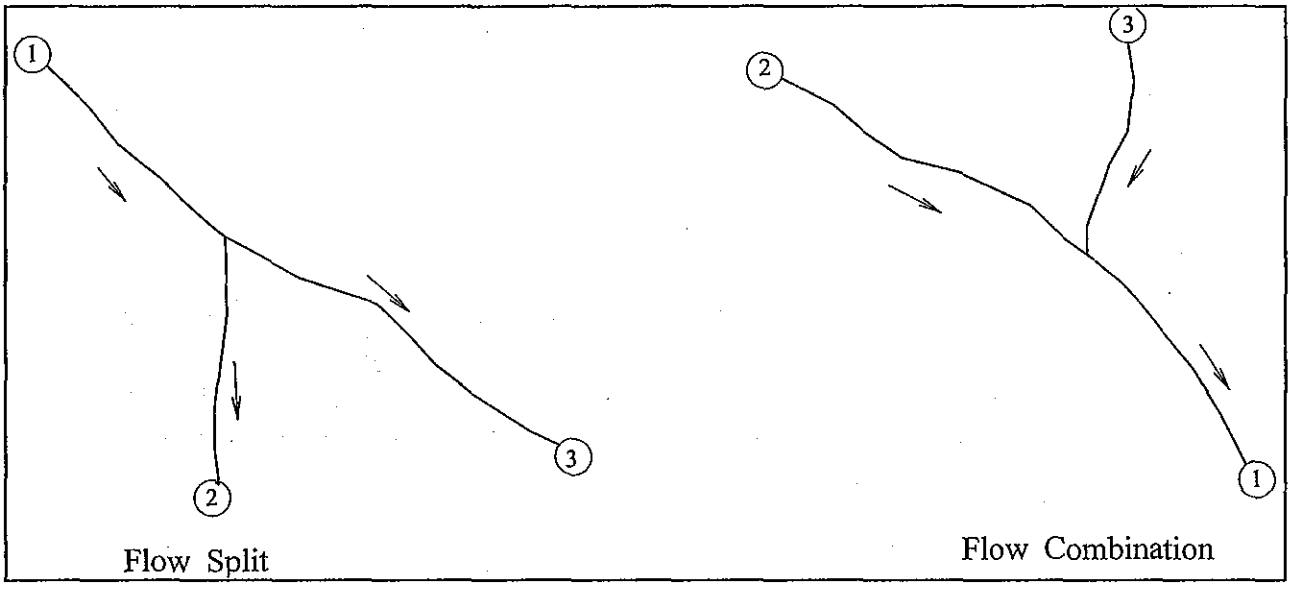

Figure 2.12 Typical flow split and combination.

Downstream Boundary Conditions

Downstream boundary conditions are required at the downstream end of all reaches which are not connected to other reaches or storage areas. Four types of downstream boundary conditions can be specified:

- a stage hydrograph,
- a flow hydrograph,
- a single-valued rating curve,
- normal depth from Manning's equation.

Stage Hydrograph. A stage hydrograph of water surface elevation versus time may be used as the downstream boundary condition if the stream flows into a backwater environment such as an estuary or bay where the water surface elevation is governed by tidal fluctuations, or where it flows into a lake or reservoir of known stage(s). At time step $(n+1)\Delta t$, the boundary condition from the stage hydrograph is given by:

$$\Delta Z_N = Z_N^{n+1} - Z_N^n \qquad (2\text{-}115)$$

The finite difference form of Equation 2-115 is:

$$CDZ_m \Delta z_N = CDB_m \tag{2-116}$$

where: $CDZ_m = 1$,
$CDB_m = z_N^{n+1} - z_N^n$.

Flow Hydrograph. A flow hydrograph may be used as the downstream boundary condition if recorded gage data is available and the model is being calibrated to a specific flood event. At time step $(n+1)\Delta t$, the boundary condition from the flow hydrograph is given by the finite difference equation:

$$CDQ_m \Delta Q_N = CDB_m \tag{2-117}$$

where: $CDQ_m = 1$,
$CDB_m = Q_N^{n+1} - Q_N^n$.

Single Valued Rating Curve. The single valued rating curve is a monotonic function of stage and flow. An example of this type of curve is the steady, uniform flow rating curve. The single valued rating curve can be used to accurately describe the stage-flow relationship of free outfalls such as waterfalls, or hydraulic control structures such as spillways, weirs or lock and dam operations. When applying this type of boundary condition to a natural stream, caution should be used. If the stream location would normally have a looped rating curve, then placing a single valued rating curve as the boundary condition can introduce errors in the solution. Too reduce errors in stage, move the boundary condition downstream from your study area, such that it no longer affects the stages in the study area. Further advice is given in (USACE, 1993).

At time $(n+1)\Delta t$ the boundary condition is given by:

$$Q_N + \theta \Delta Q_N = D_{k-1} + \frac{D_k - D_{k-1}}{S_k - S_{k-1}} (z_N + \Delta z_N - S_{k-1}) \tag{2-118}$$

where: D_k = K^{th} discharge ordinate,
S_k = K^{th} stage ordinate.

After collecting unknown terms on the left side of the equation, the finite difference form of Equation 2-118 is:

$$CDQ_m \Delta Q_N + CDZ_m \Delta z_N = CDB_m \tag{2-119}$$

where: $CDQ_m = \theta$,

$$CDZ_m = \frac{D_k - D_{k-1}}{S_k - S_{k-1}},$$

$$CDB_m = Q_N + D_{k-1} + \frac{D_k - D_{k-1}}{S_k - S_{k-1}}(z_N - S_{k-1}).$$

Normal Depth. Use of Manning's equation with a user entered friction slope produces a stage considered to be normal depth if uniform flow conditions existed. Because uniform flow conditions do not normally exist in natural streams, this boundary condition should be used far enough downstream from your study area that it does not affect the results in the study area. Manning's equation may be written as:

$$Q = K(S_f)^{0.5} \tag{2-120}$$

where: K represents the conveyance and S_f is the friction slope.

Skyline Solution of a Sparse System of Linear Equations

The finite difference equations along with external and internal boundary conditions and storage area equations result in a system of linear equations which must be solved for each time step:

$$Ax = b \tag{2-121}$$

in which: A = coefficient matrix,
x = column vector of unknowns,
b = column vector of constants.

For a single channel without a storage area, the coefficient matrix has a band width of five and can be solved by one of many banded matrix solvers.

For network problems, sparse terms destroy the banded structure. The sparse terms enter and leave at the boundary equations and at the storage areas. Figure 2.13 shows a simple system with four reaches and a storage area off of reach 2. The corresponding coefficient matrix is shown in Figure 2.14. The elements are banded for the reaches but sparse elements appear at the reach boundaries and at the storage area. This small system is a trivial problem to solve, but systems with hundreds of cross sections and tens of reaches pose a major numerical problem because of the sparse terms. Even the largest computers cannot store the coefficient matrix for a moderately sized problem, furthermore, the computer time required to

solve such a large matrix using Gaussian elimination would be very large. Because most of the elements are zero, a majority of computer time would be wasted.

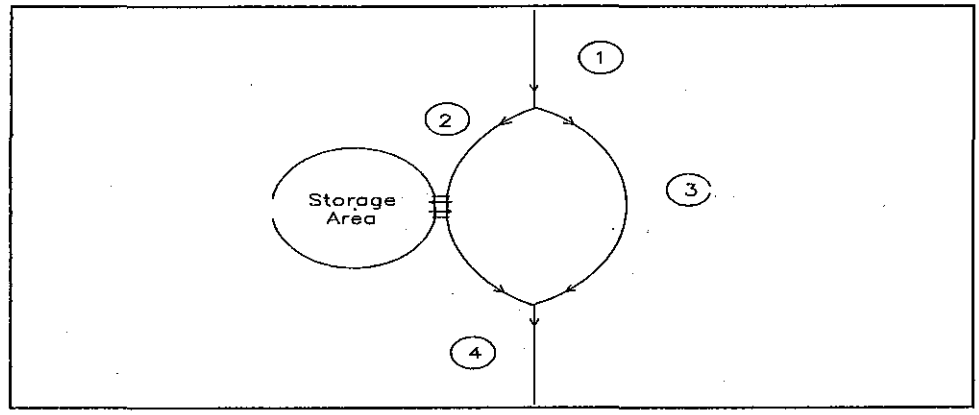

Figure 2.13 Simple network with four reaches and a storage area.

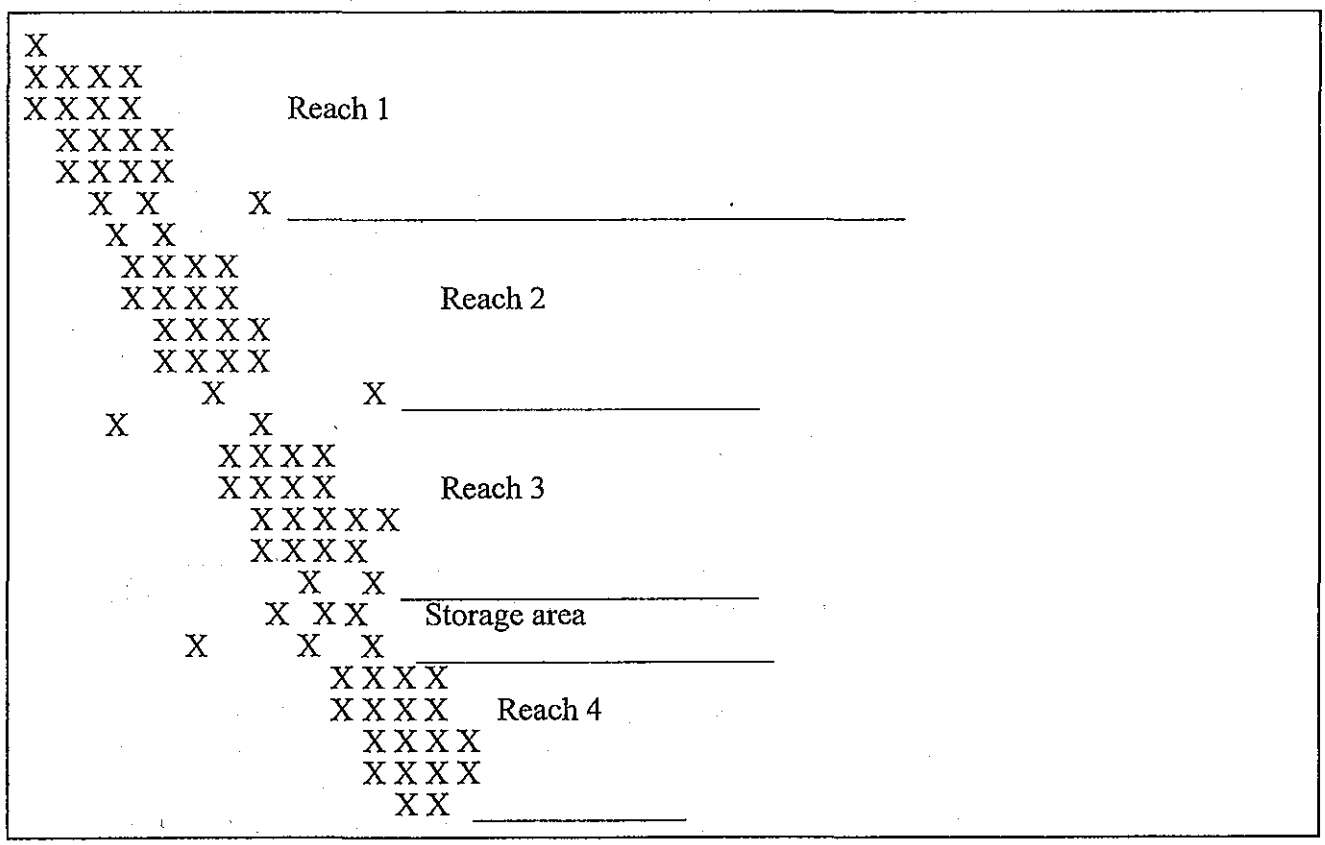

Figure 2.14 Sparse coefficient matrix resulting from simple linear system. Note, sparse terms enter and disappear at storage areas and boundary equations.

Three practical solution schemes have been used to solve the sparse

system of linear equations: Barkau (1985) used a front solver scheme to eliminate terms to the left of the diagonal and pointers to identify sparse columns to the right of the diagonal. Cunge et al. (1980) and Shaffranekk (1981) used recursive schemes to significantly reduce the size of the sparse coefficient matrix. Tucci (1978) and Chen and Simons (1979) used the skyline storage scheme (Bathe and Wilson, 1976) to store the coefficient matrix. The goal of these schemes is to more effectively store the coefficient matrix. The front solver and skyline methods identify and store only the significant elements. The recursive schemes are more elegant, significantly reducing the number of linear equations. All use Gaussian elimination to solve the simultaneous equations.

A front solver performs the reduction pass of Gauss elimination before equations are entered into a coefficient matrix. Hence, the coefficient matrix is upper triangular. To further reduce storage, Barkau (1985) proposed indexing sparse columns to the right of the band, thus, only the band and the sparse terms were stored. Since row and column operations were minimized, the procedure should be as fast if not faster than any of the other procedures. But, the procedure could not be readily adapted to a wide variety of problems because of the way that the sparse terms were indexed. Hence, the program needed to be re-dimensioned and recompiled for each new problem.

The recursive schemes are ingenious. Cunge credits the initial application to Friazinov (1970). Cunge's scheme and Schaffranek's scheme are similar in approach but differ greatly in efficiency. Through recursive upward and downward passes, each single routing reach is transformed into two transfer equations which relate the stages and flows at the upstream and downstream boundaries. Cunge substitutes the transfer equations in which M is the number of junctions. Schraffranek combines the transfer equations with the boundary equations, resulting in a system of $4N$ equations in which N is the number of individual reaches. The coefficient matrix is sparse, but the degree is much less than the original system.

By using recursion, the algorithms minimize row and column operations. The key to the algorithm's speed is the solution of a reduced linear equation set. For smaller problems Gaussian elimination on the full matrix would suffice. For larger problems, some type of sparse matrix solver must be used, primarily to reduce the number of elementary operations. Consider, for example, a system of 50 reaches. Schaffranek's matrix would be 200 X 200 and Cunge's matrix would be 50 X 50, 2.7 million and 42,000 operations respectively (the number of operations is approximately 1/3 n^3 where n is the number of rows).

Another disadvantage of the recursive scheme is adaptability. Lateral weirs which discharge into storage areas or which discharge into other

reaches disrupt the recursion algorithm. These weirs may span a short distance or they may span an entire reach. The recursion algorithm, as presented in the above references, will not work for this problem. The algorithm can be adapted, but no documentation has yet been published.

Skyline is the name of a storage algorithm for a sparse matrix. In any sparse matrix, the non-zero elements from the linear system and from the Gaussian elimination procedure are to the left of the diagonal and in a column above the diagonal. This structure is shown in Figure A.4. Skyline stores these inverted "L shaped" structures in a vector, keeping the total storage at a minimum. Elements in skyline storage are accessed by row and column numbers. Elements outside the "L" are returned as zero, hence the skyline matrix functions exactly as the original matrix. Skyline storage can be adapted to any problem.

The efficiency of Gaussian elimination depends on the number of pointers into skyline storage. Tucci (1978) and Chen and Simons (1979) used the original algorithm as proposed by Bathe and Wilson (1976). This algorithm used only two pointers, the left limit and the upper limit of the "L", thus, a large number of unnecessary elementary operations are performed on zero elements and in searching for rows to reduce. Their solution was acceptable for small problems, but clearly deficient for large problems. Using additional pointers reduces the number of superfluous calculations. If the pointers identify all the sparse columns to the right of the diagonal, then the number of operations is minimized and the performance is similar to the front solver algorithm.

Skyline Solution Algorithm

The skyline storage algorithm was chosen to store the coefficient matrix. The Gauss elimination algorithm of Bathe and Wilson was abandoned because of its poor efficiency. Instead a modified algorithm with seven pointers was developed. The pointers are:

1) IDIA(IROW) - index of the diagonal element in row IROW in skyline storage.
2) ILEFT(IROW) - number of columns to the left of the diagonal.
3) IHIGH(IROW) - number of rows above the diagonal.
4) IRIGHT(IROW) - number of columns in the principal band to the right of the diagonal.
5) ISPCOL(J,IROW) - pointer to sparse columns to the right of the principal band.
6) IZSA(IS) - the row number of storage area IS.
7) IROWZ(N) - the row number of the continuity equation for segment N.

The pointers eliminate the meaningless operations on zero elements. This

code is specifically designed for flood routing through a full network.

CHAPTER 3

Basic Data Requirements

This chapter describes the basic data requirements for performing the one-dimensional flow calculations within HEC-RAS. The basic data are defined and discussions of applicable ranges for parameters are provided.

Contents

General

The main objective of the HEC-RAS program is quite simple - to compute water surface elevations at all locations of interest for either a given set of flow data (steady flow simulation), or by routing hydrographs through the system (unsteady flow simulation). The data needed to perform these computations are divided into the following categories: geometric data; steady flow data; unsteady flow data; and sediment data (not available yet). Geometric data are required for any of the analyses performed within HEC-RAS. The other data types are only required if you are going to do that specific type of analysis (i.e., steady flow data are required to perform a steady flow water surface profile computation). The current version of HEC-RAS can perform either steady or unsteady flow computations.

Geometric Data

The basic geometric data consist of establishing the connectivity of the river system (River System Schematic); cross section data; reach lengths; energy loss coefficients (friction losses, contraction and expansion losses); and stream junction information. Hydraulic structure data (bridges, culverts, spillways, weirs, etc...), which are also considered geometric data, will be described in later chapters.

Study Limit Determination

When performing a hydraulic study, it is normally necessary to gather data both upstream of and downstream of the study reach. Gathering additional data upstream is necessary in order to evaluate any upstream impacts due to construction alternatives that are being evaluated within the study reach (Figure 3.1). The limits for data collection upstream should be at a distance such that the increase in water surface profile resulting from a channel modification converges with the existing conditions profile. Additional data collection downstream of the study reach is necessary in order to prevent any user-defined boundary condition from affecting the results within the study reach. In general, the water surface at the downstream boundary of a model is not normally known. The user must estimate this water surface for each profile to be computed. A common practice is to use Manning's equation and compute normal depth as the starting water surface. The actual water surface may be higher or lower than normal depth. The use of normal depth will introduce an error in the water surface profile at the boundary. In general, for subcritical flow, the error at the boundary will diminish as the computations proceed upstream. In order to prevent any computed errors within the study reach, the unknown boundary condition should be placed far enough downstream such that the computed profile will converge to a consistent answer by the time the computations reach the downstream limit of the study.

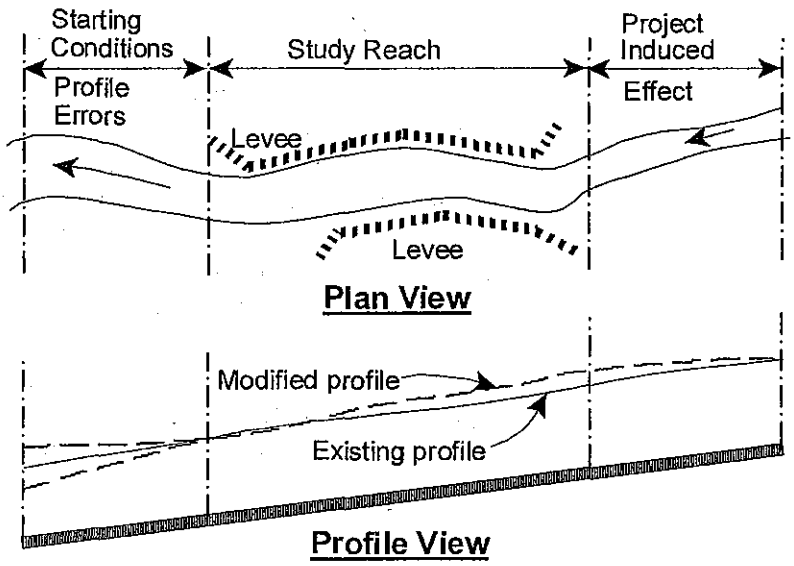

Figure 3.1 Example Study Limit Determination

The River System Schematic

The river system schematic is required for any geometric data set within the HEC-RAS system. The schematic defines how the various river reaches are connected, as well as establishing a naming convention for referencing all the other data. The river system schematic is developed by drawing and connecting the various reaches of the system within the geometric data editor (see Chapter 6 of the HEC-RAS User's Manual for details on how to develop the schematic from within the user interface). The user is required to develop the river system schematic before any other data can be entered.

Each river reach on the schematic is given a unique identifier. As other data are entered, the data are referenced to a specific reach of the schematic. For example, each cross section must have a "River", "Reach" and "River Station" identifier. The river and reach identifiers defines which reach the cross section lives in, while the river station identifier defines where that cross section is located within the reach, with respect to the other cross sections for that reach.

The connectivity of reaches is very important in order for the model to understand how the computations should proceed from one reach to the next. The user is required to draw each reach from upstream to downstream, in what is considered to be the positive flow direction. The connecting of reaches is considered a junction. Junctions should only be established at

locations where two or more streams come together or split apart. Junctions cannot be established with a single reach flowing into another single reach. These two reaches must be combined and defined as one reach. An example river system schematic is shown in Figure 3.2.

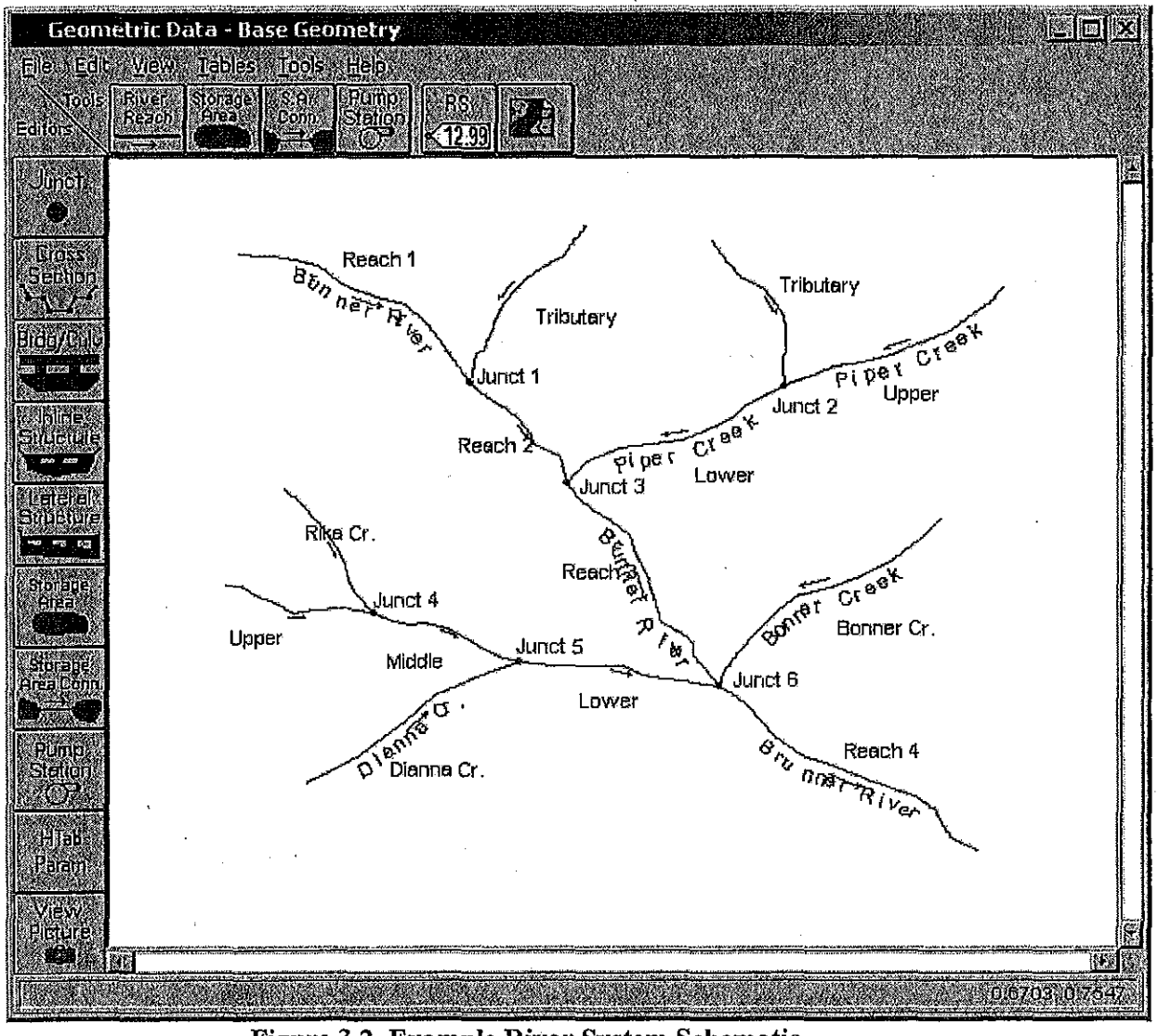

Figure 3.2 Example River System Schematic.

The example schematic shown in Figure 3.2 is for a dendritic river system. Arrows are automatically drawn on the schematic in the assumed positive flow direction. Junctions (red circles) are automatically formed as reaches are connected. As shown, the user is require to provide a river and reach identifier for each reach, as well as an identifier for each junction.

HEC-RAS has the ability to model river systems that range from a single reach model to complicated networks. A "network" model is where river reaches split apart and then come back together, forming looped systems. An example schematic of a looped stream network is shown in Figure 3.3.

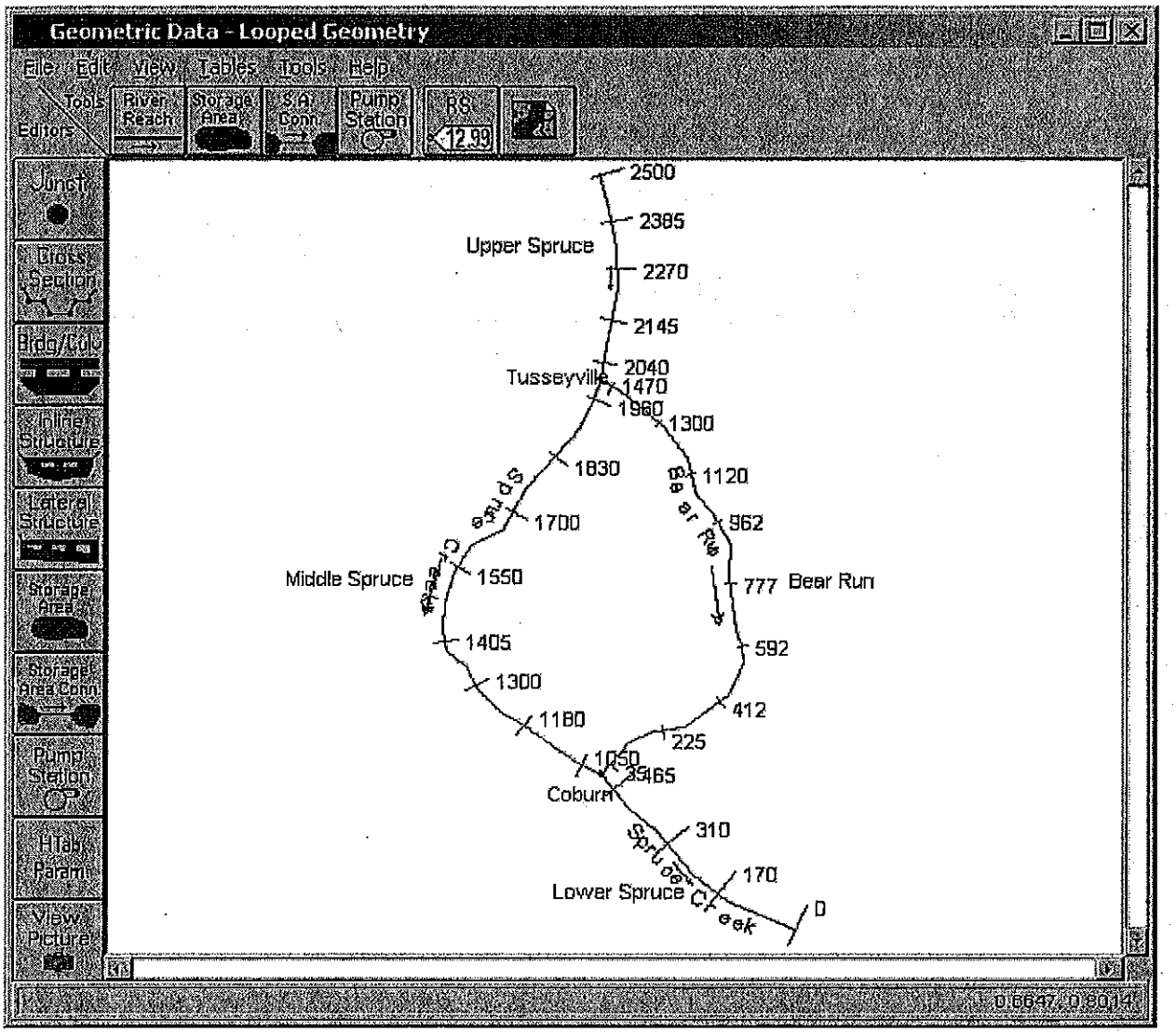

Figure 3.3 Example Schematic for a Looped Network of Reaches

The river system schematic shown in Figure 3.3 demonstrates the ability of HEC-RAS to model flow splits as well as flow combinations. The current version of the steady flow model within HEC-RAS does not determine the amount of flow going to each reach at a flow split. It is currently up to the user to define the amount of flow in each reach. After a simulation is made, the user should adjust the flow in the reaches in order to obtain a balance in energy around the junction of a flow split.

Cross Section Geometry

Boundary geometry for the analysis of flow in natural streams is specified in terms of ground surface profiles (cross sections) and the measured distances between them (reach lengths). Cross sections are located at intervals along a stream to characterize the flow carrying capability of the stream and its adjacent floodplain. They should extend across the entire floodplain and

should be perpendicular to the anticipated flow lines. Occasionally it is necessary to layout cross-sections in a curved or dog-leg alignment to meet this requirement. Every effort should be made to obtain cross sections that accurately represent the stream and floodplain geometry.

Cross sections are required at representative locations throughout a stream reach and at locations where changes occur in discharge, slope, shape, or roughness, at locations where levees begin or end and at bridges or control structures such as weirs. Where abrupt changes occur, several cross sections should be used to describe the change regardless of the distance. Cross section spacing is also a function of stream size, slope, and the uniformity of cross section shape. In general, large uniform rivers of flat slope normally require the fewest number of cross sections per mile. The purpose of the study also affects spacing of cross sections. For instance, navigation studies on large relatively flat streams may require closely spaced (e.g., 200 feet) cross sections to analyze the effect of local conditions on low flow depths, whereas cross sections for sedimentation studies, to determine deposition in reservoirs, may be spaced at intervals on the order of miles.

The choice of friction loss equation may also influence the spacing of cross sections. For instance, cross section spacing may be maximized when calculating an M1 profile (backwater profile) with the average friction slope equation or when the harmonic mean friction slope equation is used to compute M2 profiles (draw down profile). The HEC-RAS software provides the option to let the program select the averaging equation.

Each cross section in an HEC-RAS data set is identified by a River, Reach, and River Station label. The cross section is described by entering the station and elevation (X-Y data) from left to right, with respect to looking in the downstream direction. The River Station identifier may correspond to stationing along the channel, mile points, or any fictitious numbering system. The numbering system must be consistent, in that the program assumes that higher numbers are upstream and lower numbers are downstream.

Each data point in the cross section is given a station number corresponding to the horizontal distance from a starting point on the left. Up to 500 data points may be used to describe each cross section. Cross section data are traditionally defined looking in the downstream direction. The program considers the left side of the stream to have the lowest station numbers and the right side to have the highest. Cross section data are allowed to have negative stationing values. Stationing must be entered from left to right in increasing order. However, more than one point can have the same stationing value. The left and right stations separating the main channel from the overbank areas must be specified on the cross section data editor. End points of a cross section that are too low (below the computed water surface elevation) will automatically be extended vertically and a note indicating that the cross section had to be extended will show up in the output for that section. The program adds additional wetted perimeter for any water that comes into contact with the extended walls.

Other data that are required for each cross section consist of: downstream reach lengths; roughness coefficients; and contraction and expansion coefficients. These data will be discussed in detail later in this chapter.

Numerous program options are available to allow the user to easily add or modify cross section data. For example, when the user wishes to repeat a surveyed cross section, an option is available from the interface to make a copy of any cross section. Once a cross section is copied, other options are available to allow the user to modify the horizontal and vertical dimensions of the repeated cross section data. For a detailed explanation on how to use these cross section options, see chapter 6 of the HEC-RAS user's manual.

Optional Cross Section Properties

A series of program options are available to restrict flow to the effective flow areas of cross sections. Among these capabilities are options for: ineffective flow areas; levees; and blocked obstructions. All of these capabilities are available from the "Options" menu of the Cross Section Data editor.

Ineffective Flow Areas. This option allows the user to define areas of the cross section that will contain water that is not actively being conveyed (ineffective flow). Ineffective flow areas are often used to describe portions of a cross section in which water will pond, but the velocity of that water, in the downstream direction, is close to zero. This water is included in the storage calculations and other wetted cross section parameters, but it is not included as part of the active flow area. When using ineffective flow areas, no additional wetted perimeter is added to the active flow area. An example of an ineffective flow area is shown in Figure 3.4. The cross-hatched area on the left of the plot represents what is considered to be the ineffective flow.

Two alternatives are available for setting ineffective flow areas. The first option allows the user to define a left station and elevation and a right station and elevation (normal ineffective areas). When this option is used, and if the water surface is below the established ineffective elevations, the areas to the left of the left station and to the right of the right station are considered ineffective. Once the water surface goes above either of the established elevations, then that specific area is no longer considered ineffective.

The second option allows for the establishment of blocked ineffective flow areas. Blocked ineffective flow areas require the user to enter an elevation, a left station, and a right station for each ineffective block. Up to ten blocked ineffective flow areas can be entered at each cross section. Once the water surface goes above the elevation of the blocked ineffective flow area, the blocked area is no longer considered ineffective.

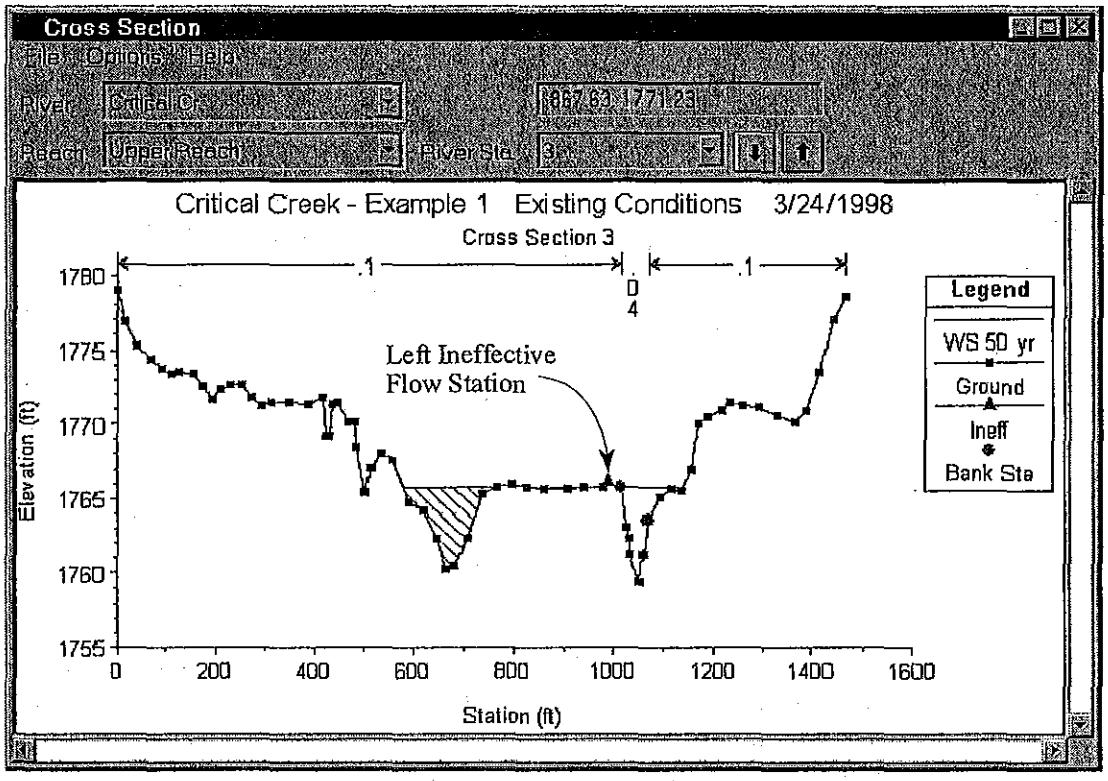

Figure 3.4 Cross section with normal ineffective flow areas

Levees. This option allows the user to establish a left and/or right levee station and elevation on any cross section. When levees are established, no water can go to the left of the left levee station or to the right of the right levee station until either of the levee elevations are exceeded. Levee stations must be defined explicitly, or the program assumes that water can go anywhere within the cross section. An example of a cross section with a levee on the left side is shown in Figure 3.5. In this example the levee station and elevation is associated with an existing point on the cross section.

The user may want to add levees into a data set in order to see what effect a levee will have on the water surface. A simple way to do this is to set a levee station and elevation that is above the existing ground. If a levee elevation is placed above the existing geometry of the cross section, then a vertical wall is placed at that station up to the established levee height. Additional wetted perimeter is included when water comes into contact with the levee wall. An example of this is shown in Figure 3.6.

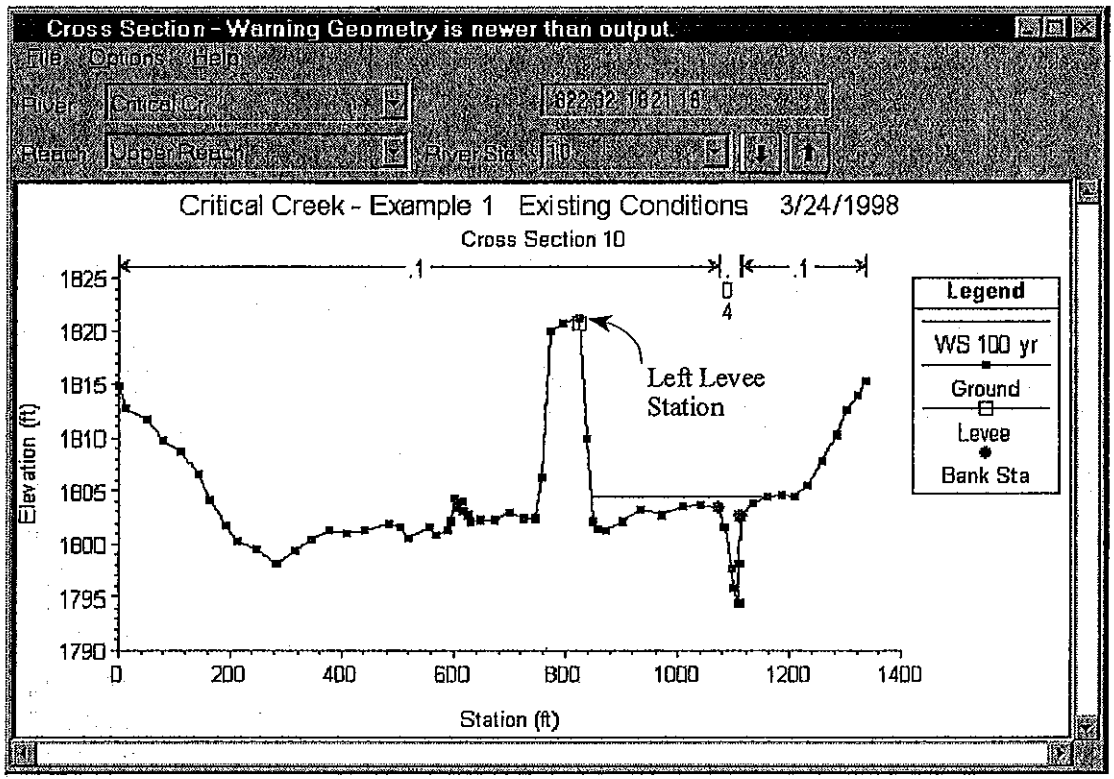

Figure 3.5 Example of the Levee Option

Obstructions. This option allows the user to define areas of the cross section that will be permanently blocked out. Obstructions decrease flow area and add wetted perimeter when the water comes in contact with the obstruction. A obstruction does not prevent water from going outside of the obstruction.

Two alternatives are available for entering obstructions. The first option allows the user to define a left station and elevation and a right station and elevation (normal obstructions). When this option is used, the area to the left of the left station and to the right of the right station will be completely blocked out. An example of this type of obstruction is shown in Figure 3.7.

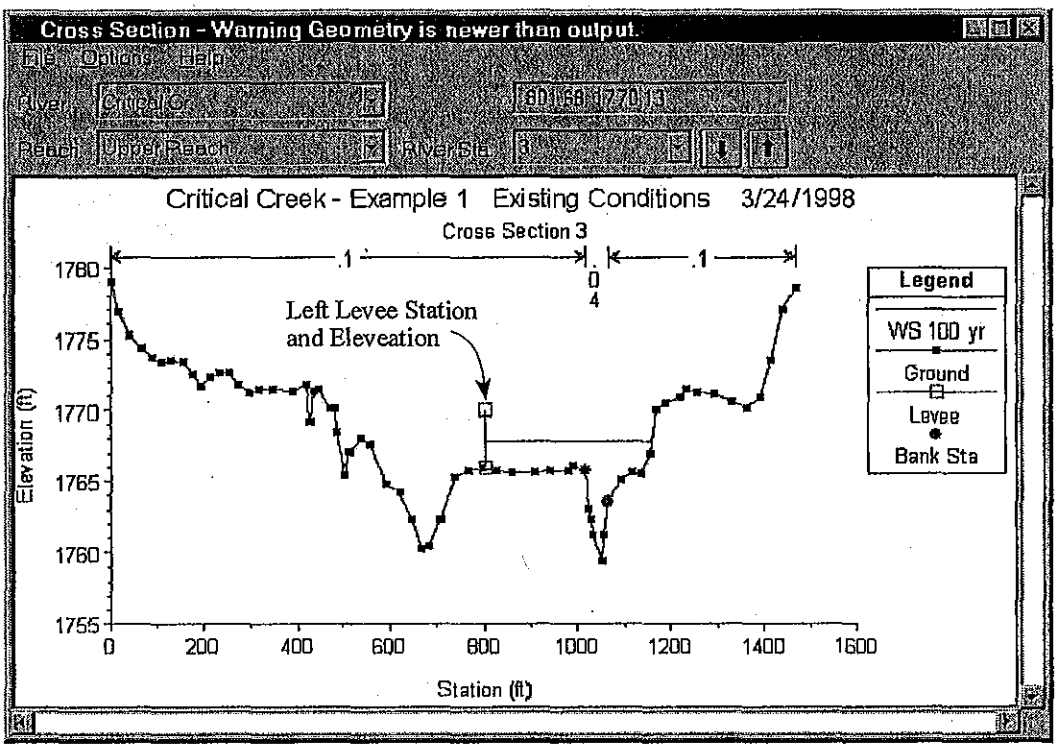

Figure 3.6 Example Levee Added to a Cross Section

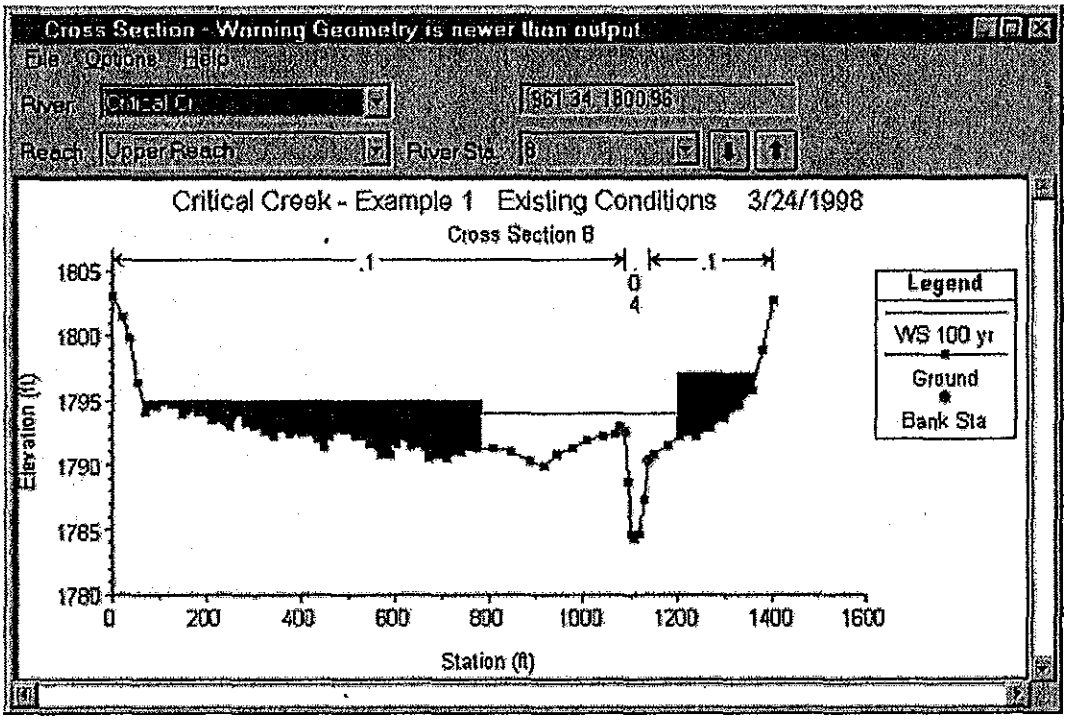

Figure 3.7 Example of Normal Obstructions

The second option, for obstructions, allows the user to enter up to 20 individual blocks (Multiple Blocks). With this option the user enters a left station, a right station, and an elevation for each of the blocks. An example of a cross section with multiple blocked obstructions is shown in Figure 3.8.

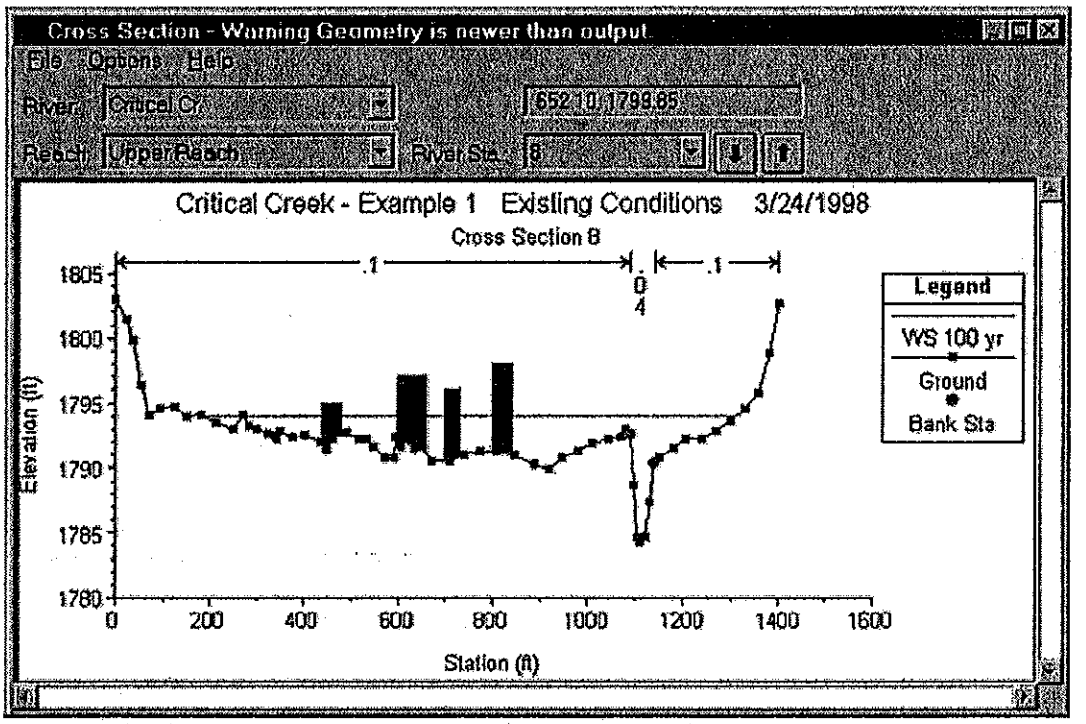

Figure 3.8 Example Cross Section With Multiple Blocked Obstructions

Reach Lengths

The measured distances between cross sections are referred to as reach lengths. The reach lengths for the left overbank, right overbank and channel are specified on the cross section data editor. Channel reach lengths are typically measured along the thalweg. Overbank reach lengths should be measured along the anticipated path of the center of mass of the overbank flow. Often, these three lengths will be of similar value. There are, however, conditions where they will differ significantly, such as at river bends, or where the channel meanders and the overbanks are straight. Where the distances between cross sections for channel and overbanks are different, a discharge-weighted reach length is determined based on the discharges in the main channel and left and right overbank segments of the reach (see Equation 2-3, of chapter 2).

Energy Loss Coefficients

Several types of loss coefficients are utilized by the program to evaluate energy losses: (1) Manning's n values or equivalent roughness "k" values for friction loss, (2) contraction and expansion coefficients to evaluate transition (shock) losses, and (3) bridge and culvert loss coefficients to evaluate losses related to weir shape, pier configuration, pressure flow, and entrance and exit conditions. Energy loss coefficients associated with bridges and culverts will be discussed in chapters 5 and 6 of this manual.

Manning's n. Selection of an appropriate value for Manning's n is very significant to the accuracy of the computed water surface profiles. The value of Manning's n is highly variable and depends on a number of factors including: surface roughness; vegetation; channel irregularities; channel alignment; scour and deposition; obstructions; size and shape of the channel; stage and discharge; seasonal changes; temperature; and suspended material and bedload.

In general, Manning's n values should be calibrated whenever observed water surface profile information (gaged data, as well as high water marks) is available. When gaged data are not available, values of n computed for similar stream conditions or values obtained from experimental data should be used as guides in selecting n values.

There are several references a user can access that show Manning's n values for typical channels. An extensive compilation of n values for streams and floodplains can be found in Chow's book "Open-Channel Hydraulics" [Chow, 1959]. Excerpts from Chow's book, for the most common types of channels, are shown in Table 3.1 below. Chow's book presents additional types of channels, as well as pictures of streams for which n values have been calibrated.

Table 3.1
Manning's 'n' Values

Type of Channel and Description	Minimum	Normal	Maximum
A. *Natural Streams*			
1. **Main Channels**			
a. Clean, straight, full, no rifts or deep pools	0.025	0.030	0.033
b. Same as above, but more stones and weeds	0.030	0.035	0.040
c. Clean, winding, some pools and shoals	0.033	0.040	0.045
d. Same as above, but some weeds and stones	0.035	0.045	0.050
e. Same as above, lower stages, more ineffective slopes and sections	0.040	0.048	0.055
f. Same as "d" but more stones	0.045	0.050	0.060
g. Sluggish reaches, weedy. deep pools	0.050	0.070	0.080
h. Very weedy reaches, deep pools, or floodways with heavy stands of timber and brush	0.070	0.100	0.150
2. **Flood Plains**			
a. Pasture no brush			
1. Short grass	0.025	0.030	0.035
2. High grass	0.030	0.035	0.050
b. Cultivated areas			
1. No crop	0.020	0.030	0.040
2. Mature row crops	0.025	0.035	0.045
3. Mature field crops	0.030	0.040	0.050
c. Brush			
1. Scattered brush, heavy weeds	0.035	0.050	0.070
2. Light brush and trees, in winter	0.035	0.050	0.060
3. Light brush and trees, in summer	0.040	0.060	0.080
4. Medium to dense brush, in winter	0.045	0.070	0.110
5. Medium to dense brush, in summer	0.070	0.100	0.160
d. Trees			
1. Cleared land with tree stumps, no sprouts	0.030	0.040	0.050
2. Same as above, but heavy sprouts	0.050	0.060	0.080
3. Heavy stand of timber, few down trees, little undergrowth, flow below branches	0.080	0.100	0.120
4. Same as above, but with flow into branches	0.100	0.120	0.160
5. Dense willows, summer, straight	0.110	0.150	0.200
3. **Mountain Streams, no vegetation in channel, banks usually steep, with trees and brush on banks submerged**			
a. Bottom: gravels, cobbles, and few boulders	0.030	0.040	0.050
b. Bottom: cobbles with large boulders	0.040	0.050	0.070

Table 3.1 (Continued)
Manning's 'n' Values

Type of Channel and Description	Minimum	Normal	Maximum
B. *Lined or Built-Up Channels*			
1. **Concrete**			
a. Trowel finish	0.011	0.013	0.015
b. Float Finish	0.013	0.015	0.016
c. Finished, with gravel bottom	0.015	0.017	0.020
d. Unfinished	0.014	0.017	0.020
e. Gunite, good section	0.016	0.019	0.023
f. Gunite, wavy section	0.018	0.022	0.025
g. On good excavated rock	0.017	0.020	
h. On irregular excavated rock	0.022	0.027	
2. **Concrete bottom float finished with sides of:**			
a. Dressed stone in mortar	0.015	0.017	0.020
b. Random stone in mortar	0.017	0.020	0.024
c. Cement rubble masonry, plastered	0.016	0.020	0.024
d. Cement rubble masonry	0.020	0.025	0.030
e. Dry rubble on riprap	0.020	0.030	0.035
3. **Gravel bottom with sides of:**			
a. Formed concrete	0.017	0.020	0.025
b. Random stone in mortar	0.020	0.023	0.026
c. Dry rubble or riprap	0.023	0.033	0.036
4. **Brick**			
a. Glazed	0.011	0.013	0.015
b. In cement mortar	0.012	0.015	0.018
5. **Metal**			
a. Smooth steel surfaces	0.011	0.012	0.014
b. Corrugated metal	0.021	0.025	0.030
6. **Asphalt**			
a. Smooth	0.013	0.013	
b. Rough	0.016	0.016	
7. **Vegetal lining**	0.030		0.500

Table 3.1 (Continued)
Manning's 'n' Values

Type of Channel and Description	Minimum	Normal	Maximum
C. *Excavated or Dredged Channels*			
1. **Earth, straight and uniform**			
a. Clean, recently completed	0.016	0.018	0.020
b. Clean, after weathering	0.018	0.022	0.025
c. Gravel, uniform section, clean	0.022	0.025	0.030
d. With short grass, few weeds	0.022	0.027	0.033
2. **Earth, winding and sluggish**			
a. No vegetation	0.023	0.025	0.030
b. Grass, some weeds	0.025	0.030	0.033
c. Dense weeds or aquatic plants in deep channels	0.030	0.035	0.040
d. Earth bottom and rubble side	0.028	0.030	0.035
e. Stony bottom and weedy banks	0.025	0.035	0.040
f. Cobble bottom and clean sides	0.030	0.040	0.050
3. **Dragline-excavated or dredged**			
a. No vegetation	0.025	0.028	0.033
b. Light brush on banks	0.035	0.050	0.060
4. **Rock cuts**			
a. Smooth and uniform	0.025	0.035	0.040
b. Jagged and irregular	0.035	0.040	0.050
5. **Channels not maintained, weeds and brush**			
a. Clean bottom, brush on sides	0.040	0.050	0.080
b. Same as above, highest stage of flow	0.045	0.070	0.110
c. Dense weeds, high as flow depth	0.050	0.080	0.120
d. Dense brush, high stage	0.080	0.100	0.140

Other sources that include pictures of selected streams as a guide to n value determination are available (Fasken, 1963; Barnes, 1967; and Hicks and Mason, 1991). In general, these references provide color photos with tables of calibrated n values for a range of flows.

Although there are many factors that affect the selection of the n value for the channel, some of the most important factors are the type and size of materials that compose the bed and banks of a channel, and the shape of the channel. Cowan (1956) developed a procedure for estimating the effects of these factors to determine the value of Manning's n of a channel. In Cowan's procedure, the value of n is computed by the following equation:

$$n = (n_b + n_1 + n_2 + n_3 + n_4)m \qquad (3\text{-}1)$$

where: n_b = Base value of n for a straight uniform, smooth channel in natural materials

n_1 = Value added to correct for surface irregularities

n_2 = Value for variations in shape and size of the channel

n_3 = Value for obstructions

n_4 = Value for vegetation and flow conditions

m = Correction factor to account for meandering of the channel

A detailed description of Cowan's method can be found in "Guide for Selecting Manning's Roughness Coefficients for Natural Channels and Flood Plains" (FHWA, 1984). This report was developed by the U.S. Geological Survey (Arcement, 1989) for the Federal Highway Administration. The report also presents a method similar to Cowan's for developing Manning's n values for flood plains, as well as some additional methods for densely vegetated flood plains.

Limerinos (1970) related n values to hydraulic radius and bed particle size based on samples from 11 stream channels having bed materials ranging from small gravel to medium size boulders. The Limerinos equation is as follows:

$$n = \frac{(0.0926)R^{1/6}}{1.16 + 2.0\log\left(\frac{R}{d_{84}}\right)} \qquad (3\text{-}2)$$

where: R = Hydraulic radius, in feet (data range was 1.0 to 6.0 feet)

d_{84} = Particle diameter, in feet, that equals or exceeds that of 84 percent of the particles (data range was 1.5 mm to 250 mm)

The Limerinos equation (3-2) fit the data that he used very well, in that the coefficient of correlation $\overline{R}^2 = 0.88$ and the standard error of estimates for values of $n/R^{1/6} = 0.0087$. Limerinos selected reaches that had a minimum amount of roughness, other than that caused by the bed material. The Limerinos equation provides a good estimate of the base n value. The base n value should then be increased to account for other factors, as shown above in Cowen's method.

Jarrett (1984) developed an equation for high gradient streams (slopes greater than 0.002). Jarrett performed a regression analysis on 75 data sets that were surveyed from 21 different streams. Jarrett's equation for Manning's n is as follows:

$$n = 0.39 S^{0.38} R^{-0.16} \tag{3-3}$$

where: S = The friction slope. The slope of the water surface can be used when the friction slope is unknown.

Jarrett (1984) states the following limitations for the use of his equation:

1. The equations are applicable to natural main channels having stable bed and bank materials (gravels, cobbles, and boulders) without backwater.

2. The equations can be used for slopes from 0.002 to 0.04 and for hydraulic radii from 0.5 to 7.0 feet (0.15 to 2.1 m). The upper limit on slope is due to a lack of verification data available for the slopes of high-gradient streams. Results of the regression analysis indicate that for hydraulic radius greater than 7.0 feet (2.1 m), n did not vary significantly with depth; thus extrapolating to larger flows should not be too much in error as long as the bed and bank material remain fairly stable.

3. During the analysis of the data, the energy loss coefficients for contraction and expansion were set to 0.0 and 0.5, respectively.

4. Hydraulic radius does not include the wetted perimeter of bed particles.

5. These equations are applicable to streams having relatively small amounts of suspended sediment.

Because Manning's n depends on many factors such as the type and amount of vegetation, channel configuration, stage, etc., several options are available in HEC-RAS to vary n. When three n values are sufficient to describe the channel and overbanks, the user can enter the three n values directly onto the cross section editor for each cross section. Any of the n values may be changed at any cross section. Often three values are not enough to adequately describe the lateral roughness variation in the cross section; in this case the "Horizontal Variation of n Value" should be selected from the "Options" menu of the cross section editor. If n values change within the channel, the criterion described in Chapter 2, under composite n values, is used to determine whether the n values should be converted to a composite value using Equation 2-5.

Equivalent Roughness "k". An equivalent roughness parameter "k",

commonly used in the hydraulic design of channels, is provided as an option for describing boundary roughness in HEC-RAS. Equivalent roughness, sometimes called "roughness height," is a measure of the linear dimension of roughness elements, but is not necessarily equal to the actual, or even the average, height of these elements. In fact, two roughness elements with different linear dimensions may have the same "k" value because of differences in shape and orientation [Chow, 1959].

The advantage of using equivalent roughness "k" instead of Manning's "n" is that "k" reflects changes in the friction factor due to stage, whereas Manning's "n" alone does not. This influence can be seen in the definition of Chezy's "C" (English units) for a rough channel (Equation 2-6, USACE, 1991):

$$C = 32.6 \log_{10}\left[\frac{12.2R}{k}\right] \tag{3-4}$$

where: C = Chezy roughness coefficient

R = hydraulic radius (feet)

k = equivalent roughness (feet)

Note that as the hydraulic radius increases (which is equivalent to an increase in stage), the friction factor "C" increases. In HEC-RAS, "k" is converted to a Manning's "n" by using the above equation and equating the Chezy and Manning's equations (Equation 2-4, USACE, 1991) to obtain the following:

English Units:

$$n = \frac{1.486R^{1/6}}{32.6 \log_{10}\left[12.2\frac{R}{k}\right]} \tag{3-5}$$

Metric Unit:

$$n = \frac{R^{1/6}}{18 \log_{10}\left[12.2\frac{R}{k}\right]} \tag{3-6}$$

where: n = Manning's roughness coefficient

Again, this equation is based on the assumption that all channels (even concrete-lined channels) are "hydraulically rough." A graphical illustration of this conversion is available [USACE, 1991].

Horizontal variation of "k" values is described in the same manner as horizontal variation of Manning's "n" values. See chapter 6 of the HEC-RAS user's manual, to learn how to enter k values into the program. Up to twenty

values of "k" can be specified for each cross section.

Tables and charts for determining "k" values for concrete-lined channels are provided in EM 1110-2-1601 [USACE, 1991]. Values for riprap-lined channels may be taken as the theoretical spherical diameter of the median stone size. Approximate "k" values [Chow, 1959] for a variety of bed materials, including those for natural rivers are shown in Table 3.2.

Table 3.2
Equivalent Roughness Values of Various Bed Materials

	k (Feet)
Brass, Cooper, Lead, Glass	0.0001 - 0.0030
Wrought Iron, Steel	0.0002 - 0.0080
Asphalted Cast Iron	0.0004 - 0.0070
Galvanized Iron	0.0005 - 0.0150
Cast Iron	0.0008 - 0.0180
Wood Stave	0.0006 - 0.0030
Cement	0.0013 - 0.0040
Concrete	0.0015 - 0.0100
Drain Tile	0.0020 - 0.0100
Riveted Steel	0.0030 - 0.0300
Natural River Bed	0.1000 - 3.0000

The values of "k" (0.1 to 3.0 ft.) for natural river channels are normally much larger than the actual diameters of the bed materials to account for boundary irregularities and bed forms.

Contraction and Expansion Coefficients. Contraction or expansion of flow due to changes in the cross section is a common cause of energy losses within a reach (between two cross sections). Whenever this occurs, the loss is computed from the contraction and expansion coefficients specified on the cross section data editor. The coefficients, which are applied between cross sections, are specified as part of the data for the upstream cross section. The coefficients are multiplied by the absolute difference in velocity heads between the current cross section and the next cross section downstream, which gives the energy loss caused by the transition (Equation 2-2 of Chapter 2). Where the change in river cross section is small, and the flow is subcritical, coefficients of contraction and expansion are typically on the order of 0.1 and 0.3, respectively. When the change in effective cross section area is abrupt such as at bridges, contraction and expansion coefficients of 0.3 and 0.5 are often used. On occasion, the coefficients of contraction and expansion around bridges and culverts may be as high as 0.6 and 0.8, respectively. These values may be changed at any cross section. For

additional information concerning transition losses and for information on bridge loss coefficients, see chapter 5, Modeling Bridges. Typical values for contraction and expansion coefficients, for subcritical flow, are shown in Table 3.3 below.

Table 3.3
Subcritical Flow Contraction and Expansion Coefficients

	Contraction	Expansion
No transition loss computed	0.0	0.0
Gradual transitions	0.1	0.3
Typical Bridge sections	0.3	0.5
Abrupt transitions	0.6	0.8

The maximum value for the contraction and expansion coefficient is one (1.0). **In general, the empirical contraction and expansion coefficients should be lower for supercritical flow.** In supercritical flow the velocity heads are much greater, and small changes in depth can cause large changes in velocity head. Using contraction and expansion coefficients that would be typical for subcritical flow can result in over estimation of the energy losses and oscillations in the computed water surface profile. In constructed trapezoidal and rectangular channels, designed for supercritical flow, the user should set the contraction and expansion coefficients to zero in the reaches where the cross sectional geometry is not changing shape. In reaches where the flow is contracting and expanding, the user should select contraction and expansion coefficients carefully. Typical values for gradual transitions in supercritical flow would be around 0.05 for the contraction coefficient and 0.10 for the expansion coefficient. As the natural transitions begin to become more abrupt, it may be necessary to use higher values, such as 0.1 for the contraction coefficient and 0.2 for the expansion coefficient. If there is no contraction or expansion, the user may want to set the coefficients to zero for supercritical flow.

Stream Junction Data

Stream junctions are defined as locations where two or more streams come together or split apart. Junction data consists of reach lengths across the junction and tributary angles (only if the momentum equation is selected). Reach lengths across the junction are entered in the Junction Data editor. This allows for the lengths across very complicated confluences (e.g., flow splits) to be accommodated. An example of this is shown in Figure 3.9.

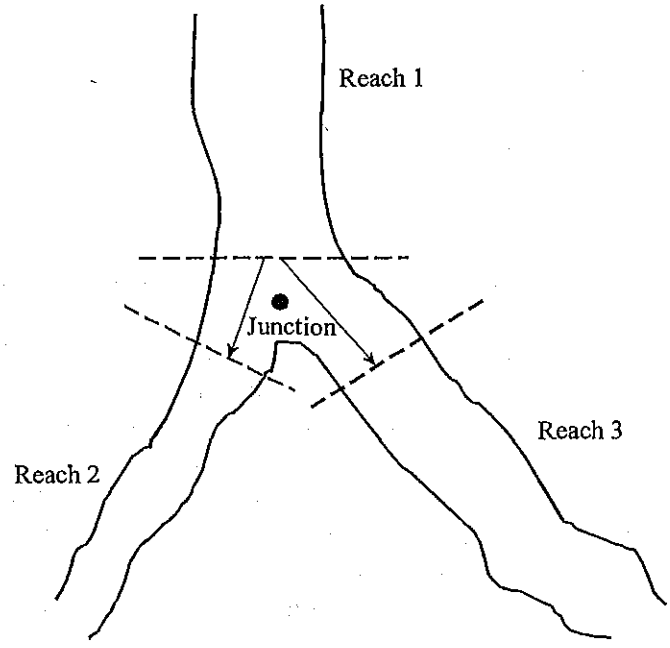

Figure 3.9 Example of a Stream Junction

As shown in Figure 3.9, using downstream reach lengths, for the last cross section in Reach 1, would not adequately describe the lengths across the junction. It is therefore necessary to describe lengths across junctions in the Junction Data editor. For the example shown in Figure 3.9, two lengths would be entered. These lengths should represent the average distance that the water will travel from the last cross section in Reach 1 to the first cross section of the respective reaches.

In general, the cross sections that bound a junction should be placed as close together as possible. This will minimize the error in the calculation of energy losses across the junction.

In HEC-RAS a junction can be modeled by either the energy equation (Equation 2-1 of chapter 2) or the momentum equation. The energy equation does not take into account the angle of any tributary coming in or leaving the main stream, while the momentum equation does. In most cases, the amount of energy loss due to the angle of the tributary flow is not significant, and using the energy equation to model the junction is more than adequate. However, there are situations where the angle of the tributary can cause significant energy losses. In these situations it would be more appropriate to use the momentum approach. When the momentum approach is selected, an angle for all tributaries of the main stem must be entered. A detailed description of how junction calculations are made can be found in Chapter 4 of this manual.

Steady Flow Data

Steady flow data are required in order to perform a steady water surface profile calculation. Steady flow data consist of: flow regime; boundary conditions; and peak discharge information.

Flow Regime

Profile computations begin at a cross section with known or assumed starting conditions and proceed upstream for subcritical flow or downstream for supercritical flow. The flow regime (subcritical, supercritical, or mixed flow regime) is specified on the Steady Flow Analysis window of the user interface. Subcritical profiles computed by the program are constrained to critical depth or above, and supercritical profiles are constrained to critical depth or below. In cases where the flow regime will pass from subcritical to supercritical, or supercritical to subcritical, the program should be run in a mixed flow regime mode. For a detailed discussion of mixed flow regime calculations, see Chapter 4 of this manual.

Boundary Conditions

Boundary conditions are necessary to establish the starting water surface at the ends of the river system (upstream and downstream). A starting water surface is necessary in order for the program to begin the calculations. In a subcritical flow regime, boundary conditions are only necessary at the downstream ends of the river system. If a supercritical flow regime is going to be calculated, boundary conditions are only necessary at the upstream ends of the river system. If a mixed flow regime calculation is going to be made, then boundary conditions must be entered at all ends of the river system.

The boundary conditions editor contains a table listing every reach. Each reach has an upstream and a downstream boundary condition. Connections to junctions are considered internal boundary conditions. Internal boundary conditions are automatically listed in the table, based on how the river system was defined in the geometric data editor. The user is only required to enter the necessary external boundary conditions. There are four types of boundary conditions available to the user:

Known Water Surface Elevations - For this boundary condition the user must enter a known water surface elevation for each of the profiles to be computed.

Critical Depth - When this type of boundary condition is selected, the user is not required to enter any further information. The program will calculate critical depth for each of the profiles and use that as the boundary condition.

Normal Depth - For this type of boundary condition, the user is required to enter an energy slope that will be used in calculating normal depth (using Manning's equation) at that location. A normal depth will be calculated for each profile based on the user-entered slope. In general, the energy slope can be approximated by using the average slope of the channel, or the average slope of the water surface in the vicinity of the cross section.

Rating Curve - When this type of boundary condition is selected, a pop up window appears allowing the user to enter an elevation versus flow rating curve. For each profile, the elevation is interpolated from the rating curve given the flow, using linear interpolation between the user-entered points.

Whenever the water surface elevations at the boundaries of the study are unknown; and a user defined water surface is required at the boundary to start the calculations; the user must either estimate the water surface, or select normal depth or critical depth. Using an estimated water surface will incorporate an error in the water surface profile in the vicinity of the boundary condition. If it is important to have accurate answers at cross sections near the boundary condition, additional cross sections should be added. If a subcritical profile is being computed, then additional cross sections need only be added below the downstream boundaries. If a supercritical profile is being computed, then additional cross sections should be added upstream of the relevant upstream boundaries. If a mixed flow regime profile is being computed, then cross sections should be added upstream and downstream of all the relevant boundaries. In order to test whether the added cross sections are sufficient for a particular boundary condition, the user should try several different starting elevations at the boundary condition, for the same discharge. If the water surface profile converges to the same answer, by the time the computations get to the cross sections that are in the study area, then enough sections have been added, and the boundary condition is not affecting the answers in the study area.

Discharge Information

Discharge information is required at each cross section in order to compute the water surface profile. Discharge data are entered from upstream to downstream for each reach. At least one flow value must be entered for each reach in the river system. Once a flow value is entered at the upstream end of a reach, it is assumed that the flow remains constant until another flow value is encountered with the same reach. The flow rate can be changed at any cross section within a reach. However, the flow rate cannot be changed in the middle of a bridge, culvert, or stream junction. Flow data must be entered for the total number of profiles that are to be computed.

Unsteady Flow Data

Unsteady flow data are required in order to perform an unsteady flow analysis. Unsteady flow data consists of boundary conditions (external and internal), as well as initial conditions.

Boundary Conditions

Boundary conditions must be established at all of the open ends of the river system being modeled. Upstream ends of a river system can be modeled with the following types of boundary conditions: flow hydrograph; stage hydrograph; flow and stage hydrograph. Downstream ends of the river system can be modeled with the following types of boundary conditions: rating curve, normal depth (Manning's equation); stage hydrograph; flow hydrograph; stage and flow hydrograph.

Boundary conditions can also be established at internal locations within the river system. The user can specify the following types of boundary conditions at internal cross sections: lateral inflow hydrograph; uniform lateral inflow hydrograph; groundwater interflow. Additionally, any gated structures that are defined within the system (inline, lateral, or between storage areas) could have the following types of boundary conditions in order to control the gates: time series of gate openings; elevation controlled gate; navigation dam; or internal observed stage and flow.

Initial Conditions

In addition to boundary conditions, the user is required to establish the initial conditions (flow and stage) at all nodes in the system at the beginning of the simulation. Initial conditions can be established in two different ways. The most common way is for the user to enter flow data for each reach, and then have the program compute water surface elevations by performing a steady flow backwater analysis. A second method can only be done if a previous run was made. This method allows the user to write a file of flow and stage from

a previous run, which can then be used as the initial conditions for a subsequent run.

In addition to establishing the initial conditions within the river system, the user must define the starting water surface elevation in any storage areas that are defined. This is accomplished from the initial conditions editor. The user must enter a stage for each storage area within the system.

For more information on unsteady flow data, please review chapter 8 of the HEC-RAS User's manual.

CHAPTER 4

Overview of Optional Capabilities

HEC-RAS has numerous optional capabilities that allow the user to model unique situations. These capabilities include: multiple profile analysis; multiple plan analysis; optional friction loss equations; cross section interpolation; mixed flow regime calculations; modeling stream junctions; flow distribution calculations; and split flow optimization.

Contents

Multiple Profile Analysis

HEC-RAS can compute up to 500 profiles, for the same geometric data, within a single execution of the steady flow computations. The number of profiles to be computed is defined as part of the steady flow data. When more than one profile is requested, the user must ensure that flow data and boundary conditions are established for each profile. Once a multiple profile computation is made, the user can view output, in a graphical and tabular mode, for any single profile or combination of profiles.

For an unsteady flow analysis, the user can have detailed output computed for the maximum water surface profile, as well as profiles that represent specific instances in time during the unsteady flow simulation. The user can request detailed output for up to 500 specific time slices.

Warning, as the number of profiles (steady flow) or time slices (unsteady flow) is increased, the size of the output files will also increase.

Multiple Plan Analysis

The HEC-RAS system has the ability to compute water surface profiles for a number of different characterizations (plans) of the river system. Modifications can be made to the geometry and/or flow data, and then saved in separate files. Plans are then formulated by selecting a particular geometry file and a particular flow file. The multiple plan option is useful when, for example, a comparison of existing conditions and future channel modifications are to be analyzed. Channel modifications can consist of any change in the geometric data, such as: the addition of a bridge or culvert; channel improvements; the addition of levees; changes in n values due to development or changes in vegetation; etc. The multiple plan option can also be used to perform a design of a specific geometric feature. For example, if you were sizing a bridge opening, a separate geometry file could be developed for a base condition (no bridge), and then separate geometry files could be developed for each possible bridge configuration. A plan would then consist of selecting a flow file and one of the geometry files. Computations are performed for each plan individually. Once the computations are performed for all the plans, the user can then view output in a graphical and tabular mode for any single plan or combination of plans.

Optional Friction Loss Equations

This option can be used in both steady flow and unsteady flow water surface profile calculations. The friction loss between adjacent cross sections is computed as the product of the representative rate of friction loss (friction slope) and the weighted-average reach length. The program allows the user

to select from the following previously defined friction loss equations:

- Average Conveyance (Equation 2-13)
- Average Friction Slope (Equation 2-14)
- Geometric Mean Friction Slope (Equation 2-15)
- Harmonic Mean Friction Slope (Equation 2-16)

Any of the above friction loss equations will produce satisfactory estimates provided that reach lengths are not too long. The advantage sought in alternative friction loss formulations is to be able to maximize reach lengths without sacrificing profile accuracy.

Equation 2-13, the average conveyance equation, is the friction loss formulation that has been set as the default method within HEC-RAS. This equation is viewed as giving the best overall results for a range of profile types (M1, M2, etc). Research (Reed and Wolfkill, 1976) indicates that Equation 2-14 is the most suitable for M1 profiles. (Suitability as indicated by Reed and Wolfkill is the most accurate determination of a known profile with the least number of cross sections.) Equation 2-15 is the standard friction loss formulation used in the FHWA/USGS step-backwater program WSPRO (Sherman, 1990). Equation 2-16 has been shown by Reed and Wolfkill to be the most suitable for M2 profiles.

Another feature of this capability is to select the most appropriate of the preceding four equations on a cross section by cross section basis depending on flow conditions (e.g., M1, S1, etc.) within the reach. At present, however, the criteria for this automated method (shown in Table 4.1), does not select the best equation for friction loss analysis in reaches with significant lateral expansion, such as the reach below a contracted bridge opening.

The selection of friction loss equations is accomplished from the Options menu on the Steady Flow Analysis window.

Table 4.1
Criteria Utilized to Select Friction Equation

Profile Type	Is friction slope at current cross section greater than friction slope at preceding cross section?	Equation Used
Subcritical (M1, S1)	Yes	Average Friction Slope (2-14)
Subcritical (M2)	No	Harmonic Mean (2-16)
Supercritical (S2)	Yes	Average Friction Slope (2-14)
Supercritical (M3, S3)	No	Geometric Mean (2-15)

Cross Section Interpolation

Occasionally it is necessary to supplement surveyed cross section data by interpolating cross sections between two surveyed sections. Interpolated cross sections are often required when the change in velocity head is too large to accurately determine the change in the energy gradient. An adequate depiction of the change in energy gradient is necessary to accurately model friction losses as well as contraction and expansion losses. When cross sections are spaced too far apart, the program may end up defaulting to critical depth.

The HEC-RAS program has the ability to generate cross sections by interpolating the geometry between two user entered cross sections. The geometric interpolation routines in HEC-RAS are based on a string model, as shown in Figure 4.1

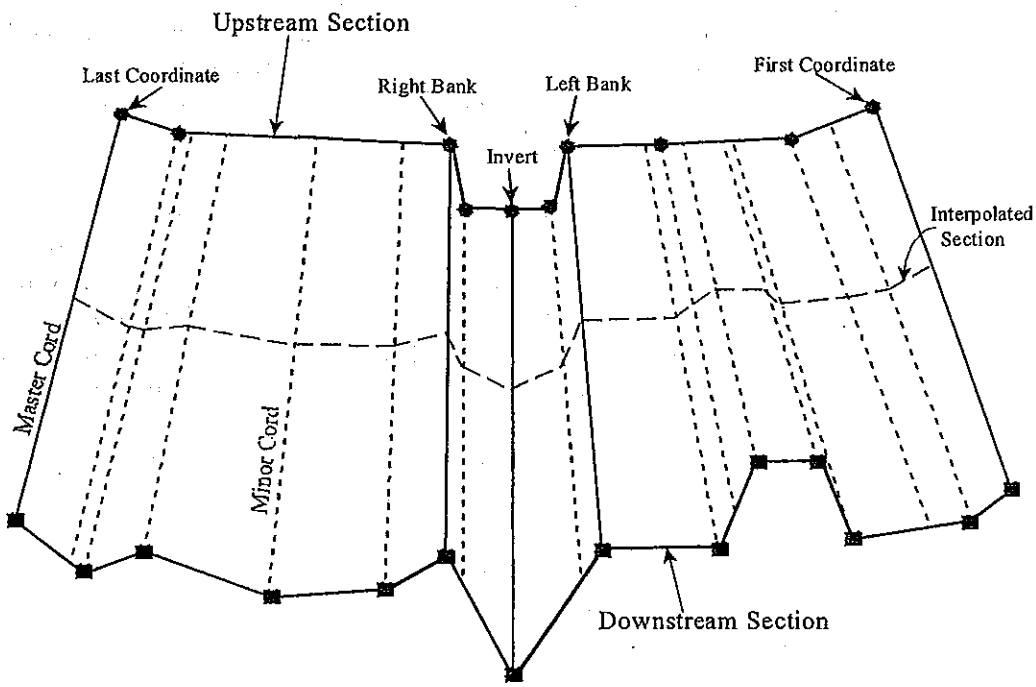

Figure 4.1 String Model for Geometric Cross Section Interpolation

The string model in HEC-RAS consists of cords that connect the coordinates of the upstream and downstream cross sections. The cords are classified as "Master Cords" and "Minor Cords." The master cords are defined explicitly as to the number and starting and ending location of each cord. The default number of master cords is five. The five default master cords are based on the following location criteria:

1. First coordinate of the cross section (May be equal to left bank).

2. Left bank of main channel (Required to be a master cord).

3. Minimum elevation point in the main channel.

4. Right bank of main channel (Required to be a master cord).

5. Last coordinate of the cross section (May be equal to right bank).

The interpolation routines are not restricted to a set number of master cords. At a minimum, there must be two master cords, but there is no maximum. Additional master cords can be added by the user. This is explained in Chapter 6 of the HEC-RAS user's manual, under cross section interpolation.

The minor cords are generated automatically by the interpolation routines. A minor cord is generated by taking an existing coordinate in either the upstream or downstream section and establishing a corresponding coordinate at the opposite cross section by either matching an existing coordinate or interpolating one. The station value at the opposite cross section is determined by computing the proportional distance that the known coordinate represents between master chords, and then applying the proportion to the distance between master cords of the opposite section. The number of minor cords will be equal to the sum of all the coordinates in the upstream and downstream sections minus the number of master cords.

Once all the minor cords are computed, the routines can then interpolate any number of sections between the two known cross sections. Interpolation is accomplished by linearly interpolating between the elevations at the ends of a cord. Interpolated points are generated at all of the minor and master cords. The elevation of a particular point is computed by distance weighting, which is based on how far the interpolated cross section is from the user known cross sections.

The interpolation routines will also interpolate roughness coefficients (Manning's n). Interpolated cross section roughness is based on a string model similar to the one used for geometry. Cords are used to connect the breaks in roughness coefficients of the upstream and downstream sections. The cords are also classified as master and minor cords. The default number of master cords is set to four, and are located based on the following criteria:

1. First coordinate of the cross section (may be equal to left bank).

2. Left bank of main channel.

3. Right bank of main channel.

4. Last coordinate of the cross section (may be equal to right bank).

When either of the two cross sections has more than three n values, additional minor cords are added at all other n value break points. Interpolation of roughness coefficients is then accomplished in the same manner as the geometry interpolation.

In addition to the Manning's n values, the following information is interpolated automatically for each generated cross section: downstream reach lengths; main channel bank stations; contraction and expansion coefficients; normal ineffective flow areas; levees; and normal blocked obstructions. Ineffective flow areas, levees, and blocked obstructions are only interpolated if both of the user-entered cross sections have these features turned on.

Cross section interpolation is accomplished from the user interface. To learn how to perform the interpolation, review the section on interpolating in Chapter 6 of the HEC-RAS user's manual.

Mixed Flow Regime Calculations

The HEC-RAS software has the ability to perform subcritical, supercritical, or mixed flow regime calculations. The Specific Force equation is used in HEC-RAS to determine which flow regime is controlling, as well as locating any hydraulic jumps. The equation for Specific Force is derived from the momentum equation (Equation 2-37). When applying the momentum equation to a very short reach of river, the external force of friction and the force due to the weight of water are very small, and can be ignored. The momentum equation then reduces to the following equation:

$$\frac{Q_1^2 \beta_1}{g A_1} + A_1 \bar{Y}_1 = \frac{Q_2^2 \beta_2}{g A_2} + A_2 \bar{Y}_2 \qquad (4\text{-}1)$$

Where: Q = Discharge at each section
β = Momentum coefficient (similar to alpha)
A = Total flow area
$\bar{Y}$ = Depth from the water surface to centroid of the area
g = Gravitational acceleration

The two sides of the equation are analogous, and may be expressed for any channel section as a general function:

$$SF = \frac{Q^2 \beta}{g A} + A\bar{Y} \qquad (4\text{-}2)$$

The generalized function (equation 4-2) consists of two terms. The first term is the momentum of the flow passing through the channel cross section per unit time. This portion of the equation is considered the dynamic component. The second term represents the momentum of the static component, which is the force exerted by the hydrostatic pressure of the water. Both terms are essentially a force per unit weight of water. The sum of the two terms is called the Specific Force (Chow, 1959).

When the specific force equation is applied to natural channels, it is written in the following manner:

$$SF = \frac{Q^2 \beta}{g A_m} + A_t \bar{Y} \qquad (4\text{-}3)$$

Where: A_m = Flow area in which there is motion
A_t = Total flow area, including ineffective flow areas

The mixed flow regime calculations for steady flow analysis in HEC-RAS are performed as follows:

1. First, a subcritical water surface profile is computed starting from a known downstream boundary condition. During the subcritical calculations, all locations where the program defaults to critical depth are flagged for further analysis.

2. Next the program begins a supercritical profile calculation starting upstream. The program starts with a user specified upstream boundary condition. If the boundary condition is supercritical, the program checks to see if it has a greater specific force than the previously computed subcritical water surface at this location. If the supercritical boundary condition has a greater specific force, then it is assumed to control, and the program will begin calculating a supercritical profile from this section. If the subcritical answer has a greater specific force, then the program begins searching downstream to find a location where the program defaulted to critical depth in the subcritical run. When a critical depth is located, the program uses it as a boundary condition to begin a supercritical profile calculation.

3. The program calculates a supercritical profile in the downstream direction until it reaches a cross section that has both a valid subcritical and a supercritical answer. When this occurs, the program calculates the specific force of both computed water surface elevations. Whichever answer has the greater specific force is considered to be the correct solution. If the supercritical answer has a greater specific force, the program continues making supercritical calculations in the downstream direction and comparing the specific force of the two solutions. When the program reaches a cross section whose subcritical answer has a greater specific force than the supercritical answer, the program assumes that a hydraulic jump occurred between that section and the previous cross section.

4. The program then goes to the next downstream location that has a critical depth answer and continues the process.

An example mixed flow profile, from HEC-RAS, is shown in Figure 4.2. This example was adapted from problem 9-8, page 245, in Chow's "Open Channel Hydraulics" (Chow, 1959).

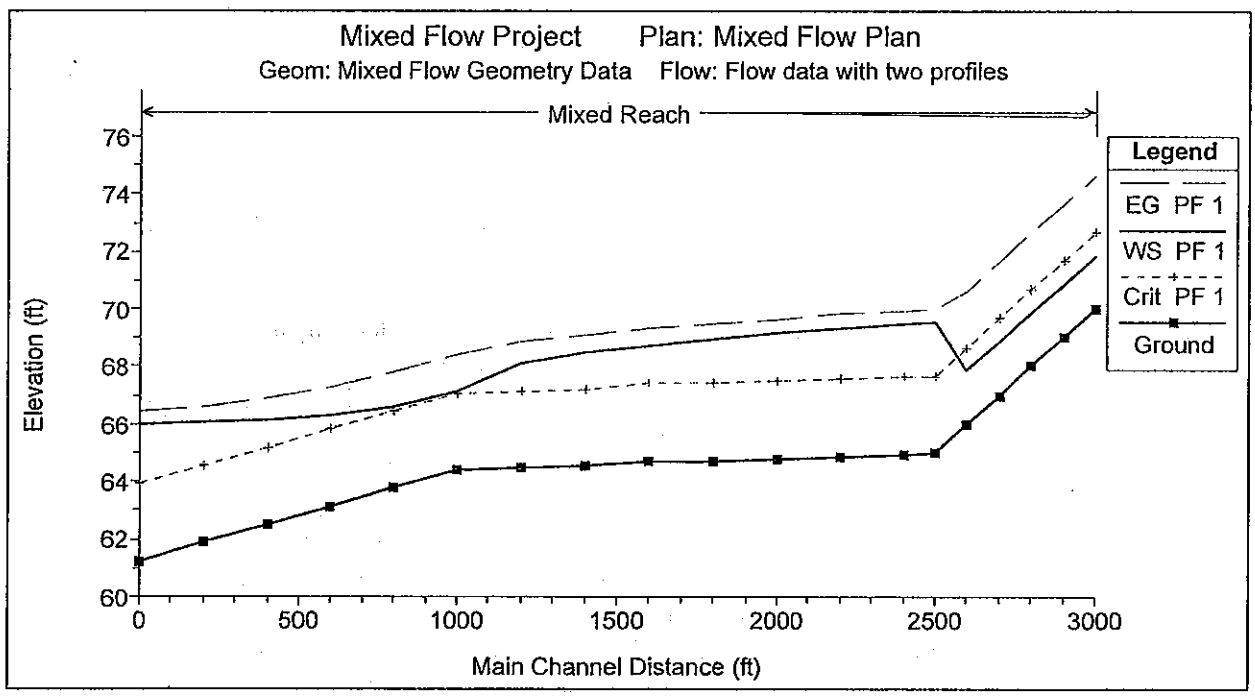

Figure 4.2 Example Mixed Flow Regime Profile from HEC-RAS

As shown in Figure 4.2, the flow regime transitions from supercritical to subcritical just before the first break in slope.

Modeling Stream Junctions

This option is only available for steady flow water surface profile calculations. Stream junctions can be modeled in two different ways within HEC-RAS. The default method is an energy based solution. This method solves for water surfaces across the junction by performing standard step backwater and forewater calculations through the junction. The method does not account for the angle of any of the tributary flows. Because most streams are highly subcritical flow, the influence of the tributary flow angle is often insignificant. If the angle of the tributary plays an important role in influencing the water surface around the junction, then the user should switch to the alternative method available in HEC-RAS, which is a momentum based method. The momentum based method is a one dimensional formulation of the momentum equation, but the angles of the tributaries are used to evaluate the forces associated with the tributary flows. There are six possible flow conditions that HEC-RAS can handle at a junction:

1. Subcritical flow - flow combining
2. Subcritical flow - flow split
3. Supercritical flow - flow combining
4. Supercritical flow- flow split
5. Mixed flow regime - flow combining
6. Mixed flow regime - flow split

The most common situations are the subcritical flow cases (1) and (2). The following is a discussion of how the energy method and the momentum based method are applied to these six flow cases.

Energy Based Junction Method

The energy-based method solves for water surfaces across the junction by performing standard step calculations with the one dimensional energy equation (Equation 2-1). Each of the six cases are discussed individually.

Case 1: *Subcritical Flow - Flow Combining.*

An example junction with flow combining is shown in Figure 4.3. In this case, subcritical flow calculations are performed up to the most upstream section of reach 3. From here, backwater calculations are performed separately across the junction for each of the two upstream reaches. The water surface at reach 1, station 4.0 is calculated by performing a balance of energy from station 3.0 to 4.0. Friction losses are based on the length from station 4.0 to 3.0 and the average friction slope between the two sections. Contraction or expansion losses are also evaluated across the junction. The water surface for the downstream end of reach 2 is calculated in the same manner. The energy equation from station 3.0 to 4.0 is written as follows:

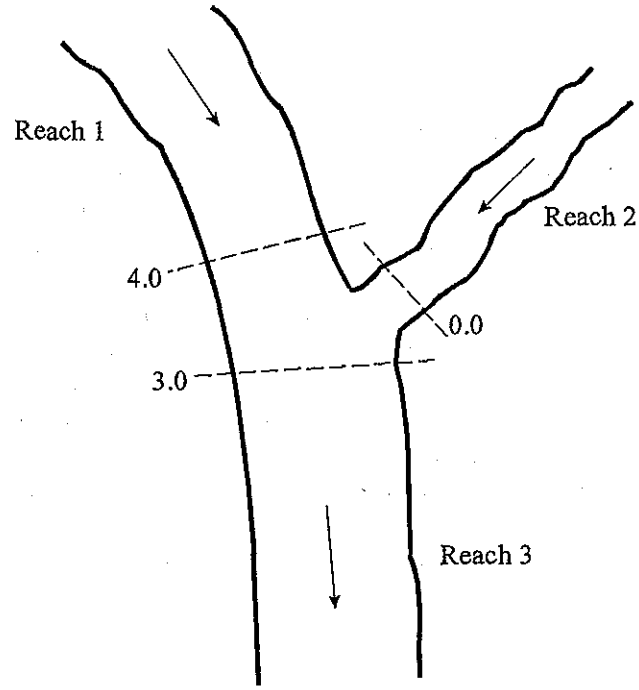

Figure 4.3 Example Junction with Flow Combining.

$$WS_4 + \frac{\alpha_4 V_4^2}{2g} = WS_3 + \frac{\alpha_3 V_3^2}{2g} + L_{4-3}\,\overline{S}_{f_{4-3}} + C\left|\frac{\alpha_4 V_4^2}{2g} - \frac{\alpha_3 V_3^2}{2g}\right| \qquad (4\text{-}4)$$

Case 2: *Subcritical Flow - Flow Split*

For this case, a subcritical water surface profile is calculated for both reaches 2 and 3, up to river stations 2.0 and 3.0 (see Figure 4.4). The program then calculates the specific force (momentum) at the two locations. The cross section with the greater specific force is used as the downstream boundary for calculating the water surface across the junction at river station 4.0. For example, if cross section 3.0 had a greater specific force than section 2.0, the program will compute a backwater profile from station 3.0 to station 4.0 in order to get the water surface at 4.0.

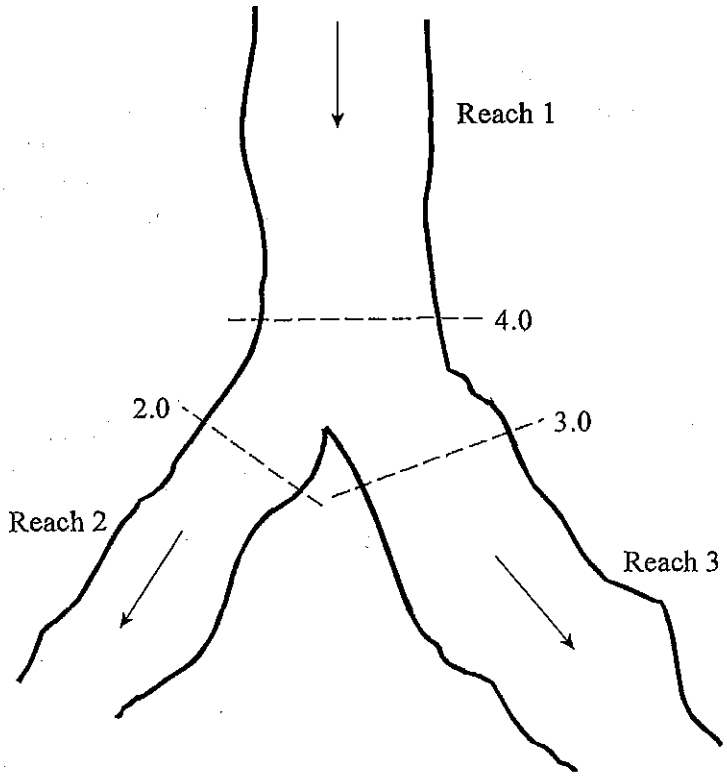

Figure 4.4 Example Flow Split at a Junction

Currently the HEC-RAS program assumes that the user has entered the correct flow for each of the three reaches. In general, the amount of flow going to reach 2 and reach 3 is unknown. In order to obtain the correct flow distribution at the flow split, the user must perform a trial and error process. This procedure involves the following:

1. Assume an initial flow split at the junction.

2. Run the program in order to get energies and water surfaces at all the locations around the junction.

3. Compare the energy at stations 2.0 and 3.0. If they differ by a significant magnitude, then the flow distribution is incorrect. Re-distribute the flow by putting more flow into the reach that had the lower energy.

4. Run the program again and compare the energies. If the energy at stations 2.0 and 3.0 still differ significantly, then re-distribute the flow again.

5. Keep doing this until the energies at stations 2.0 and 3.0 are within a reasonable tolerance.

Ideally it would be better to perform a backwater from station 2.0 to 4.0 and also from station 3.0 to 4.0, and then compare the two computed energies at the same location. Since the program only computes one energy at station 4.0, the user must compare the energies at the downstream cross sections. This procedure assumes that the cross sections around the junction are spaced closely together.

Case 3: *Supercritical Flow - Flow Combining*

In this case, a supercritical water surface profile is calculated for all of reach 1 and 2, down to stations 4.0 and 0.0 (see Figure 4.5). The program calculates the specific force at stations 4.0 and 0.0, and then takes the stream with the larger specific force as the controlling stream. A supercritical forewater calculation is made from the controlling upstream section down to station 3.0.

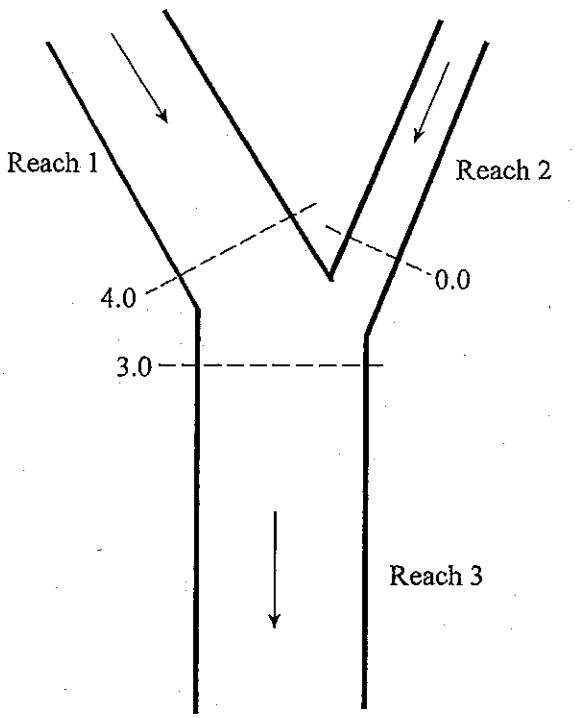

Figure 4.5 Example Supercritical Flow Combine

Case 4: *Supercritical Flow - Flow Split*

In this case a supercritical water surface profile is calculated down to station 4.0 of reach 1 (see Figure 4.6). The water surfaces at sections 3.0 and 2.0 are calculated by performing separate forewater calculations from station 4.0 to station 2.0, and then from station 4.0 to 3.0.

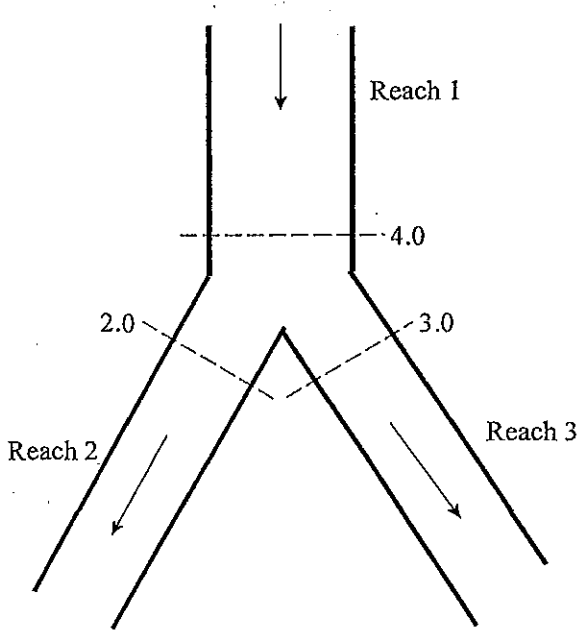

Figure 4.6 Example Supercritical Flow Split

Case 5: *Mixed Flow Regime - Flow Combining*

In the case of mixed flow, a subcritical profile calculation is made through the junction as described previously (see Figure 4.7). If the flow remains subcritical during the supercritical flow calculations, then the subcritical answers are assumed to be correct. If, however, the flow at either or both of the cross sections upstream of the junction is found to have supercritical flow controlling, then the junction must be re-calculated. When one or more of the upstream sections is supercritical, the program will calculate the specific force of all the upstream sections. If the supercritical sections have a greater specific force than the subcritical sections, then the program assumes that supercritical flow will control. The program then makes a forewater calculation from the upstream section with the greatest specific force (let's say section 4.0) to the downstream section (section 3.0).

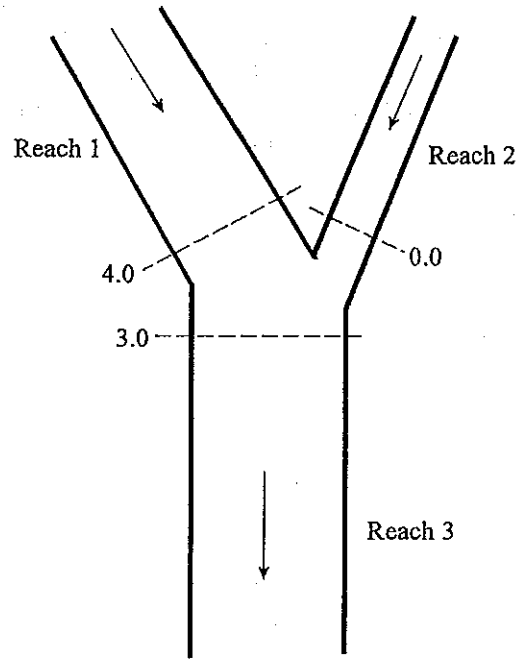

Figure 4.7 Example of Mixed Flow Regime at a Flow Combine

The program next computes the specific force of both the subcritical and supercritical answers at section 3.0. If the supercritical answer at section 3.0 has a lower specific force than the previously computed subcritical answer, then the program uses the subcritical answer and assumes that a hydraulic jump occurred at the junction. If the supercritical answer has a greater specific force, then the program continues downstream with forewater calculations until a hydraulic jump is encountered. Also, any upstream reach that is subcritical must be recomputed. For example, if reach two is subcritical, the water surface at section 0.0 was based on a backwater calculation from section 3.0 to 0.0. If section 3.0 is found to be supercritical, the water surface at section 0.0 is set to critical depth, and backwater calculations are performed again for reach 2. If there are any reaches above reach 2 that are affected by this change, then they are also recomputed.

Case 6: *Mixed Flow Regime - Split Flow*

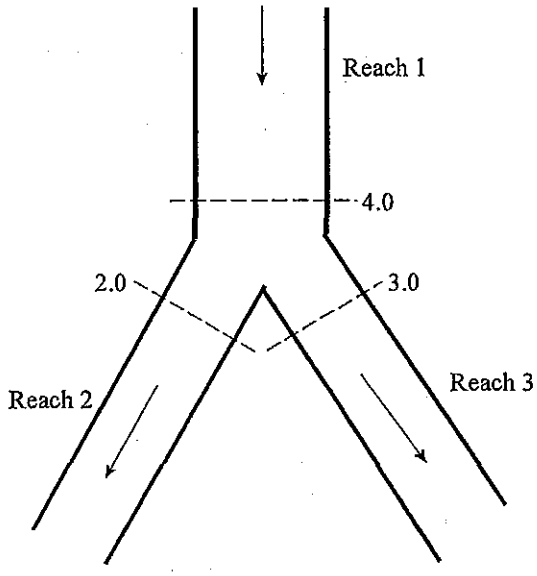

Figure 4.8 Example of Mixed Flow Regime at a Flow Split

In this case, a subcritical profile through the junction is computed as described previously. If during the supercritical flow pass it is found that section 4.0 (Figure 4.8) is actually supercritical, the program will perform forewater calculations across the junction. The program will make a forewater calculation from section 4.0 to 2.0 and then from 4.0 to 3.0. The program will then calculate the specific force of the subcritical and supercritical answers at sections 2.0 and 3.0. Which ever answer has the greater specific force is assumed to be correct for each location. Normal mixed flow regime calculations continue on downstream from the junction.

Momentum Based Junction Method

The user can choose a momentum-based method to solve the junction problem instead of the default energy based method. As described previously, there are six possible flow conditions at the junction. The momentum-based method uses the same logic as the energy based method for solving the junction problem. The only difference is that the momentum-based method solves for the water surfaces across the junction with the momentum equation.

Also, the momentum equation is formulated such that it can take into account the angles at which reaches are coming into or leaving the junction. To use the momentum based method, the user must supply the angle for any reach who's flow lines are not parallel to the main stem's flow lines. An example of a flow combining junction is shown below in Figure 4.9. In this example, angles for both reaches 1 and 2 could be entered. Each angle is taken from a line that is perpendicular to cross-section 3.0 of reach 3.

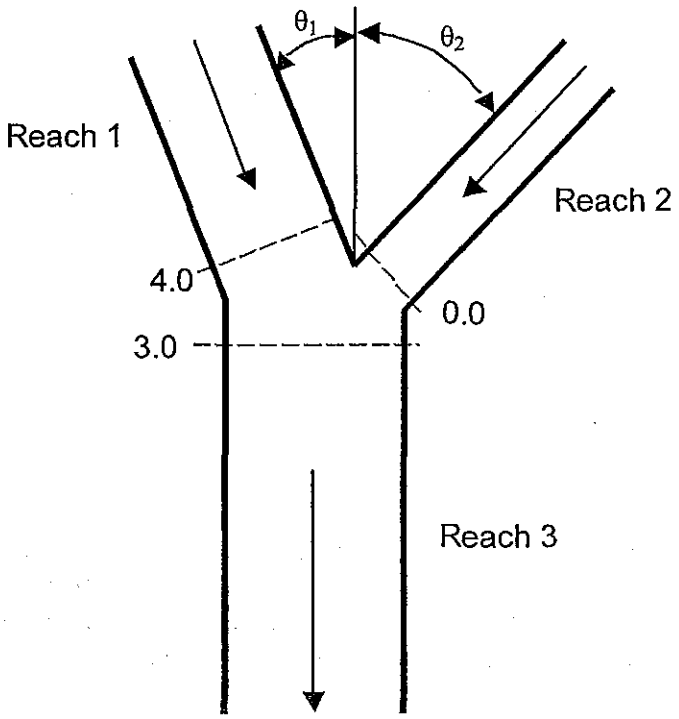

Figure 4.9 Example Geometry for Applying the Momentum Equation to a Flow Combining Junction

For subcritical flow, the water surface is computed up to section 3.0 of reach 3 by normal standard step backwater calculations. If the momentum equation is selected, the program solves for the water surfaces at sections 4.0 and 0.0 by performing a momentum balance across the junction. The momentum balance is written to only evaluate the forces in the X direction (the direction of flow based on cross section 3.0 of reach 3). For this example the equation is as follows:

$$SF_3 = SF_4 \cos\theta_1 - F_{f_{4-3}} + W_{x_{4-3}} + SF_0 \cos\theta_2 - F_{f_{0-3}} + W_{x_{0-3}} \quad (4\text{-}5)$$

Where: SF = Specific Force (as define in Equation 4.3)

The frictional and the weight forces are computed in two segments. For example, the friction and weight forces between sections 4.0 and 3.0 are based on the assumption that the centroid of the junction is half the distance between the two sections. The first portion of the forces are computed from section 4.0 to the centroid of the junction, utilizing the area at cross section 4.0. The second portion of the forces are computed from the centroid of the junction to section 3.0, using a flow weighted area at section 3.0. The equations to compute the friction and weight forces for this example are as follows:

Forces due to friction:

$$F_{f_{4-3}} = \overline{S}_{f_{4-3}} \frac{L_{4-3}}{2} A_4 \cos\theta_1 + \overline{S}_{f_{4-3}} \frac{L_{4-3}}{2} A_3 \frac{Q_4}{Q_3} \quad (4\text{-}6)$$

$$F_{f_{0-3}} = \overline{S}_{f_{0-3}} \frac{L_{0-3}}{2} A_0 \cos\theta_2 + \overline{S}_{f_{0-3}} \frac{L_{0-3}}{2} A_3 \frac{Q_0}{Q_3} \quad (4\text{-}7)$$

Forces due to weight of water:

$$W_{x_{4-3}} = S_{0_{4-3}} \frac{L_{4-3}}{2} A_4 \cos\theta_1 + S_{0_{4-3}} \frac{L_{4-3}}{2} A_3 \frac{Q_4}{Q_3} \quad (4\text{-}8)$$

$$W_{x_{0-3}} = S_{0_{0-3}} \frac{L_{0-3}}{2} A_0 \cos\theta_2 + S_{0_{0-3}} \frac{L_{0-3}}{2} A_3 \frac{Q_0}{Q_3} \quad (4\text{-}9)$$

To solve the momentum balance equation (Equation 4-5) for this example, the following assumptions are made:

1. The water surface elevations at section 4.0 and 0.0 are solved simultaneously, and are assumed to be equal to each other. This is a rough approximation, but it is necessary in order to solve Equation 4-5. Because of this assumption, the cross sections around the junction should be closely spaced in order to minimize the error associated with this assumption.

2. The area used at section 3.0 for friction and weight forces is distributed between the upper two reaches by using a flow weighting. This is necessary in order not to double account for the flow volume and

frictional area.

When evaluating supercritical flow at this type of junction (Figure 4.9), the water surface elevations at sections 4.0 and 0.0 are computed from forewater calculations, and therefore the water surface elevations at section 3.0 can be solved directly from equation 4-5.

For mixed flow regime computations, the solution approach is the same as the energy based method, except the momentum equation is used to solve for the water surfaces across the junction.

An example of applying the momentum equation to a flow split is shown in Figure 4.10 below:

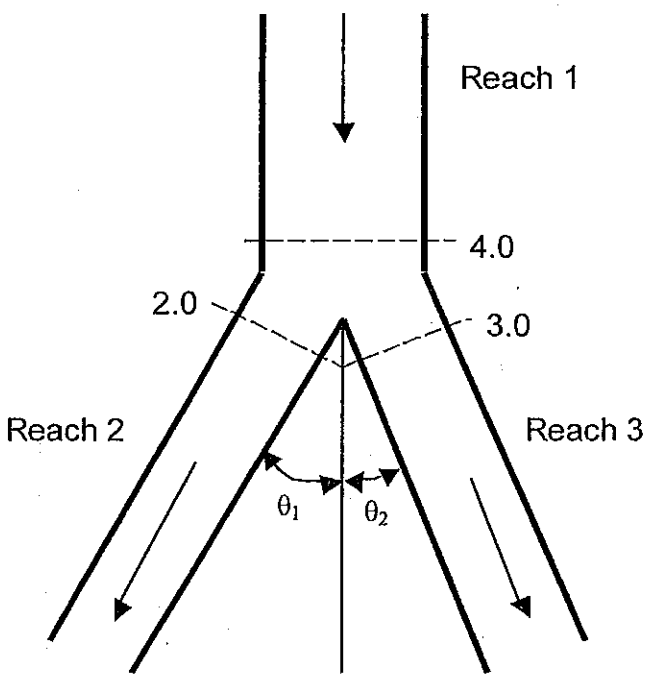

Figure 4.10 Example Geometry for Applying the Momentum Equation To a Flow Split Type of Junction

For the flow split shown in Figure 4.10, the momentum equation is written as follows:

$$SF_4 = SF_2 \cos\theta_1 + F_{f_{4-2}} - W_{x_{4-2}} + SF_3 \cos\theta_2 \; F_{f_{4-3}} - W_{x_{4-3}} \qquad (4\text{-}10)$$

For subcritical flow, the water surface elevation is known at sections 2.0 and 3.0, and the water surface elevation at section 4.0 can be found by solving Equation 4-10. For supercritical flow, the water surface is known at section 4.0 only, and, therefore, the water surface elevations at sections 3.0 and 2.0 must be solved simultaneously. In order to solve Equation 4-10 for supercritical flow, it is assumed that the water surface elevations at sections 2.0 and 3.0 are equal.

Mixed flow regime computations for a flow split are handled in the same manner as the energy based solution, except the momentum equation (Equation 4-10) is used to solve for the water surface elevations across the junction.

Flow Distribution Calculations

The general cross section output shows the distribution of flow in three subdivisions of the cross section: left overbank, main channel, and the right overbank. Additional output, showing the distribution of flow for multiple subdivisions of the left and right overbanks, as well as the main channel, can be requested by the user.

The flow distribution output can be obtained by first defining the locations that the user would like to have this type of output. The user can either select specific locations or all locations in the model. Next, the number of slices for the flow distribution computations must be defined for the left overbank, main channel, and the right overbank. The user can define up to 45 total slices. Each flow element (left overbank, main channel, and right overbank) must have at least one slice. The user can change the number of slices used at each of the cross sections. The final step is to perform the normal profile calculations. During the computations, at each cross section where flow distribution is requested, the program will calculate the flow (discharge), area, wetted perimeter, percentage of conveyance, hydraulic depth, and average velocity for each of the user defined slices. For further details on how to request and view flow distribution output, see Chapters 7 and 8 of the HEC-RAS User's manual.

The computations for the flow distribution are performed after the program has calculated a water surface elevation and energy by the normal methodology described in Chapter 2 of this manual. The flow distribution computations are performed as follows:

1. First, the water surface is computed in the normal manner of using the three flow subdivisions (left overbank, main channel, and right overbank), and balancing the energy equation.

2. Once a water surface elevation is computed, the program slices the cross section into the user defined flow distribution slices, and then computes an area, wetted perimeter, and hydraulic depth (area over top width) for each slice.

3. Using the originally computed energy slope (S_f), the cross section Manning's n values, the computed area and wetted perimeter for each slice, and Manning's equation, the program computes the conveyance and percentage of discharge for each of the slices.

4. The program sums up the computed conveyance for each of the slices. In general, the slice computed conveyance will not be the same as the originally computed conveyance (from the traditional methods for conveyance subdivision described in Chapter 2 of this manual). Normally, as a cross section is subdivided further and further, the computed conveyance, for a given water surface elevation, will increase.

5. In order to correct for the difference in computed conveyances, the program computes a ratio of the original total conveyance (from the normal calculations) divided by the total slice conveyance. This ratio is then applied to each of the slices, in order to achieve the same conveyance as was originally computed.

6. The final step is to compute an average velocity for each slice. The average velocity is computed by taking the discharge and dividing by the area for each of the user defined slices.

An example of the flow distribution output is shown in Figure 4.11.

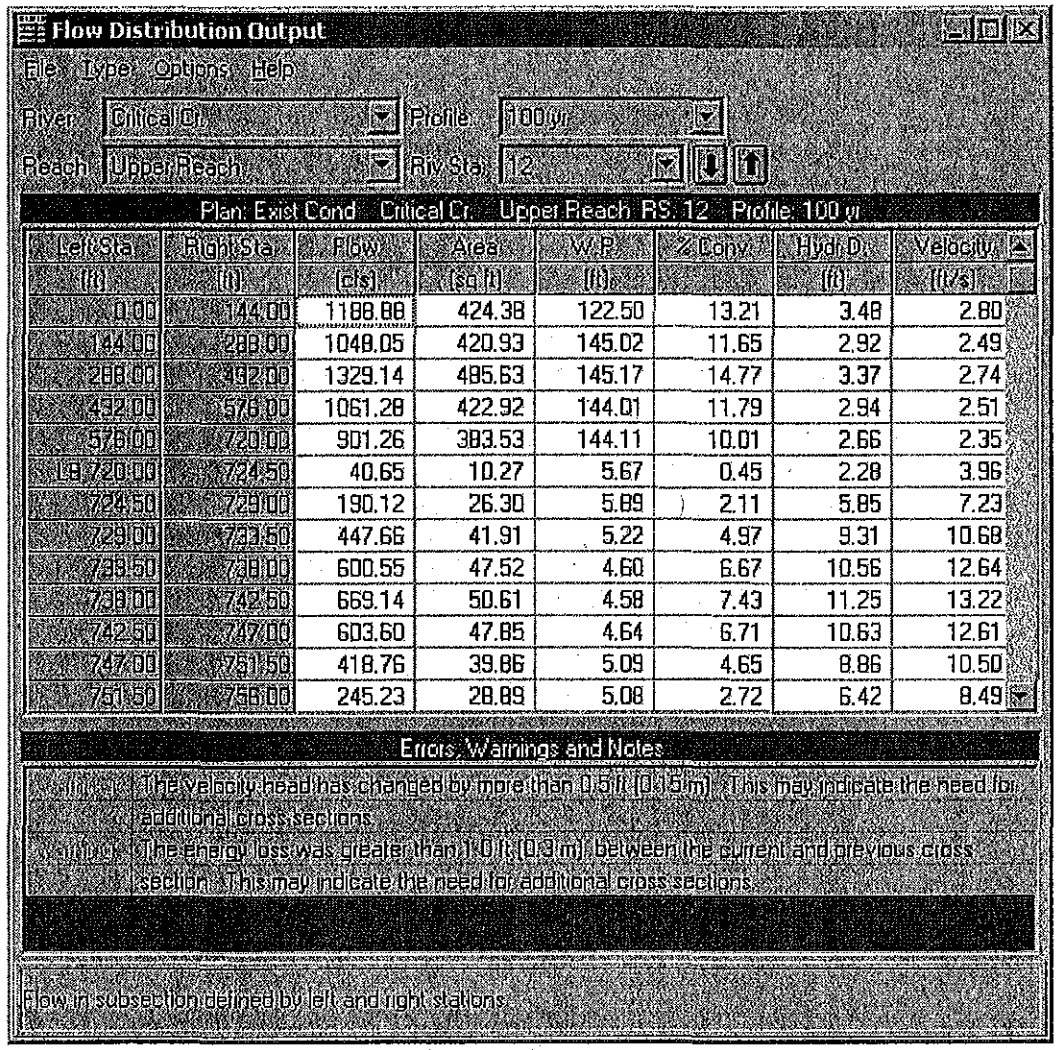

Figure 4.11 Example Output for the Flow Distribution Option.

In general, the results of the flow distribution computations should be used cautiously. Specifically, the velocities and percentages of discharge are based on the results of a one-dimensional hydraulic model. A true velocity and flow distribution varies vertically as well as horizontally. To achieve such detail, the user would need to use a three-dimensional hydraulic model, or go out and measure the flow distribution in the field. While the results for the flow distribution, provided by HEC-RAS, are better than the standard three subdivisions (left overbank, main channel, and right overbank) provided by the model, the values are still based on average estimates of the one-dimensional results. Also, the results obtained from the flow distribution option can vary with the number of slices used for the computations. In general, it is better to use as few slices as possible.

Split Flow Optimization

This feature is for Steady Flow Analyses only. The HEC-RAS software has the capability to optimize flow splits at lateral weirs/spillways, hydraulic connections, storage areas, and stream junctions. This feature is available by selecting "Split Flow Optimizations" from the "Options" menu of the Steady Flow Analysis" window. When this option is selected, a window will appear as shown below.

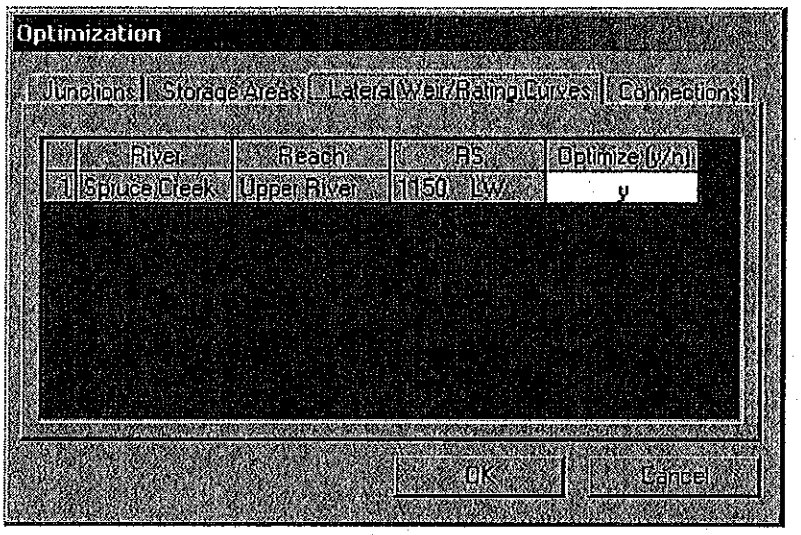

Figure 4.12 Split Flow Optimization Window

When the split flow optimization is turned on, the program will calculate a water surface profile with the first assumed flows. From the computed profile, new flows are calculated for the hydraulic structures and junctions and the profile is re-run. This process continues until the calculated and assumed flows match within a given tolerance. For more information on split flow optimization, please review Example 15 of the Applications Guide.

CHAPTER 5

Modeling Bridges

HEC-RAS computes energy losses caused by structures such as bridges and culverts in three parts. One part consists of losses that occur in the reach immediately downstream from the structure, where an expansion of flow generally takes place. The second part is the losses at the structure itself, which can be modeled with several different methods. The third part consists of losses that occur in the reach immediately upstream of the structure, where the flow is generally contracting to get through the opening. This chapter discusses how bridges are modeled using HEC-RAS. Discussions include: general modeling guidelines; hydraulic computations through the bridge; selecting a bridge modeling approach; and unique bridge problems and suggested approaches.

Contents

General Modeling Guidelines

Considerations for modeling the geometry of a reach of river in the vicinity of a bridge are essentially the same for any of the available bridge modeling approaches within HEC-RAS. Modeling guidelines are provided in this section for locating cross sections; defining ineffective flow areas; and evaluating contraction and expansion losses around bridges.

Cross Section Locations

The bridge routines utilize four user-defined cross sections in the computations of energy losses due to the structure. During the hydraulic computations, the program automatically formulates two additional cross sections inside of the bridge structure. A plan view of the basic cross section layout is shown in Figure 5.1. The cross sections in Figure 5.1 are labeled as river stations 1, 2, 3, and 4 for the purpose of discussion within this chapter. Whenever the user is performing water surface profile computations through a bridge (or any other hydraulic structure), additional cross sections should always be included both downstream and upstream of the bridge. This will prevent any user-entered boundary conditions from affecting the hydraulic results through the bridge.

Cross section 1 is located sufficiently downstream from the structure so that the flow is not affected by the structure (i.e., the flow has fully expanded). This distance (the expansion reach length, L_e) should generally be determined by field investigation during high flows. The expansion distance will vary depending upon the degree of constriction, the shape of the constriction, the magnitude of the flow, and the velocity of the flow.

Table 5.1 offers ranges of expansion ratios, which can be used for different degrees of constriction, different slopes, and different ratios of the overbank roughness to main channel roughness. Once an expansion ratio is selected, the distance to the downstream end of the expansion reach (the distance L_e on Figure 5.1) is found by multiplying the expansion ratio by the average obstruction length (the average of the distances A to B and C to D from Figure 5.1). The average obstruction length is half of the total reduction in floodplain width caused by the two bridge approach embankments. In Table 5.1, b/B is the ratio of the bridge opening width to the total floodplain width, n_{ob} is the Manning n value for the overbank, n_c is the n value for the main channel, and S is the longitudinal slope. The values in the interior of the table are the ranges of the expansion ratio. For each range, the higher value is typically associated with a higher discharge.

Table 5.1
Ranges of Expansion Ratios

		$n_{ob} / n_{c=1}$	$n_{ob} / n_{c=2}$	$n_{ob} / n_{c=4}$
b/B = 0.10	S = 1 ft/mile	1.4 – 3.6	1.3 – 3.0	1.2 – 2.1
	5 ft/mile	1.0 – 2.5	0.8 – 2.0	0.8 – 2.0
	10 ft/mile	1.0 – 2.2	0.8 – 2.0	0.8 – 2.0
b/B = 0.25	S = 1 ft/mile	1.6 – 3.0	1.4 – 2.5	1.2 – 2.0
	5 ft/mile	1.5 – 2.5	1.3 – 2.0	1.3 – 2.0
	10 ft/mile	1.5 – 2.0	1.3 – 2.0	1.3 – 2.0
b/B = 0.50	S = 1 ft/mile	1.4 – 2.6	1.3 – 1.9	1.2 – 1.4
	5 ft/mile	1.3 – 2.1	1.2 – 1.6	1.0 – 1.4
	10 ft/mile	1.3 – 2.0	1.2 – 1.5	1.0 – 1.4

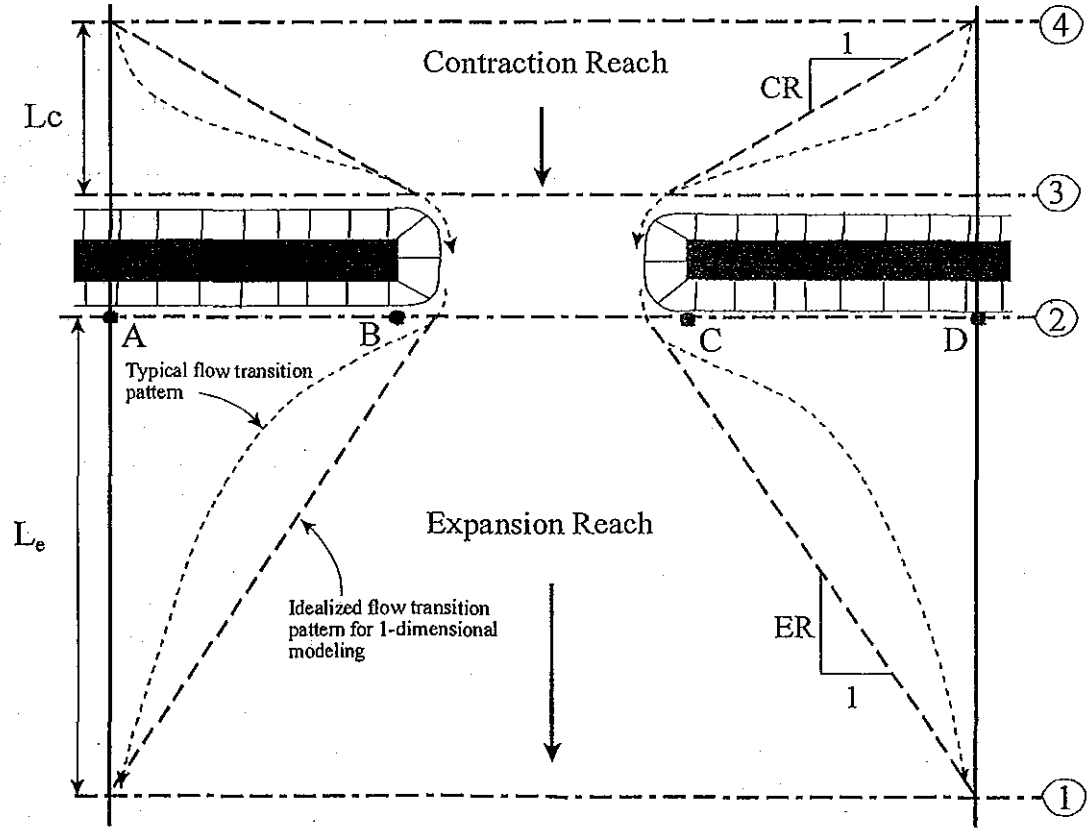

Figure 5.1 Cross Section Locations at a Bridge

A detailed study of flow contraction and expansion zones has been completed by the Hydrologic Engineering Center entitled "Flow Transitions in Bridge Backwater Analysis" (RD-42, HEC, 1995). The purpose of this study was to provide better guidance to hydraulic engineers performing water surface profile computations through bridges. Specifically the study focused on

determining the expansion reach length, L_e; the contraction reach length, L_c; the expansion energy loss coefficient, C_e; and the contraction energy loss coefficient, C_c. A summary of this research, and the final recommendations, can be found in Appendix B of this document.

The user should not allow the distance between cross section 1 and 2 to become so great that friction losses will not be adequately modeled. If the modeler thinks that the expansion reach will require a long distance, then intermediate cross sections should be placed within the expansion reach in order to adequately model friction losses. The ineffective flow option can be used to limit the effective flow area of the intermediate cross sections in the expansion reach.

Cross section 2 is located a short distance downstream from the bridge (i.e., commonly placed at the downstream toe of the road embankment). This cross section should represent the area just outside the bridge.

Cross section 3 should be located a short distance upstream from the bridge (commonly placed at the upstream toe of the road embankment). The distance between cross section 3 and the bridge should only reflect the length required for the abrupt acceleration and contraction of the flow that occurs in the immediate area of the opening. Cross section 3 represents the effective flow area just upstream of the bridge. Both cross sections 2 and 3 will have ineffective flow areas to either side of the bridge opening during low flow and pressure flow profiles. In order to model only the effective flow areas at these two sections, the modeler should use the ineffective flow area option at both of these cross sections.

Cross section 4 is an upstream cross section where the flow lines are approximately parallel and the cross section is fully effective. In general, flow contractions occur over a shorter distance than flow expansions. The distance between cross section 3 and 4 (the contraction reach length, L_c) should generally be determined by field investigation during high flows. Traditionally, the Corps of Engineers used a criterion to locate the upstream cross section one times the average length of the side constriction caused by the structure abutments (the average of the distance from A to B and C to D on Figure 5.1). The contraction distance will vary depending upon the degree of constriction, the shape of the constriction, the magnitude of the flow, and the velocity of the flow. As mentioned previously, the detailed study "Flow Transitions in Bridge Backwater Analysis" (RD-42, HEC, 1995) was performed to provide better guidance to hydraulic engineers performing water surface profile computations through bridges. A summary of this research, and the final recommendations, can be found in Appendix B of this document.

During the hydraulic computations, the program automatically formulates two additional cross sections inside of the bridge structure. The geometry inside of the bridge is a combination of the bounding cross sections (sections 2 and 3) and the bridge geometry. The bridge geometry consists of the bridge deck

and roadway, sloping abutments if necessary, and any piers that may exist. The user can specify different bridge geometry for the upstream and downstream sides of the structure if necessary. Cross section 2 and the structure information on the downstream side of the bridge are used as the geometry just inside the structure at the downstream end. Cross section 3 and the upstream structure information are used as the bridge geometry just inside the structure at the upstream end.

Defining Ineffective Flow Areas

A basic problem in defining the bridge data is the definition of ineffective flow areas near the bridge structure. Referring to Figure 5-1, the dashed lines represent the effective flow boundary for low flow and pressure flow conditions. Therefore, for cross sections 2 and 3, ineffective flow areas to either side of the bridge opening (along distance AB and CD) should not be included as part of the active flow area for low flow or pressure flow.

The bridge example shown in Figure 5.2 is a typical situation where the bridge spans the entire floodway and its abutments obstruct the natural floodplain. This is a similar situation as was shown in plan view in Figure 5.1. The cross section numbers and locations are the same as those discussed in the "Cross Section Locations" section of this chapter. The problem is to convert the natural ground profile at cross sections 2 and 3 from the cross section shown in part B to that shown in part C of Figure 5.2. The elimination of the ineffective overbank areas can be accomplished by redefining the geometry at cross sections 2 and 3 or by using the natural ground profile and requesting the program's ineffective area option to eliminate the use of the overbank area (as shown in part C of Figure 5.2). Also, for high flows (flows over topping the bridge deck), the area outside of the main bridge opening may no longer be ineffective, and will need to be included as active flow area. If the modeler chooses to redefine the cross section, a fixed boundary is used at the sides of the cross section to contain the flow, when in fact a solid boundary is not physically there. The use of the ineffective area option is more appropriate and it does not add wetted perimeter to the active flow boundary above the given ground profile.

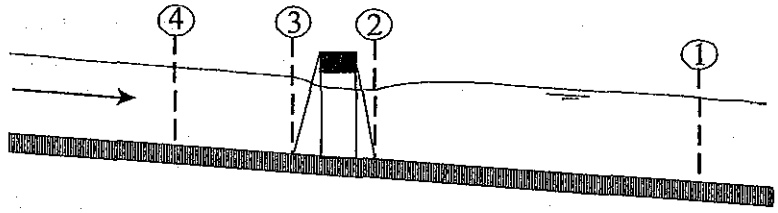

A. Channel Profile and cross section locations

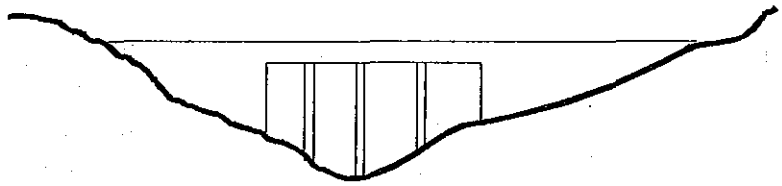

B. Bridge cross section on natural ground

C. Portion of cross sections 2 & 3 that is ineffective for low flow

Figure 5.2 Cross Sections Near Bridges

The ineffective area option is used at sections 2 and 3 to keep all the active flow in the area of the bridge opening until the elevations associated with the left and/or right ineffective flow areas are exceeded by the computed water surface elevation. The program allows the stations and controlling elevations of the left and right ineffective flow areas to be specified by the user. Also, the stations of the ineffective flow areas do not have to coincide with stations of the ground profile, the program will interpolate the ground station.

The ineffective flow areas should be set at stations that will adequately describe the active flow area at cross sections 2 and 3. In general, these stations should be placed outside the edges of the bridge opening to allow for the contraction and expansion of flow that occurs in the immediate vicinity of the bridge. On the upstream side of the bridge (section 3) the flow is contracting rapidly. A practical method for placing the stations of the ineffective flow areas is to assume a 1:1 contraction rate in the immediate vicinity of the bridge. In other words, if cross section 3 is 10 feet from the upstream bridge face, the ineffective flow areas should be placed 10 feet away from each side of the bridge opening. On the downstream side of the bridge (section 2), a similar assumption can be applied. The active flow area on the downstream side of the bridge may be less than, equal to, or greater than the width of the bridge opening. As flow converges into the bridge opening,

depending on the abruptness of the abutments, the active flow area may constrict to be less than the bridge opening. As the flow passes through and out of the bridge it begins to expand. Because of this phenomenon, estimating the stationing of the ineffective flow areas at cross section 2 can be very difficult. In general, the user should make the active flow area equal to the width of the bridge opening or wider (to account for flow expanding), unless the bridge abutments are very abrupt (vertical wall abutments with no wing walls).

The elevations specified for ineffective flow should correspond to elevations where significant weir flow passes over the bridge. For the downstream cross section, the threshold water surface elevation for weir flow is not usually known on the initial run, so an estimate must be made. An elevation below the minimum top-of-road, such as an average between the low chord and minimum top-of-road, can be used as a first estimate.

Using the ineffective area option to define the ineffective flow areas allows the overbank areas to become effective as soon as the ineffective area elevations are exceeded. The assumption is that under weir flow conditions, the water can generally flow across the whole bridge length and the entire overbank in the vicinity of the bridge would be effectively carrying flow up to and over the bridge. If it is more reasonable to assume only part of the overbank is effective for carrying flow when the bridge is under weir flow, then the overbank n values can be increased to reduce the amount of conveyance in the overbank areas under weir flow conditions.

Cross section 3, just upstream from the bridge, is usually defined in the same manner as cross section 2. In many cases the cross sections are identical. The only difference generally is the stations and elevations to use for the ineffective area option. For the upstream cross section, the elevation should initially be set to the low point of the top-of-road. When this is done the user could possibly get a solution where the bridge hydraulics are computing weir flow, but the upstream water surface elevation comes out lower than the top of road. Both the weir flow and pressure flow equations are based on the energy grade line in the upstream cross section. Once an upstream energy is computed from the bridge hydraulics, the program tries to compute a water surface elevation in the upstream cross section that corresponds to that energy. Occasionally the program may get a water surface that is confined by the ineffective flow areas and lower than the minimum top of road. When this happens, the user should decrease the elevations of the upstream ineffective flow areas in order to get them to turn off. Once they turn off, the computed water surface elevation will be much closer to the computed energy gradeline (which is higher than the minimum high chord elevation).

Using the ineffective area option in the manner just described for the two cross sections on either side of the bridge provides for a constricted section when all of the flow is going under the bridge. When the water surface is higher than the control elevations used, the entire cross section is used. The program user should check the computed solutions on either side of the bridge section to ensure they are consistent with the type of flow. That is, for low flow or pressure flow solutions, the output should show the effective area restricted to the bridge opening. When the bridge output indicates weir flow, the solution should show that the entire cross section is effective. During overflow situations, the modeler should ensure that the overbank flow around the bridge is consistent with the weir flow.

Contraction and Expansion Losses

Losses due to contraction and expansion of flow between cross sections are determined during the standard step profile calculations. Manning's equation is used to calculate friction losses, and all other losses are described in terms of a coefficient times the absolute value of the change in velocity head between adjacent cross sections. When the velocity head increases in the downstream direction, a contraction coefficient is used; and when the velocity head decreases, an expansion coefficient is used.

As shown in Figure 5.1, the flow contraction occurs between cross sections 4 and 3, while the flow expansion occurs between sections 2 and 1. The contraction and expansion coefficients are used to compute energy losses associated with changes in the shape of river cross-sections (or effective flow areas). The loss due to expansion of flow is usually larger than the contraction loss, and losses from short abrupt transitions are larger than losses from gradual transitions. Typical values for contraction and expansion coefficients under subcritical flow conditions are shown in Table 5.2 below:

Table 5.2
Subcritical Flow Contraction and Expansion Coefficients

	Contraction	Expansion
No transition loss computed	0.0	0.0
Gradual transitions	0.1	0.3
Typical Bridge sections	0.3	0.5
Abrupt transitions	0.6	0.8

The maximum value for the contraction and expansion coefficient is 1.0. As mentioned previously, a detailed study was completed by the Hydrologic Engineering Center entitled "Flow Transitions in Bridge Backwater Analysis" (HEC, 1995). A summary of this research, as well as recommendations for contraction and expansion coefficients, can be found in Appendix B.

In general, contraction and expansion coefficients for supercritical flow

should be lower than subcritical flow. For typical bridges that are under class C flow conditions (totally supercritical flow), the contraction and expansion coefficients should be around 0.05 and 0.1 respectively. For abrupt bridge transitions under class C flow, values of 0.1 and 0.2 may be more appropriate.

Hydraulic Computations Through the Bridge

The bridge routines in HEC-RAS allow the modeler to analyze a bridge with several different methods without changing the bridge geometry. The bridge routines have the ability to model low flow (Class A, B, and C), low flow and weir flow (with adjustments for submergence on the weir), pressure flow (orifice and sluice gate equations), pressure and weir flow, and highly submerged flows (the program will automatically switch to the energy equation when the flow over the road is highly submerged). This portion of the manual describes in detail how the program models each of these different flow types.

Low Flow Computations

Low flow exists when the flow going through the bridge opening is open channel flow (water surface below the highest point on the low chord of the bridge opening). For low flow computations, the program first uses the momentum equation to identify the class of flow. This is accomplished by first calculating the momentum at critical depth inside the bridge at the upstream and downstream ends. The end with the higher momentum (therefore most constricted section) will be the controlling section in the bridge. If the two sections are identical, the program selects the upstream bridge section as the controlling section. The momentum at critical depth in the controlling section is then compared to the momentum of the flow downstream of the bridge when performing a subcritical profile (upstream of the bridge for a supercritical profile). If the momentum downstream is greater than the critical depth momentum inside the bridge, the class of flow is considered to be completely subcritical (i.e., class A low flow). If the momentum downstream is less than the momentum at critical depth, in the controlling bridge section, then it is assumed that the constriction will cause the flow to pass through critical depth and a hydraulic jump will occur at some distance downstream (i.e., class B low flow). If the profile is completely supercritical through the bridge, then this is considered class C low flow.

Class A low flow. Class A low flow exists when the water surface through the bridge is completely subcritical (i.e., above critical depth). Energy losses through the expansion (sections 2 to 1) are calculated as friction losses and expansion losses. Friction losses are based on a weighted friction slope times a weighted reach length between sections 1 and 2. The weighted friction slope is based on one of the four available alternatives in the HEC-RAS, with the average-conveyance method being the default. This option is user

selectable. The average length used in the calculation is based on a discharge-weighted reach length. Energy losses through the contraction (sections 3 to 4) are calculated as friction losses and contraction losses. Friction and contraction losses between sections 3 and 4 are calculated in the same way as friction and expansion losses between sections 1 and 2.

There are four methods available for computing losses through the bridge (sections 2 to 3):

- Energy Equation (standard step method)

- Momentum Balance

- Yarnell Equation

- FHWA WSPRO method

The user can select any or all of these methods to be computed. This allows the modeler to compare the answers from several techniques all in a single execution of the program. If more than one method is selected, the user must choose either a single method as the final solution or direct the program to use the method that computes the greatest energy loss through the bridge as the final solution at section 3. Minimal results are available for all the methods computed, but detailed results are available for the method that is selected as the final answer. A detailed discussion of each method follows:

Energy Equation (standard step method):

The energy-based method treats a bridge in the same manner as a natural river cross-section, except the area of the bridge below the water surface is subtracted from the total area, and the wetted perimeter is increased where the water is in contact with the bridge structure. As described previously, the program formulates two cross sections inside the bridge by combining the ground information of sections 2 and 3 with the bridge geometry. As shown in Figure 5.3, for the purposes of discussion, these cross sections will be referred to as sections BD (Bridge Downstream) and BU (Bridge Upstream).

The sequence of calculations starts with a standard step calculation from just downstream of the bridge (section 2) to just inside of the bridge (section BD) at the downstream end. The program then performs a standard step through the bridge (from section BD to section BU). The last calculation is to step out of the bridge (from section BU to section 3).

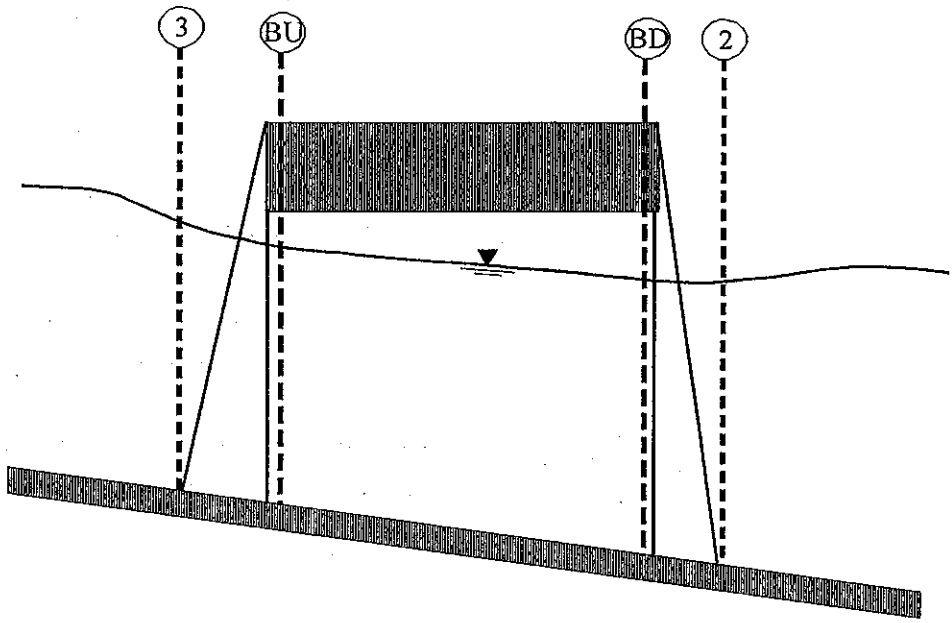

Figure 5.3 Cross Sections Near and Inside the Bridge

The energy-based method requires Manning's n values for friction losses and contraction and expansion coefficients for transition losses. The estimate of Manning's n values is well documented in many hydraulics text books, as well as several research studies. Basic guidance for estimating roughness coefficients is provided in Chapter 3 of this manual. Contraction and expansion coefficients are also provided in Chapter 3, as well as in earlier sections of this chapter. Detailed output is available for cross sections inside the bridge (sections BD and BU) as well as the user entered cross sections (sections 2 and 3).

Momentum Balance Method:

The momentum method is based on performing a momentum balance from cross section 2 to cross-section 3. The momentum balance is performed in three steps. The first step is to perform a momentum balance from cross section 2 to cross-section BD inside the bridge. The equation for this momentum balance is as follows:

$$A_{BD}\,\overline{Y}_{BD} + \frac{\beta_{BD}\,Q_{BD}^2}{g\,A_{BD}} = A_2\,\overline{Y}_2 + \frac{\beta_2\,Q_2^2}{g\,A_2} - A_{p_{BD}}\,\overline{Y}_{p_{BD}} + F_f - W_x \qquad (5\text{-}1)$$

where: A_2, A_{BD} = Active flow area at section 2 and BD, respectively

$A_{p_{BD}}$ = Obstructed area of the pier on downstream side

$\overline{Y}_2, \overline{Y}_{BD}$ = Vertical distance from water surface to center of gravity of flow area A_2 and A_{BD}, respectively

$\overline{Y}_{p_{BD}}$ = Vertical distance from water surface to center of gravity of wetted pier area on downstream side

β_2, β_{BD} = Velocity weighting coefficients for momentum equation

Q_2, Q_{BD} = Discharge

g = Gravitational acceleration

F_f = External force due to friction, per unit weight of water

W_x = Force due to weight of water in the direction of flow, per unit weight of water

The second step is a momentum balance from section BD to BU (see Figure 5.3). The equation for this step is as follows:

$$A_{BU}\,\overline{Y}_{BU} + \frac{\beta_{BU}\,Q_{BU}^2}{g\,A_{BU}} = A_{BD}\,\overline{Y}_{BD} + \frac{\beta_{BD}\,Q_{BD}^2}{g\,A_{BD}} + F_f - W_x \qquad (5\text{-}2)$$

The final step is a momentum balance from section BU to section 3 (see Figure 5.3). The equation for this step is as follows:

$$A_3\,\overline{Y}_3 + \frac{\beta_3\,Q_3^2}{g\,A_3} = A_{BU}\,\overline{Y}_{BU} + \frac{\beta_{BU}\,Q_{BU}^2}{g\,A_{BU}} + A_{p_{BU}}\,\overline{Y}_{p_{BU}} + \frac{1}{2}C_D\,\frac{A_{p_{BU}}\,Q_3^2}{g\,A_3^2} + F_f - W_x \qquad (5\text{-}3)$$

where: C_D = Drag coefficient for flow going around the piers. Guidance on selecting drag coefficients can be found under Table 5.3 below.

The momentum balance method requires the use of roughness coefficients for the estimation of the friction force and a drag coefficient for the force of drag on piers. As mentioned previously, roughness coefficients are described in Chapter 3 of this manual. Drag coefficients are used to estimate the force due to the water moving around the piers, the separation of the flow, and the resulting wake that occurs downstream. Drag coefficients for various cylindrical shapes have been derived from experimental data (Lindsey, 1938). The following table shows some typical drag coefficients that can be used for piers:

Table 5.3
Typical drag coefficients for various pier shapes

Pier Shape	**Drag Coefficient C_D**
Circular pier	1.20
Elongated piers with semi-circular ends	1.33
Elliptical piers with 2:1 length to width	0.60
Elliptical piers with 4:1 length to width	0.32
Elliptical piers with 8:1 length to width	0.29
Square nose piers	2.00
Triangular nose with 30 degree angle	1.00
Triangular nose with 60 degree angle	1.39
Triangular nose with 90 degree angle	1.60
Triangular nose with 120 degree angle	1.72

The momentum method provides detailed output for the cross sections inside the bridge (BU and BD) as well as outside the bridge (2 and 3). The user has the option of turning the friction and weight force components off. The default is to include the friction force but not the weight component. The computation of the weight force is dependent upon computing a mean bed slope through the bridge. Estimating a mean bed slope can be very difficult with irregular cross section data. A bad estimate of the bed slope can lead to large errors in the momentum solution. The user can turn this force on if they feel that the bed slope through the bridge is well behaved for their application.

During the momentum calculations, if the water surface (at sections BD and BU) comes into contact with the maximum low chord of the bridge, the momentum balance is assumed to be invalid and the results are not used.

Yarnell Equation:

The Yarnell equation is an empirical equation that is used to predict the change in water surface from just downstream of the bridge (section 2 of Figure 5.3) to just upstream of the bridge (section 3). The equation is based on approximately 2600 lab experiments in which the researchers varied the shape of the piers, the width, the length, the angle, and the flow rate. The Yarnell equation is as follows (Yarnell, 1934):

$$H_{3-2} = 2K\left(K + 10\omega - 0.6\right)\left(\alpha + 15\alpha^4\right)\frac{V^2}{2g} \qquad (5\text{-}4)$$

Where: H_{3-2} = Drop in water surface elevation from section 3 to 2

K = Yarnell's pier shape coefficient

ω = Ratio of velocity head to depth at section 2

α = Obstructed area of the piers divided by the total unobstructed area at section 2

V_2 = Velocity downstream at section 2

The computed upstream water surface elevation (section 3) is simply the downstream water surface elevation plus H_{3-2}. With the upstream water surface known the program computes the corresponding velocity head and energy elevation for the upstream section (section 3). When the Yarnell method is used, hydraulic information is only provided at cross sections 2 and 3 (no information is provided for sections BU and BD).

The Yarnell equation is sensitive to the pier shape (K coefficient), the pier obstructed area, and the velocity of the water. The method is not sensitive to the shape of the bridge opening, the shape of the abutments, or the width of the bridge. Because of these limitations, the Yarnell method should only be used at bridges where the majority of the energy losses are associated with the piers. When Yarnell's equation is used for computing the change in water surface through the bridge, the user must supply the Yarnell pier shape coefficient, K. The following table gives values for Yarnell's pier coefficient, K, for various pier shapes:

Table 5.4
Yarnell's pier coefficient, K, for various pier shapes

Pier Shape	Yarnell K Coefficient
Semi-circular nose and tail	0.90
Twin-cylinder piers with connecting diaphragm	0.95
Twin-cylinder piers without diaphragm	1.05
90 degree triangular nose and tail	1.05
Square nose and tail	1.25
Ten pile trestle bent	2.50

FHWA WSPRO Method:

The low flow hydraulic computations of the Federal Highway Administration's (FHWA) WSPRO computer program, has been adapted as an option for low flow hydraulics in HEC-RAS. The WSPRO methodology had to be modified slightly in order to fit into the HEC-RAS concept of cross-section locations around and through a bridge.

The WSPRO method computes the water surface profile through a bridge by solving the energy equation. The method is an iterative solution performed from the exit cross section (1) to the approach cross-section (4). The energy balance is performed in steps from the exit section (1) to the cross section just downstream of the bridge (2); from just downstream of the bridge (2) to inside of the bridge at the downstream end (BD); from inside of the bridge at the downstream end (BD) to inside of the bridge at the upstream end (BU); From inside of the bridge at the upstream end (BU) to just upstream of the bridge (3); and from just upstream of the bridge (3) to the approach section (4). A general energy balance equation from the exit section to the approach section can be written as follows:

$$h_4 + \frac{\alpha_4 V_4^2}{2g} = h_1 + \frac{\alpha_1 V_1^2}{2g} h_{L_{4-1}} \qquad (5\text{-}5)$$

where: h_1 = Water surface elevation at section 1

V_1 = Velocity at section 1

h_4 = Water surface elevation at section 4

V_4 = Velocity at section 4

h_L = Energy losses from section 4 to 1

The incremental energy losses from section 4 to 1 are calculated as follows:

From Section 1 to 2

Losses from section 1 to section 2 are based on friction losses and an expansion loss. Friction losses are calculated using the geometric mean friction slope times the flow weighted distance between sections 1 and 2. The following equation is used for friction losses from 1 to 2:

$$h_{f_{1-2}} = \frac{BQ^2}{K_2 K_1} \tag{5-6}$$

Where B is the flow weighted distance between sections 1 and 2, and K_1 and K_2 are the total conveyance at sections 1 and 2 respectively. The expansion loss from section 2 to section 1 is computed by the following equation:

$$h_e = \frac{Q^2}{2g A_1^2}\left[2\beta_1 - \alpha_1 - 2\beta_2\left(\frac{A_1}{A_2}\right) + \alpha_2\left(\frac{A_1}{A_2}\right)^2\right] \tag{5-7}$$

Where α and β are energy and momentum correction factors for non-uniform flow. α_1 and β_1 are computed as follows:

$$\alpha_1 = \frac{\sum\left(K_i^3/A_i^2\right)}{K_T^3/A_T^2} \tag{5-8}$$

$$\beta_1 = \frac{\sum\left(K_i^2/A_i\right)}{K_T^2/A_T} \tag{5-9}$$

α_2 and β_2 are related to the bridge geometry and are defined as follows:

$$\alpha_1 = \frac{1}{C^2} \tag{5-10}$$

$$\beta_1 = \frac{1}{C} \tag{5-11}$$

where C is an empirical discharge coefficient for the bridge, which was originally developed as part of the Contracted Opening method by Kindswater, Carter, and Tracy (USGS, 1953), and subsequently modified by Matthai (USGS, 1968). The computation of the discharge coefficient, C, is explained in detail in appendix D of this manual.

From Section 2 to 3

Losses from section 2 to section 3 are based on friction losses only. The energy balance is performed in three steps: from section 2 to BD; BD to BU; and BU to 3. Friction losses are calculated using the geometric mean friction slope times the flow weighted distance between sections. The following equation is used for friction losses from BD to BU:

$$h_{f(BU-BD)} = \frac{L_B Q^2}{K_{BU} K_{BD}} \tag{5-12}$$

Where K_{BU} and K_{BD} are the total conveyance at sections BU and BD respectively, and L_B is the length through the bridge. Similar equations are used for the friction losses from section 2 to BD and BU to 3.

From Section 3 to 4

Energy losses from section 3 to 4 are based on friction losses only. The equation for computing the friction loss is as follows:

$$h_{f(3-4)} = \frac{L_{av} Q^2}{K_3 K_4} \tag{5-13}$$

Where L_{av} is the effective flow length in the approach reach, and K_3 and K_4 are the total conveyances at sections 3 and 4. The effective flow length is computed as the average length of 20 equal conveyance stream tubes (FHWA, 1986). The computation of the effective flow length by the stream tube method is explained in appendix D of this manual.

Class B low flow. Class B low flow can exist for either subcritical or supercritical profiles. For either profile, class B flow occurs when the profile passes through critical depth in the bridge constriction. For a **subcritical profile**, the momentum equation is used to compute an upstream water surface (section 3 of Figure 5.3) above critical depth and a downstream water surface (section 2) below critical depth. For a **supercritical profile**, the bridge is acting as a control and is causing the upstream water surface elevation to be above critical depth. Momentum is used to calculate an upstream water surface above critical depth and a downstream water surface below critical depth. If for some reason the momentum equation fails to converge on an answer during the class B flow computations, the program will automatically switch to an energy-based method for calculating the class B profile through the bridge.

Whenever class B flow is found to exist, the user should run the program in a mixed flow regime mode. If the user is running a mixed flow regime profile the program will proceed with backwater calculations upstream, and later with forewater calculations downstream from the bridge. Also, any hydraulic jumps that may occur upstream and downstream of the bridge can be located if they exist.

Class C low flow. Class C low flow exists when the water surface through the bridge is completely supercritical. The program can use either the energy equation or the momentum equation to compute the water surface through the bridge for this class of flow.

High Flow Computations

The HEC-RAS program has the ability to compute high flows (flows that come into contact with the maximum low chord of the bridge deck) by either the Energy equation (standard step method) or by using separate hydraulic equations for pressure and/or weir flow. The two methodologies are explained below.

Energy Equation (standard step method). The energy-based method is applied to high flows in the same manner as it is applied to low flows. Computations are based on balancing the energy equation in three steps through the bridge. Energy losses are based on friction and contraction and expansion losses. Output from this method is available at the cross sections inside the bridge as well as outside.

As mentioned previously, friction losses are based on the use of Manning's equation. Guidance for selecting Manning's n values is provided in Chapter 3 of this manual. Contraction and expansion losses are based on a coefficient times the change in velocity head. Guidance on the selection of contraction and expansion coefficients has also been provided in Chapter 3, as well as previous sections of this chapter.

The energy-based method performs all computations as though they are open channel flow. At the cross sections inside the bridge, the area obstructed by the bridge piers, abutments, and deck is subtracted from the flow area and additional wetted perimeter is added. Occasionally the resulting water surfaces inside the bridge (at sections BU and BD) can be computed at elevations that would be inside of the bridge deck. The water surfaces inside of the bridge reflect the hydraulic grade line elevations, not necessarily the actual water surface elevations. Additionally, the active flow area is limited to the open bridge area.

Pressure and Weir Flow Method. A second approach for the computation of high flows is to utilize separate hydraulic equations to compute the flow as pressure and/or weir flow. The two types of flow are presented below.

Pressure Flow Computations:

Pressure flow occurs when the flow comes into contact with the low chord of the bridge. Once the flow comes into contact with the upstream side of the bridge, a backwater occurs and orifice flow is established. The program will handle two cases of orifice flow; the first is when only the upstream side of the bridge is in contact with the water; and the second is when the bridge opening is flowing completely full. The HEC-RAS program will automatically select the appropriate equation, depending upon the flow situation. For the first case (see Figure 5.4), a sluice gate type of equation is used (FHWA, 1978):

$$Q = C_d A_{BU} \sqrt{2g} \left[Y_3 - \frac{Z}{2} + \frac{\alpha_3 V_3^2}{2g} \right]^{1/2} \qquad (5\text{-}14)$$

Where: Q = Total discharge through the bridge opening

C_d = Coefficient of discharge for pressure flow

A_{BU} = Net area of the bridge opening at section BU

Y_3 = Hydraulic depth at section 3

Z = Vertical distance from maximum bridge low chord to the mean river bed elevation at section BU

The discharge coefficient C_d, can vary depending upon the depth of water upstream. Values for C_d range from 0.27 to 0.5, with a typical value of 0.5 commonly used in practice. The user can enter a fixed value for this coefficient or the program will compute one based on the amount that the inlet is submerged. A diagram relating C_d to Y_3/Z is shown in Figure 5.5.

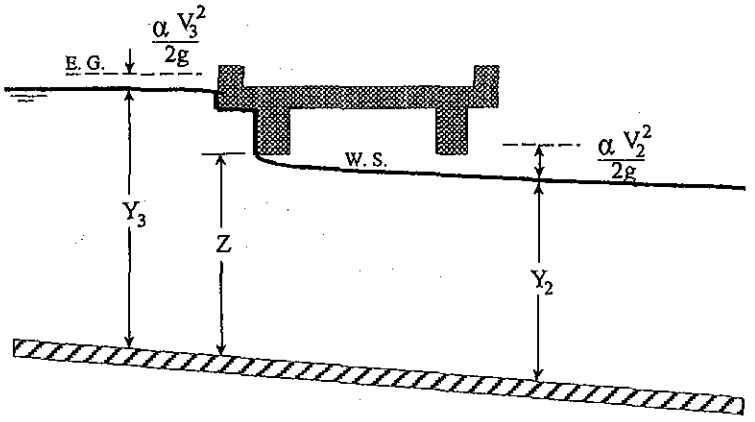

Figure 5.4 Example of a bridge under sluice gate type of pressure flow

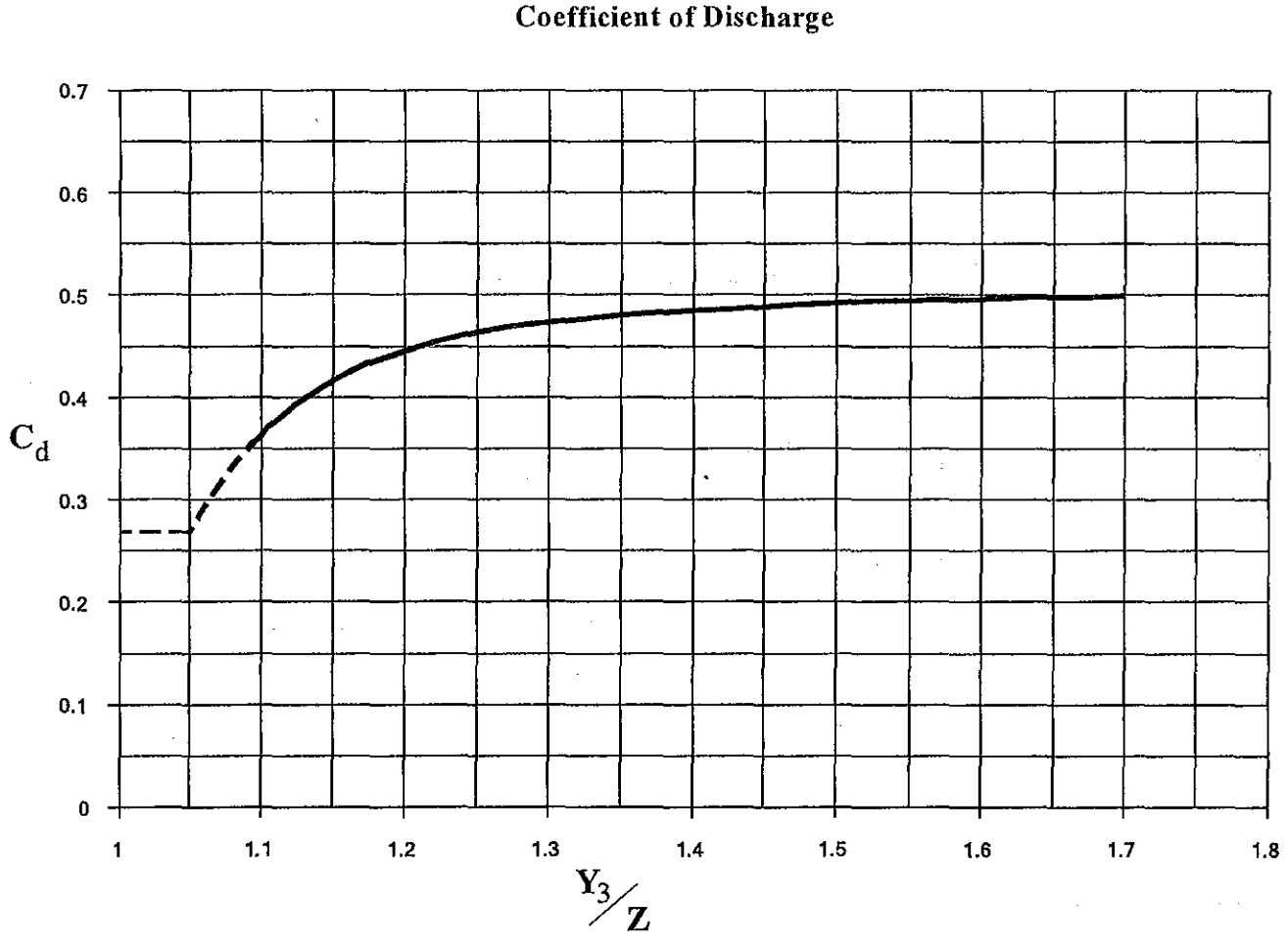

Figure 5.5 Coefficient of discharge for sluice gate type flow

As shown in Figure 5.5, the limiting value of Y_3/Z is 1.1. There is a transition zone somewhere between Y_3/Z = 1.0 and 1.1 where free surface flow changes to orifice flow. The type of flow in this range is unpredictable, and equation 5-14 is not applicable.

In the second case, when both the upstream and downstream side of the bridge are submerged, the standard full flowing orifice equation is used (see Figure 5.6). This equation is as follows:

$$Q = C A\sqrt{2gH} \tag{5-15}$$

Where: C = Coefficient of discharge for fully submerged pressure flow. Typical value of C is 0.8.

H = The difference between the energy gradient elevation upstream and the water surface elevation downstream.

A = Net area of the bridge opening.

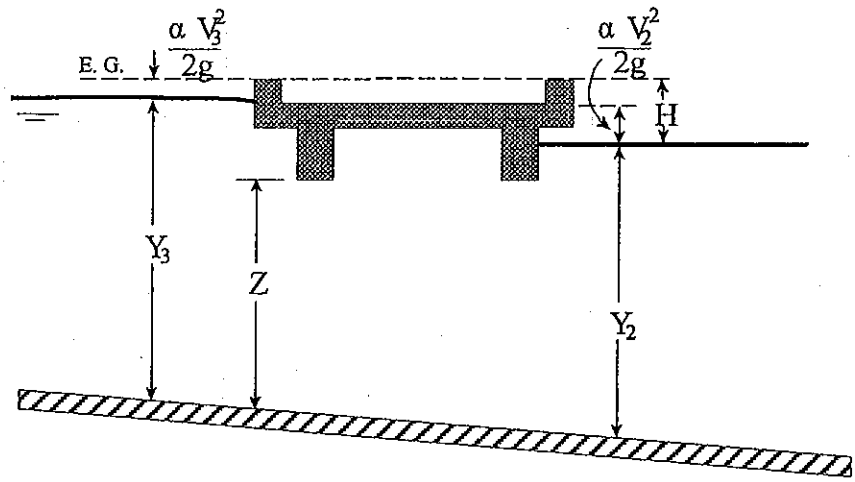

Figure 5.6 Example of a bridge under fully submerged pressure flow

Typical values for the discharge coefficient C range from 0.7 to 0.9, with a value of 0.8 commonly used for most bridges. The user must enter a value for C whenever the pressure flow method is selected. The discharge coefficient C can be related to the total loss coefficient, which comes from the form of the orifice equation that is used in the HEC-2 computer program (HEC, 1991):

$$Q = A\sqrt{\frac{2gH}{K}} \tag{5-16}$$

Where: K = Total loss coefficient

The conversion from K to C is as follows:

$$C = \sqrt{\frac{1}{K}} \tag{5-17}$$

The program will begin checking for the possibility of pressure flow when the computed low flow energy grade line is above the maximum low chord elevation at the upstream side of the bridge. Once pressure flow is computed, the pressure flow answer is compared to the low flow answer, the higher of the two is used. The user has the option to tell the program to use the water surface, instead of energy, to trigger the pressure flow calculation.

Weir Flow Computations:

Flow over the bridge, and the roadway approaching the bridge, is calculated using the standard weir equation (see Figure 5.7):

$$Q = CLH^{3/2} \tag{5-18}$$

where: Q = Total flow over the weir

C = Coefficient of discharge for weir flow

L = Effective length of the weir

H = Difference between energy upstream and road crest

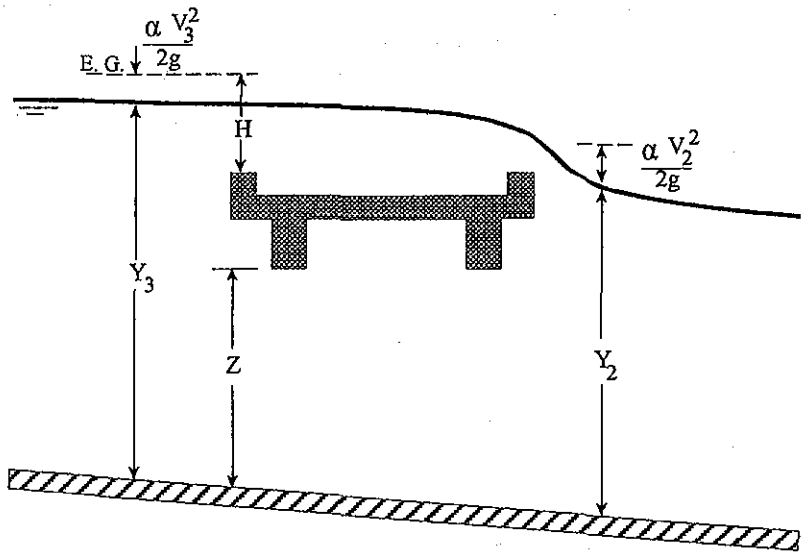

Figure 5.7 Example bridge with pressure and weir flow

The approach velocity is included by using the energy grade line elevation in lieu of the upstream water surface elevation for computing the head, H.

Under free flow conditions (discharge independent of tailwater) the coefficient of discharge C, ranges from 2.5 to 3.1 (1.38 - 1.71 metric) for broad-crested weirs depending primarily upon the gross head on the crest (C increases with head). Increased resistance to flow caused by obstructions such as trash on bridge railings, curbs, and other barriers would decrease the value of C.

Tables of weir coefficients, C, are given for broad-crested weirs in King's Handbook (King, 1963), with the value of C varying with measured head H and breadth of weir. For rectangular weirs with a breadth of 15 feet and a H of 1 foot or more, the given value is 2.63 (1.45 for metric). Trapezoidal shaped weirs generally have a larger coefficient with typical values ranging from 2.7 to 3.08 (1.49 to 1.70 for metric).

"Hydraulics of Bridge Waterways" (FHWA, 1978) provides a curve of C versus the head on the roadway. The roadway section is shown as a trapezoid and the coefficient rapidly changes from 2.9 for a very small H to 3.03 for H = 0.6 feet. From there, the curve levels off near a value of 3.05 (1.69 for metric).

With very little prototype data available, it seems the assumption of a rectangular weir for flow over the bridge deck (assuming the bridge can withstand the forces) and a coefficient of 2.6 (1.44 for metric) would be reasonable. If the weir flow is over the roadway approaches to the bridge, a value of 3.0 (1.66 for metric) would be consistent with available data. If weir flow occurs as a combination of bridge and roadway overflow, then an average coefficient (weighted by weir length) could be used.

For high tailwater elevations, the program will automatically reduce the amount of weir flow to account for submergence on the weir. Submergence is defined as the depth of water above the minimum weir elevation on the downstream side (section 2) divided by the height of the energy gradeline above the minimum weir elevation on the upstream side (section 3). The reduction of weir flow is accomplished by reducing the weir coefficient based on the amount of submergence. Submergence corrections are based on a trapezoidal weir shape or optionally an ogee spillway shape. The total weir flow is computed by subdividing the weir crest into segments, computing L, H, a submergence correction, and a Q for each section, then summing the incremental discharges. The submergence correction for a trapezoidal weir shape is from "Hydraulics of Bridge Waterways" (Bradley, 1978). Figure 5.8 shows the relationship between the percentage of submergence and the flow reduction factor.

When the weir becomes highly submerged the program will automatically switch to calculating the upstream water surface by the energy equation (standard step backwater) instead of using the pressure and weir flow equations. The criteria for when the program switches to energy based calculations is user controllable. A default maximum submergence is set to 0.95 (95 percent).

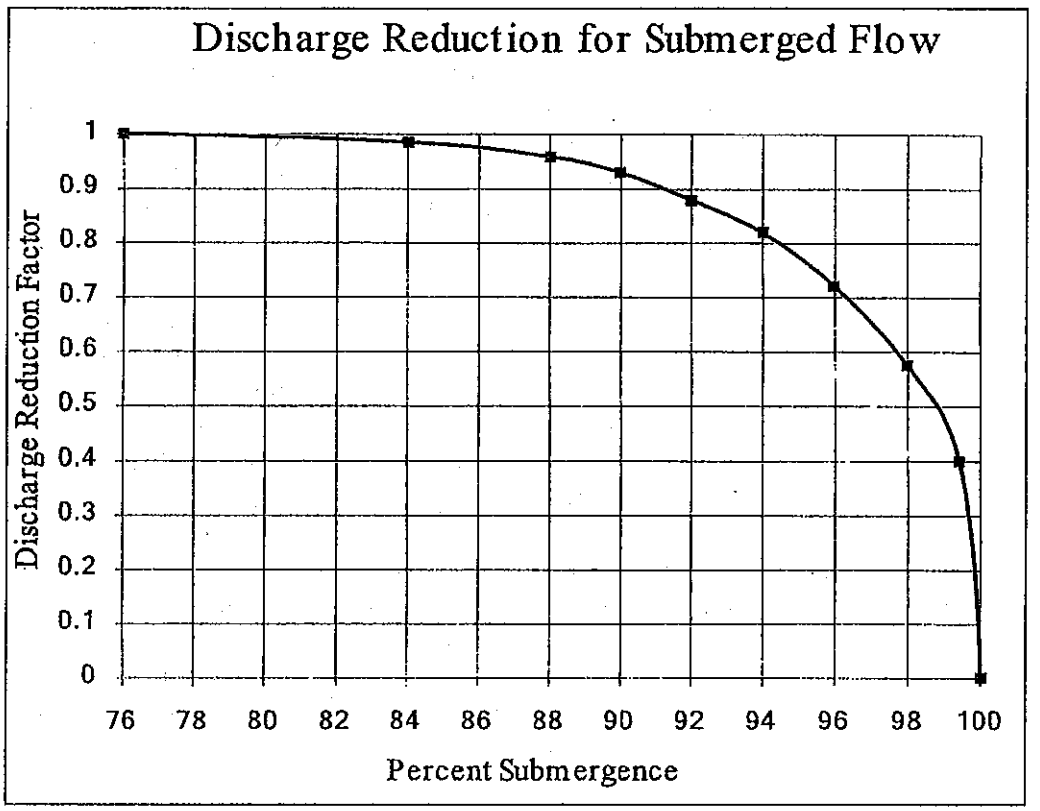

Figure 5.8 Factor for reducing weir flow for submergence

Combination Flow.

Sometimes combinations of low flow or pressure flow occur with weir flow. In these cases, an iterative procedure is used to determine the amount of each type of flow. The program continues to iterate until both the low flow method (or pressure flow) and the weir flow method have the same energy (within a specified tolerance) upstream of the bridge (section 3). The combination of low flow and weir flow can only be computed with the energy and Yarnell low flow method.

Selecting a Bridge Modeling Approach

There are several choices available to the user when selecting methods for computing the water surface profile through a bridge. For low flow (water surface is below the maximum low chord of the bridge deck), the user can select any or all of the four available methods. For high flows, the user must choose between either the energy based method or the pressure and weir flow approach. The choice of methods should be considered carefully. The following discussion provides some basic guidelines on selecting the appropriate methods for various situations.

Low Flow Methods

For low flow conditions (water surface below the highest point on the low chord of the bridge opening), the Energy and Momentum methods are the most physically based, and in general are applicable to the widest range of bridges and flow situations. Both methods account for friction losses and changes in geometry through the bridge. The energy method accounts for additional losses due to flow transitions and turbulence through the use of contraction and expansion losses. The momentum method can account for additional losses due to pier drag. The FHWA WSPRO method was originally developed for bridge crossings that constrict wide flood plains with heavily vegetated overbank areas. The method is an energy-based solution with some empirical attributes (the expansion loss equation in the WSPRO method utilizes an empirical discharge coefficient). The Yarnell equation is an empirical formula. When applying the Yarnell equation, the user should ensure that the problem is within the range of data that the method was developed for. The following examples are some typical cases where the various low flow methods might be used:

1. In cases where the bridge piers are a small obstruction to the flow, and friction losses are the predominate consideration, the energy based method, the momentum method, and the WSPRO method should give the best answers.

2. In cases where pier losses and friction losses are both predominant, the momentum method should be the most applicable. But any of the methods can be used.

3. Whenever the flow passes through critical depth within the vicinity of the bridge, both the momentum and energy methods are capable of modeling this type of flow transition. The Yarnell and WSPRO methods are for subcritical flow only.

4. For supercritical flow, both the energy and the momentum method can be used. The momentum-based method may be better at locations that have a substantial amount of pier impact and drag losses. The

Yarnell equation and the WSPRO method are only applicable to subcritical flow situations.

5. For bridges in which the piers are the dominant contributor to energy losses and the change in water surface, either the momentum method or the Yarnell equation would be most applicable. However, the Yarnell equation is only applicable to Class A low flow.

6. For long culverts under low flow conditions, the energy based standard step method is the most suitable approach. Several sections can be taken through the culvert to model changes in grade or shape or to model a very long culvert. This approach also has the benefit of providing detailed answers at several locations within the culvert, which is not possible with the culvert routines in HEC-RAS. However, if the culvert flows full, or if it is controlled by inlet conditions, the culvert routines would be the best approach. For a detailed discussion of the culvert routines within HEC-RAS, see Chapter 6 of this manual.

High Flow Methods

For high flows (flows that come into contact with the maximum low chord of the bridge deck), the energy-based method is applicable to the widest range of problems. The following examples are some typical cases where the various high flow methods might be used.

1. When the bridge deck is a small obstruction to the flow, and the bridge opening is not acting like an pressurized orifice, the energy based method should be used.

2. When the bridge deck and road embankment are a large obstruction to the flow, and a backwater is created due to the constriction of the flow, the pressure and weir method should be used.

3. When the bridge and/or road embankment is overtopped, and the water going over top of the bridge is not highly submerged by the downstream tailwater, the pressure and weir method should be used. The pressure and weir method will automatically switch to the energy method if the bridge becomes 95 percent submerged. The user can change the percent submergence at which the program will switch from the pressure and weir method to the energy method. This is accomplished from the Deck/Roadway editor in the Bridge/Culvert Data editor.

4. When the bridge is highly submerged, and flow over the road is not acting like weir flow, the energy-based method should be used.

Unique Bridge Problems and Suggested Approaches

Many bridges are more complex than the simple examples presented in the previous sections. The following discussion is intended to show how HEC-RAS can be used to calculate profiles for more complex bridge crossings. The discussion here will be an extension of the previous discussions and will address only those aspects that have not been discussed previously.

Perched Bridges

A perched bridge is one for which the road approaching the bridge is at the floodplain ground level, and only in the immediate area of the bridge does the road rise above ground level to span the watercourse (Figure 5.9). A typical flood-flow situation with this type of bridge is low flow under the bridge and overbank flow around the bridge. Because the road approaching the bridge is usually not much higher than the surrounding ground, the assumption of weir flow is often not justified. A solution based on the energy method (standard step calculations) would be better than a solution based on weir flow with correction for submergence. Therefore, this type of bridge should generally be modeled using the energy-based method, especially when a large percentage of the total discharge is in the overbank areas.

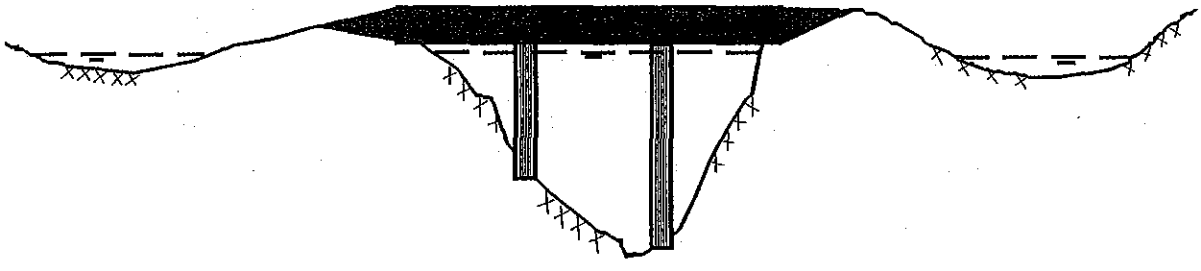

Figure 5.9 Perched Bridge Example

Low Water Bridges

A low water bridge (Figure 5.10) is designed to carry only low flows under the bridge. Flood flows are carried over the bridge and road. When modeling this bridge for flood flows, the anticipated solution is a combination of pressure and weir flow. However, with most of the flow over the top of the bridge, the correction for submergence may introduce considerable error. If the tailwater is going to be high, it may be better to use the energy-based method.

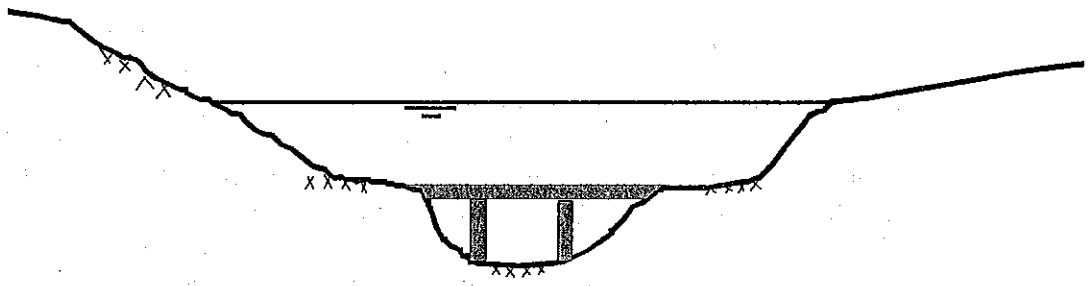

Figure 5.10 Low Water Bridge Example

Bridges on a Skew

Skewed bridge crossings (Figure 5.11) are generally handled by making adjustments to the bridge dimensions to define an equivalent cross section perpendicular to the flow lines. The bridge information, and cross sections that bound the bridge, can be adjusted from the bridge editor. An option called **Skew Bridge/Culvert** is available from the bridge/culvert editor.

In the publication "Hydraulics of Bridge Waterways" (Bradley, 1978) the effect of skew on low flow is discussed. In model testing, skewed crossings with angles up to 20 degrees showed no objectionable flow patterns. For increasing angles, flow efficiency decreased. A graph illustrating the impact of skew indicates that using the projected length is adequate for angles up to 30 degrees for small flow contractions.

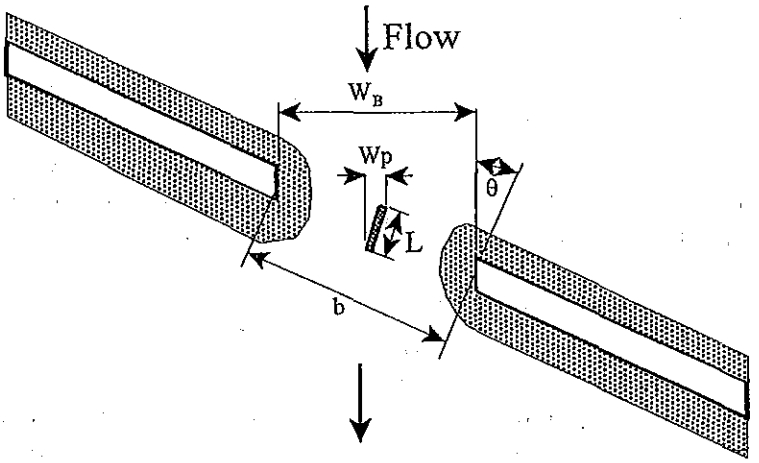

Figure 5.11 Example Bridge on a Skew

For the example shown in figure 5.11, the projected width of the bridge opening, perpendicular to the flow lines, will be computed with the following equation:

$$W_B = \cos\theta * b \tag{5-19}$$

Where: W_B = Projected width of the bridge opening, perpendicular to the flow lines

b = The length of the bridge opening as measured along the skewed road crossing

θ = The bridge skew angle in degrees

The pier information must also be adjusted to account for the skew of the bridge. HEC-RAS assumes the piers are continuous, as shown in Figure 5.11, thus the following equation will be applied to get the projected width of the piers, perpendicular to the flow lines:

$$W_p = \sin\theta * L + \cos\theta * w_p \tag{5-20}$$

Where: W_p = The projected width of the pier, perpendicular to the flow lines

L = The actual length of the pier

w_p = The actual width of the pier

Parallel Bridges

With the construction of divided highways, a common modeling problem involves parallel bridges (Figure 5.12). For new highways, these bridges are often identical structures. The hydraulic loss through the two structures has been shown to be between one and two times the loss for one bridge [Bradley, 1978]. The model results [Bradley, 1978] indicate the loss for two bridges ranging from 1.3 to 1.55 times the loss for one bridge crossing, over the range of bridge spacings tested. Presumably if the two bridges were far enough apart, the losses for the two bridges would equal twice the loss for one. If the parallel bridges are very close to each other, and the flow will not be able to expand between the bridges, the bridges can be modeled as a single bridge. If there is enough distance between the bridge, in which the flow has room to expand and contract, the bridges should be modeled as two separate bridges. If both bridges are modeled, care should be exercised in depicting the expansion and contraction of flow between the bridges. Expansion and contraction rates should be based on the same procedures as single bridges.

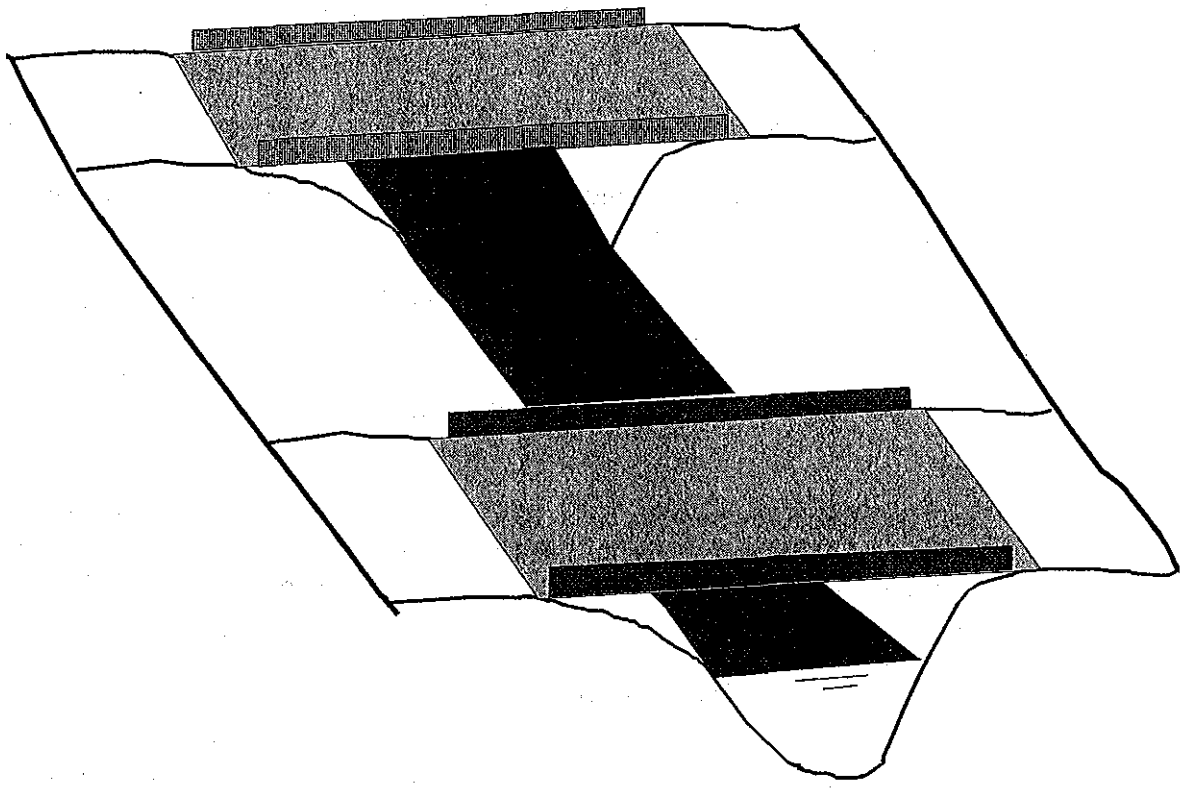

Figure 5.12 Parallel Bridge Example

Multiple Bridge Opening

Some bridges (Figure 5.13) have more than one opening for flood flow, especially over a very wide floodplain. Multiple culverts, bridges with side relief openings, and separate bridges over a divided channel are all examples of multiple opening problems. With more than one bridge opening, and possible different control elevations, the problem can be very complicated. HEC-RAS can handle multiple bridge and/or culvert openings. Detailed discussions on how to model multiple bridge and/or culvert openings is covered under Chapter 7 of the HEC-RAS Hydraulic Reference manual and Chapter 6 of the User's manual.

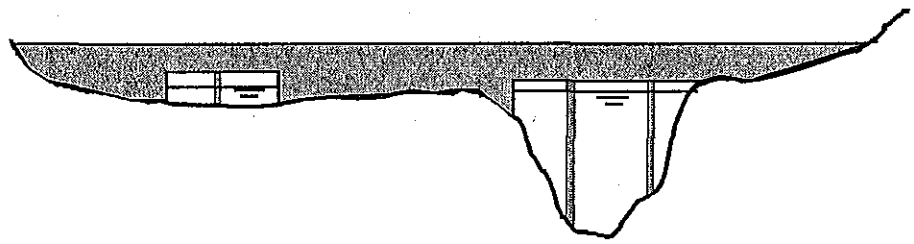

Figure 5.13 Example Multiple Bridge Opening

Modeling Floating Pier Debris

Trash, trees, and other debris may accumulate on the upstream side of a pier. During high flow events, this debris may block a significant portion of the bridge opening. In order to account for this effect, a pier debris option has been added to HEC-RAS.

The pier debris option blocks out a rectangular shaped area in front of the given pier. The user enters the height and the width of the given block. The program then adjusts the area and wetted perimeter of the bridge opening to account for the pier debris. The rectangular block is centered on the centerline of the upstream pier. The pier debris is assumed to float at the top of the water surface. That is, the top of the rectangular block is set at the same elevation as the water surface. For instance, assume a bridge opening that has a pier that is six feet wide with a centerline station of 100 feet, the elevation of water inside of the bridge is ten feet, and that the user wants to model pier debris that sticks out two feet past either side of the pier and is [vertically] four feet high. The user would enter a pier debris rectangle that is 10 feet wide (six feet for the pier plus two feet for the left side and two feet for the right side) and 4 feet high. The pier debris would block out the flow that is between stations 95 and 105 and between an elevation of six and ten feet (from an elevation of six feet to the top of the water surface).

The pier debris does not form until the given pier has flow. If the bottom of the pier is above the water surface, then there is no area or wetted perimeter adjustment for that pier. However, if the water surface is above the top of the pier, the debris is assumed to lodge underneath the bridge, where the top of the pier intersects the bottom of the bridge deck. It is assumed that the debris entirely blocks the flow and that the debris is physically part of the pier. (The Yarnell and momentum bridge methods require the area of the pier, and pier debris is included in these calculations.)

The program physically changes the geometry of the bridge in order to model the pier debris. This is done to ensure that there is no double accounting of area or wetted perimeter. For instance, pier debris that extends past the abutment, or into the ground, or that overlaps the pier debris of an adjacent pier is ignored.

Shown in Figure 5.14 is the pier editor with the pier debris option turned on. Note that there is a check box to turn the floating debris option on. Once this option is turned on, two additional fields will appear to enter the height and overall width of the pier debris. Additionally, there is a button that the user can use to set the entered height and width for the first pier as being the height and width of debris that will be used for all piers at this bridge location. Otherwise, the debris data can be defined separately for every pier.

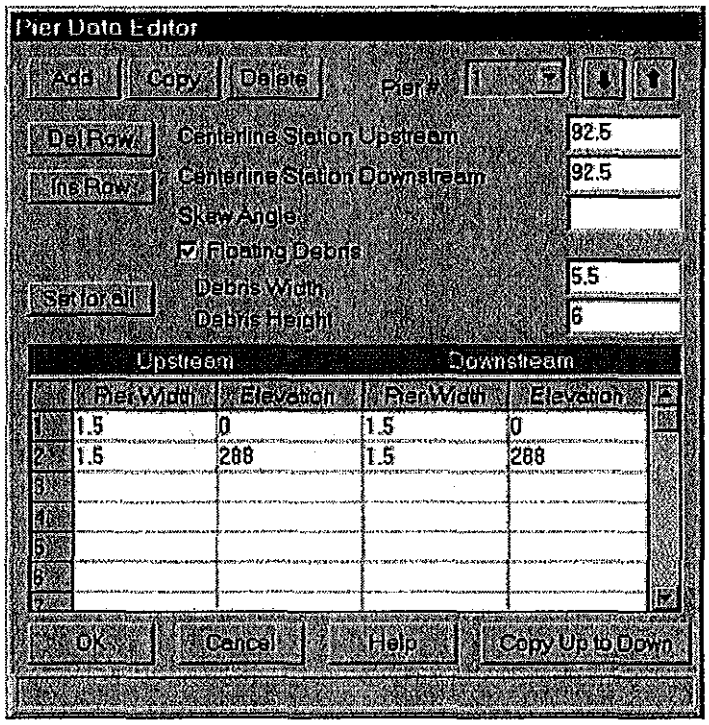

Figure 5.14 Pier Editor With Floating Debris Option

After the user has run the computational program with the pier debris option turned on, the pier debris will then be displayed on the cross section plots of the upstream side of the bridge (this is the cross sections with the labels "BR U," for inside of the bridge at the upstream end). An example cross-section plot with pier debris is shown in Figure 5.15.

CHAPTER 7

Modeling Multiple Bridge and/or Culvert Openings

The HEC-RAS program has the ability to model multiple bridge and/or culvert openings at a single location. A common example of this type of situation is a bridge opening over the main stream and a relief bridge (or group of culverts) in the overbank area. The HEC-RAS program is capable of modeling up to seven opening types at any one location.

Contents

General Modeling Guidelines

Occasionally you may need to model a river crossing that cannot be modeled adequately as a single bridge opening or culvert group. This often occurs in wide floodplain areas where there is a bridge opening over the main river channel, and a relief bridge or group of culverts in the overbank areas. There are two ways you can model this type of problem within HEC-RAS. The first method is to use the multiple opening capability in HEC-RAS, which is discussed in detail in the following section. A second method is to model the two openings as divided flow. This method would require the user to define the flow path for each opening as a separate reach. This option is discussed in the last section of this chapter.

Multiple Opening Approach

The multiple opening features in HEC-RAS allow users to model complex bridge and/or culvert crossings within a one dimensional flow framework. HEC-RAS has the ability to model three types of openings: Bridges; Culvert Groups (a group of culverts is considered to be a single opening); and Conveyance Areas (an area where water will flow as open channel flow, other than a bridge or culvert opening). Up to seven openings can be defined at any one river crossing. The HEC-RAS multiple opening methodology is limited to subcritical flow profiles. The program can also be run in mixed flow regime mode, but only a subcritical profile will be calculated in the area of the multiple opening. An example of a multiple opening is shown in Figure 7.1.

As shown in Figure 7.1, the example river crossing has been defined as three openings, labeled as #1, #2, and #3. Opening #1 represents a Conveyance Area, opening #2 is a Bridge opening, and opening #3 is a Culvert Group.

The approach used in HEC-RAS is to evaluate each opening as a separate entity. An iterative solution is applied, in which an initial flow distribution between openings is assumed. The water surface profile and energy gradient are calculated through each opening. The computed upstream energies for each opening are compared to see if they are within a specified tolerance (the difference between the opening with the highest energy and the opening with the lowest energy must be less than the tolerance). If the difference in energies is not less than the tolerance, the program makes a new estimate of the flow distribution through the openings and repeats the process. This iterative technique continues until either a solution that is within the tolerance is achieved, or a predefined maximum number of iterations is reached (the default maximum is 30).

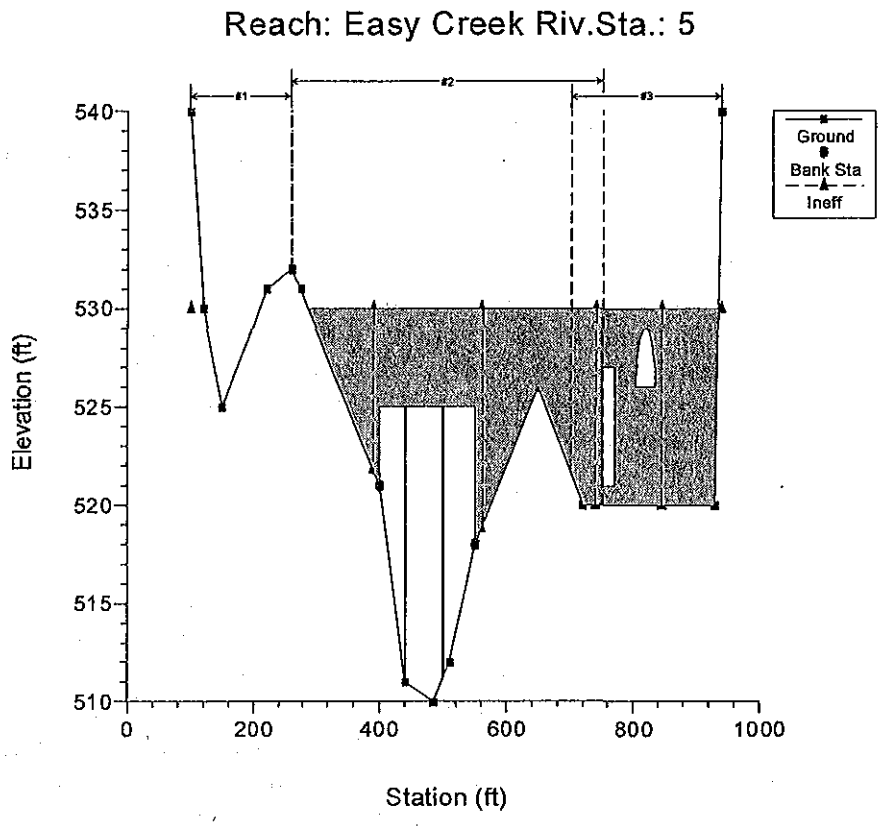

Figure 7.1 Example Multiple Opening River Crossing

The distribution of flow requires the establishment of flow boundaries both upstream and downstream of the openings. The flow boundaries represent the point at which flow separates between openings. These flow boundaries are referred to as "Stagnation Points" (the term "stagnation points" will be used from this point on when referring to the flow separation boundaries). A plan view of a multiple opening is shown in Figure 7.2.

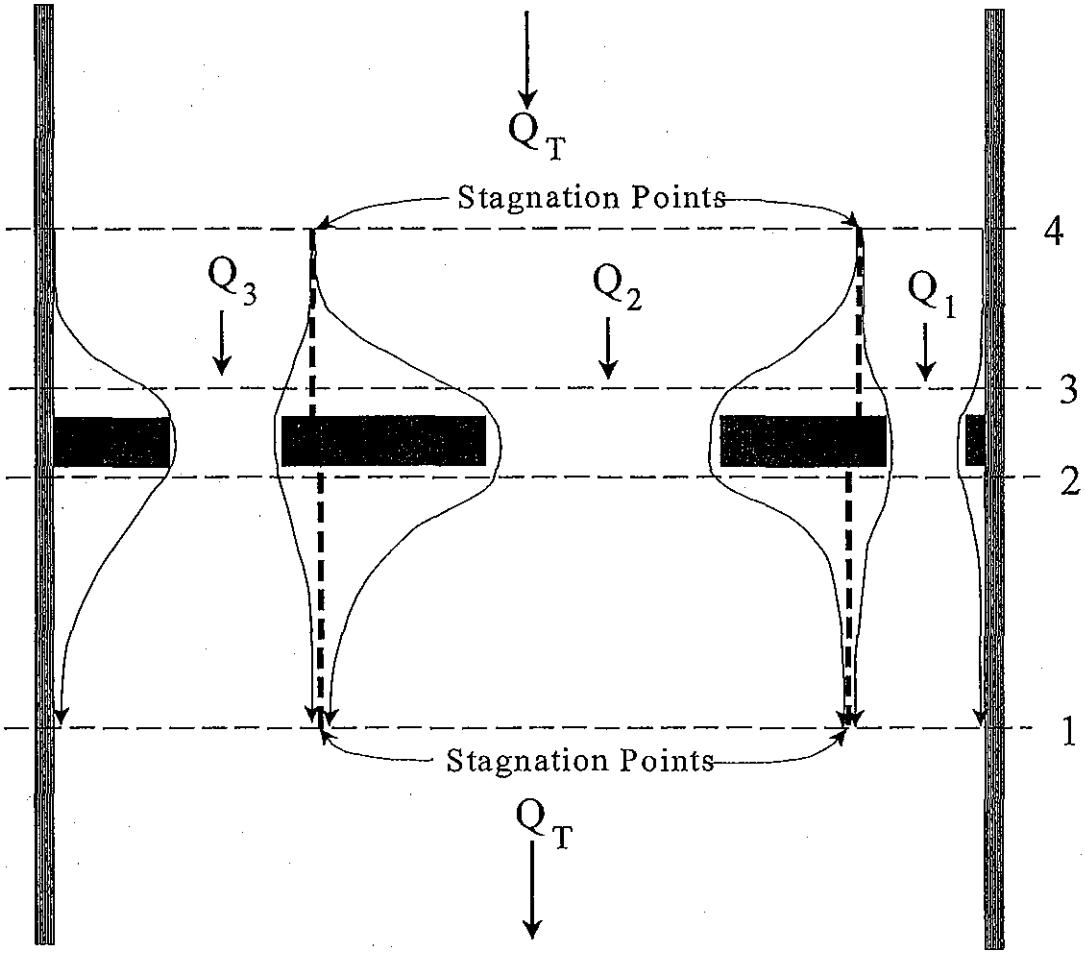

Figure 7.2 Plan view of a Multiple Opening Problem

Locating the Stagnation Points

The user has the option of fixing the stagnation point locations or allowing the program to solve for them within user defined limits. In general, it is better to let the program solve for the stagnation points, because it provides the best flow distribution and computed water surfaces. Also, allowing the stagnation points to migrate can be important when evaluating several different flow profiles in the same model. Conversely though, if the range in which the stagnation points are allowed to migrate is very large, the program may have difficulties in converging to a solution. Whenever this occurs, the user should either reduce the range over which the stagnation points can migrate or fix their location.

Within HEC-RAS, stagnation points are allowed to migrate between any bridge openings and/or culvert groups. However, if the user defines a conveyance area opening, the stagnation point between this type of opening and any other must be a fixed location. Also, conveyance area openings are limited to the left and right ends of the cross section.

Computational Procedure for Multiple Openings

HEC-RAS uses an iterative procedure for solving the multiple opening problem. The following approach is used when performing a multiple opening computation:

1. The program makes a first guess at the upstream water surface by setting it equal to the computed energy on the downstream side of the river crossing.

2. The assumed water surface is projected onto the upstream side of the bridge. A flow distribution is computed based on the percent of flow area in each opening.

3. Once a flow distribution is estimated, the stagnation points are calculated based on the upstream cross section. The assumed water surface is put into the upstream section. The hydraulic properties are calculated based on the assumed water surface and flow distribution. Stagnation points are located by apportioning the conveyance in the upstream cross section, so that the percentage of conveyance for each section is equal to the percentage of flow allocated to each opening.

4. The stagnation points in the downstream cross section (section just downstream of the river crossing) are located in the same manner.

5. Once a flow distribution is assumed, and the upstream and downstream stagnation points are set, the program calculates the water surface profiles through each opening, using the assumed flow.

6. After the program has computed the upstream energy for each opening, a comparison is made between the energies to see if a balance has been achieved (i.e., the difference between the highest and lowest computed energy is less than a predefined tolerance). If the energies are not within the tolerance, the program computes an average energy by using a flow weighting for each opening.

7. The average energy computed in step 6 is used to estimate the new flow distribution. This estimate of the flow distribution is based on adjusting the flow in each opening proportional to the percentage that the computed energy for that opening is from the weighted average

energy. An opening with a computed energy higher than the weighted mean will have its flow reduced, while an opening with a computed energy that is lower than the weighted mean will have its flow increased. Once the flow for all the openings is adjusted, a continuity check is made to ensure that the sum of the flows in all the openings is equal to the total flow. If this is not true, the flow in each opening is adjusted to ensure that the sum of flows is equal to the total flow.

8. Steps 3 through 7 continue until either a balance in energy is reached or the program gets to the fifth iteration. If the program gets to the fifth iteration, then the program switches to a different iterating method. In the second iteration method, the program formulates a flow versus upstream energy curve for each opening. The rating curve is based on the first four iterations. The rating curves are combined to get a total flow verses energy curve for the entire crossing. A new upstream energy guess is based on entering this curve with the total flow and interpolating an energy. Once a new energy is estimated, the program goes back to the individual opening curves with this energy and interpolates a flow for each opening. With this new flow distribution the program computes the water surface and energy profiles for each opening. If all the energies are within the tolerance, the calculation procedure is finished. If it is not within the tolerance the rating curves are updated with the new computed points, and the process continues. This iteration procedure continues until either a solution within the tolerance is achieved, or the program reaches the maximum number of iterations. The tolerance for balancing the energies between openings is 5 times the normal cross section water surface tolerance (0.05 feet or 0.015 meters). The default number of iterations for the multiple opening solutions scheme is 1.5 times the normal cross section maximum (the default is 30).

9. Once a solution is achieved, the program places the mean computed energy into the upstream cross section and computes a corresponding water surface for the entire cross section. In general, this water surface will differ from the water surfaces computed from the individual openings. This mean energy and water surface are reported as the final solution at the upstream section. User=s can obtain the results of the computed energies and water surfaces for each opening through the cross section specific output table, as well as the multiple opening profile type of table.

Limitations of the Multiple Opening Approach

The multiple opening method within HEC-RAS is a one-dimensional flow approach to a complex hydraulic problem. The methodology has the following limitations: the energy grade line is assumed to be constant upstream and downstream of the multiple opening crossing; the stagnation points are not allowed to migrate past the edge of an adjacent opening; and the stagnation points between a conveyance area and any other type of opening must be fixed (i.e. can not float). The model is limited to a maximum of seven openings. There can only be up to two conveyance type openings, and these openings must be located at the far left and right ends of the cross sections. Given these limitations, if you have a multiple opening crossing in which the water surface and energy vary significantly between openings, then this methodology may not be the most appropriate approach. An alternative to the multiple opening approach is the divided flow approach. This method is discussed below.

Divided Flow Approach

An alternative approach for solving a multiple opening problem is to model the flow paths of each opening as a separate river reach. This approach is more time consuming, and requires the user to have a greater understanding of how the flow will separate between openings. The benefit of using this approach is that varying water surfaces and energies can be obtained between openings. An example of a divided flow application is shown in Figure 7.3.

In the example shown in Figure 7.3, high ground exist between the two openings (both upstream and downstream). Under low flow conditions, there are two separate and distinct channels. Under high flow conditions the ground between the openings may be submerged, and the water surface continuous across both openings. To model this as a divided flow the user must create two separate river reaches around the high ground and through the openings. Cross sections 2 through 8 must be divided at what the user believes is the appropriate stagnation points for each cross section. This can be accomplished in several ways. The cross sections could be physically split into two, or the user could use the same cross sections in both reaches. If the same cross sections are used, the user must block out the area of each cross section (using the ineffective flow option) that is not part of the flow path for that particular reach. In other words, if you were modeling the left flow path, you would block out everything to the right of the stagnation points. For the reach that represents the right flow path, everything to the left of the stagnation points would be blocked out.

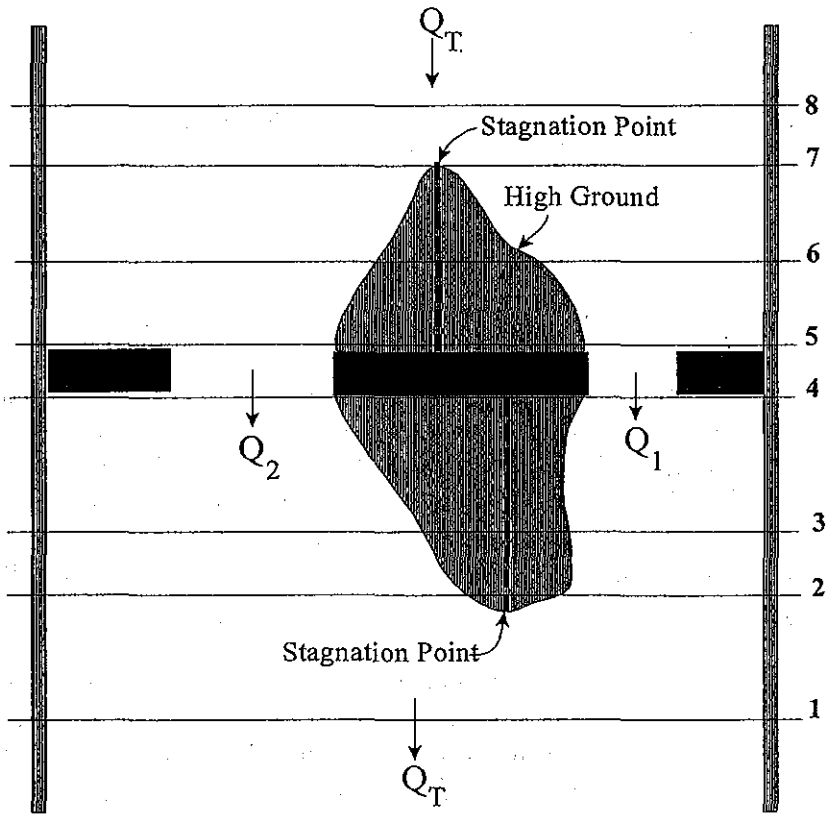

Figure 7.3 Example of a Divided Flow Problem

When modeling a divided flow, you must define how much flow is going through each reach. The current version of HEC-RAS can optimize the flow split. The user makes a first guess at the flow distribution, and then runs the model with the split flow optimization option turned on. The program uses an iterative procedure to calculate the correct flow in each reach. More information on split flow optimization can be found in chapter 7 of the User's Manual, chapter 4 of the Hydraulic Reference Manual, and Example 15 of the Applications Guide.

CHAPTER 8

Modeling Gated Spillways, Weirs and Drop Structures

This version of HEC-RAS allows the user to model inline structures, such as gated spillways, overflow weirs, drop structures, as well as lateral structures. HEC-RAS has the ability to model radial gates (often called tainter gates) or vertical lift gates (sluice gates). The spillway crest of the gates can be modeled as either an ogee shape or a broad crested weir shape. In addition to the gate openings, the user can also define a separate uncontrolled overflow weir.

This chapter describes the general modeling guidelines for using the gated spillway and weir capability within HEC-RAS, as well as the hydraulic equations used. Information on modeling drop structures with HEC-RAS is also provided. For information on how to enter gated spillway and weir data, as well as viewing gated spillway and weir results, see Chapter 6 and Chapter 8 of the HEC-RAS User's Manual, respectively.

Contents

General Modeling Guidelines

The gated spillway and weir option within HEC-RAS can be used to model inline (structures across the main stream) or lateral (structures along the side of the stream) weirs, gated spillways, or a combination of both. An example of a dam with a gated spillway and overflow weir is shown in Figure 8.1.

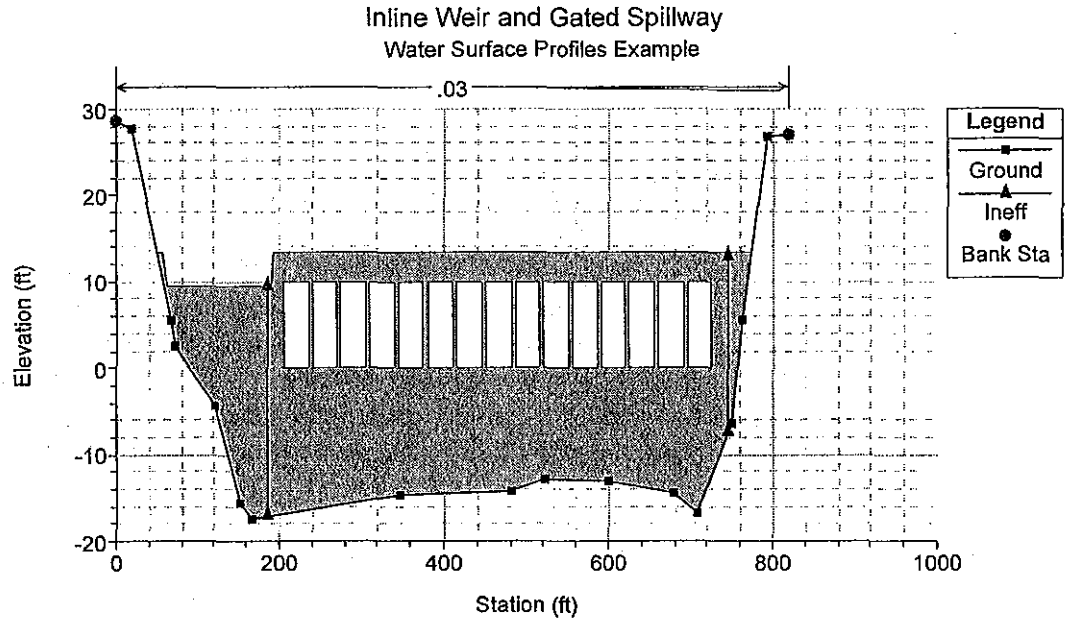

Figure 8.1 Example of Inline Gated Spillway and Weir

In the example shown in Figure 8.1 there are 15 identical gate openings and the entire top of the embankment is specified as an overflow weir.

Gated Spillways within HEC-RAS can be modeled as radial gates (often called tainter gates) or vertical lift gates (sluice gates). The equations used to model the gate openings can handle both submerged and unsubmerged conditions at the inlet and outlet of the gates. If the gates are opened far enough, such that unsubmerged conditions exist at the upstream end, the program automatically switches to a weir flow equation to calculate the hydraulics of the flow. The spillway crest through the gate openings can be specified as either an ogee crest shape or a broad crested weir. The program has the ability to calculate both free flowing and submerged weir flow through the gate openings. Figure 8.2 is a diagram of the two gate types with different spillway crests.

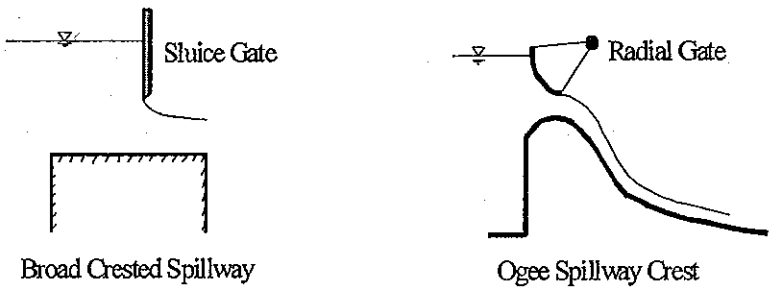

Figure 8.2 Example Sluice and Radial Gates

Up to 10 gate groups can be entered into the program at any one river crossing. Each gate group can have up to 25 identical gate openings. Identical gate openings must be the same gate type; size; elevation; and have identical gate coefficients. If anything about the gates is different, except their physical location across the stream, the gates must be entered as separate gate groups.

The overflow weir capability can be used by itself or in conjunction with the gated spillway option. The overflow weir is entered as a series of station and elevation points across the stream, which allows for complicated weir shapes. The user must specify if the weir is broad crested or an ogee shape. The software has the ability to account for submergence due to the downstream tailwater. Additionally, if the weir has an ogee shaped crest, the program can calculate the appropriate weir coefficient for a given design head. The weir coefficient will automatically be decreased or increased when the actual head is lower or higher than the design head.

Cross Section Locations

The inline weir and gated spillway routines in HEC-RAS require the same cross sections as the bridge and culvert routines. Four cross sections in the vicinity of the hydraulic structure are required for a complete model, two upstream and two downstream. In general, there should always be additional cross sections downstream from any structure (bridge, culvert, weir, etc...), such that the user entered downstream boundary condition does not affect the hydraulics of flow through the structure. In order to simplify the discussion of cross sections around the inline weir and gated spillway structure, only the four cross sections in the vicinity will be discussed. These four cross sections include: one cross section sufficiently downstream such that the flow is fully expanded; one at the downstream end of the structure (representing the tailwater location); one at the upstream end of the structure (representing the headwater location); and one cross section located far enough upstream at the

point in which the flow begins to contract. Note, the cross sections that bound the structure represent the channel geometry outside of the embankment. Figure 8.3 illustrates the cross sections required for an inline weir and gated spillway model.

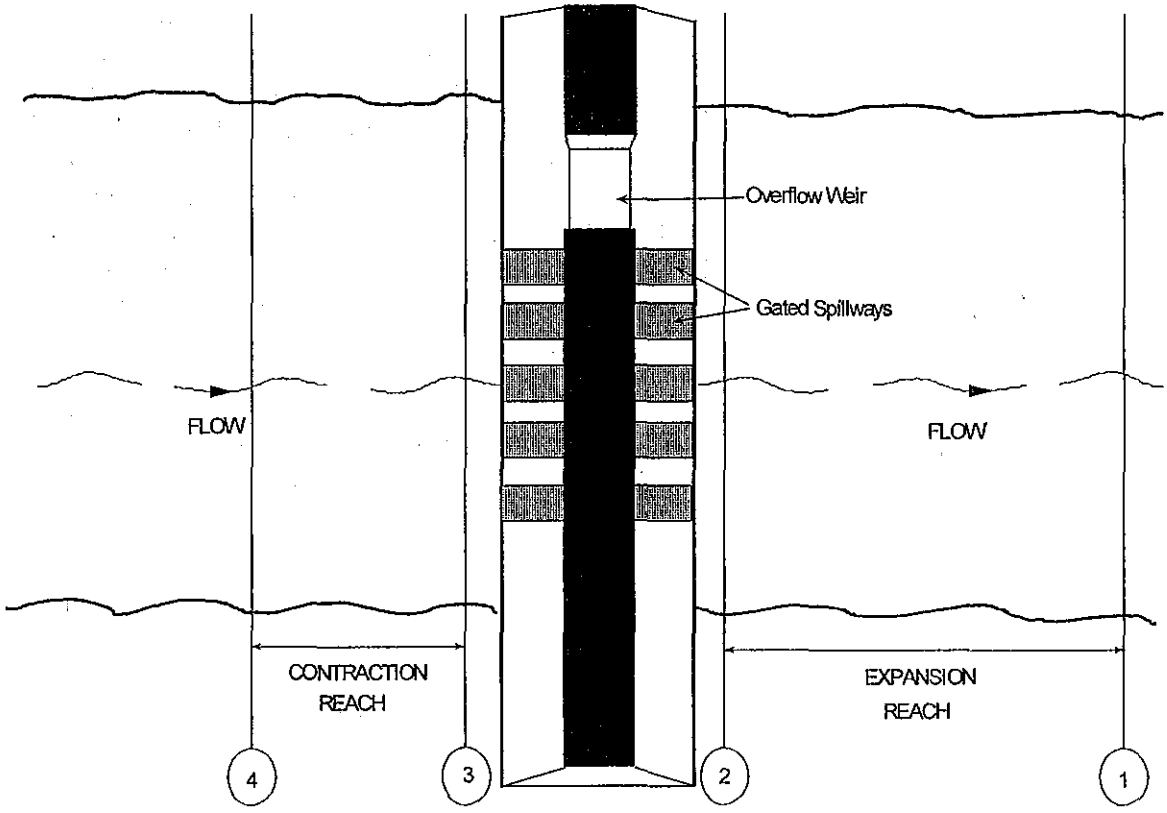

Figure 8.3 Cross Section Layout for Inline Gated Spillways and Weirs

Cross Section 1. Cross Section 1 for a weir and/or gated spillway should be located at a point where flow has fully expanded from its constricted top width caused by the constriction. The entire area of Cross Section 1 is usually considered to be effective in conveying flow.

Cross Section 2. Cross Section 2 is located a short distance downstream from the structure. The computed water surface at this cross section will represent the tailwater elevation of the weir and the gated spillways. This cross section should not include any of the structure or embankment, but represents the physical shape of the channel just downstream of the structure. The shape and location of this cross section is entered separately from the Inline Weir and Gated Spillway data (from the cross section editor).

The HEC-RAS ineffective area option is used to restrict the effective flow area of Cross Section 2 to the flow area around or near the edges of the gated spillways, until flow overtops the overflow weir and/or embankment. The ineffective flow areas are used to represent the correct amount of active flow area just downstream of the structure. Establishing the correct amount of effective flow area is very important in computing an accurate tailwater elevation at Cross Section 2. Because the flow will begin to expand as it exits the gated spillways, the active flow area at Section 2 is generally wider than the width of the gate openings. The width of the active flow area will depend upon how far downstream Cross Section 2 is from the structure. In general, a reasonable assumption would be to assume a 1:1 expansion rate over this short distance. Figure 8.4 illustrates Cross Section 2 of a typical inline weir and gated spillway model. On Figure 8.4, the channel bank locations are indicated by small circles and the stations and elevations of the ineffective flow areas are indicated by triangles.

Cross Sections 1 and 2 are located so as to create a channel reach downstream of the structure in which the HEC-RAS program can accurately compute the friction losses and expansion losses that occur as the flow fully expands.

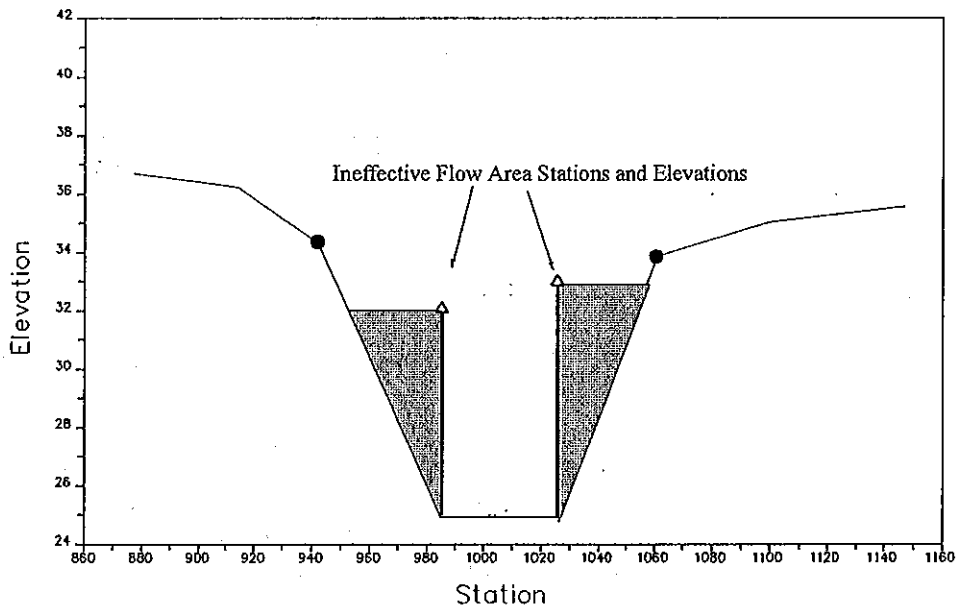

Figure 8.4 Cross Section 2 of Inline Gated Spillway and Weir Model

Cross Section 3. Cross Section 3 of an inline weir and gated spillway model is located a short distance upstream of the embankment, and represents the physical configuration of the upstream channel. The water surface computed at this cross section represents the upstream headwater for the overflow weir and the gated spillways. The software uses a combination of the deck/road embankment data, Cross Section 3, and the gated spillway data, to describe the hydraulic structure and the roadway embankment. The inline weir and gated spillway data is located at a river station between Cross Section 2 and

Cross Section 3.

The HEC-RAS ineffective area option is used to restrict the effective flow area of Cross Section 3 until the flow overtops the roadway. The ineffective flow area is used to represent the correct amount of active flow area just upstream of the structure. Because the flow is contracting rapidly as it enters the gate openings, the active flow area at Section 3 is generally wider than the width of the gates. The width of the active flow area will depend upon how far upstream Cross Section 3 is placed from the structure. In general, a reasonable assumption would be to assume a 1:1 contraction rate over this short distance. Figure 8.5 illustrates Cross Section 3 for a typical model, including the embankment profile and the gated spillways. On Figure 8.5, the channel bank locations are indicated by small circles, and the stations and elevations of ineffective areas are indicated by triangles.

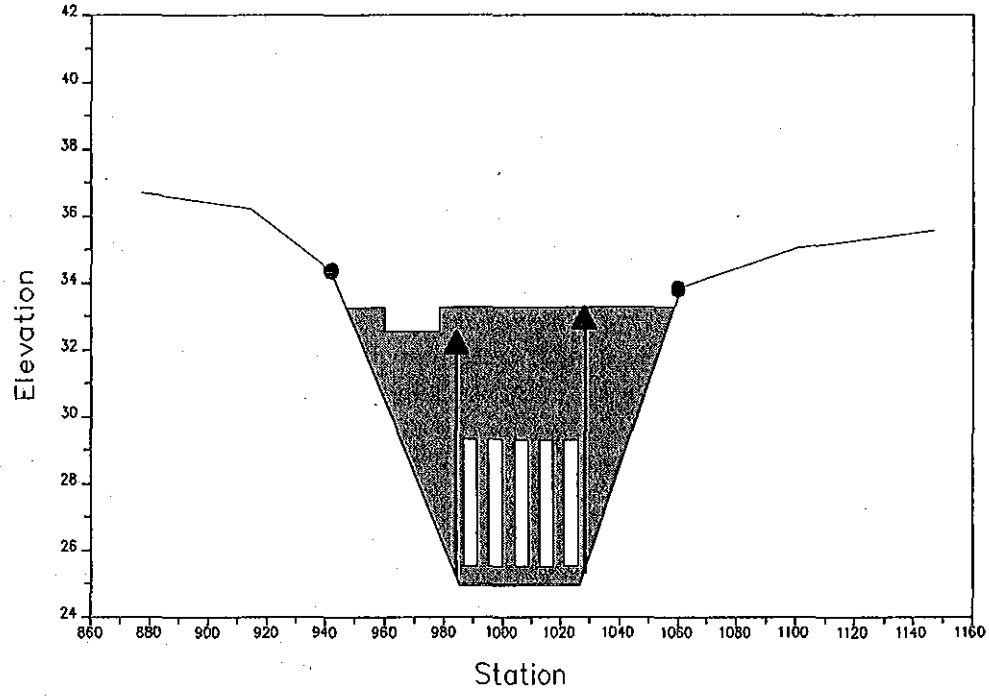

Figure 8.5 Cross Section 3 of Inline Gated Spillway and Weir

Cross Section 4. The final cross section in the inline weir and gated spillway model is located at a point where flow has not yet begun to contract from its unrestrained top width upstream of the structure. This distance is normally determined assuming a one to one contraction of flow. In other words, the average rate at which flow can contract to pass through the gate openings is assumed to be one foot laterally for every one foot traveled in the downstream direction. The entire area of Cross Section 4 is usually considered to be effective in conveying flow.

Expansion and Contraction Coefficients

User-defined coefficients are required to compute head losses due to the contraction and expansion of flows upstream and downstream of an inline weir and gated spillway structure. These losses are computed by multiplying an expansion or contraction coefficient by the absolute difference in velocity head between two cross sections.

If the velocity head increases in the downstream direction, a contraction coefficient is applied. When the velocity head decreases in the downstream direction, an expansion coefficient is used. Recommended values for the expansion and contraction coefficients have been given in Chapter 3 of this manual (table 3.2). As indicated by the tabulated values, the expansion of flow causes more energy loss than the contraction. Also, energy losses increase with the abruptness of the transition.

Hydraulic Computations Through Gated Spillways

As mentioned previously, the program is capable of modeling both radial gates (often called tainter gates) and vertical lift gates (sluice gates). The equations used to model the gate openings can handle both submerged and unsubmerged conditions at the inlet and the outlet of the gates. When the gates are opened to an elevation greater than the upstream water surface elevation, the program automatically switches to modeling the flow through the gates as weir flow. When the upstream water surface is greater than or equal to 1.25 times the height of the gate opening (with respect to the gates spillway crest), the gate flow equations are applied. When the upstream water surface is between 1.0 and 1.25 times the gate opening, the flow is in a zone of transition between weir flow and gate flow. The program computes the upstream head with both equations and then calculates a linear weighted average of the two values (this is an iterative process to obtain the final headwater elevation for a flow in the transition range). When the upstream water surface is equal to or less than 1.0 times the gate opening, then the flow through the gate opening is calculated as weir flow.

Radial Gates

An example radial gate with an ogee spillway crest is shown in Figure 8.6.

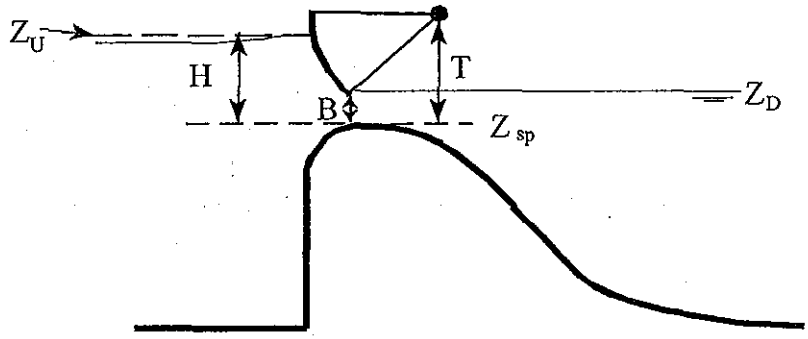

Figure 8.6 Example Radial Gate with an Ogee Spillway Crest

The flow through the gate is considered to be "Free Flow" when the downstream tailwater elevation (Z_D) is not high enough to cause an increase in the upstream headwater elevation for a given flow rate. The equation used for a Radial gate under free flow conditions is as follows:

$$Q = C\sqrt{2g}\, W\, T^{TE}\, B^{BE}\, H^{HE} \qquad (8\text{-}1)$$

Where: Q = Flow rate in cfs
C = Discharge coefficient (typically ranges from 0.6 - 0.8)
W = Width of the gated spillway in feet
T = Trunnion height (from spillway crest to trunnion pivot point)
TE = Trunnion height exponent, typically about 0.16 (default 0.0)
B = Height of gate opening in feet
BE = Gate opening exponent, typically about 0.72 (default 1.0)
H = Upstream Energy Head above the spillway crest Z_U - Z_{sp}
HE = Head exponent, typically about 0.62 (default 0.5)
Z_U = Elevation of the upstream energy grade line
Z_D = Elevation of the downstream water surface
Z_{sp} = Elevation of the spillway crest through the gate

When the downstream tailwater increases to the point at which the gate is no longer flowing freely (downstream submergence is causing a greater upstream headwater for a given flow), the program switches to the following form of

the equation:

$$Q = C\sqrt{2g}\, W\, T^{TE}\, B^{BE}\, (3H)^{HE} \qquad (8\text{-}2)$$

where: H = $Z_U - Z_D$

Submergence begins to occur when the tailwater depth divided by the headwater energy depth above the spillway, is greater than 0.67. Equation 8-2 is used to transition between free flow and fully submerged flow. This transition is set up so the program will gradually change to the fully submerged Orifice equation when the gates reach a submergence of 0.80. The fully submerged Orifice equation is shown below:

$$Q = CA\sqrt{2gH} \qquad (8\text{-}3)$$

Where: A = Area of the gate opening.
H = $Z_U - Z_D$
C = Discharge coefficient (typically 0.8)

Sluice Gate

An example sluice gate with a broad crest is shown in Figure 8.7.

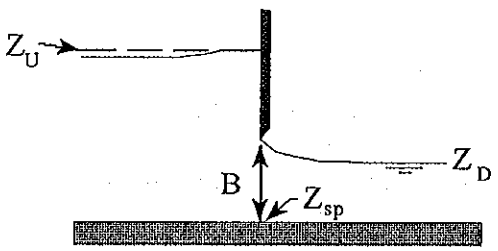

Figure 8.7 Example Sluice Gate with Broad Crested Spillway

The equation for a free flowing sluice gate is as follows:

$$Q = CW\, B\sqrt{2gH} \qquad (8\text{-}4)$$

Where: H = Upstream energy head above the spillway crest ($Z_U - Z_{sp}$)
C = Coefficient of discharge, typically 0.5 to 0.7

When the downstream tailwater increases to the point at which the gate is no longer flowing freely (downstream submergence is causing a greater upstream headwater for a given flow), the program switches to the following form of the equation:

$$Q = CW\,B\sqrt{2g3H} \tag{8-5}$$

Where: H $= Z_U - Z_D$

Submergence begins to occur when the tailwater depth above the spillway divided by the headwater energy above the spillway, is greater than 0.67. Equation 8-5 is used to transition between free flow and fully submerged flow. This transition is set up so the program will gradually change to the fully submerged Orifice equation (Equation 8-3) when the gates reach a submergence of 0.80.

Low Flow Through The Gates

When the upstream water surface is equal to or less than the top of the gate opening, the program calculates the flow through the gates as weir flow. An example of low flow through a gated structure is shown in Figure 8.8.

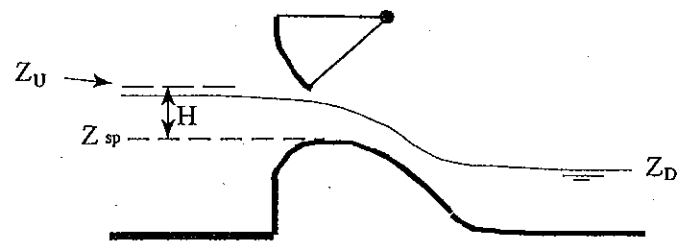

Figure 8.8 Example Radial Gate Under Low Flow Conditions

The standard weir equation used for this calculation is shown below:

$$Q = C\,L\,H^{3/2} \tag{8-6}$$

where: C = Weir flow coefficient, typical values will range from 2.6 to 4.0 depending upon the shape of the spillway crest (i.e., broad crested or ogee shaped).

L = Length of the spillway crest.

H = Upstream energy head above the spillway crest.

The user can specify either a broad crested or ogee weir shape for the spillway crest of the gate. If the crest of the spillway is ogee shaped, the weir coefficient will be automatically adjusted when the upstream energy head is higher or lower than a user specified design head. The adjustment is based on the curve shown in Figure 8.9 (Bureau of Reclamation, 1977). The curve provides ratios for the discharge coefficient, based on the ratio of the actual head to the design head of the spillway. In Figure 8.9, H_e is the upstream energy head; H_o is the design head; C_o is the coefficient of discharge at the design head; and C is the coefficient of discharge for an energy head other than the design head.

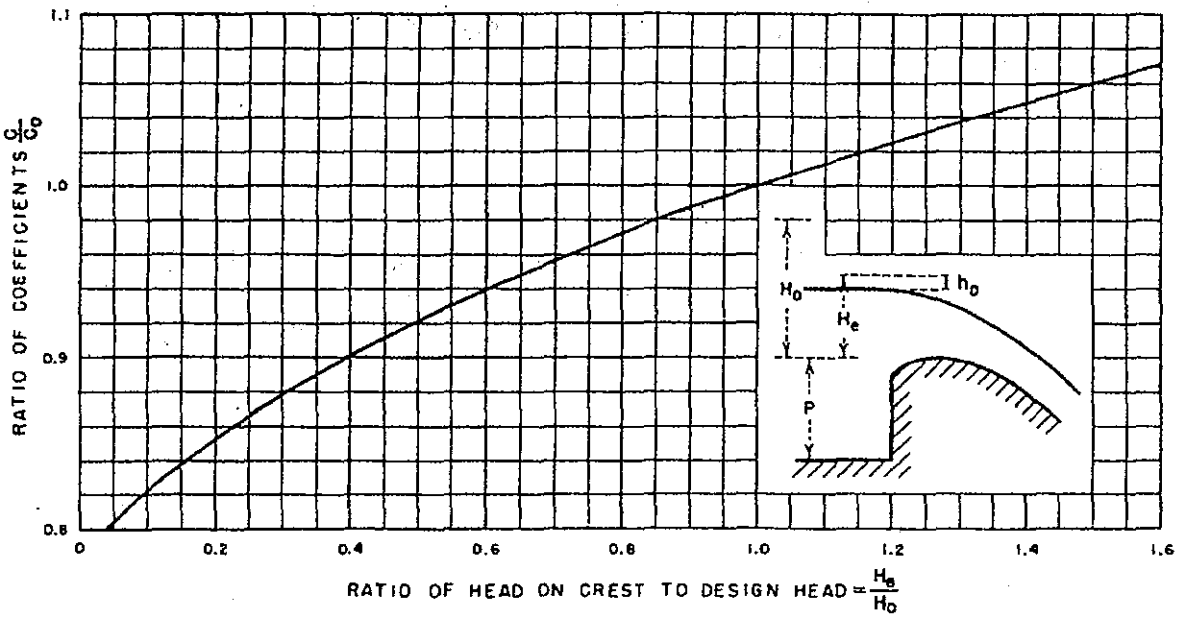

Figure 8.9 Weir Flow Coefficient for Other Than Design Head

The program automatically accounts for submergence on the weir when the tailwater is high enough to slow down the flow. Submergence is defined as the depth of water above the weir on the downstream side divided by the headwater energy depth of water above the weir on the upstream side. As the degree of submergence increases, the program reduces the weir flow coefficient. Submergence corrections are based on a trapezoidal (broad crested) or ogee shaped weir.

Uncontrolled Overflow Weirs

In addition to the gate openings, the user can define an uncontrolled overflow weir at the same river crossing. The weir could represent an emergency spillway or the entire top of the structure and embankment. Weir flow is computed using the standard weir equation (equation 8-6). The uncontrolled overflow weir can be specified as either a broad crested or ogee shaped weir. If the weir is ogee shaped, the program will allow for fluctuations in the discharge coefficient to account for upstream energy heads that are either higher or lower than the design head (figure 8.9). The program will automatically account for any submergence of the downstream tailwater on the weir, and reduce the flow over the weir. The modeler is referred to Chapter 5 of the Hydraulic Reference Manual for additional discussions concerning uncontrolled overflow weirs, including submergence criteria and selection of weir coefficients.

Modeling Lateral Structures

HEC-RAS has the ability to model lateral weirs, gated spillways, and culverts. The modeler can insert a lateral weir only, or a separate gated spillway structure, or any combination of the three types. An example diagram of a lateral structure is shown in Figure 8.10.

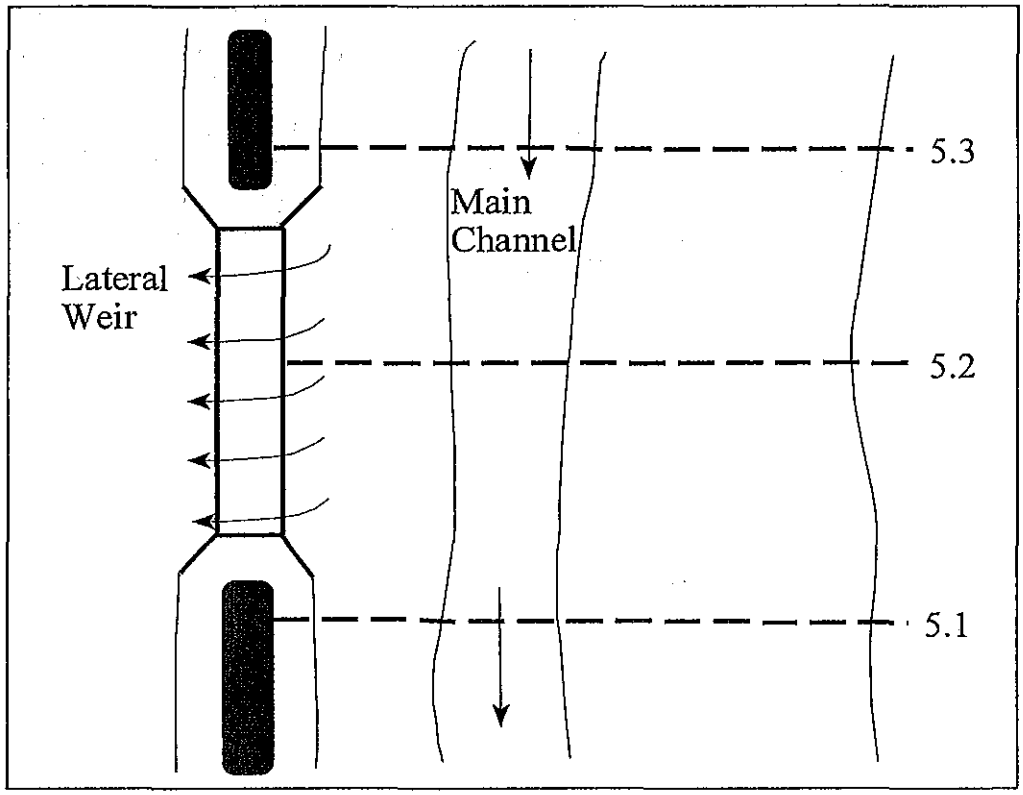

Figure 8.10 Plan View of an Example Lateral Weir

At a minimum there must be a cross section upstream of, and a cross section downstream of the lateral structure. The upstream cross section can either be right at the beginning of the structure, or it can be a short distance upstream. The downstream cross section can be right at the downstream end of the structure or it can be a short distance downstream. The user can have any number of additional cross sections in the middle of the structure.

If there are gated openings in the structure, the hydraulic computations for lateral gated spillways are exactly the same as those described previously for inline gated spillways. The only difference is that the headwater energy is computed separately for each gate, based on its centerline location along the stream. The headwater energy for each gate is interpolated linearly between computed points at each cross section.

An example lateral structure is shown in Figure 8.11 as a profile view.

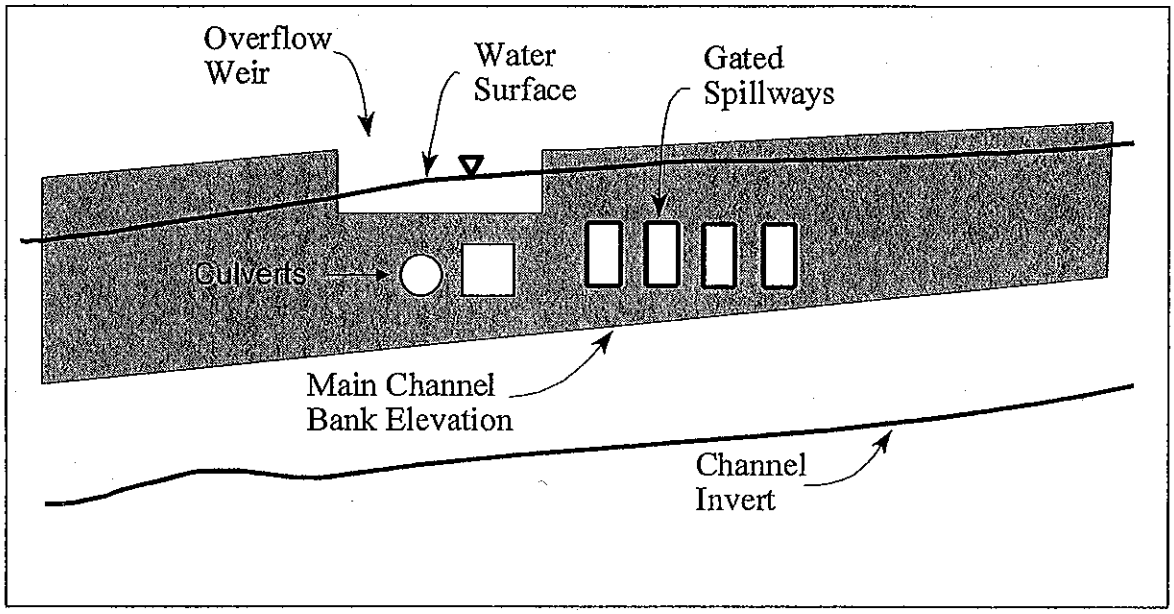

Figure 8.11 Example Lateral Weir and Gated Spillway

As shown in Figure 8.11, the water surface across the weir has a slope to it. Additionally, the weir itself could be on a slope. Because of this, an equation for weir flow with a sloping water surface and weir sill had to be derived. Shown in Figure 8.12 is a sloping weir segment with a sloping water surface. The equation for a sloping line representing the water surface and the weir segment are shown. The constants a_{ws} and a_w represent the slope of the water surface and the weir segment, respectively, while the variable C_{ws} and C_w are constants representing the initial elevations.

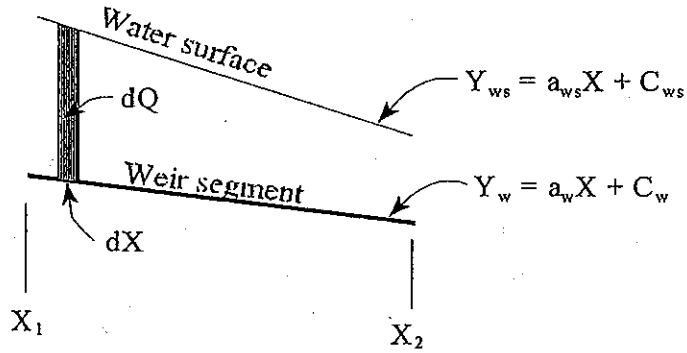

Figure 8.12 Sloping Weir Segment and Water Surface

The standard weir equation (8-6) assumes that the weir is parallel with the water surface (i.e. that the depth of water is constant from one end of the weir segment to the other). The following general equation is derived for a sloping weir and water surface by integrating the standard weir equation:

$$dQ = C(y_{ws} - y_w)^{3/2}\, dx \tag{8-7}$$

$$dQ = C(a_{ws}x + C_{ws} - a_w x - C_w)^{3/2}\, dx \tag{8-8}$$

$$dQ = C((a_{ws} - a_w)x + C_{ws} - C_w)^{3/2}\, dx \tag{8-9}$$

Assuming: $a_1 = a_{ws} - a_w$ and $C_1 = C_{ws} - C_w$

$$\int_{x_1}^{x_2} dQ = C\int_{x_1}^{x_2} (a_1 x + C_1)^{3/2}\, dx = \frac{2C}{5a_1}(a_1 x + C_1)^{5/2}\Big]_{x_1}^{x_2} \tag{8-10}$$

$$Q_{x_1 - x_2} = \frac{2C}{5a_1}((a_1 x_2 + C_1)^{5/2} - (a_1 x_1 + C_1)^{5/2}) \tag{8-11}$$

The above equation is valid as long as a_1 is not zero. When a_1 is zero, this implies that the water surface and the weir segment are parallel. When this is true, the original weir equation (equation 8-6) is used.

Within HEC-RAS, flow over a lateral weir can be computed from either the energy grade line or the water surface elevation. The standard weir equation is derived with the upstream energy head being based on the distance from the weir sill to the upstream energy gradeline. The energy gradeline is the default for a lateral weir as well. However, the user has the option of instructing the program to use the water surface elevation when computing the head term of the weir equation. This would be most appropriate when the weir is located close to the main channel. In this situation the energy due to the velocity head is in the downstream direction, and not over the top of the lateral weir. Therefore, the computation of the energy head over the lateral weir is best depicted by using the water surface of the flow in the channel.

The predecessor to HEC-RAS (HEC-2 program) used the water surface elevation as the default for lateral weir calculations. This is an important point to remember when comparing results between HEC-RAS and HEC-2. However, both programs allow the user to select either the energy gradeline or the water surface elevation for this calculation.

Drop Structures

Drop structures can be modeled with the inline weir option or as a series of cross sections. If you are just interested in getting the water surface upstream and downstream of the drop structure, then the inline weir option would probably be the most appropriate (as described in a previous section of this chapter). However, if you want to compute a more detailed profile upstream of and through the drop, then you will need to model it as a series of cross sections.

When modeling a drop structure as a series of cross sections, the most important thing is to have enough cross sections at the correct locations. Cross sections need to be closely spaced where the water surface and velocity is changing rapidly (i.e. just upstream and downstream of the drop). An example of a drop structure is shown in Figure 8.13.

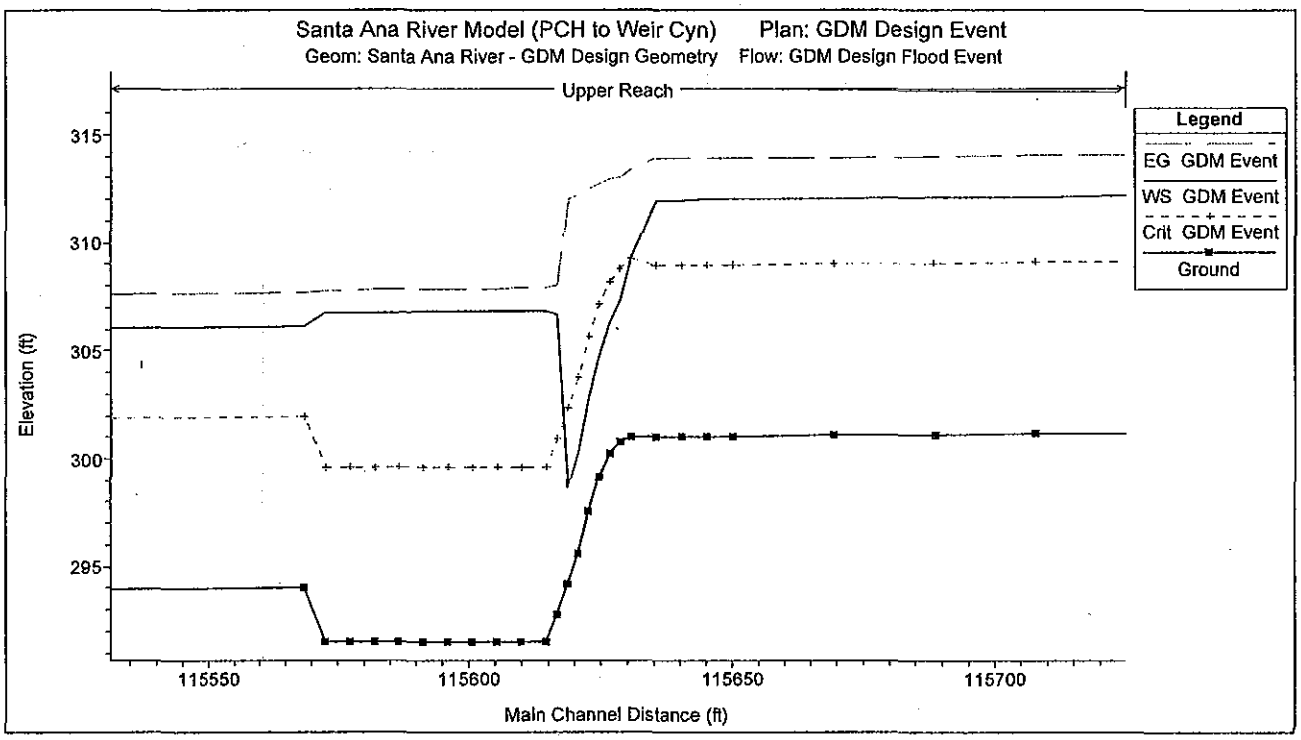

Figure 8.13 Drop Structure Modeled With Cross Sections

As shown in Figure 8.13, the spacing between cross sections should decrease as you get closer to the drop structure (cross sections are located at each square shown on the ground profile). Additionally, if the drop itself is on a slope, then additional cross sections should be placed along the sloping drop in order to model the transition from subcritical to supercritical flow. Several cross sections should also be placed in the stilling basin (location of energy dissipaters) in order to correctly locate where the hydraulic jump will occur

(i.e. the hydraulic jump could occur on the slope of the drop, or it may occur inside of the stilling basin). Manning's n values should be increased inside of the stilling basin to represent the increased roughness do to the energy dissipater blocks.

In order to evaluate this method of modeling drop structures, a comparison was made between a physical model study and an HEC-RAS model of the drop structure. During the design phase of improvements to the Santa Ana river, the Waterways Experiment Station (WES) was contracted to study the drop structures and make recommendations. The results of this study were reported in General Design for Replacement of or Modifications to the Lower Santa Ana River Drop Structures, Orange County, California (Technical Report HL-94-4, April 1994, USACE). Over 50 different designs were tested in 1:25 scale flume models and 1:40 scale full width models. The designs evaluated existing structures, modifying original structures and replacing them with entirely new designs. The drop structure design used in the Santa Ana River is similar to one referred to as Type 10 in the report. A HEC-RAS model was developed to model the Type 10 drop structure and the model results were compared to the flume results.

The geometry for the HEC-RAS model was developed from the following design diagram in the WES report.

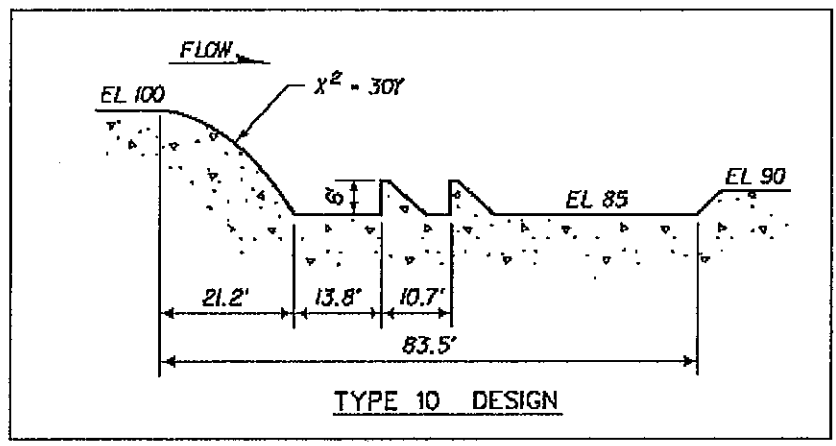

Figure 8.14 WES Report Plate 13.

The total reach in the model was 350 feet, 150 upstream of the crest of the drop structure and 200 feet below the crest. The cross sections were rectangular, with the following spacing used in the HEC-RAS model:

Location	Reach Lengths
Upstream of Drop structure:	10 feet
Over the drop:	2 feet
Inside the stilling basin:	10 feet
Downstream of Structure:	10 feet

The expansion and contraction coefficients were set to 0.3 and 0.1 respectively. Two Manning's n values were used in the HEC-RAS model of the flume. Inside the stilling basin where the bottom elevation was 85 feet, the Manning's n values were set to 0.05. In all other cross sections the Manning's n values were set to 0.03. The higher n value was used in the stilling basin to account for the additional energy loss due to the rows of baffles that exist in the flume but were not added into the cross sections data of HEC-RAS.

The original data from the flume experiments were obtained from the Waterways Experiment Station, and entered in HEC-RAS as observed data. The results of the HEC-RAS model are compared in profile to the observed water surface elevations in the flume study in Figure 8.15. These results show that HEC-RAS was able to adequately model the drop structures, both upstream and downstream of the crest.

Some differences occur right at the crest and through the hydraulic jump. The differences at the crest are due to the fact that the energy equation will always show the flow passing through critical depth at the top of the crest. Whereas, in the field it has been shown that the flow passes through critical depth at a distance upstream of 3-4 times critical depth. However, as shown in Figure 8.15, a short distance upstream of the crest the HEC-RAS program converges to the same depth as the observed data. Correctly obtaining the maximum upstream water surface in the most important part of modeling the drop structure.

Downstream of the drop, the flow is supercritical and then goes through a hydraulic jump. The flume data shows the jump occurring over a distance of 50 to 60 feet with a lot of turbulence. The HEC-RAS model cannot predict how long of a distance it will take for the jump to occur, but it can predict where the jump will begin. The HEC-RAS model will always show the jump occurring between two adjacent cross sections. The HEC-RAS model shows the higher water surface inside of the stilling basin and then going down below the stilling basin. The model shows all of this as a fairly smooth transition, whereas it is actually a turbulent transition with the water surface bouncing up and down. In general, the results from the HEC-RAS model are very good at predicting the stages upstream, inside, and downstream of the drop structure.

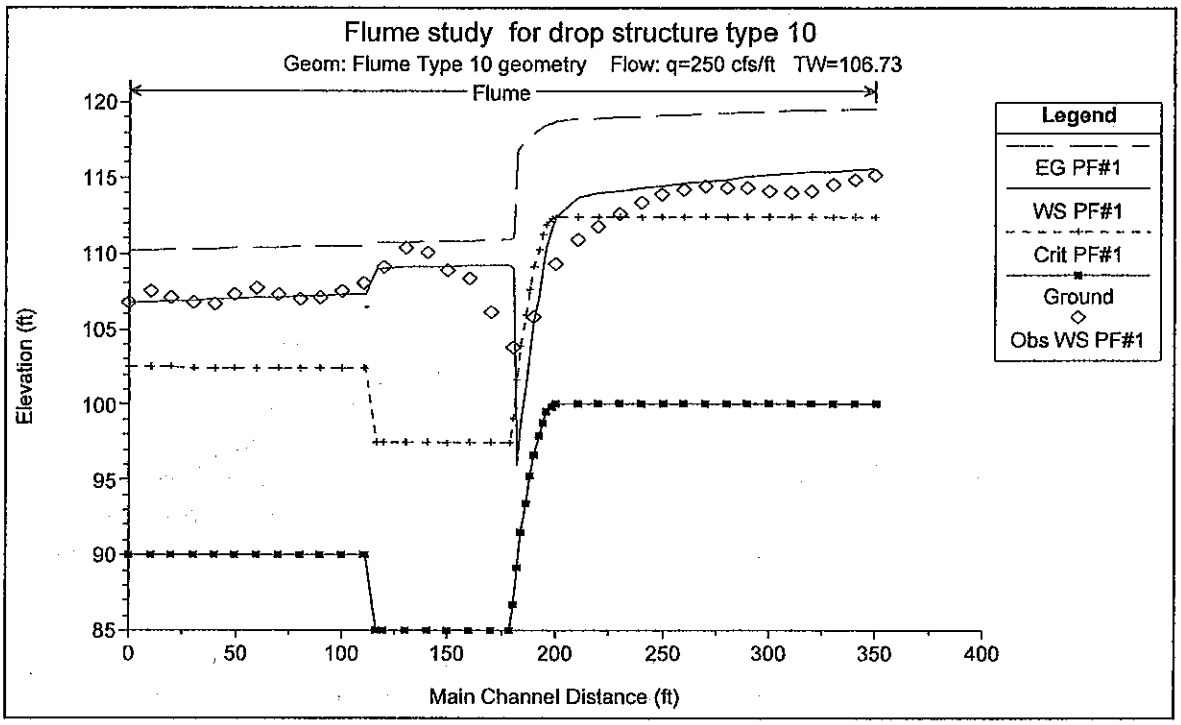

Figure 8.15 Comparison Between Flume Data and HEC-RAS For a Drop Structure

CHAPTER 9

Floodplain Encroachment Calculations

The evaluation of the impact of floodplain encroachments on water surface profiles can be of substantial interest to planners, land developers, and engineers. It is also a significant aspect of flood insurance studies. HEC-RAS contains five optional methods for specifying floodplain encroachments within a steady flow analysis. This chapter describes the computational details of each of the five encroachment methods, as well as special considerations for encroachments at bridges, culverts, and multiple openings. Discussions are also provided on a general modeling approach for performing an encroachment analysis.

For information on how to enter encroachment data, how to perform the encroachment calculations, and viewing encroachment results, see Chapter 9 of the HEC-RAS user's manual.

Contents

Introduction

The HEC-RAS floodway procedure for steady flow analyses is based on calculating a natural profile (existing conditions geometry) as the first profile in a multiple profile run. Other profiles in a run are calculated using various encroachment options, as desired. Before performing an encroachment analysis, the user should have developed a model of the existing river system. This model should be calibrated to the fullest extent that is possible. Verification that the model is adequately modeling the river system is an extremely important step before attempting to perform an encroachment analysis.

Encroachment Methods

HEC-RAS contains five optional methods for specifying floodplain encroachments. Each method is illustrated in the following paragraphs.

Encroachment Method 1

With encroachment method 1 the user specifies the exact locations of the encroachment stations for each individual cross section. The encroachment stations can also be specified differently for each profile. An example of encroachment method 1 is shown in Figure 9.1.

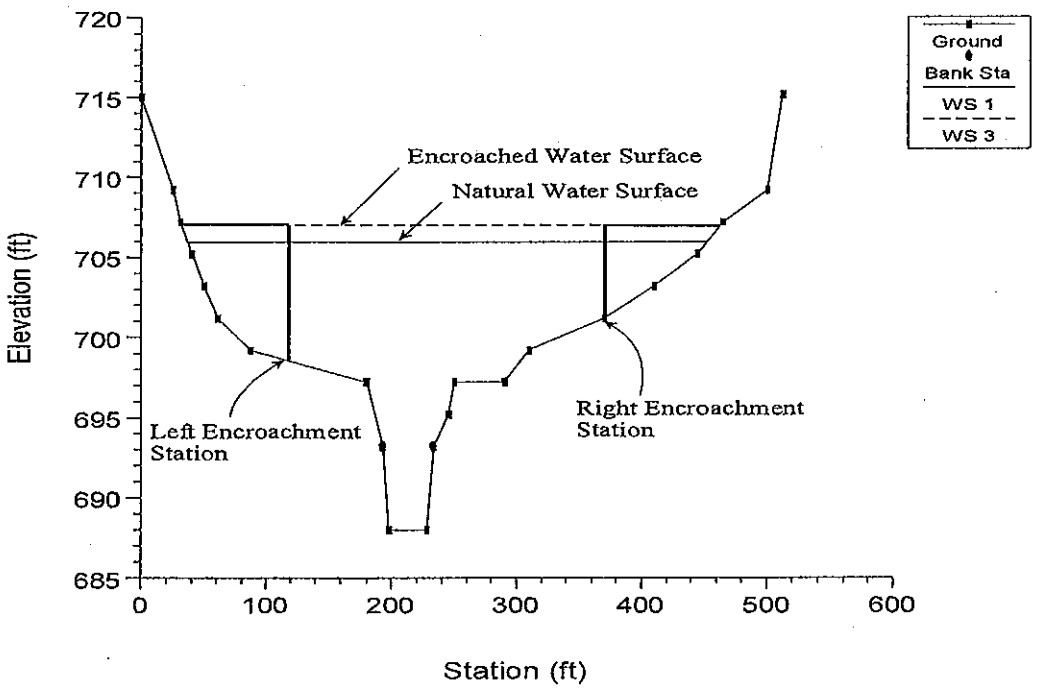

Figure 9.1 Example of Encroachment Method 1

Encroachment Method 2

Method 2 utilizes a fixed top width. The top width can be specified separately for each cross section. The left and right encroachment stations are made equal distance from the centerline of the channel, which is halfway between the left and right bank stations. If the user specified top width would end up with an encroachment inside the channel, the program sets that encroachment (left and/or right) to the channel bank station. An example of encroachment method 2 is shown in Figure 9.2.

HEC-RAS also allows the user to establish a left and right offset. The left and right offset is used to establish a buffer zone around the main channel for further limiting the amount of the encroachments. For example, if a user established a right offset of 5 feet and a left offset of 10 feet, the model will limit all encroachments to 5 feet from the right bank station and 10 feet from the left bank station. If a user entered top width would end up inside of an offset, the program will set the encroachment at the offset stationing.

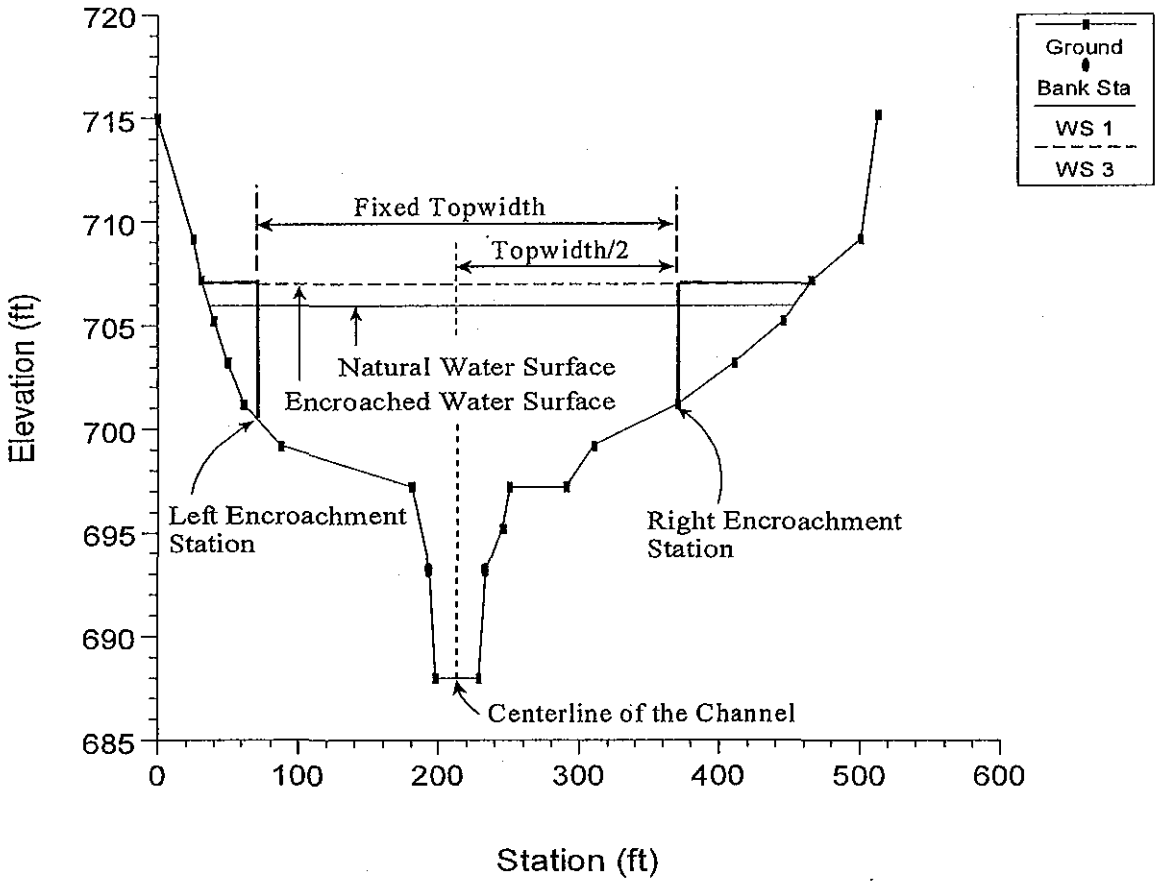

Figure 9.2 Example of Encroachment Method 2

Encroachment Method 3

Method 3 calculates encroachment stations for a specified percent reduction in the conveyance (%K Reduction) of the natural profile for each cross section. One-half of the conveyance is eliminated on each side of the cross section (if possible). The computed encroachments cannot infringe on the main channel or any user specified encroachment offsets. If one-half of the conveyance exceeds either overbank conveyance, the program will attempt to make up the difference on the other side. If the percent reduction in cross section conveyance cannot be accommodated by both overbank areas combined, the encroachment stations are made equal to the stations of left and right channel banks (or the offset stations, if specified). An example of encroachment method 3 is shown in Figure 9.3.

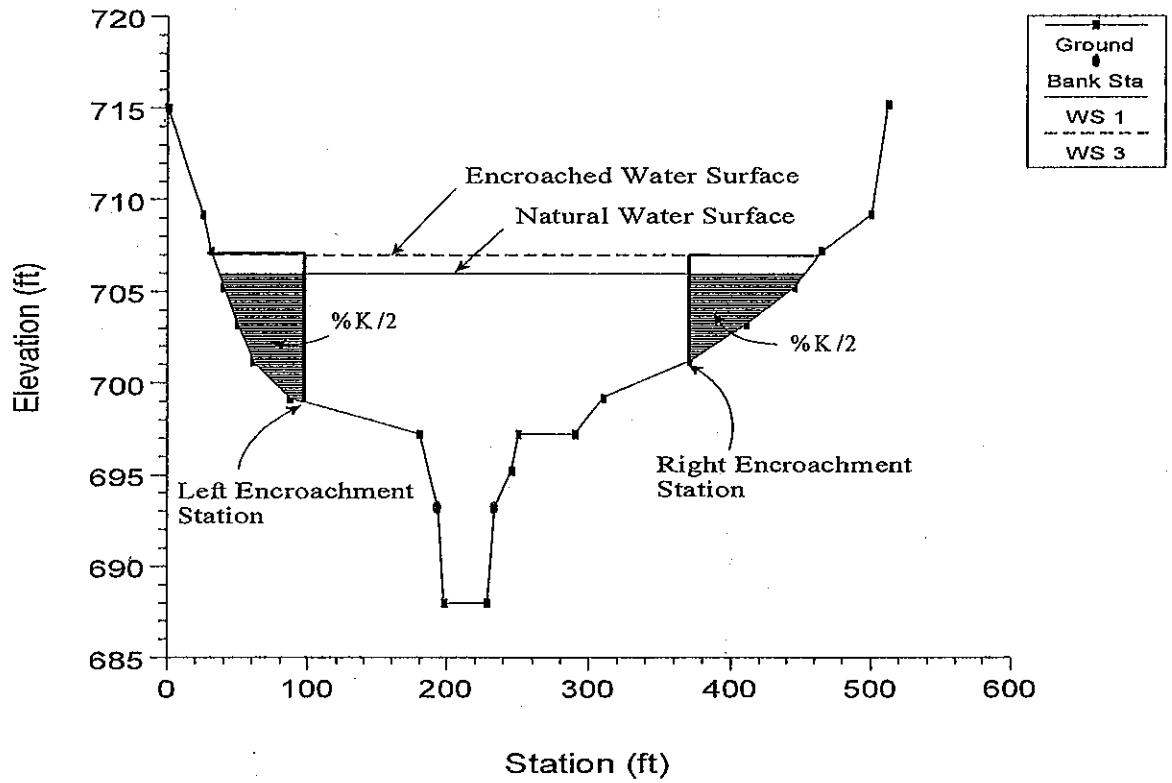

Figure 9.3 Example of Encroachment Method 3

Encroachment Method 3 requires that the first profile (of a multiple profile run) must be a natural (un-encroached) profile. Subsequent profiles (profiles 2-15) of a multiple profile run may be utilized for Method 3 encroachments. The percentage of reduction in conveyance can be changed for any cross section. A value of 10 percent for the second profile would indicate that 10 percent of the conveyance based on the natural profile (first profile) will be eliminated - 5 percent from each overbank. Equal conveyance reduction is the default.

An alternate scheme to **equal** conveyance reduction is conveyance reduction in **proportion** to the distribution of natural overbank conveyance. For instance, if the natural cross section had twice as much conveyance in the left overbank as in the right overbank, a 10 percent conveyance reduction value would reduce 6.7 percent from the left overbank and 3.3 percent from the right overbank.

Encroachment Method 4

Method 4 computes encroachment stations so that conveyance within the encroached cross section (at some higher elevation) is equal to the conveyance of the natural cross section at the natural water level. This higher elevation is specified as a fixed amount (target increase) above the natural (e.g., 100 year) profile. The encroachment stations are determined so that an equal loss of conveyance (at the higher elevation) occurs on each overbank, if possible. If half of the loss cannot be obtained in one overbank, the difference will be made up, if possible, in the other overbank, except that encroachments will not be allowed to fall within the main channel.

A target increase of 1.0 indicates that a 1 foot rise will be used to determine the encroachments based on equal conveyance. An alternate scheme to **equal** conveyance reduction is to reduce conveyance in **proportion** to the distribution of natural overbank conveyance. See Method 3 for an explanation of this. A key difference between Method 4 and Method 3 is that the reduction in conveyance is based on the higher water surface (target water surface) for Method 4, while Method 3 uses the lower water surface (natural water surface). An example of a Method 4 encroachment is shown in Figure 9.4.

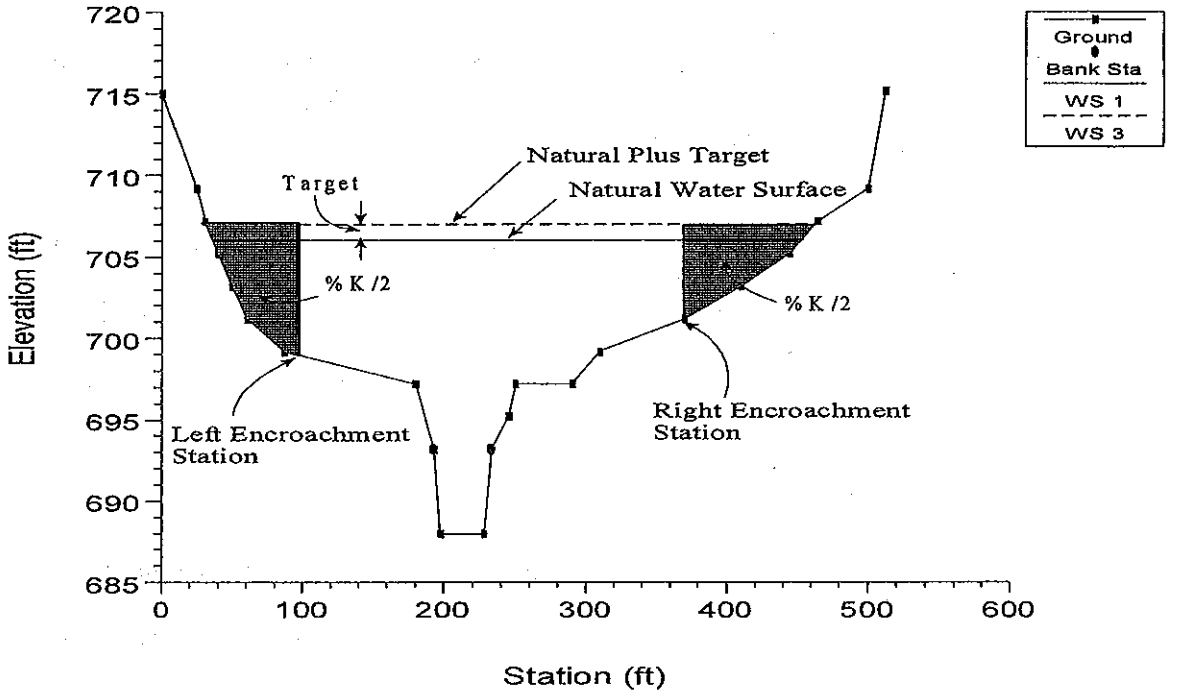

Figure 9.4 Example of Encroachment Method 4

Encroachment Method 5

Method 5 operates much like Method 4 except that an optimization scheme is used to obtain the target difference in water surface elevation between natural and encroached conditions. A maximum of 20 trials is allowed in attempting a solution. Equal conveyance reduction is attempted in each overbank, unless this is not possible (i.e., the encroachment goes all the way into the bank station before the target is met). The input data for method 5 consists of a target water surface increase and a target energy increase. The program objective is to match the target water surface without exceeding the target energy. If this is not possible, the program will then try to find the encroachments that match the target energy. If no target energy is entered, the program will keep encroaching until the water surface target is met. If only a target energy is entered, the program will keep encroaching until the target energy is met. If neither of the criteria is met after 20 trials, the program will take the best answer from all the trials and use it as the final result. The target water surface and energy can be changed at any cross section, like Methods 1 through 4. An example of method 5 is shown in Figure 9.5.

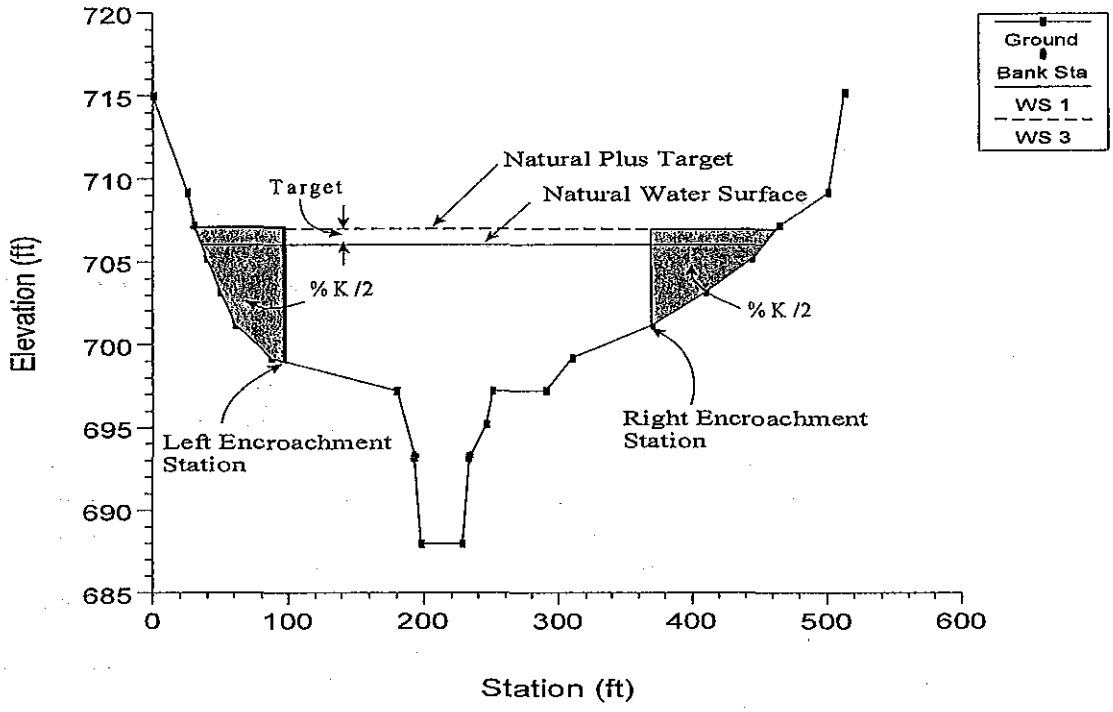

Figure 9.5 Example of Encroachment Method 5

Bridge, Culvert, and Multiple Opening Encroachments

In general, the default methodology for encroachments at bridges, culverts, and multiple openings, is to use the downstream computed encroachments through the structure, and at the cross section just upstream of the structure (the program does this automatically). There are a few exceptions to this rule.

First, when using Method 1, the user can enter separate encroachment stations downstream of the structure, inside the structure, and upstream of the structure. Only one set of encroachments can be entered for inside of the structure.

Second, for encroachment methods 2 through 5, the program will allow for separate encroachment calculations at a bridge, when using the energy based bridge computation method. For all other bridge computation methods (Momentum, Yarnell, WSPRO, Pressure Flow, Pressure and Weir Flow, and Low Flow and Weir Flow) the program will use the computed downstream encroachments through the bridge and at the cross section just upstream.

At a culvert crossing or a multiple opening, when using encroachment methods 2 through 5, the program will always use the computed downstream encroachments through the structure and just upstream of the structure. The

only way to override this is to use Method 1 encroachments.

Also, encroachments can be turned off at any bridge, culvert, or multiple opening.

General Modeling Guidelines

The HEC-RAS floodway procedure is based on calculating a natural profile (no encroachments) as the first profile of a multiple profile run. Subsequent profiles are calculated with the various encroachment options available in the program.

In general, when performing a floodway analysis, encroachment methods 4 and 5 are normally used to get a first cut at the encroachment stations. Recognizing that the initial floodway computations may provide changes in water surface elevations greater, or less, than the "target" increase, initial computer runs are usually made with several "target" values. The initial computer results should then be analyzed for increases in water surface elevations, changes in velocities, changes in top width, and other parameters. Also, plotting the results with the X-Y-Z perspective plot, or onto a topographic map, is recommended. From these initial results, new estimates can be made and tried.

The increase in water surface elevation will frequently exceed the "target" used to compute the conveyance reduction and encroachment stations for the section. That is why several target increase values are generally used in the initial floodway computations.

After a few initial runs, the encroachment stations should become more defined. Because portions of several computed profiles may be used, additional runs with method 4 or 5 should be made with varying targets along the stream. The final computer runs are usually made with encroachment Method 1 defining the specific encroachment stations at each cross section. Additional runs are often made with Method 1, allowing the user to adjust encroachment stations at specific cross sections to further define the floodway.

While the floodway analysis generally focuses on the change in water surface elevation, it is important to remember that the floodway must be consistent with local development plans and provide reasonable hydraulic transitions through the study reach. Sometimes the computed floodway solution, which provides computed water surfaces at or near the target maximum, may be unreasonable when transferred to the map of the actual study reach. If this occurs, the user may need to change some of the encroachment stations, based on the visual inspection of the topographic map. The floodway computations should be re-run with the new encroachment stations to ensure that the target maximum is not exceeded.

CHAPTER 10

Estimating Scour at Bridges

The computation of scour at bridges within HEC-RAS is based upon the methods outlined in Hydraulic Engineering Circular No. 18 (HEC No. 18, FHWA, 2001). Before performing a scour analysis with the HEC-RAS software, the engineer should thoroughly review the procedures outlined in that report. This chapter presents the methods and equations for computing contraction scour and local scour at piers and abutments. Most of the material in this chapter was taken directly from the HEC No. 18 publication (FHWA, 2001).

For information on how to enter bridge scour data into HEC-RAS, to perform the bridge scour computations, and to view the bridge scour results, see Chapter 11 of the HEC-RAS user's manual.

Contents

General Modeling Guidelines

In order to perform a bridge scour analysis, the user must first develop a hydraulic model of the river reach containing the bridge to be analyzed. This model should include several cross sections downstream from the bridge, such that any user defined downstream boundary condition does not affect the hydraulic results inside and just upstream of the bridge. The model should also include several cross sections upstream of the bridge, in order to evaluate the long-term effects of the bridge on the water surface profile upstream.

The hydraulic modeling of the bridge should be based on the procedures outlined in Chapter 5 of this manual. If observed data are available, the model should be calibrated to the fullest extent possible. Once the hydraulic model has been calibrated (if observed data are available), the modeler can enter the design events to be used for the scour analysis. In general, the design event for a scour analysis is usually the 100 year (1 percent chance) event. In addition to this event, it is recommended that a 500 year (0.2 percent chance) event also be used to evaluate the bridge foundation under a super-flood condition.

After performing the water surface profile calculations for the design events, the bridge scour can then be evaluated. The total scour at a highway crossing is comprised of three components: long-term aggradation or degradation; contraction scour; and local scour at piers and abutments. The scour computations in the HEC-RAS software allow the user to compute contraction scour and local scour at piers and abutments. The current version of the HEC-RAS software does not allow the user to evaluate long-term aggradation and degradation. Long term aggradation and degradation should be evaluated before performing the bridge scour analysis. Procedures for performing this type of analysis are outlined in the HEC No. 18 report, and are beyond the scope of this discussion. The remaining discussions in this chapter are limited to the computation of contraction scour and local pier and abutment scour.

Computing Contraction Scour

Contraction scour occurs when the flow area of a stream is reduced by a natural contraction or a bridge constricting the flow. At a bridge crossing, many factors can contribute to the occurrence of contraction scour. These factors may include: the main channel naturally contracts as it approaches the bridge opening; the road embankments at the approach to the bridge cause all or a portion of the overbank flow to be forced into the main channel; the bridge abutments are projecting into the main channel; the bridge piers are blocking a significant portion of the flow area; and a drop in the downstream tailwater which causes increased velocities inside the bridge. There are two forms of contraction scour that can occur depending on how much bed material is already being transported upstream of the bridge contraction reach.

The two types of contraction scour are called live-bed contraction scour and clear-water contraction scour. Live-bed contraction scour occurs when bed material is already being transported into the contracted bridge section from upstream of the approach section (before the contraction reach). Clear-water contraction scour occurs when the bed material sediment transport in the uncontracted approach section is negligible or less than the carrying capacity of the flow.

Contraction Scour Conditions

Four conditions (cases) of contraction scour are commonly encountered:

Case 1. Involves overbank flow on a floodplain being forced back to the main channel by the approaches to the bridge. Case 1 conditions include:

a. The river channel width becomes narrower either due to the bridge abutments projecting into the channel or the bridge being located at a narrowing reach of the river.

b. No contraction of the main channel, but the overbank flow area is completely obstructed by the road embankments.

c. Abutments are set back away from the main channel.

Case 2. Flow is confined to the main channel (i.e., there is no overbank flow). The normal river channel width becomes narrower due to the bridge itself or the bridge site is located at a narrowing reach of the river.

Case 3. A relief bridge in the overbank area with little or no bed material transport in the overbank area (i.e., clear-water scour).

Case 4. A relief bridge over a secondary stream in the overbank area with bed material transport (similar to case one).

Determination of Live-Bed or Clear-Water Contraction Scour

To determine if the flow upstream is transporting bed material (i.e., live-bed contraction scour), the program calculates the critical velocity for beginning of motion V_c (for the D_{50} size of bed material) and compares it with the mean velocity V of the flow in the main channel or overbank area upstream of the bridge at the approach section. If the critical velocity of the bed material is greater than the mean velocity at the approach section ($V_c > V$), then clear-water contraction scour is assumed. If the critical velocity of the bed material is less than the mean velocity at the approach section ($V_c < V$), then live-bed contraction scour is assumed. The user has the option of forcing the program to calculate contraction scour by the live-bed or clear-water contraction scour

equation, regardless of the results from the comparison. To calculate the critical velocity, the following equation by Laursen (1963) is used:

$$V_c = K_u \, y_1^{1/6} \, D_{50}^{1/3} \tag{10-1}$$

Where: V_c = Critical velocity above which material of size D_{50} and smaller will be transported, ft/s (m/s)

y_1 = Average depth of flow in the main channel or overbank area at the approach section, ft (m)

D_{50} = Bed material particle size in a mixture of which 50% are smaller, ft (m)

K_u = 11.17 (English Units), 6.19 (S.I. Units)

Live-Bed Contraction Scour

The HEC No. 18 publication recommends using a modified version of Laursen's (1960) live-bed scour equation:

$$y_2 = y_1 \left[\frac{Q_2}{Q_1} \right]^{6/7} \left[\frac{W_1}{W_2} \right]^{K_1} \tag{10-2}$$

$$y_s = y_2 - y_0 \tag{10-3}$$

Where: y_s = Average depth of contraction scour in feet (m).

y_2 = Average depth after scour in the contracted section, feet (m). This is taken as the section inside the bridge at the upstream end in HEC-RAS (section BU).

y_1 = Average depth in the main channel or floodplain at the approach section, feet (m).

y_0 = Average depth in the main channel or floodplain at the contracted section before scour, feet (m).

Q_1 = Flow in the main channel or floodplain at the approach section, which is transporting sediment, cfs (m^3/s).

Q_2 = Flow in the main channel or floodplain at the contracted section, which is transporting sediment, cfs (m^3/s).

W_1 = Bottom width in the main channel or floodplain at the approach section, feet (m). This is approximated as the top width of the active flow area in HEC-RAS.

W_2 = Bottom width of the main channel or floodplain at the contracted section less pier widths, feet (m). This is approximated as the top width of the active flow area.

k_1 = Exponent for mode of bed material transport.

V_* / ω	k_1	**Mode of Bed Material Transport**
< 0.50	0.59	Mostly contact bed material discharge
0.50 to 2.0	0.64	Some suspended bed material discharge
> 2.0	0.69	Mostly suspended bed material discharge

V_* = $(g\, y_1\, S_1)^{1/2}$, shear velocity in the main channel or floodplain at the approach section, ft/s (m/s).
ω = Fall velocity of bed material based on D_{50}, ft/s (m/s).
g = Acceleration of gravity, ft/s^2 (m/s^2).
S_1 = Slope of the energy grade line at the approach section, ft/ft (m/m).

Clear-Water Contraction Scour

The recommended clear-water contraction scour equation by the HEC No. 18 publication is an equation based on research from Laursen (1963):

$$y_2 = \left[\frac{Q_2^2}{C\, D_m^{2/3}\, W_2^2} \right]^{3/7} \tag{10-4}$$

$$y_s = y_2 - y_0 \tag{10-5}$$

Where D_m = Diameter of the smallest non-transportable particle in the bed material (1.25 D_{50}) in the contracted section, feet (m).
D_{50} = Median diameter of the bed material, feet (m).
C = 130 for English units (40 for metric).

Note: If the bridge opening has overbank area, then a separate contraction scour computation is made for the main channel and each of the overbanks.

Computing Local Scour at Piers

Pier scour occurs due to the acceleration of flow around the pier and the formation of flow vortices (known as the horseshoe vortex). The horseshoe vortex removes material from the base of the pier, creating a scour hole. As the depth of scour increases, the magnitude of the horshoe vortex decreases, thereby reducing the rate at which material is removed from the scour hole. Eventually an equilibrium between bed material inflow and outflow is reached, and the scour hole ceases to grow.

The factors that affect the depth of local scour at a pier are: velocity of the flow just upstream of the pier; depth of flow; width of the pier; length of the pier if skewed to the flow; size and gradation of bed material; angle of attack of approach flow; shape of the pier; bed configuration; and the formation of ice jams and debris.

The HEC No. 18 report recommends the use of the Colorado State University (CSU) equation (Richardson, 1990) for the computation of pier scour under both live-bed and clear-water conditions. The CSU equation is the default equation in the HEC-RAS software. In addition to the CSU equation, an equation developed by Dr. David Froehlich (1991) has also been added as an alternative pier scour equation. The Froehlich equation is not recommended in the HEC No. 18 report, but has been shown to compare well with observed data.

Computing Pier Scour With The CSU Equation

The CSU equation predicts maximum pier scour depths for both live-bed and clear-water pier scour. The equation is:

$$y_s = 2.0 K_1 K_2 K_3 K_4 a^{0.65} y_1^{0.35} Fr_1^{0.43} \qquad (10\text{-}6)$$

Where: y_s = Depth of scour in feet (m)
K_1 = Correction factor for pier nose shape
K_2 = Correction factor for angle of attack of flow
K_3 = Correction factor for bed condition
K_4 = Correction factor for armoring of bed material
a = Pier width in feet (m)
y_1 = Flow depth directly upstream of the pier in feet (m). This is taken from the flow distribution output for the cross section just upstream from the bridge.
Fr_1 = Froude Number directly upstream of the pier. This is taken from the flow distribution output for the cross section just upstream from the bridge.

Note: For round nose piers aligned with the flow, the maximum scour depth is limited as follows:

$y_s \leq 2.4$ times the pier width (a) for $Fr_1 \leq 0.8$
$y_s \leq 3.0$ times the pier width (a) for $Fr_1 > 0.8$

An optional correction factor, Kw for wide piers in shallow water can be applied to the CSU equation.

$$K_w = 2.58\left(\frac{y}{a}\right)^{0.34} F^{0.65} \qquad \text{for } V/V_c < 1$$

$$K_w = 1.0\left(\frac{y}{a}\right)^{0.13} F^{0.25} \qquad \text{for } V/V_c \geq 1$$

Because this correction factor was developed based on limited flume data, it is not automatically accounted for in HEC-RAS. The user, however, can manually apply this factor to the computed scour depth, or can combine it with one of the user-entered correction factors (K_1 through K_4). See section 6.3 of HEC-18.

The correction factor for pier nose shape, K_1, is given in Table 10.1 below:

Table 10.1
Correction Factor, K_1, for Pier Nose Shape

Shape of Pier Nose	K_1
(a) Square nose	1.1
(b) Round nose	1.0
(c) Circular cylinder	1.0
(d) Group of cylinders	1.0
(e) Sharp nose (triangular)	0.9

The correction factor for angle of attack of the flow, K_2, is calculated in the program with the following equation:

$$K_2 = \left(\cos\theta + \frac{L}{a}\sin\theta\right)^{0.65} \qquad (10\text{-}7)$$

Where: L = Length of the pier along the flow line, feet (m)
θ = Angle of attack of the flow, with respect to the pier

Note: If L/a is larger than 12, the program uses L/a = 12 as a maximum in equation 10-7. If the angle of attack is greater than 5 degrees, K_2 dominates and K_1 should be set to 1.0 (the software does this automatically).

The correction factor for bed condition, K_3, is shown in table 10.2.

Table 10.2
Increase in Equilibrium Pier Scour Depth, K_3, For Bed Condition

Bed Condition	Dune Height H feet	K_3
Clear-Water Scour	N/A	1.1
Plane Bed and Antidune Flow	N/A	1.1
Small Dunes	$10 > H \geq 2$	1.1
Medium Dunes	$30 > H \geq 10$	1.1 to 1.2
Large Dunes	$H \geq 30$	1.3

The correction factor K_4 decreases scour depths for armoring of the scour hole for bed materials that have a D_{50} equal to or larger than 0.007 feet (0.002 m) and a D_{95} equal to or larger than 0.066 feet (0.020 m). The correction factor results from recent research by A. Molinas at CSU, which showed that when the velocity (V_1) is less than the critical velocity (V_{c90}) of the D_{90} size of the bed material, and there is a gradation in sizes in the bed material, the D_{90} will limit the scour depth. The equation developed by J. S. Jones from analysis of the data is:

$$K_4 = 0.4(V_R)^{0.15} \tag{10-8}$$

Where:

$$V_R = \left[\frac{V_1 - V_{i50}}{V_{c50} - V_{i95}}\right] \tag{10-9}$$

$$V_{i50} = 0.645\left[\frac{D_{50}}{a}\right]^{0.053} V_{c50} \tag{10-10}$$

$$V_{i95} = 0.645\left[\frac{D_{95}}{a}\right]^{0.053} V_{c95}$$

V_R' = Velocity ratio
V_1 = Average velocity in the main channel or overbank area at the cross section just upstream of the bridge, ft/s (m/s)
V_{i50} = Approach velocity required to initiate scour at the pier for grain size D50, ft/s (m/s)
V_{i95} = Approach velocity required to initiate scour at the pier for grain size D95, ft/s (m/s)
V_{c50} = Critical velocity for D_{50} bed material size, ft/s (m/s)
V_{c95} = Critical velocity for D_{95} bed material size, ft/s (m/s)
a = Pier width, ft (m)

$$V_{c50} = K_u\, y^{1/6}\, D_{50}^{1/3} \qquad (10\text{-}11)$$
$$V_{c95} = K_u\, y^{1/6}\, D_{95}^{1/3}$$

Where: y = The depth of water just upstream of the pier, ft (m)
K_u = 11.17 (English Units), 6.19 (S.I. Units)

Limiting K_4 values and bed material size are given in Table 10.3.

Table 10.3
Limits for Bed Material Size and K_4 Values

Factor	Minimum Bed Material Size	Minimum K_4 Value
K_4	$D_{50} \geq 0.006$ ft (0.002 m) D95≥0.06 ft (0.02 m)	0.4

Computing Pier Scour With The Froehlich Equation

A local pier scour equation developed by Dr. David Froehlich (Froehlich, 1991) has been added to the HEC-RAS software as an alternative to the CSU equation. This equation has been shown to compare well against observed data (FHWA, 1996). The equation is:

$$y_s = 0.32\phi\,(a')^{0.62}\, y_1^{0.47}\, Fr_1^{0.22}\, D_{50}^{-0.09} + a \qquad (10\text{-}12)$$

where: ϕ = Correction factor for pier nose shape: $\phi = 1.3$ for square nose piers; $\phi = 1.0$ for rounded nose piers; and $\phi = 0.7$ for

sharp nose (triangular) piers.

a' = Projected pier width with respect to the direction of the flow, feet (m)

Note: This form of Froehlich's equation is use to predict maximum pier scour for design purposes. The addition of one pier width (+ a) is placed in the equation as a factor of safety. If the equation is to be used in an analysis mode (i.e. for predicting the scour of a particular event), Froehlich suggests dropping the addition of the pier width (+ a). The HEC-RAS program always includes the addition of the pier width (+ a) when computing pier scour. The pier scour from this equation is limited to a maximum in the same manner as the CSU equation. Maximum scour $y_s \leq 2.4$ times the pier width (a) for $Fr_1 \leq 0.8$, and $y_s \leq 3.0$ times the pier width (a) for $Fr_1 > 0.8$.

Computing Local Scour at Abutments

Local scour occurs at abutments when the abutment obstructs the flow. The obstruction of the flow forms a horizontal vortex starting at the upstream end of the abutment and running along the toe of the abutment, and forms a vertical wake vortex at the downstream end of the abutment.

The HEC No. 18 report recommends two equations for the computation of live-bed abutment scour. When the wetted embankment length (L) divided by the approach flow depth (y_1) is greater than 25, the HEC No. 18 report suggests using the HIRE equation (Richardson, 1990). When the wetted embankment length divided by the approach depth is less than or equal to 25, the HEC No. 18 report suggests using an equation by Froehlich (Froehlich, 1989).

The HIRE Equation

The HIRE equation is based on field data of scour at the end of spurs in the Mississippi River (obtained by the USACE). The HIRE equation is:

$$y_s = 4\, y_1 \left(\frac{K_1}{0.55}\right) K_2\, Fr_1^{0.33} \qquad (10\text{-}13)$$

where: y_s = Scour depth in feet (m)

y_1 = Depth of flow at the toe of the abutment on the overbank or in the main channel, ft (m), taken at the cross section just upstream of the bridge.

K_1 = Correction factor for abutment shape, Table 10.4

K_2 = Correction factor for angle of attack (θ) of flow with abutment. $\theta = 90$ when abutments are perpendicular to the

flow, $\theta < 90$ if embankment points downstream, and $\theta > 90$ if embankment points upstream. $K_2 = (\theta/90)^{0.13}$

Fr_1 = Froude number based on velocity and depth adjacent and just upstream of the abutment toe

Table 10.4
Correction Factor for Abutment Shape, K_1

Description	K_1
Vertical-wall Abutment	1.00
Vertical-wall Abutment with wing walls	0.82
Spill-through Abutment	0.55

The correction factor, K_2, for angle of attack can be taken from Figure 10.1.

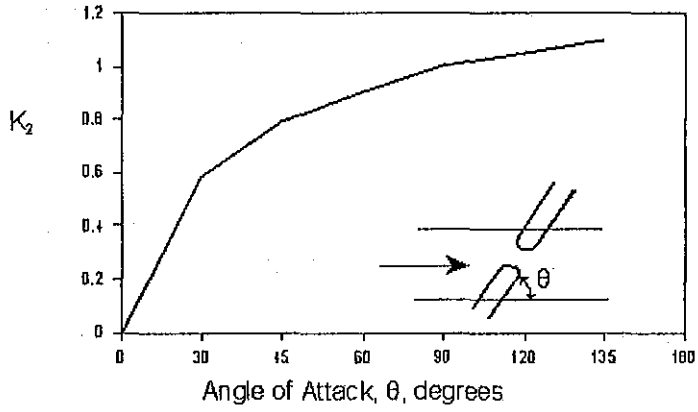

Figure 10.1 Correction Factor for Abutment Skew, K_2

Froehlich's Equation

Froehlich analyzed 170 live-bed scour measurements in laboratory flumes by regression analysis to obtain the following equation:

$$y_s = 2.27 K_1 K_2 (L')^{0.43} y_a^{0.57} Fr^{0.61} + y_a \qquad (10\text{-}14)$$

where: y_s = Scour depth in feet (m)
K_1 = Correction factor for abutment shape, Table 10.4
K_2 = Correction factor for angle of attack (θ) of flow with abutment. $\theta = 90$ when abutments are perpendicular to the

flow, $\theta < 90$ if embankment points downstream, and $\theta > 90$ if embankment points upstream (Figure 10.1). $K_2 = (\theta/90)^{0.13}$

L' = Length of abutment (embankment) projected normal to flow, ft (m)

y_a = Average depth of flow on the floodplain at the approach section, ft (m)

Fr = Froude number of the floodplain flow at the approach section, $Fr = V_e/(gy_a)^2$

V_e = Average velocity of the approach flow $V_e = Q_e/A_e$ ft/s

Q_e = Flow obstructed by the abutment and embankment at the approach section, cfs (m^3/s)

A_e = Flow area of the approach section obstructed by the abutment and embankment, ft^2 (m^2)

Note: The above form of the Froehlich equation is for design purposes. The addition of the average depth at the approach section, y_a, was added to the equation in order to envelope 98 percent of the data. If the equation is to be used in an analysis mode (i.e. for predicting the scour of a particular event), Froehlich suggests dropping the addition of the approach depth ($+ y_a$). The HEC-RAS program always calculates the abutment scour with the ($+y_a$) included in the equation.

Clear-Water Scour at Abutments

Clear-water scour can be calculated with equation 9-13 or 9-14 for live-bed scour because clear-water scour equations potentially decrease scour at abutments due to the presence of coarser material. This decrease is unsubstantiated by field data.

Total Scour Depths Inside The Bridge

The total depth of scour is a combination of long-term bed elevation changes, contraction scour, and local scour at each individual pier and abutment. Once the scour is computed, the HEC-RAS software automatically plots the scour at the upstream bridge cross section. An example plot is shown in Figure 10.2 below.

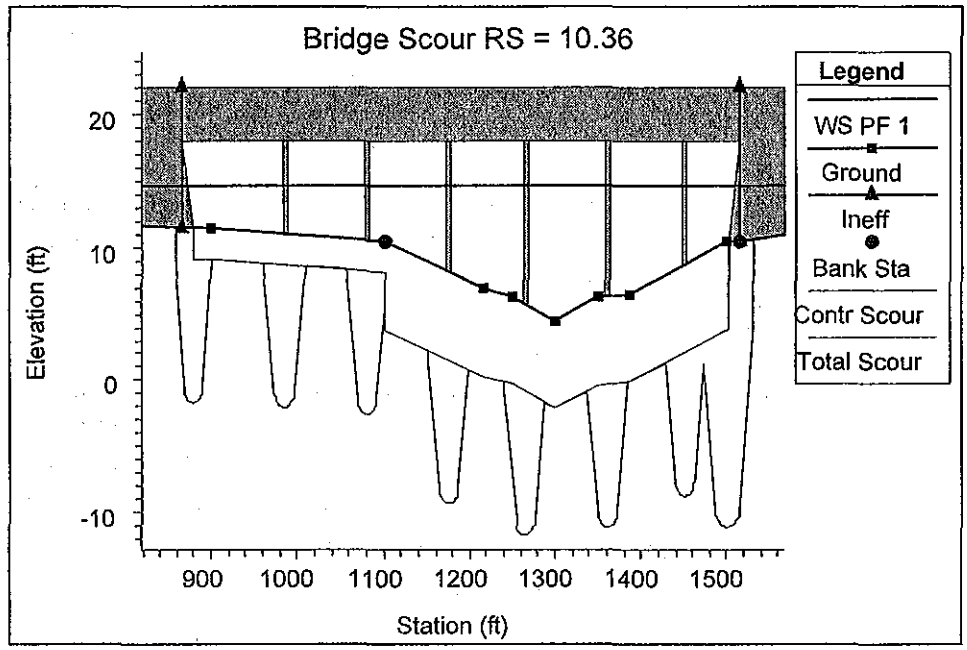

Figure 10.2 Graphic of Contraction and Total Scour at a Bridge

As shown in figure 10.2, the program plots both contraction scour and total local scour. The contraction scour is plotted as a separate line below the existing conditions cross section data. The local pier and abutment scour are added to the contraction scour, and then plotted as total scour depths. The topwidth of the local scour hole around a pier is computed as 2.0 y_s to each side of the pier. Therefore, the total topwidth of the scour hole at a pier is plotted as (4.0 y_s + a). The topwidth of the local scour hole at abutments is plotted as 2.0 y_s around each side of the abutment toe. Therefore, the total topwidth of the scour hole at abutments is plotted as 4.0 y_s.

CHAPTER 11

Modeling Ice-covered Rivers

HEC-RAS allows the user to model ice-covered channels at two levels. The first level is an ice cover with known geometry. In this case, the user specifies the ice cover thickness and roughness at each cross section. Different ice cover thicknesses and roughness can be specified for the main channel and for each overbank and both can vary along the channel. The second level is a wide-river ice jam. In this case, the ice jam thickness is determined at each section by balancing the forces on it. The ice jam can be confined to the main channel or can include both the main channel and the overbanks. The material properties of the wide-river jam can be selected by the user and can vary from cross section to cross section. The user can specify the hydraulic roughness of the ice jam or HEC-RAS will estimate the hydraulic roughness on the basis of empirical data.

This chapter describes the general guidelines for modeling ice-covered channels with HEC-RAS. It contains background material and the equations used. For information on how to enter ice cover data and to view results, see Chapter 6 and Chapter 8 of the HEC-RAS User's Manual.

Contents

Modeling Ice Covers with Known Geometry

Ice covers are common on rivers during the cold winter months and they form in a variety of ways. The actual ways in which an ice cover forms depend on the channel flow conditions and the amount and type of ice generated. In most cases, river ice covers float in hydrostatic equilibrium because they react both elastically and plastically (the plastic response is termed creep) to changes in water level. The thickness and roughness of ice covers can vary significantly along the channel and even across the channel. A stationary, floating ice cover creates an additional fixed boundary with an associated hydraulic roughness. An ice cover also makes a portion of the channel cross sectional area unavailable for flow. The net result is generally to reduce the channel conveyance, largely by increasing the wetted perimeter and reducing the hydraulic radius of a channel, but also by modifying the effective channel roughness and reducing the channel flow area.

The conveyance of a channel or any subdivision of an ice-covered channel, K_i, can be estimated using Manning's equation:

$$K_i = \frac{1.486}{n_c} A_i R_i^{2/3} \tag{11-1}$$

Where: n_c = the composite roughness.
A_i = the flow area beneath the ice cover.
R_i = the hydraulic roughness modified to account for the presence of ice.

The composite roughness of an ice-covered river channel can be estimated using the Belokon-Sabaneev formula as:

$$n_c = \left(\frac{n_b^{3/2} + n_i^{3/2}}{2} \right)^{2/3} \tag{11-2}$$

Where: n_b = the bed Manning's roughness value.
n_i = the ice Manning's roughness value.

The hydraulic radius of an ice-covered channel is found as:

$$R_i = \frac{A_i}{P_b + B_i} \tag{11-3}$$

Where: P_b = the wetted perimeter associated with the channel bottom and side slopes

B_i = the width of the underside of the ice cover

It is interesting to estimate the influence that an ice cover can have on the channel conveyance. For example, if a channel is roughly rectangular in shape and much wider than it is deep, then its hydraulic radius will be cut approximately in half by the presence of an ice cover. Assuming the flow area remains constant, we see that the addition of an ice cover, whose roughness is equivalent to the beds, results in a reduction of conveyance of 37%.

Separate ice thickness and roughness can be entered for the main channel and each overbank, providing the user with the ability to have three separate ice thicknesses and ice roughness at each cross section. The ice thickness in the main channel and each overbank can also be set to zero. The ice cover geometry can change from section to section along the channel. The suggested range of Manning's n values for river ice covers is listed in Table 1.

The amount of a floating ice cover that is beneath the water surface is determined by the relative densities of ice and water. The ratio of the two densities is called the specific gravity of the ice. In general, the density of fresh water ice is about 1.78 slugs per cubic foot (the density of water is about 1.94 slugs per cubic foot), which corresponds to a specific gravity of 0.916. The actual density of a river ice cover will vary, depending on the amount of unfrozen water and the number and size of air bubbles incorporated into the ice. Accurate measurements of ice density are tedious, although possible. They generally tell us that the density of freshwater ice does not vary significantly from its nominal value of 0.916. In any case the user can specify a different density if necessary.

Table 11.1
Suggested Range of Manning's n Values for Ice Covered Rivers

The suggested range of Manning's n values for a single layer of ice

Type of Ice	Condition	Manning's n value
Sheet ice	Smooth	0.008 to 0.012
	Rippled ice	0.01 to 0.03
	Fragmented single layer	0.015 to 0.025
Frazil ice	New 1 to 3 ft thick	0.01 to 0.03
	3 to 5 ft thick	0.03 to 0.06
	Aged	0.01 to 0.02

The suggested range of Manning's n values for ice jams

Thickness	Manning's n values		
ft	Loose frazil	Frozen frazil	Sheet ice
0.3	-	-	0.015
1.0	0.01	0.013	0.04
1.7	0.01	0.02	0.05
2.3	0.02	0.03	0.06
3.3	0.03	0.04	0.08
5.0	0.03	0.06	0.09
6.5	0.04	0.07	0.09
10.0	0.05	0.08	0.10
16.5	0.06	0.09	-

Modeling Wide-River Ice Jams

The wide river ice jam is probably the most common type of river ice jam. In this type, all stresses acting on the jam are ultimately transmitted to the channel banks. The stresses are estimated using the ice jam force balance equation:

$$\frac{d\left(\overline{\sigma}_x t\right)}{dx} + \frac{2\tau_b t}{B} = \rho' g S_w t + \tau_i \qquad (11\text{-}4)$$

where: $\overline{\sigma_x}$ = the longitudinal stress (along stream direction)
t = the accumulation thickness
τ_b = the shear resistance of the banks
B = the accumulation width
ρ' = the ice density
g = the acceleration of gravity
S_w = the water surface slope
τ_i = the shear stress applied to the underside of the ice by the flowing water

This equation balances changes in the longitudinal stress in the ice cover and the stress acting on the banks with the two external forces acting on the jam: the gravitational force attributable to the slope of the water surface and the shear stress of the flowing water on the jam underside.

Two assumptions are implicit in this force balance equation: that $\overline{\sigma_x}$, t, and τ_i are constant across the width, and that none of the longitudinal stress is transferred to the channel banks through changes in stream width, or horizontal bends in the plan form of the river. In addition, the stresses acting on the jam can be related to the mean vertical stress using the passive pressure concept from soil mechanics, and the mean vertical stress

results only from the hydrostatics forces acting in the vertical direction. In the present case, we also assume that there is no cohesion between individual pieces of ice (reasonable assumption for ice jams formed during river ice breakup). A complete discussion of the granular approximation can be found elsewhere (Beltaos 1996).

In this light, the vertical stress, $\overline{\sigma_z}$, is:

$$\overline{\sigma}_z = \gamma_e t \tag{11-5}$$

Where:

$$\gamma_e = 0.5\rho' g(1-s)(1-e) \tag{11-6}$$

Where: e = the ice jam porosity (assumed to be the same above and below the water surface)

s = the specific gravity of ice

The longitudinal stress is then:

$$\overline{\sigma}_x = k_x \overline{\sigma}_z \tag{11-7}$$

Where:

$$k_x = \tan^2\left(45 + \frac{\varphi}{2}\right) \tag{11-8}$$

φ = the angle of internal friction of the ice jam

The lateral stress perpendicular to the banks can also be related to the longitudinal stress as

$$\overline{\sigma}_y = k_1 \overline{\sigma}_x \tag{11-9}$$

Where: k_1 = the coefficient of lateral thrust

Finally, the shear stress acting on the bank can be related to the lateral stress:

$$\tau_b = k_0 \bar{\sigma}_y \tag{11-10}$$

Where:

$$k_0 = \tan\varphi \tag{11-11}$$

Using the above expressions, we can restate the ice jam force balance as:

$$\frac{dt}{dx} = \frac{1}{2 k_x \gamma_e}\left[\rho' g S_w + \frac{\tau_i}{t}\right] - \frac{k_0 k_1 t}{B} = F \tag{11-12}$$

where: F = a shorthand description of the force balance equation

To evaluate the force balance equation, the under-ice shear stress must be estimated. The under-ice shear stress is:

$$\tau_i = \rho g R_{ic} S_f \tag{11-13}$$

Where: R_{ic} = the hydraulic radius associated with the ice cover
S_f = the friction slope of the flow

R_{ic} can be estimated as:

$$R_{ic} = \left(\frac{n_i}{n_c}\right)^{1.5} R_i \tag{11-14}$$

The hydraulic roughness of an ice jam can be estimated using the empirical relationships derived from the data of Nezhikovsky (1964). For ice accumulations found in wide river ice jams that are greater than 1.5 ft thick, Manning's n value can be estimated as:

$$n_i = 0.069 H^{-0.23} t_i^{0.40} \tag{11-15}$$

and for accumulations less than 1.5 ft thick

$$n_i = 0.0593 H^{-0.23} t_i^{0.77} \tag{11-16}$$

where: H = the total water depth
t_i = the accumulation thickness

Solution Procedure

The ice jam force balance equation is solved using an approach analogous to the standard step method. In this, the ice thickness at each cross section is found, starting from a known ice thickness at the upstream end of the ice jam. The ice thickness at the next downstream section is assumed and the value of F found. The ice jam thickness at this downstream cross section, t_{ds}, is then computed as:

$$t_{ds} = t_{us} + \overline{F} L \tag{11-17}$$

Where: t_{us} = the thickness at the upstream section
L = the distance between sections

and $$\overline{F} = \frac{F_{us} + F_{ds}}{2} \tag{11-18}$$

The assumed value and computed value of t_{ds} are then compared. The new assumed value of the downstream ice jam thickness set equal to the old assumed value plus 33% of the difference between the assumed and computed value. This "local relaxation" is necessary to ensure that the ice jam calculations converge smoothly to a fixed value at each cross section. A maximum of 25 iterations is allowed for convergence. The above steps are repeated until the values converge to within 0.1 ft (0.03 m) or to a user defined tolerance.

After the ice thickness is calculated at a section, the following tests are made:

1. The ice thickness cannot completely block the river cross section. At least 1.0 ft must remain between the bottom of the ice and the minimum elevation in the channel available for flow.

2. The water velocity beneath the ice cover must be less than 5 fps (1.5 m/s) or a user defined maximum velocity. If the flow velocity beneath the ice jam at a section is greater than this, the ice thickness is reduced to produce a flow velocity of approximately 5 fps or the user defined maximum water velocity.

3. The ice jam thickness cannot be less than the thickness supplied by the user. If the calculated ice thickness is less than this value, it is set equal to the user supplied thickness.

It is necessary to solve the force balance equation and the energy equation (eq. 2-1) simultaneously for the wide river ice jam. However, difficulties arise because the energy equation is solved using the standard step method, starting from the downstream end of the channel and proceeding upstream, while the force balance equation is solved starting from the upstream end and proceeding downstream. The energy equation can only be solved in the upstream direction because ice covers and wide river jams exist only under conditions of subcritical flow. To overcome this incompatibility and to solve both the energy and the ice jam force balance equations, the following solution scheme was adopted.

A first guess of the ice jam thickness is provided by the user to start this scheme. The energy equation is then solved using the standard step method starting at the downstream end. Next, the ice jam force balance equation is solved from the upstream to the downstream end of the channel. The energy equation and ice jam force balance equation are solved alternately until the ice jam thickness and water surface elevations converge to fixed values at each cross section. This is "global convergence."

Global convergence occurs when the water surface elevation at any cross section changes less than 0.06 ft, or a user supplied tolerance, and the ice jam thickness at any section changes less than 0.1 ft, or a user supplied tolerance, between successive solutions of the ice jam force balance equation. A total of 50 iterations (or a user defined maximum number) are allowed for convergence. Between iterations of the energy equation, the ice jam thickness at each section is allowed to vary by only 25% of the calculated change. This "global relaxation" is necessary to ensure that the entire water surface profile converges smoothly to a final profile.

Appendix A References

Ackers, P., and White, W.R. November 1973. "Sediment Transport: New Approach and Analysis," Journal of the Hydraulics Division, American Society of Civil Engineers, Vol. 99, No. HY 11, pp. 2040-2060.

American Iron and Steel Institute (AISI), 1980. Modern Sewer Design, Washington D.C.

American Society of Civil Engineers. 1977. "Sedimentation Engineering, "Vito A. Vanoni, ed., American Society of Civil Engineers Task Committee, American Society of Engineers, New York.

Amein, M. and Fang, C.S., 1970, "Implicit Flood Routing in Natural Channels," Journal of the Hydraulics Division, ASCE, Vol. 96, No. HY12, Proc. Paper 7773, pp. 2481-2500.

Amin, M.I., and Murphy, P.J. August 1981. "Two Bed-Load Formulas: An Evaluation," Journal of the Hydraulics Division, American Society of Civil Engineers, Vol. 107, No. HY8, pp. 961-972.

Arcement, G. J., Jr., and V. R. Schneider, 1989. "Guide for Selecting Manning's Roughness Coefficient for Natural Channels and Floodplains," U.S. Geological Survey, Water Supply Paper 2339, 38 p., Washington D.C.

Barkau, R.L., 1981, "Simulation of the Failure of Illinois River Levees," Memo to File, St. Louis District, Corps of Engineers, St. Louis, MO.

Barkau, R.L., 1982, "Simulation of the July 1981 Flood Along the Salt River," Report for CE695BV, Special Problems in Hydraulics, Department of Civil Engineering, Colorado State University, Ft. Collins, CO.

Barkau, R.L., 1985, "A Mathematical Model of Unsteady Flow Through a Dendritic Network," Ph.D. Dissertation, Department of Civil Engineering, Colorado State University, Ft. Collins, CO.

Barkau, Robert L., 1992. *UNET, One-Dimensional Unsteady Flow Through a Full Network of Open Channels*, Computer Program, St. Louis, MO.

Bathe, K. and Wilson, E.L., 1976, Numerical Methods in Finite Element Analysis, Prentice-Hall, Inc., Englewood Cliffs, NJ.

Barnes, Harry H,, Jr., 1967. "Roughness Characteristics of Natural Channels," U.S. Geological Survey, Water Supply Paper 1849, Washington D.C.

Blench, T. , 1970, "Regime Theory Design of Canals with Sand Beds." Journal of the Irrigation and Drainage Division, ASCE, Vol. 96, No. IR2, Proc. Paper 7381, pp 205-213.

Bodhaine, G.L., 1982, "Measurement of Peak Discharge at Culverts by Indirect Methods," Techniques of Water Resources Investigations of the United States Geological Survey, Book 3, Chapter A3, U.S. Geological Survey, WA.

Bradley, J.N., 1978. *Hydraulics of Bridge Waterways*, Hydraulic Design Series No. 1, Federal Highway Administration, U.S. Department of Transportation, Second Edition, revised March 1978, Washington D.C.

Brownlie, William R., 1981 (Nov). "Prediction of Flow Depth and Sediment Discharge in Open Channels," Report No. KH-R-43A, California Institute of Technology, W.M Keck Laboratory of Hydraulics and Water Resources, Report No. KH-R-43A, November 1981. Pasadena, CA.

Brownlie, Williem R. 1983 (Jul). "Flow Depth in Sand Bed Channels." Journal of Hydraulic Engineering. American Society of Civil Engineers, Vol 109, No 7, pp 959-990.

Bureau of Public Roads (BPR), 1965. *Hydraulic Charts for the Selection of Highway Culverts*, Hydraulic Engineering Circular No. 5, U.S. Department of Commerce.

Bureau of Reclamation, 1977. *Design of Small Dams*, Water Resources Technical Publication, Washington D.C..

Burkham, Durl E. and David R. Dawdy. 1976. Resistance Equation.

Chanson, Hubert. 1999. "The Hydraulics of Open Channel Flow." John Wiley & Sons Inc., New York.

Chen, Y.H., 1973, "Mathematical Modeling of Water and Sediment Routing in Natural Channels," Ph.D. Dissertation, Department of Civil Engineering, Colorado State University, Ft. Collins, CO.

Chen, Y.H. and Simons, D.B., 1979, "A Mathematical Model of the Lower Chippewa River Network System," Report CER-79 DBS-YHC-58, Department of Civil Engineering, Colorado State University, Ft. Collins, CO.

Chow, V.T., 1959, *Open Channel Hydraulics*, McGraw-Hill Book Company, NY.

Colby, B.R. March 1964. "Practical Computations of Bed-Material Discharge," Journal of the Hydraulics Division, American Society of Civil Engineers, Vol 90, No. HY2, pp 217-246.

Copeland, Ronald R., and Thomas, William A. 1989. "Corte Madera Creek Sedimentation Study." Numerical Model Investigation. US Army Engineer Waterways Experiment Station, Vicksburg, MS. TR-HL-89-6

Copeland, Ronald R. 1994 (Sep). "Application of Channel Stability Methods—Case Studies." US Army Engineer Waterways Experiment Station, Vicksburg, MS. TR-HL-94-11.

Cunge, J.A., Holly, F.M., and Verwey, A., 1980, Practical Aspects of Computational River Hydraulics, Pitman Advanced Publishing Program, Boston, MA.

Cowan, W.L., 1956. "Estimating Hydraulic Roughness Coefficients," Agricultural Engineering, Vol. 37, No. 7, pp 473-475.

Einstein, Hans A. 1950. "The Bed Load Function for Sediment Transportation in Open Channels," Technical Bulletin 1026, US Department of Agricultural, Soil Conservation Service, Washington, D.C.

Fasken, G.B., 1963. "Guide for Selecting Roughness Coefficient n Values for Channels," Soil Conservation Service, US department of Agriculture, 45 p.

Federal Emergency Management Agency, 1985. *Flood Insurance Study Guidelines and Specifications for Study Contractors*, FEMA 37, Washington D.C., September 1985.

Federal Highway Administration, 1984. "Guide for Selecting Manning's Roughness Coefficients for Natural Channels and Flood Plains," Report No. FHWA-TS-84-204, McLean, Virginia.

Federal Highway Administration, 1985. *Hydraulic Design of Highway Culverts*, Hydraulic Design Series No. 5, U.S. Department of Transportation, September 1985, Washington D.C..

Federal Highway Administration, 1986. *Bridge Waterways Analysis Model: Research Report*, Report No. FHWA/RD-86/108, July 1986, Washington D.C..

Federal Highway Administration, 1990. User's Manual for WSPRO - A Computer Model for Water Surface Profile Computations, Publication No. FHWA-IP-89-027, September 1990.

Federal Highway Administration, 1995. *Evaluating Scour at Bridges*, Federal Highway Administration, HEC No. 18, Publication No. FHWA-IP-90-017, 3rd Edition, November 1995, Washington D.C.

Federal Highway Administration, 1996. *Channel Scour at Bridges in the United States*, Publication No. FHWA-RD-95-184, August 1996, Washington D.C.

Fread, D.L., 1974, Numerical Properties of the Implicit Four Point Finite Difference Equations of Unsteady Flow," NOAA Technical Memorandum NWS Hydro-18, U.S. Department of Commerce, NOAA, NWS, Silver Spring, MD, 123pp.

Fread, D.L., 1976, "Theoretical Development of an Implicit Dynamic Routing Model," Hydrologic Research Laboratory, Office of Hydrology, U.S. Department of Commerce, NOAA, NWS, Silver Spring, MD., presented at Dynamic Routing Seminar, Lower Mississippi River Forecast Center, Slidell, LA., 13-17 Dec 1976.

French, R.H., 1985, Open-Channel Hydraulics, McGraw-Hill Book Company, New York.

Friazinov, 1970, "Solution Algorithm for Finite Difference Problems on Directed Graphs," Journal of Mathematics and Mathematical Physics, Vol. 10, No. 2, (in Russian).
Froehlich, D.C., 1989. *Local Scour at Bridge Abutments*, Proceedings of the 1989 National Conference on Hydraulic Engineering, ASCE, New Orleans, LA, pp. 13-18.

Froehlich, D.C., 1991. *Analysis of Onsite Measurements of Scour at Piers*, Proceedings of the ASCE National Hydraulic Engineering Conference, Colorado Springs, CO.

Graf, Walter Hans. 1971. "Hydraulics of Sediment Transport." McGraw Hill, Inc.,

Hicks, D.M. and P.D. Mason, 1991. *Roughness Characteristics of New Zealand Rivers*, Water Resources Survey, DSIR Marine and Freshwater, New Zealand, June 1991.

Hydrologic Engineering Center, 1986. "Accuracy of Computed Water Surface Profiles," Research Document 26, U.S. Army Corps of Engineers, Davis CA.

Hydrologic Engineering Center, 1991. *HEC-2, Water Surface Profiles*, User's Manual, U.S. Army Corps of Engineers, Davis CA.

Hydrologic Engineering Center, August 1993. HEC-6 Generalized Computer Program. "Scour and Deposition in Rivers and Reservoirs," User's Manual. U.S. Army Corps of Engineers, Davis CA.

Hydrologic Engineering Center, 1994. HECDSS, User's Guide and Utility Programs Manual, U.S. Army Corps of Engineers, Davis CA.

Hydrologic Engineering Center, 1995. RD-41, A Comparison of the One-Dimensional Bridge Hydraulic Routines from: HEC-RAS, HEC-2, and WSPRO, U.S. Army Corps of Engineers, Davis CA., September 1995

Hydrologic Engineering Center, 1995. RD-42, Flow Transitions in Bridge Backwater Analysis, U.S. Army Corps of Engineers, Davis CA., September 1995

Hydrologic Engineering Center, 1997. *UNET, One-Dimensional Unsteady Flow Through a Full Network of Open Channels*, User's Manual, U.S. Army Corps of Engineers, Davis, CA.
Henderson, F.M., 1966, Open Channel Flow, Macmillan Publishing Co., Inc., NY, 523pp.

Iwagaki, Yuichi. 1954. "On the Law of Resistance to Turbulent Flow in Open Rough Channels," Proceedings of the 4th Japan National Congress for Applied Mechanics, pp 229-233.

Jansen, P.Ph. 1979. "Principles of River Engineering, the Non-Tidal Alluvial River." Delftse Uitgevers Maatsschappij, Delft, The Netherlands.

Jarrett, R.D., 1984. "Hydraulics of High Gradient Streams," A.S.C.E. Journal of Hydraulic Engineering, Vol. 110, No. 11, November 1984.

Keulegan, Garbis H. 1938. "Laws of Turbulent Flow in Open Channels," Research Paper RP 1151, National Bureau of Standards, Journal of Research, vol 21: PP 701-741.

King, H.W. and E.F. Brater 1963. *Handbook of Hydraulics*, Fifth Edition, McGraw Hill Book Company, New York.

Lane, E.W., 1953, "Design of Stable Channels." American Society of Civil Engineers, Transactions, Paper number 2776, pp 1234-1261.

Laursen, Emmett M., 1958 (Feb). "Total Sediment Load of Streams," Journal of the Hydraulics Division, American Society of Civil Engineers, 84(HY1), 1530-1 to 1530-36.

Laursen, E.M., 1960. *Scour at Bridge Crossings*, ASCE Journal of Hydraulic Engineering, Vol. 89, No. HY 3.

Laursen, E.M., 1963. *An Analysis of Relief Bridges*, ASCE Journal of Hydraulic Engineering, Vol. 92, No. HY 3.

Liggett, J.A., and Cunge, J.A., 1975, "Numerical Methods of Solution of the Unsteady Flow Equations," in Unsteady Flow in Open Channels, edited by K. Mahmood and V. Yevjevich, Vol. I, Chapter 4, Water Resources Publications, Ft. Collins, CO.

Limerinos, J.T. 1970. "Determination of the Manning Coefficient from Measured Bed Roughness in Natural Channels," Geological Survey Water-Supply Paper 1898-B, Prepared in cooperation with the California Department of Water Resources, US Government Printing Office, Washington DC, 20402.

Lindsey, W.F., 1938. "Typical Drag Coefficients for Various Cylinders in Two Dimensional Flow," NACA Technical Report 619.

Microsoft Corporation, 2000. *Microsoft Windows 2000*, User's Manual, Redmond WA.

Parmakian, J., 1963, Waterhammer Analysis, Dover Publications, Inc., NY.

Proffitt, G.T., and Sutherland, A.J. 1983. "Transport of Non-Uniform Sediments," Journal of Hydraulic Research, vol. 21, No. 1, pp. 33-43.

Raudkivi, Arved J. 1998. "Loose Boundary Hydraulics," A.A. Balkema, Rotterdam, pp 8-28.

Rubey, W.W. 1933. "Settling Velocities of Gravel, Sand, and Silt Particles," American Journal of Science, 5th Series, Vol. 25, No 148, 1933, pp. 325-338.

Reed, J.R. and A.J. Wolfkill, 1976. "Evaluation of Friction Slope Models," River 76, Symposium on Inland Waterways for Navigation Flood Control and Water Diversions, Colorado State University, CO.

Richardson, E.V., D.B. Simons and P. Julien, 1990. *Highways in the River Environment*, FHWA-HI-90-016, Federal Highway Administration, U.S. Department of Transportation, Washington, D.C.

Schaffranek, R.W., et al., 1981, "A Model for the Simulation of Flow in Singular and an Interconnected Network of Channels," Techniques of Water Resources Investigations, Chapter 3, U.S. Geological Survey, Reston, VA.

Schlichting, Hermann. 1968. "Boundary-Layer Theory," Translated by J. Kestin. McGraw-Hill Book Company, New York, pp 578-586.

Shearman, J. O., 1990. User's Manual for WSPRO - A computer model for water surface profile computations, Federal Highway Administration, Publication No. FHWA-IP-89-027, 177 p.

Shames, I.H., 1962, Mechanics of Fluids, McGraw-Hill Book Company, NY.

Simons, Daryl B., and Senturk, Fuat. 1992. "Sediment Transport Technology." Water Resources Publications, Littleton, Colorado.

Smith, R.H., 1978, "Development of a Flood Routing Model for Small Meandering Rivers," Ph.D. Dissertation, Department of Civil Engineering, University of Missouri at Rolla, MO.

Stelczer, K. 1981. "Bed-Load Transport." Water Resources Publications, Littleton, Colorado.

Streeter, V.L. and Wylie, E.B., 1967, Hydraulic Transients, McGraw-Hill Book Company, NY.

Toffaleti, F.B. 1968. Technical Report No. 5. "A Procedure for Computation of Total River Sand Discharge and Detailed Distribution, Bed to Surface", Committee on Channel Stabilization, U.S. Army Corps of Engineers, November, 1968

Tucci, C.E.M., 1978, "Hydraulic and Water Quality Model for a River Network," Ph.D. Dissertation, Department of Civil Engineering, Colorado State University, Ft. Collins, CO.

U.S. Army Corps of Engineers, 1965. *Hydraulic Design of Spillways*, EM 1110-2-1603, Plate 33.

USACE, 1993, River Hydraulics, Engineer Manual 1110-2-1416, Headquarters, U.S. Army Corps of Engineers, Washington, DC, October 1993.

US Army Corps of Engineers. 1994. "Channel Stability Assessment for Flood Control Projects," EM 1110-2-1418, US Army Corps of Engineers, Washington DC.

US Army Corps of Engineers. 1994. "Engineering and Design – Hydraulic Design of Flood Control Channels," EM 1110-2-1601, US Army Corps of Engineers, Washington DC.

US Army Corps of Engineers, Waterways Experiment Station. 1998. "SAM Hydraulic Design Package for Channels User's Manual," Vicksburg, MS.

U.S. Bureau of Reclamation (USBR), 1985, Canal Radial Gate Structure Design for Arizona Canal System, WCPM 11.04.

U.S. Geological Survey, 1953. Computation of Peak Discharge at Contractions, Geological Survey Circular No. 284, Washington, D.C.

U.S. Geological Survey, 1968. Measurement of Peak Discharge at Width Contractions By Indirect Methods, Water Resources Investigation, Book 3, Chapter A4, Washington, D.C.

Van Rijn, Leo C. 1984. "Sediment Transport, Part I: Bed Load Transport," Journal of Hydraulic Engineering, American Society of Civil Engineers, Vol 110, No. 10, pp 1412-1430.

Van Rijn, Leo C. 1993. "Principles of Sediment Transport in Rivers, Estuaries, Coastal Seas and Oceans," International Institute for Infrastructural, Hydraulic, and Environmental Engineering, Delft, The Netherlands.

Waterways Experiment Station (WES), 1973, Bridge Pier Losses, Section 010-6, Hydraulic Design Criteria, U.S. Army Corps of Engineers, Vicksburg, MS.

Yang, C.T. 1973. "Incipient Motion and Sediment Transport," Journal of the Hydraulics Division, American Society of Civil Engineers, Vol. 99, No HY10, October, 1973, pp 1679-1704.

Yang, C.T. 1984. "Unit Stream Power Equation for Gravel," Journal of the Hydraulics Division, American Society of Civil Engineers, Vol. 110, No. 12, December 1984, pp1783-1797.

Yang, C.T., Schenggan, Wan, 1991. "Comparison of Selected Bed-Material Load Formulas," Journal of Hydraulic Engineering, American Society of Civil Engineers, Vol 117, No. 8, August 1991, pp 973-989.

Yarnell, D.L., 1934. "Bridge Piers as Channel Obstructions," Technical Bulletin 442, U.S. Department of Agriculture, Washington D.C.

APPENDIX C

Computational Differences Between HEC-RAS and HEC-2

HEC-RAS is a completely new software product. None of the computational routines in the HEC-2 program were used in the HEC-RAS software. When HEC-RAS was being developed, a significant effort was spent on improving the computational capabilities over those in the HEC-2 program. Because of this, there are computational differences between the two programs. This appendix describes all of the major areas in which computational differences can occur.

Cross Section Conveyance Calculations

Both HEC-RAS and HEC-2 utilize the Standard Step method for balancing the energy equation to compute a water surface for a cross section. A key element in the solution of the energy equation is the calculation of conveyance. The conveyance is used to determine friction losses between cross sections, the flow distribution at a cross section, and the velocity weighing coefficient alpha. The approach used in HEC-2 is to calculate conveyance between every coordinate point in the cross section overbanks (Figure 1). The conveyance is then summed to get the total left overbank and right overbank values. HEC-2 does not subdivide the main channel for conveyance calculations. This method of computing overbank conveyance can lead to different amounts of total conveyance when additional points are added to the cross section, with out actually changing the geometry. The HEC-RAS program supports this method for calculating conveyance, but the default method is to make conveyance calculations only at n-value break points (Figure 2).

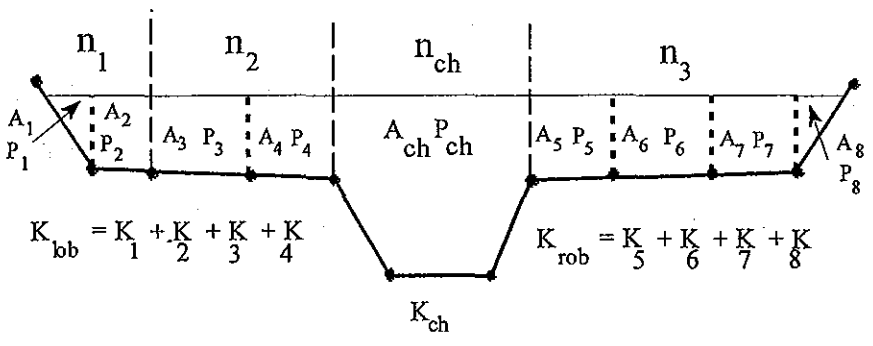

Figure C-1. HEC-2 Conveyance Subdivision

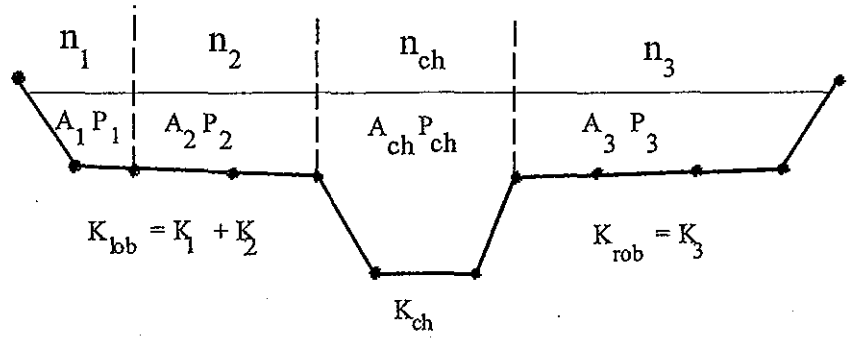

Figure C-2. HEC-RAS Default Conveyance Subdivision Method

Testing Using HEC-2 Conveyance Calculation Approach

Comparisons of HEC-RAS results with those from HEC-2 were performed using 97 data sets from the HEC profile accuracy study (HEC, 1986). Water surface profiles were computed for 10% and 1% chance floods using HEC-2 and HEC-RAS, both programs using the HEC-2 approach for computing overbank conveyance. Table 1 shows the percentage, of approximately 2000 cross sections, within ±0.02 feet (±6 mm). For the 10% chance flood, 53 cross sections had difference greater than ±0.02 feet (±6 mm). For those sections, 62.2% were caused by differences in computation of critical depth and 34% resulted from propagation of the difference upstream. For the 1% chance flood, 88 sections had elevation differences over ±0.02 feet (6 mm), of which 60.2% resulted from critical depth and 36.4% from the upstream propagation of downstream differences. HEC-RAS uses 0.01 feet (3 mm) for the critical depth error criterion, while HEC-2 uses 2.5% of the depth of flow.

Table 1.
Computed Water Surface Elevation Difference (HEC-RAS - HEC-2)

Difference (feet)	-0.02	-0.01	0.0	0.01	0.02	Total
10% Chance Flood	0.8%	11.2%	73.1%	11.2%	0.6%	96.9%
1% Chance Flood	2.0%	11.6%	70.1%	10.8%	1.3%	95.8%

Testing Using HEC-RAS and HEC-2 Approach

The two methods for computing conveyance will produce different answers whenever portions of the overbanks have ground sections with significant vertical slopes. In general, the HEC-RAS default approach will provide a lower total conveyance for the same elevation and, therefore, a higher computed water surface elevation. In order to test the significance of the two ways of computing conveyance, comparisons were performed using the same 97 data sets. Water surface profiles were computed for the 1% chance event using the two methods for computing conveyance in HEC-RAS. The results confirmed that the HEC-RAS default approach will generally produce a higher computed water surface elevation. Out of the 2048 cross section locations, 47.5% had computed water surface elevations within 0.10 feet (30.5 mm), 71% within 0.20 feet (61 mm), 94.4% within 0.40 feet (122 mm), 99.4% within 1.0 feet (305 mm), and one cross section had a difference of 2.75 feet (0.84 m). Because the differences tend to be in the same direction, some effects can be attributed to propagation.

The results from these comparisons do not show which method is more accurate, they only show differences. In general, it is felt that the HEC-RAS default method is more commensurate with the Manning equation and the concept of separate flow elements. The default method in HEC-RAS is also more consistent, in that the computed conveyance is based on the geometry, and not on how many points are used in the cross section. Further research, with observed water surface profiles, will be needed to make any final conclusions about the accuracy of the two methods.

Critical Depth Calculations

During the water surface profile calculations, each of the two programs may need to calculate critical depth at a cross section if any of the following conditions occur:

(1) The supercritical flow regime has been specified by the user.

(2) The calculation of critical depth has been requested by the user.

(3) The current cross section is an external boundary cross section and critical depth must be determined to ensure the user-entered boundary condition is in the correct flow regime.

(4) The Froude number check for a subcritical profile indicates that critical depth needs to be determined to verify the flow regime of the computed water surface elevation.

(5) The program could not balance the energy equation within the specified tolerance before reaching the maximum number of iterations.

The HEC-RAS program has two methods for calculating critical depth: a "parabolic" method and a "secant" method. The HEC-2 program has one method, which is very similar to the HEC-RAS "parabolic" method. The parabolic method is computationally faster, but it is only able to locate a single minimum energy. For most cross sections there will only be one minimum on the total energy curve; therefore, the parabolic method has been set as the default method for HEC-RAS (the default method can be changed from the user interface). If the parabolic method is tried and it does not converge, then the HEC-RAS program will automatically try the secant method. The HEC-RAS version of the parabolic method calculates critical depth to a numerical accuracy of 0.01 feet, while HEC-2's version of the parabolic method calculates critical depth to a numerical accuracy of 2.5 percent of the flow depth. This, in its self, can lead to small differences in the calculation of critical depth between the two programs.

In certain situations it is possible to have more than one minimum on the total energy curve. Multiple minimums are often associated with cross sections that have breaks in the total energy curve. These breaks can occur due to very wide and flat overbanks, as well as cross sections with levees and ineffective flow areas. When the parabolic method is used on a cross section that has multiple minimums on the total energy curve, the method will converge on the first minimum that it locates. This approach can lead to incorrect estimates of critical depth, in that the returned value for critical depth may be the top of a levee or an ineffective flow elevation. When this occurs in the HEC-RAS program, the software automatically switches to the secant method. The HEC-RAS secant method is capable of finding up to three minimums on the energy versus depth curve. Whenever more than one minimum energy is found, the program selects the lowest valid minimum energy (a minimum energy at the top of a levee or ineffective flow elevation is not considered a valid critical depth solution).

Given that HEC-RAS has the capability to find multiple critical depths, and detect possible invalid answers, the final critical depth solutions between HEC-2 and HEC-RAS could be quite different. In general the critical depth answer from the HEC-RAS program will always be more accurate than HEC-2.

Bridge Hydraulic Computations

A vast amount of effort has been spent on the development of the new bridge routines used in the HEC-RAS software. The bridge routines in HEC-RAS allow the modeler to analyze a bridge by several different methods with the same bridge geometry. The model utilizes four user defined cross sections in the computations of energy losses due to the structure. Cross sections are

automatically formulated inside the bridge on an as need basis by combining the bridge geometry with the two cross sections that bound the structure. The HEC-2 program requires the user to use one of two possible methods, the special bridge routine or the normal bridge routine. The data requirements for the two methods are different, and therefore the user must decide a prior which method to use.

Differences between the HEC-2 and HEC-RAS bridge routines will be addressed by discussing the two HEC-2 bridge methodologies separately.

HEC-2 Special Bridge Methodology

The largest computational differences will be found when comparing the HEC-2 special bridge routines to the equivalent HEC-RAS bridge methodologies. The following is a list of what is different between the two programs:

1. The HEC-2 special bridge routines use a trapezoidal approximation for low flow calculations (Yarnell equation and class B flow check with the momentum equation). The HEC-RAS program uses the actual bridge opening geometry for all of the low flow methodologies.

2. Also for low flow, the HEC-2 program uses a single pier (of equivalent width to the sum total width of all piers) placed in the middle of the trapezoid. In the HEC-RAS software, all of the piers are defined separately, and the hydraulic computations are performed by evaluating the water surface and impact on each pier individually. While this is more data for the user to enter, the results are much more physically based.

3. For pressure flow calculations, HEC-2 requires the net flow area of the bridge opening. The HEC-RAS software calculates the area of the bridge opening from the bridge and cross section geometry. Because of the potential error involved in calculating the bridge opening area by hand, differences between the programs may occur for pressure flow calculations.

4. The HEC-RAS software has two equations that can be used for pressure flow. The first equation is for a fully submerged condition (i.e. when both the upstream side and downstream side of the bridge is submerged). The fully submerged equation is also used in HEC-2. A second equation is available in HEC-RAS, which is automatically applied when only the upstream side of the bridge is submerged. This equation computes pressure flow as if the bridge opening were acting as a sluice gate. The HEC-2 program only has the fully submerged pressure flow equation. Therefore, when only the upstream side of the bridge is submerged, the two programs will compute different

answers for pressure flow because they will be using different equations.

5. When using the HEC-2 special bridge routines, it is not necessary for the user to specify low chord information in the bridge table (BT data). The bridge table information is only used for weir flow in HEC-2. When HEC-2 special bridge data is imported into HEC-RAS, the user must enter the low chord information in order to define the bridge opening. This is due to the fact that the trapezoidal approximation used in HEC-2 is not used in HEC-RAS, and therefore the opening must be completely defined.

6. When entering bridge table (BT records) information in the HEC-2 special bridge method, the user had to enter stations that followed along the ground in the left overbank, then across the bridge deck/road embankment; and then along the ground of the right overbank. This was necessary in order for the left and right overbank area to be used in the weir flow calculations. In HEC-RAS this is not necessary. The bridge deck/roadway information only needs to reflect the additional blocked out area that is not part of the ground. HEC-RAS will automatically merge the ground information and the high chord data of the bridge deck/roadway.

HEC-2 Normal Bridge Methodology

In general, when importing HEC-2 normal bridge data into HEC-RAS there should not be any problems. The program automatically selects the energy-based methods for low flow and high flow conditions, which is equivalent to the normal bridge method. The following is a list of possible differences that can occur.

1. In HEC-2 pier information is either entered as part of the bridge table (BT data) or the ground information (GR data). If the user stays with the energy based methods in HEC-RAS the results should be about the same. If the user wishes to use either the Momentum or Yarnell methods for low flow, they must first delete the pier information from the BT or GR data, and then re-enter it as separate pier information in HEC-RAS. If this is not done, HEC-RAS will not know about the pier information, and will therefore incorrectly calculate the losses with either the Momentum or Yarnell methods.

2. The HEC-2 Normal bridge method utilizes six cross sections. HEC-RAS uses only four cross sections in the vicinity of the bridge. The two cross sections inside the bridge are automatically formulated from the cross sections outside the bridge and the bridge geometry. In general, it is common for HEC-2 users to repeat cross sections through the bridge opening (i.e. the cross sections used inside the bridge were a repeat of the downstream section). If however, the HEC-2 user entered completely different cross sections inside the

bridge than outside, the HEC-RAS software will add two additional cross sections just outside of the bridge, in order to get the correct geometry inside of the bridge. This however gives the HEC-RAS data set two more cross-sections than the original HEC-2 data set. The two cross sections are placed at zero distance from the bridge, but could still cause some additional losses due to contraction and expansion of flow. The user may want to make some adjustments to the data when this happens.

3. In HEC-2 the stationing of the bridge table (BT Records) had to match stations on the ground (GR data). This is not required in HEC-RAS. The stationing of the data that makes up a bridge (ground, deck/roadway, piers, and abutments) does not have to match in any way, HEC-RAS will interpolate any points that it needs.

Culvert Hydraulic Computations

The culvert routines in HEC-RAS and HEC-2 were adapted from the Federal Highway Administrations Hydraulic Design of Highway Culverts publication, HDS No. 5 (FHWA, 1985). The following is a list of the differences between the two programs.

1. HEC-2 can only perform culvert calculations for box and circular culvert shapes. HEC-RAS can handle the following shapes: box; circular pipe; semi-circle; arch; pipe arch, vertical ellipse; horizontal ellipse; low profile arch; high profile arch; and ConSpan.

2. HEC-RAS also has the ability to mix the culvert shapes, sizes, and all other parameters at any single culvert crossing. In HEC-2 the user is limited to the same shape and size barrels.

3. HEC-RAS has the ability to use two roughness coefficients inside the culvert barrel (one for the top and sides, and one for the bottom). This allows for better modeling of culverts that have a natural bottom, or culverts that were designed for fish passage.

4. HEC-RAS allows the user to fill in a portion of a culvert. This allows users to model culverts that are buried.

Floodway Encroachment Computations

The floodway encroachment capabilities in HEC-RAS were adapted from those found in HEC-2. For the most part, encroachment methods 1-3 in HEC-RAS are the same as methods 1-3 in HEC-2. The following is a list of the differences between the two programs.

1. HEC-RAS has an additional capability of allowing the user to specify a left and right encroachment offset. While in general the encroachments can go all the way up to the main channel bank stations, the offset establishes an additional buffer zone around the main channel bank stations for limiting the encroachments. The offset is applicable to methods 2-5 in HEC-RAS.

2. The logic of method 4 in HEC-RAS is the same as method 4 in HEC-2. The only difference is that the HEC-RAS method 4 will locate the final encroachment to an accuracy of 0.01 feet, while the HEC-2 method 4 uses a parabolic interpolation method between the existing cross section points. Since conveyance is non-linear with respect to the horizontal stationing, the interpolation in HEC-2 does not always find the encroachment station as accurately as HEC-RAS.

3. Method 5 in HEC-RAS is a combination of HEC-2's methods 5 and 6. The HEC-RAS method five can be used to optimize for a change in water surface (HEC-2 method 5); a change in energy (HEC-2 method 6); or both parameters at the same time (new feature).

4. At bridges and culverts, the default in HEC-RAS is to perform the encroachment, while in HEC-2 the default was not to perform the encroachment. Both programs have the ability to turn encroachments at bridges and culverts on or off.

5. At bridges where the energy based modeling approach is being used (similar to HEC-2's normal bridge method), HEC-RAS will calculate the encroachment for each of the cross sections through the bridge individually. HEC-2 will take the encroachments calculated at the downstream side of the bridge and fix those encroachment stations the whole way through the bridge.

6. In HEC-2, if the user specifies a fixed set of encroachments on the X3 record, this would override anything on the ET record. In HEC-RAS, when the data is imported the X3 record encroachment is converted into a blocked obstruction. Therefore any additional encroachment information found on the ET record will be used in addition to the blocked obstruction.

New Computational Features in HEC-RAS

The following is a list of some of the new computational features found in HEC-RAS that are not available in HEC-2.

1. HEC-RAS can perform sub-critical, supercritical, or mixed flow regime calculations all in a single execution of the program. The cross section order does not have to be reversed (as in HEC-2), the user simply presses a single button to select the computational flow regime. When in a mixed flow regime mode, HEC-RAS can also locate hydraulic jumps.

2. HEC-RAS has the ability to perform multiple bridge and/or culvert openings at the same road crossing.

3. At bridges, the user has the ability to use a momentum-based solution for class A, B, and C low flow. In HEC-2 the momentum equation was used for class B and C flow, and requires the trapezoidal approximation. The HEC-RAS momentum solution also takes into account friction and weight forces that HEC-2 does not.

4. HEC-RAS can model single reaches, dendritic stream systems, or fully looped network systems. HEC-2 can only do single reaches and a limited number of tributaries (up two three stream orders).

5. At stream junctions, HEC-RAS has the ability to perform the calculations with either an energy-based method or a momentum based method. HEC-2 only has the energy based method.

6. HEC-RAS has the following new cross section properties not found in HEC-2: blocked ineffective flow areas; normal ineffective flow areas can be located at any station (in HEC-2 they are limited to the main channel bank stations); blocked obstructions; and specification of levees.

7. In HEC-RAS the user can enter up to 500 points in a cross section. HEC-2 has a limit of 100.

8. HEC-RAS has the ability to perform geometric cross section interpolation. HEC-2 interpolation is based on a ratio of the current cross section and a linear elevation adjustment.

9. HEC-RAS has an improved flow distribution calculation routine. The new routine can subdivide the main channel as well as the overbanks, and the user has control over how many subdivisions are used. The HEC-2 flow distribution option is limited to the overbank areas and breaks at existing coordinate points.

APPENDIX E

Sediment Transport Functions – Sample Calculations

The following sample calculations were the basis for the algorithms used in the HEC-RAS sediment transport functions. They were computed for a single grain size, however they were adapted in the code to account for multiple grain sizes.

Ackers-White Sediment Transport Function

by Ackers-White (ASCE Jour. Of Hyd, Nov 1973)

Input Parameters

Temperature, F	T = 55	Average Velocity, ft/s	V = 2
Kinetic viscosity, ft^2/s	$\nu = 0.00001315$	Discharge, ft^3/s	Q = 5000
Depth, ft	D = 10	Unit Weight water, lb/ft^3	$\gamma_w = 62.385$
Slope	S = 0.001	Overall d50, ft	$d_{50} = 0.00232$
Median Particle Diamter, ft	$d_{si} = 0.00232$		
Specific Gravity of Sediment,	s = 2.65		

Constants

Acceleration of gravity, ft/s^2	g = 32.2

Solution

*note: Ackers-White required the use of d_{35} as the representative grain size for computations in their original paper. In the HEC-RAS approach, the median grain size will be used as per the 1993 update. The overall d_{50} is used for the hiding factor computations.

Hiding Factor from Profitt and Sutherland has been added for this procedure, but will be included as an option in HEC-RAS.

Computations are updated as per Acker's correction in Institution of Civil Engineers Water Maritime and Energy, Dec 1993.

Dimensionless grain diameter,

$$d_{gr} = d_{si} \cdot \left[\frac{g \cdot (s-1)}{\nu^2} \right]^{\frac{1}{3}} \qquad d_{gr} = 15.655$$

Shear velocity u,

$$u_{star} = \sqrt{g \cdot D \cdot S} \qquad u_{star} = 0.567$$

Sediment size-related transition exponent n,

$$n = \begin{cases} 1 & \text{if } d_{gr} \le 1 \\ \left(1 - .056 \cdot \log\left(d_{gr}\right)\right) & \text{if } 1 < d_{gr} \le 60 \\ 0 & \text{if } d_{gr} > 60 \end{cases} \qquad n = 0.331$$

Initial motion parameter A,

$$A = \begin{cases} \left(\frac{0.23}{\sqrt{d_{gr}}} + 0.14\right) & \text{if } d_{gr} \le 60 \\ 0.17 & \text{otherwise} \end{cases} \qquad A = 0.198$$

Sediment mobility number F_{gr},

$\alpha = 10$ (assumed value used in HEC6 and SAM) $\qquad \alpha = 10$

$$F_{gr} = \frac{u_{star}^{\,n}}{\sqrt{g \cdot d_{si} \cdot (s-1)}} \cdot \left(\frac{V}{\sqrt{32} \cdot \log\left(\alpha \cdot \frac{D}{d_{si}}\right)} \right)^{1-n} \qquad F_{gr} = 0.422$$

Hiding Factor HF,

Shield's Mobility Parameter θ,

$$\theta = \frac{u_{star}^{\,2}}{g \cdot (s-1) d_{50}} \qquad \theta = 2.612$$

$$dRatio = \begin{cases} 1.1 & \text{if } \theta \le 0.04 \\ \left(2.3 - 30 \cdot \theta\right) & \text{if } 0.04 < \theta \le 0.045 \\ \left(1.4 - 10 \cdot \theta\right) & \text{if } 0.045 < \theta \le 0.095 \\ 0.45 & \text{otherwise} \end{cases} \qquad dRatio = 0.45$$

$dAdjust = d_{50} \cdot dRatio$ $\qquad dAdjust = 1.044 \times 10^{-3}$

$$HFRatio = \frac{d_{si}}{dAdjust} \qquad HFRatio = 2.222$$

$$HF = \begin{cases} 1.30 & \text{if HFRatio} \geq 3.7 \\ (0.53 \cdot \log(\text{HFRatio}) + 1) & \text{if } 0.075 \leq \text{HFRatio} < 3.7 \\ 0.40 & \text{otherwise} \end{cases} \qquad HF = 1.184$$

Adjust Sediment Mobility Number for Hiding Factor

$$F_{gr} = HF \cdot F_{gr} \qquad F_{gr} = 0.5$$

Check for too fine sediment based on F_{gr} and A,

$$\text{Check} = \frac{F_{gr}}{A} \qquad \text{Check} = 2.522$$

Sediment transport function exponent m,

$$m = \begin{cases} \left(\frac{6.83}{d_{gr}} + 1.67\right) & \text{if } d_{gr} \leq 60 \\ 1.78 & \text{otherwise} \end{cases} \qquad m = 2.106$$

Check for too fine sediment based on m,

$$Check = \begin{cases} 0 & \text{if } m > 6 \\ Check & \text{otherwise} \end{cases} \qquad \text{Check} = 2.522$$

Sediment transport function coefficient C,

$$C = \begin{cases} 10^{2.79 \cdot \log(d_{gr}) - 0.98(\log(d_{gr}))^2 - 3.46} & \text{if } d_{gr} \leq 60 \\ 0.025 & \text{otherwise} \end{cases} \qquad C = 0.0298$$

Transport parameter G_{gr},

$$G_{gr} = C \cdot \left(\frac{F_{gr}}{A} - 1\right)^m \qquad G_{gr} = 0.072$$

Sediment flux X, in parts per million by fluid weight,

$$X = \frac{G_{gr} sd_{si}}{D\left(\frac{u_{star}}{V}\right)^n} \qquad X = 6.741 \times 10^{-5}$$

Sediment Discharge, lb/s

$$G = \gamma_w Q X \qquad G = 21.027$$

Sediment Discharge, tons/day

$$G_s = \frac{86400}{2000} \cdot G \qquad G_s = 908$$

Check to make sure particle diameter and mobility functions are not too low,

$$G_s = \begin{cases} G_s & \text{if Check} > 1 \\ 0 & \text{otherwise} \end{cases} \qquad G_s = 908$$

Engelund Hansen Sediment Transport Function

by Vanoni (1975), and Raudkivi (1976)

Input Parameters

Temperature, F	T = 55	Average Velocity, ft/s	V = 5.46
Kinematic viscosity, ft^2/s	$\nu = 0.00001315$		
Depth, ft	D = 22.9	Unit Weight water, lb/ft^3	$\gamma_w = 62.385$
Slope	S = 0.0001		
Median Particle Diamter, ft	$d_{si} = 0.00232$	Channel Width, ft	B = 40
Specific Gravity of Sediment,	s = 2.65		

Constants

Acceleration of gravity, ft/s^2 $g = 32.2$

Solution

Bed level shear stress τ_o,

$$\tau_o = \gamma_w \cdot D \cdot S \qquad \tau_o = 0.143$$

Fall diameter d_f,

$$d_f = \begin{cases} \left(-69.07 \cdot d_{si}^{\,2} + 1.0755 \cdot d_{si} + 0.000007\right) & \text{if } d_{si} \le 0.00591 \\ \left(0.1086 \cdot d_{si}^{\,0.6462}\right) & \text{otherwise} \end{cases} \qquad d_f = 2.13 \times 10^{-3}$$

Sediment discharge lb/s,

$$g_s = 0.05 \cdot \gamma_w \cdot s \cdot V^2 \cdot \sqrt{\frac{d_f}{g \cdot (s-1)}} \cdot \left[\frac{\tau_o}{(\gamma_w \cdot s - \gamma_w) \cdot d_f}\right]^{\frac{3}{2}} \cdot B \qquad g_s = 32.82$$

Sediment discharge ton/day,

$$G_s = g_s \cdot \frac{86400}{2000} \qquad G_s = 1418$$

Laursen-Copeland Sediment Transport Function

by Copeland (from SAM code, 1996)

Input Parameters

Temperature, F	T = 55	Average Velocity, ft/s	V = 5.46
Kinematic viscosity, ft^2/s	$\nu = 0.00001315$	Discharge, ft^3/s	Q = 5000
Depth, ft	D = 22.90	Unit Weight water, lb/ft^3	$\gamma_w = 62.385$
Slope	S = 0.0001	84% Particle diameter, ft	$d_{84} = 0.00294$
Median Particle Diamter, ft	$d_{sl} = 0.00232$		
Specific Gravity of Sediment	s = 2.65		

Constants

Acceleration of gravity, ft/s^2	g = 32.2

Solution

*Note: the difference between the final result presented here and the result in SAM is due to the method for determining fall velocity. Rubey is used here, whereas SAM computes a value based on a drag coefficient determined from Reynolds number. Calculation routine taken from SAM.

Because the grain distribution is reduced to standard grade sizes representing each present grade class, the d_{84} will equal the standard grade size, d_{si}, in this procedure.

$$d_{84} = d_{si}$$

Grain-related hydraulic radius R

$$R' = \frac{0.0472 \cdot V^{\frac{3}{2}} \cdot (3.5 \cdot d_{84})^{\frac{1}{4}}}{(g \cdot S)^{\frac{3}{4}}} \qquad R' = 14.189$$

R' = 15.248

$$u_*' = \sqrt{g \cdot R' \cdot S} \qquad u_*' = 0.222$$

$$FNRP = \left(\frac{V}{u_*'}\right) - 3.28 - 5.75 \cdot \log\left(\frac{R'}{d_{84}}\right)$$

$$FNRP = 5.195 \times 10^{-4}$$

$$DFNRP = \frac{V + 5 \cdot u_*'}{2.0 \cdot u_*' \cdot R'} \qquad DFNRP = 0.972$$

$$RPRI2 = R' + \frac{FNRP}{DFNRP} \qquad RPRI2 = 15.249$$

$$\Delta R = |RPRI2 - R'| \qquad \Delta R = 5.345 \times 10^{-4}$$

$$R' = \begin{cases} R' & \text{if } \Delta R \le 0.001 \\ RPRI2 & \text{otherwise} \end{cases}$$

$$R' = 15.248$$

Grain-related bed shear stress τ'_b,

$$\tau'_b = R' \cdot \gamma_w \cdot S \qquad \tau'_b = 0.095$$

$$\tau_b = D \cdot \gamma_w \cdot S \qquad \tau_b = 0.143$$

$$\tau'_b = \begin{cases} \tau'_b & \text{if } \tau'_b < \tau_b \\ \tau_b & \text{otherwise} \end{cases} \qquad \tau'_b = 0.095$$

$$u_*' = \sqrt{\frac{\tau'_b \cdot g}{\gamma_w}} \qquad u_*' = 0.222$$

$$RRP = \left(\frac{d_{si}}{R}\right)^{1.16667} \qquad RRP = 2.187 \times 10^{-5}$$

Dimensionless bed shear stress τ_b^*,

$$\tau_b^* = \frac{\tau'_b}{\gamma_w \cdot (s-1) \cdot d_{si}} \qquad \tau_b^* = 0.398$$

Shield's parameter for course grains θ^*,

$$\theta^* = 0.647 \cdot \tau_b^* + 0.0064$$

$$\theta^* = \begin{cases} 0.02 & \text{if } \theta^* < 0.02 \\ \theta^* & \text{otherwise} \end{cases} \qquad \theta^* = 0.264$$

Critical shear stress, τ_{cr}

$$\tau_{cr} = \begin{cases} \left[\theta^* \cdot \gamma_w \cdot (s-1) \cdot d_{si}\right] & \text{if } \tau_b^* \le 0.05 \\ \left[0.039 \cdot \gamma_w \cdot (s-1) \cdot d_{si}\right] & \text{otherwise} \end{cases} \qquad \tau_{cr} = 9.315 \times 10^{-3}$$

Shear stress mobility parameter TFP,

$$TFP = \frac{\tau'_b}{\tau_{cr}} - 1 \qquad TFP = 9.214$$

Fall velocity ω,

Use Rubey's equation, Vanoni p. 169

$$F_1 = \sqrt{\frac{2}{3} + \frac{36 \cdot \nu^2}{g \cdot d_{si}^3 \cdot (s-1)}} - \sqrt{\frac{36 \cdot \nu^2}{g \cdot d_{si}^3 \cdot (s-1)}} \qquad F_1 = 0.725$$

$$\omega = F_1 \cdot \sqrt{(s-1) \cdot g \cdot d_{si}} \qquad \omega = 0.255$$

Particle velocity ratio SF,

$$SF = \frac{u_*'}{\omega} \qquad SF = 0.870$$

Particle velocity ratio parameter Ψ,

$$\Psi = \begin{cases} \left[7.04 \cdot 10^{15} \cdot (SF)^{22.99}\right] & \text{if } SF \le 0.225 \\ \left(40.0 \cdot SF\right) & \text{if } 0.225 < SF \le 1.0 \\ \left(40 \cdot SF^{1.843}\right) & \text{if } SF > 1.0 \end{cases} \qquad \Psi = 34.804$$

Sediment transport G_s, tons/day

$$G_s = 0.432 \cdot \gamma_w \cdot Q \cdot RRP \cdot TFP \cdot \Psi \qquad G_s = 945$$

Meyer-Peter Muller Sediment Transport Function

by Vanoni (1975), and Schlichting's Boundary Layer Theory, 1968

Input Parameters

Temperature, F	T = 55	Average Velocity, ft/s	V = 5.46
Kinematic viscosity, ft^2/s	$\nu = 0.00001315$	Discharge, ft^3/s	Q = 5000
Depth, ft	D = 22.9	Unit Weight water, lb/ft^3	$\gamma_w = 62.385$
Slope	S = 0.0001	Overall d50, ft	$d_{90} = 0.00306$
Median Particle Diamter, ft	$d_{sl} = 0.00232$	Channel Width, ft	B = 40
Specific Gravity of Sediment,	s = 2.65		

Constants

Acceleration of gravity, ft/s^2 g = 32.2

Solution

Shear velocity u,

$$u_* = \sqrt{g \cdot D \cdot S} \qquad u_* = 0.272$$

Shear Reynold's number, R_s,

$$R_s = \frac{u_* \cdot d_{90}}{\nu} \qquad R_s = 63.189$$

Schlichting's B coefficient, Bcoeff

$$BCoeff = \begin{cases} (5.5 + 2.5 \cdot \ln(R_s)) & \text{if } R_s \le 5 \\ \left[\begin{array}{l} 0.297918 + 24.8666 \cdot \log(R_s) - 22.9885 \cdot (\log(R_s))^2 \ldots \\ + 8.5199 \cdot (\log(R_s))^3 - 1.10752 \cdot (\log(R_s))^4 \end{array} \right] & \text{if } 5 < R_s \le 70 \\ 8.5 \quad \text{otherwise} \end{cases}$$

Friction factor due to sand grains f',

$$f' = \left(\frac{2.82843}{BCoeff - 3.75 + 2.5 \cdot \ln\left(2 \cdot \frac{D}{d_{90}}\right)} \right)^2$$

$f' = 9.565 \times 10^{-3}$

Nikaradse roughness ratio RKR,

$$RKR = \sqrt{\frac{f'}{8}} \cdot \frac{V}{\sqrt{g \cdot D \cdot S}}$$

$RKR = 0.695$

Sediment discharge lb/s,

$$g_s = \left[\frac{(RKR)^{\frac{3}{2}} \cdot \gamma_w \cdot D \cdot S - 0.047 \cdot (\gamma_w \cdot s - \gamma_w) \cdot d_{si}}{0.25 \cdot \left(\frac{\gamma_w}{g}\right)^{\frac{1}{3}} \cdot \left(\frac{\gamma_w \cdot s - \gamma_w}{\gamma_w \cdot s}\right)^{\frac{2}{3}}} \right]^{\frac{3}{2}} \cdot B$$

$g_s = 7.073$

Sediment discharge ton/day,

$$G_s = g_s \cdot \frac{86400}{2000}$$

$G_s = 306$

Toffaleti Sediment Transport Function

by Vanoni, for single grain size

Input Parameters

Slope,	S = 0.0001	Temperature, F	T = 55
Hydraulic Radius, ft	R = 10.68	viscosity, ft^2/s	$\nu = 0.00001315$
Width, ft	B = 40	Median Particle Size, ft	$d_{si} = 0.00232$
Velocity, ft/s	V = 5.46	65% finer Particle Size, ft	$d_{65} = 0.00257$
		Fraction of Total Sediment	$p_i = 1$
		Unit Weight of Water, lb/ft^3	$\gamma_w = 62.385$

Constants

Acceleration of gravity, ft/s^2 $g = 32.2$

Solution

Nikaradse Roughness Value, using d_{65}, as per Einstein, 1950, p.

$k_s = d_{65}$ $\quad k_s = 2.57 \times 10^{-3}$

Grain-related shear velocity as per Einstein, 1950, p. 10

Guess $u'_{*try} = 0.199$ → Assume hydraulically rough grain first.

$$r' = \frac{u'^{2}_{*try}}{g \cdot S}$$ r' = 12.298

$$u'_{*} = \frac{V}{\left(5.75 \cdot \log\left(12.27 \cdot \frac{r'}{k_s}\right)\right)}$$

Check $u'_{*} = 0.199$

Check for hydraulically rough or smooth grains...

Guess $u'_{*try} = 0.169$

$$r' = \frac{u'^{2}_{*try}}{g \cdot S} \qquad r' = 8.87$$

$$\delta' = \frac{11.6 \cdot \nu}{u'_{*try}} \qquad \delta' = 9.026 \times 10^{-4}$$

$$\text{Check} = \frac{k_s}{\delta'} \qquad \text{Check} = 2.847 \qquad \frac{k_s}{\delta'} = 2.847$$

$$u'_* = \begin{cases} \dfrac{V}{\left(5.75 \cdot \log\left(3.67 \cdot \dfrac{r' \cdot u'_{*try}}{\nu}\right)\right)} & \text{if Check} < 5 \quad \text{Smooth} \\ u'_* \quad \text{otherwise} & \text{Rough} \end{cases}$$

Check $u'_* = 0.169$

Check for Transitional regime

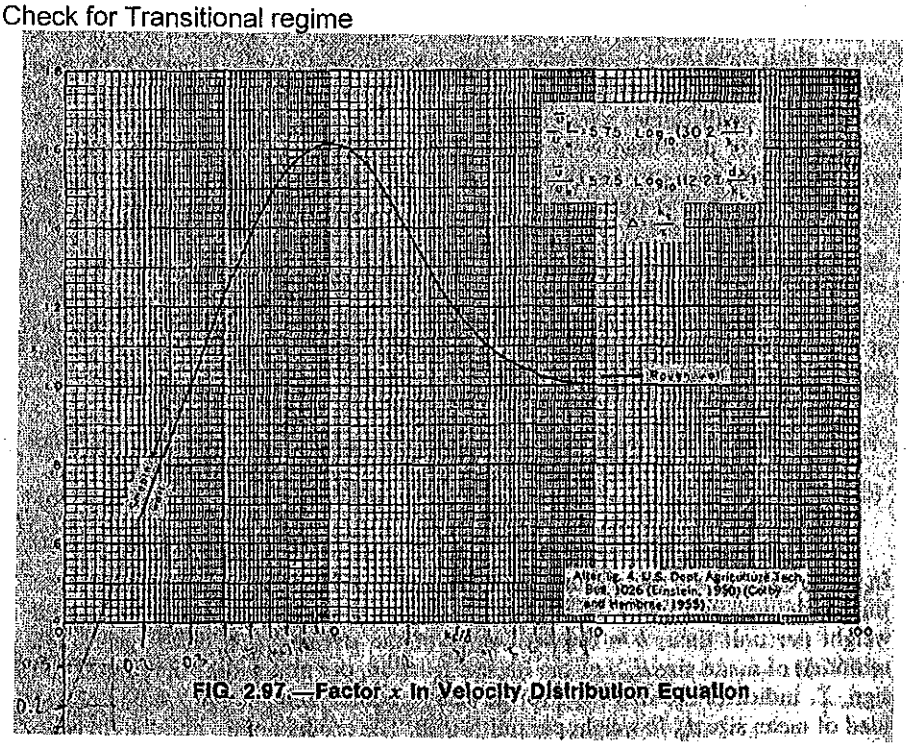

FIG. 2.97.—Factor x in Velocity Distribution Equation

$$\Phi = \frac{k_s}{\delta'} \qquad \Phi = 2.847$$

x = 1.14 from figure 2.97, Vanoni, page 196

$$u'_* = \begin{cases} \dfrac{V}{5.75 \cdot \log\left(12.27 \cdot \dfrac{r' \cdot x}{k_s}\right)} & \text{if } 0.1 < \Phi < 10 \\ u'_* & \text{otherwise} \end{cases}$$

$$\delta' = \frac{11.6 \cdot \nu}{u'_*} \qquad \Phi = \frac{k_s}{\delta'} \qquad \Phi = 3.416$$

$$u'_* = 0.203$$

****Note: Einstein's method for determining u'* was compared with Toffaleti's graphical approach. Results showed that the two methods are in acceptable agreement, with differences on the order of less than 3%. Einstein's approach was selected for its established reputation and its relative simplicity.

Toffaleti coefficients, A and k_4,

$$A_{factor} = \frac{\left(10^5 \cdot \nu\right)^{\frac{1}{3}}}{10 \cdot u'_*} \qquad A_{factor} = 0.54$$

$$A = \begin{cases} \left(9.5987 \cdot A_{factor}^{-1.5445}\right) & \text{if } A_{factor} \le 0.5 \\ \left(39.079 \cdot A_{factor}^{0.481}\right) & \text{if } 0.5 < A_{factor} \le 0.66 \\ \left(221.85 \cdot A_{factor}^{4.660}\right) & \text{if } 0.66 < A_{factor} \le 0.72 \\ 48 & \text{if } 0.72 < A_{factor} \le 1.3 \\ \left(22.594 \cdot A_{factor}^{2.872}\right) & \text{if } A_{factor} > 1.3 \end{cases} \qquad A = 29.065$$

$$k_{4Factor} = \frac{\left(10^5 \cdot \nu\right)^{\frac{1}{3}}}{10 \cdot u'_*} \cdot 10^5 \cdot S \cdot d_{65} \qquad K_{4Factor} = 0.014$$

$$k_4 = \begin{cases} (1.0) & \text{if } k_{4Facotr} \le 0.25 \\ \left(5.315 \cdot k_{4Factor}^{1.205}\right) & \text{if } 0.25 < k_{4Factor} \le 0.35 \\ \left(0.510 \cdot k_{4Factor}^{-1.028}\right) & \text{if } k_{4Factor} > 0.35 \end{cases} \qquad k_4 = 1$$

$$Ak_4 = A \cdot k_4$$

Check for too low values for the product Ak_4,

$$Ak_4 = \begin{cases} 16 & \text{if } Ak_4 < 16 \\ Ak_4 & \text{if } Ak_4 \ge 16 \end{cases} \qquad Ak_4 = 29.065$$

More Coefficients,

$$T_T = 1.10 \cdot (0.051 + 0.00009 \cdot T) \qquad T_T = 0.062$$

$$n_V = 0.1198 + 0.00048 \cdot T \qquad n_V = 0.146$$

$$c_z = 260.67 - 0.667 \cdot T \qquad c_Z = 223.985$$

Fall Velocity for Medium Sand from Toffaleti Tables at 55 degrees F,

$$w_i = 0.340$$

$$z_i = \frac{w_i \cdot V}{c_z \cdot R \cdot S} \qquad z_i = 7.76$$

$$z_i = \begin{cases} (1.5 \cdot n_V) & \text{if } z_i < n_V \\ z_i & \text{otherwise} \end{cases} \qquad z_i = 7.76$$

Empirical Relationship for g_{ssLi},

$$g_{ssLi} = \frac{0.600 \cdot p_i}{\left(\frac{T_T \cdot Ak_4}{V^2}\right)^{\frac{5}{3}} \cdot \left(\frac{d_{si}}{0.00058}\right)^{\frac{5}{3}}} \qquad g_{ssLi} = 6.473$$

$$M_i = \frac{g_{ssLi}}{\left[\frac{\left(\frac{R}{11.24}\right)^{1+n_V-0.756 \cdot z_i} - (2 \cdot d_{si})^{1+n_V-0.756 \cdot z_i}}{1+n_V-0.756 \cdot z_i}\right]} \qquad M_i = 2.948 \times 10^{-10}$$

Concentration,

$$C_{Li} = \frac{M_i}{43.2 \cdot p_i \cdot (1 + n_V) \cdot V \cdot R^{0.756 \cdot z_i - n_V}}$$

$C_{Li} = 1.425 \text{ X } 10^{-18}$

Check for unrealistically high concentration and adjust M_i if necessary,

$$C_{2d} = C_{Li} \cdot \left(\frac{2 \cdot d_{si}}{R} \right)^{-0.756 \cdot z_i}$$

$C_{2d} = 75.536$

$$C_{Li} = \begin{cases} C_{Li} & \text{if } C_{2d} < 100 \\ \dfrac{100}{\left(\dfrac{2 \cdot d_{si}}{R} \right)^{-0.756 \cdot z_i}} & \text{if } C_{2d} \geq 100 \end{cases}$$

$C_{Li} = 1.425 \text{ X } 10^{-18}$

$$M_i = C_{Li} \cdot \left[43.2 \cdot p_i \cdot (1 + n_V) \cdot V \cdot R^{0.756 \cdot z_i - n_V} \right]$$

$M_i = 2.948 \text{ X } 10^{-10}$

Bed Load Transport,

$$g_{sbi} = M_i \cdot (2 \cdot d_{si})^{(1 + n_V - 0.756 z_i)}$$

$g_{sbi} = 30.555$

Lower Layer Transport,

$$g_{ssLi} = M_i \cdot \left[\frac{\left(\dfrac{R}{11.24} \right)^{(1 + n_V - 0.756 \cdot z_i)} - (2 \cdot d_{si})^{(1 + n_V - 0.756 \cdot z_i)}}{1 + n_V - 0.756 \cdot z_i} \right]$$

$g_{ssLi} = 6.473$

Middle Layer Transport,

$$g_{ssMi} = M_i \cdot \frac{\left(\dfrac{R}{11.24} \right)^{0.244 \cdot z_i} \cdot \left[\left(\dfrac{R}{2.5} \right)^{1 + n_V - z_i} - \left(\dfrac{R}{11.24} \right)^{1 + n_V - z_i} \right]}{1 + n_V - z_i}$$

$g_{ssMi} = 5.674 \text{ X } 10^{-1}$

Upper Layer Transport,

$$g_{ssUi} = M_i \cdot \frac{\left(\dfrac{R}{11.24} \right)^{0.244 \cdot z_i} \cdot \left(\dfrac{R}{2.5} \right)^{0.5 \cdot z_i} \cdot \left[R^{(1 + n_V - 1.5 \cdot z_i)} - \left(\dfrac{R}{2.5} \right)^{1 + n_V - 1.5 \cdot z_i} \right]}{1 + n_V - 1.5 \cdot z_i}$$

$g_{ssUi} = 1.72 \text{ X } 10^{-15}$

Total Transport per Unit Width,

$$g_{si} = g_{sbi} + g_{ssLi} + g_{ssMi} + g_{ssUi} \qquad g_{si} = 37.027$$

Total Transport,

$$G = g_{si} \cdot B \qquad \underline{\text{G = 1481 tons/day}}$$

Yang Sediment Transport Function

by Yang, from ASCE Journal of Hydraulics, Oct 1973, Dec 1984

Input Parameters

Temperature, F	T = 55	Average Velocity, ft/s	V = 5.46
Kinematic viscosity, ft^2/s	$\nu = 0.00001315$	Discharge, ft^3/s	Q = 5000
Hydraulic Radius, ft	R = 10.68	Unit Weight water, lb/ft^3	$\gamma_w = 62.385$
Slope,	S = 0.0001		
Meidan Particle Diamter, ft	d_{sl} = 0.00232		
Specific Gravity of Sediment	s = 2.65		

Constants

Acceleration of gravity, ft/s^2 g = 32.2

Solution

Shear Velocity, ft/s,

$$u_* = \sqrt{g \cdot R \cdot S} \qquad u_* = 0.185$$

Particle Fall Velocity, ft/s,

Use Rubey's equation, Vanoni p. 169

$$F_1 = \sqrt{\frac{2}{3} + \frac{36 \cdot \nu^2}{g \cdot d_{si}^3 \cdot (s-1)}} - \sqrt{\frac{36 \cdot \nu^2}{g \cdot d_{si}^3 \cdot (s-1)}} \qquad F_1 = 0.725$$

$$\omega = F_1 \cdot \sqrt{(s-1) \cdot g \cdot d_{si}} \qquad \omega = 0.255$$

Shear Reynold's Number,

$$R_s = \frac{u_* \cdot d_{si}}{\nu} \qquad R_s = 32.717$$

Critical Velocity, ft/s,

$$V_{cr} = \begin{cases} \omega \cdot \left(\dfrac{2.5}{\log\left(\dfrac{u_* \cdot d_{si}}{\nu} \right) - 0.06} + 0.66 \right) & \text{if } 0 < R_s < 70 \\ (\omega \cdot 2.05) & \text{if } R_s \geq 70 \end{cases} \qquad V_{cr} = 0.606$$

Log of Concentration,

$$\log C_t = \begin{cases} \left[5.435 - 0.286\cdot\log\left(\frac{\omega\cdot d_{si}}{\nu}\right) - 0.457\cdot\log\left(\frac{u_*}{\omega}\right)\ldots \right. \\ \left. +\left(1.799 - 0.409\cdot\log\left(\frac{\omega\cdot d_{si}}{\nu}\right) - 0.314\cdot\log\left(\frac{u_*}{\omega}\right)\right)\cdot\log\left(\frac{V\cdot S}{\omega} - \frac{V_{cr}\cdot S}{\omega}\right)\right] & \text{if } d_{si} < 0.00656 \quad \text{Sand} \\ \left[\left(6.681 - 0.633\cdot\log\left(\frac{\omega\cdot d_{si}}{\nu}\right) - 4.816\cdot\log\left(\frac{u_*}{\omega}\right)\right)\ldots \right. \\ \left. +\left(2.784 - 0.305\cdot\log\left(\frac{\omega\cdot d_{si}}{\nu}\right) - 0.282\cdot\log\left(\frac{u_*}{\omega}\right)\right)\cdot\log\left(\frac{V\cdot S}{\omega} - \frac{V_{cr}\cdot S}{\omega}\right)\right] & \text{if } d_{si} \geq 0.00656 \quad \text{Gravel} \end{cases}$$

$$\log C_t = 1.853$$

Concentration, ppm

$$C_t = 10^{\log C_t} \qquad C_t = 71.284$$

Sediment Discharge, lb/s

$$G = \frac{\gamma_w \cdot Q \cdot C_t}{1000000} \qquad G = 22.235$$

Sediment Discharge, tons/day

$$G_s = \frac{86400}{2000}\cdot G \qquad G_s = 961$$